



University
of Glasgow

Carruthers, Ross David (2015) Response to ionising radiation of glioblastoma stem-like cells. PhD thesis, University of Glasgow.

<http://theses.gla.ac.uk/7022/>

Copyright and moral rights for this thesis are retained by the author

A copy can be downloaded for personal non-commercial research or study, without prior permission or charge

This thesis cannot be reproduced or quoted extensively from without first obtaining permission in writing from the Author

The content must not be changed in any way or sold commercially in any format or medium without the formal permission of the Author

When referring to this work, full bibliographic details including the author, title, awarding institution and date of the thesis must be given

Response to ionising radiation of glioblastoma stem-like cells

Ross David Carruthers

BSc Med Sci, MB ChB, MRCP, FRCR

This thesis is submitted in fulfilment of the requirements for the Degree of
Doctor of Philosophy

Institute of Cancer Sciences

College of Medical, Veterinary and Life Sciences

University of Glasgow

Dec 2015

Abstract

Introduction

Glioblastoma (GBM) is characterised by local recurrence following surgery, radiotherapy and chemotherapy. GBM has a poor prognosis and novel approaches are required. Recently, a hierarchical organisation of tumour cells in GBM has been proposed. This hypothesis suggests only a subset of cancer cells, termed ‘cancer stem-like cells’ (CSCs) drive tumour growth and possess properties of self renewal and unlimited proliferative capacity. CSCs have been described as radioresistant, implicating CSCs as a determinant of tumour recurrence following therapy. Therefore improved patient outcomes could potentially be achieved by targeting GBM CSCs. Nevertheless, reports of GBM CSC radioresistance have been conflicting, with some authors demonstrating CSC radiosensitivity. Furthermore, investigations of GBM CSC radioresponse have lacked robust radiobiological quantification and this aspect of the CSC phenotype remains controversial.

Aims

To investigate the radioresponse of GBM CSCs in comparison to non CSCs, characterise the DNA damage response (DDR) in GBM CSCs to radiation and investigate effects of inhibition of DNA damage response (DDR) in GBM CSCs.

Methods

Primary GBM cells were cultured in CSC enriching conditions and differentiating ('tumour bulk') conditions. The radioresponse of CSC and tumour bulk cultures derived from single parental tumours were thus compared by clonogenic survival assay. DDR was analysed in CSC and tumour bulk cells via Western blotting for DDR phosphoproteins and flow cytometric quantification of mitotic cells. DNA double strand break (DSB) repair was quantified by analysis of gamma H2AX foci. CSCs and tumour bulk response to irradiation in combination with inhibition of key DDR elements (ataxia telangiectasia mutated, (ATM); ataxia telangiectasia

Abstract

and Rad3 related, (ATR); and poly (ADP-ribose) polymerase, (PARP) by small molecule inhibitor agents was characterised.

Results

CSC cultures were tumourigenic or recapitulated pathological features of parental tumours in orthotopic mouse models, whereas differentiated tumour bulk cultures did not. CSC cultures exhibited upregulation of putative CSC markers relative to tumour bulk. CSC cultures were radioresistant, demonstrated upregulated DDR and more efficient activation of the G2/M checkpoint compared to tumour bulk. CSC cultures repaired DNA DSBs more efficiently at 24 hours following irradiation. Inhibition of ATM in CSCs led to abrogation of the G2/M checkpoint response, reduced efficiency of DNA DSB repair and potent radiosensitisation. Inhibition of PARP in CSCs produced an increase in unresolved DNA DSBs in GBM CSCs at 24 hours post irradiation in G2 phase cells and modest levels of radiosensitisation. Inhibition of ATR in CSCs abrogated the G2/M checkpoint in CSCs efficiently and was associated with modest radiosensitisation. Dual ATR and PARP inhibition provided highly potent radiosensitisation of GBM CSCs.

Conclusions

GBM CSCs were shown to be radioresistant relative to tumour bulk cells due to upregulated DDR, in support of the hypothesis that CSCs contribute to local recurrence, implying a need for CSC targeted therapies.

The inhibition of G2/M checkpoint activation and DNA DSB repair via ATM inhibition or combined ATR/PARP inhibition potently radiosensitised GBM CSCs suggesting targeting both checkpoint and DNA DSB repair is important for optimal radiosensitisation of GBM CSCs. This study has demonstrated that DDR is a potential therapeutic target for radiosensitisation of GBM CSCs.

Acknowledgements

I would like to acknowledge the expert guidance and mentorship given to me in the course of this PhD by my supervisor; Professor Anthony Chalmers. I am also grateful to Professor Michael Olsen for acting in the role of advisor for this project.

The help of Dr Shafiq Ahmed was invaluable during my time in the Chalmers' lab. I would also like to thank Dr Natividad Gomez-Roman, Dr Lesley Gilmour and the other members of the Chalmers' laboratory for their support and advice, (Karen Strathdee, Dr Saurabh Dayal, Katrina Stevenson, Sandy Chahal, Joanna Birch, Filip Zmuda and Antoine Vallatos). I am grateful to Dr Marie Boyd and Dr Annette Sorenson (Strathclyde University) for helping me with the neutral comet assay. Dr Patricia Roxburgh, William Clark and Andrew Keith at the Beatson CRUK Institute laboratories assisted in Sanger sequencing of the cell lines in this project.

Further supervision for this project was provided by Dr Willie Stewart, Consultant Neuropathologist. Janice Stewart and Jennifer Hay provided assistance with immunohistochemistry.

Funding for the project was provided by a University of Glasgow endowment fund. The final year of my studies was generously funded by the Beatson Cancer Charity.

Finally I'd like to thank Kate, Torin and Fergus, for reminding me of the bigger picture when my studies were not progressing as planned.

Author's Declaration

I declare that I am the sole author of this thesis. The work presented here is my own, unless otherwise acknowledged. This thesis has not been submitted for consideration for another degree in this or any other university.

Dedication

This thesis is dedicated to Kate, Torin and Fergus.

Contents

Abstract	i
Acknowledgements	iii
Author's Declaration	iv
Dedication	v
Contents	vi
Figures, tables and equations	xiv
List of Publications	xx
List of abbreviations	xxi
Chapter 1 Introduction	26
1.1 Introduction.....	26
1.2 CSC theory	26
1.2.1 Defining CSCs	27
1.2.2 Tumour heterogeneity and CSC theory	28
1.2.3 Evidence for CSCs	29
1.2.4 Experimental models of CSCs	31
1.2.5 Clinical relevance of CSCs	35
1.2.6 Quiescence of CSCs	38
1.2.7 Maintaining stemness; the influence of tumour microenvironment ...	38

Contents

1.2.8 Underlying mechanistics of CSC phenotype	40
1.2.9 Controversies surrounding the CSC hypothesis	41
1.2.10 GBM CSCs and radiotherapy resistance.....	42
1.3 The DNA Damage Response	50
1.3.1 DNA repair processes	52
1.3.2 Non Homologous End Joining (NHEJ)	53
1.3.3 Homologous Recombination (HR)	57
1.3.3 Choice of DSB repair pathway.....	60
1.3.4 Cell Cycle Checkpoint Control	61
1.3.5 Integrating, controlling and amplifying: the DDR phosphatidylinositol 3 kinase-related kinases (PIKKs)	65
1.3.6 ATM and its functions	65
1.3.7 ATR and its functions	67
1.3.8 DNA dependent protein kinase (DNAPK)	68
1.3.9 Ionising radiation induced foci (IRIF).....	68
1.3.10 The role of PARPs in the DDR	70
1.4 DDR kinase inhibition as a therapeutic strategy.....	73
1.4.1 PARP inhibition as a radiosensitising strategy	74
1.4.2 ATM inhibition as a radiosensitising strategy	82

Contents

1.4.3 ATR inhibition as a radiosensitising strategy.....	84
1.4.4 Chk1 inhibition as a radiosensitisation strategy	86
1.4.5 Combination DDR inhibition	87
1.5 DDR inhibition and GBM CSCs.....	88
1.6 Conclusion.....	90
1.7 Aims and objectives	91
1.7.1 Aims	91
1.7.2 Objectives.....	92
Chapter 2 Materials and Methods	93
2.1 Cell culture	93
2.1.1 Source and derivation of primary GBM cell cultures.....	93
2.1.2 Culture of paired GBM CSC and tumour bulk populations.....	94
2.1.3 Growth conditions	94
2.1.4 Serial passaging of cells	94
2.1.5 Counting cells.....	95
2.1.6 Cell storage and cryopreservation.....	95
2.1.7 Thawing cells from liquid nitrogen	95
2.2 Western blot analysis of DDR protein levels	96
2.2.1 Sample preparation.....	96

Contents

2.2.2 Protein estimation	96
2.2.3 Gel electrophoresis of protein	96
2.2.4 Protein transfer	97
2.2.5 Immunodetection	97
2.3 Clonogenic survival analysis	98
2.3.1 Procedure	98
2.3.2 Analysis of clonogenic survival assay.....	99
2.4 Irradiation of cells	100
2.5 Neurosphere assay	101
2.6 Gamma H2AX foci analysis.....	101
2.6.1 Procedure	101
2.6.2 Immunostaining	102
2.6.3 Confocal microscopy.....	102
2.6.4 Quantification of gamma H2AX foci	103
2.7 Neutral Comet Assay.....	104
2.7.1 Procedure	104
2.7.2 Visualisation and quantification	105
2.8 Immunohistochemistry of formalin fixed, paraffin embedded tumour sections	105

Contents

2.8.1 Procedure	105
2.9 Sanger sequencing of p53 in primary GBM cell lines	106
2.10 Flow cytometric analysis of cell cycle distribution and G2/M checkpoint activation	109
2.10.1 Procedure	109
2.11 Cell viability assays.....	114
2.12 Statistical Analyses	115
Chapter 3 Model characterisation.....	118
3.1 Introduction.....	118
3.3 Comparison of expression of putative CSC markers in GBM CSC and tumour bulk cultures.....	120
3.3 Effects of switching media on CSC markers	123
3.4 <i>In vivo</i> validation of the CSC phenotype	125
3.5 Characterisation of cell proliferation rate in CSC and tumour bulk cultures	128
3.6 Cell cycle distribution of stem and bulk cultures	129
3.7 Sanger sequencing of p53	131
3.8 Conclusions.....	132
Chapter 4 Investigation of GBM CSC radioresistance	135
4.1 Introduction.....	135

Contents

4.2 Investigation of radioresistance of GBM CSCs by clonogenic survival assay	136
4.3 Investigation of radioresistance of GBM CSCs by neurosphere formation assay	140
4.4 Investigation of cell cycle checkpoint phosphoproteins in GBM CSCs	141
4.5 Investigation of cell cycle kinetics in GBM CSC and tumour bulk cultures	144
4.6 Investigation of DNA DSB repair in GBM CSC cultures.....	148
4.7 Conclusion.....	153
Chapter 5 Effects of ATM inhibition on GBM CSC radioresistance	156
5.1 Introduction.....	156
5.2 Effect of ATM inhibition on upregulated DDR in GBM stem cells	156
5.3 Effect of ATM inhibition in the absence of radiation on cell viability in GBM CSC and bulk cells	157
5.4 Effects of ATM inhibition on G2/M checkpoint activation in GBM CSC and bulk cells	160
5.5 Effects of ATM inhibition on DNA DSB repair in GBM CSC and bulk cells by Gamma H2AX foci analysis	163
5.6 Effects of ATM inhibition on DNA DSB repair in GBM CSC and bulk tumour cells by neutral comet assay	167
5.7 Effects of ATM inhibition on clonogenic survival of GBM CSC and bulk cultures	172
5.8 Conclusions.....	175

Contents

Chapter 6 PARP and GBM CSC radioresistance	181
6.1 Introduction.....	181
6.2 PARP-1 expression in GBM tumour samples	181
6.3 Investigation of PARP-1 expression and activity in GBM CSC and bulk cultures	182
6.3 Investigation of effects of PARP-1 inhibition on GBM CSC radioresistance	183
6.4 Investigation of effects of PARP inhibition on DNA DSB repair in GBM CSCs	188
6.8 Conclusion.....	193
Chapter 7 Radiosensitisation of GBM CSCs by inhibition of ATR and PARP	197
7.1 Introduction.....	197
7.2 Effects of VE-821 on ATR function in GBM CSCs	197
7.3 Effects of VE-821 on cell viability in GBM CSC and bulk cultures	198
7.4 Effects of VE-821 on the G2/M checkpoint in GBM CSCs	199
7.5 Effects of VE-821 and radiation on clonogenic survival of GBM CSC and bulk cultures	202
7.6 Investigation of combination DDR kinase inhibition on radiosensitivity of GBM CSCs.....	204
7.7 Conclusion.....	210
Chapter 8 Discussion	214

Contents

8.1 Introduction.....	214
8.2 Modelling GBM CSCs <i>in vitro</i>	215
8.2 Radioresistance of GBM CSCs.....	218
8.3 The role of ATM in GBM CSC radioresistance.....	222
8.4 The role of Poly (ADP ribose) polymerase (PARP) in GBM CSC radioresistance.....	224
8.5 ATR inhibition and GBM CSC radioresistance.....	226
8.6 Combined checkpoint and DSB repair inhibition for optimal radiosensitisation of GBM CSCs	228
8.7 Cytotoxic effects of ATR and PARP inhibition in the absence of radiation	229
8.8 Clinical utility of DDR inhibition as a GBM radiosensitiser strategy	230
8.9 Final Conclusions	236
Appendix 1.....	238
Appendix 2.....	239
References.....	240

Figures, tables and equations

Figure 1.1 Proposed clinical significance of CSC theory	36
Figure 1.2 Responses of mammalian cells to DNA DSBs induced by gamma irradiation	51
Figure 1.3 Illustrative schematic of kinetics of DNA DSB repair following irradiation in mammalian cells	53
Figure 1.4 Schematic diagram of non homologous end joining (NHEJ) repair	56
Figure 1.5 Schematic diagrams of homologous recombination (HR) repair and its subpathways.....	58
Figure 1.6 The influence of ATR and ATM on cell cycle control in response to DNA damage.....	62
Figure 1.7 Mechanism of radiosensitisation by PARP-1 inhibition	72
Figure 2.1 Comparison of manual and automated gamma H2AX foci counts by Volocty software.....	103
Figure 2.2 Region gating to exclude debris from flow cytometry analyses	110
Figure 2.3 Region gating to exclude doublets from flow cytometry analyses ...	111
Figure 2.4 Example of cell cycle profile following analysis of PI stained cells using FlowJo software	112
Figure 2.5 Example of regional gating applied to identify mitotic cells labelled with Phosphorylated Histone H3 (pHisH3) Alexa Fluoro 488 conjugate antibody	113

Figures, tables and equations

Figure 3.1 Representative images of E2 and G7 neurospheres	119
Figure 3.2 Representative images of E2 and G7 monolayer cultures	120
Figure 3.3 Analysis of CSC markers via Western blotting	121
Figure 3.4 Quantification of CD133 expression by flow cytometry.....	122
Figure 3.5 Demonstration of immunofluorescent staining for CSC markers in E2 CSC and tumour bulk cells	123
Figure 3.6 Comparison of CSC marker and differentiation marker expression by Western blotting in CSC and bulk cultures following switching of original growth media conditions.	124
Figure 3.7 Comparison of <i>in vivo</i> tumour generation by E2 CSC and bulk cultures	126
Figure 3.8 Quantification of Ki67 and HLA immunohistochemical staining as a tumour cell marker in sections of murine xenograft tumours derived from E2 CSC and bulk cultures	127
Figure 3.9 Demonstration of patterns of CD133 immunohistochemical staining observed in E2 CSC murine orthotopic intracranial xenograft tumours	127
Figure 3.10 Demonstration of PARP-1 expression in G7 CSC and tumour bulk orthotopic xenograft tumours by immunohistochemistry	128
Figure 3.11 Cell proliferation in E2 and G7 CSC and bulk cultures measured by cell viability assay.....	129
Figure 3.12 Cell cycle profiles of E2 and G7 CSC and tumour bulk cultures under basal conditions.....	130
Figure 3.13 Analyses of cell cycle distribution of E2 and G7 CSC and tumour bulk cultures under basal conditions	131

Figures, tables and equations

Figure 4.1 Clonogenic survival analysis of CSC versus bulk cultures	138
Figure 4.2 Analysis of neurosphere formation in E2 CD133+ and CD133- cells ..	141
Figure 4.3 DDR protein and phosphoprotein expression by Western blotting in CSC and bulk cells in response to radiation	143
Figure 4.4 Cell cycle profiles of E2 and G7 CSC and tumour bulk cultures following 5Gy radiation exposure	145
Figure 4.5 Cell cycle phase quantification of cells following ionising radiation exposure in E2 and G7 CSC and tumour bulk cultures	146
Figure 4.6 Analysis of mitotic cells following ionising radiation by pHisH3	147
Figure 4.7 Quantification of mitotic cells following ionising radiation by pHisH3	148
Figure 4.8 Quantification of gamma H2AX foci following 1Gy irradiation (initial pilot experiment).....	150
Figure 4.9 Quantification of gamma H2AX foci in CENPF negative and CENPF positive E2 CSC and bulk cell nuclei	151
Figure 5.1 Comparison of phosphorylated DDR proteins in CSC and bulk cell cultures following 5Gy radiation +/- KU-55933	157
Figure 5.2 Effect of KU-55933 exposure on cell viability in CSC and bulk cultures	159
Figure 5.3 Analysis of G2/M checkpoint activation in CSC and bulk cultures following 5Gy radiation +/- KU-55933	161
Figure 5.4 Analysis of G2/M checkpoint activation in CSC and bulk cultures following 5Gy radiation +/- KU-55933	162

Figures, tables and equations

Figure 5.5 Representative images of gamma H2AX foci and CENPF immunofluorescent staining in E2 CSC and bulk cultures	164
Figure 5.6 Quantification of gamma H2AX foci in CENPF positive (G2 cell cycle phase) E2 CSC and bulk cultures following 1Gy +/- 10µM KU-55933	165
Figure 5.7 Quantification of gamma H2AX foci in CENPF negative (G1 cell cycle phase) E2 CSC and bulk cultures following 1Gy +/- 10µM KU-55933	166
Figure 5.8 Quantification of DNA DSBs in E2 CSC and bulk cultures following radiation +/- 10µM KU-55933 by neutral comet assay	168
Figure 5.9 Quantification of DNA DSBs in E2 CSC cultures following radiation +/- KU-55933 by neutral comet assay.....	169
Figure 5.10 Immunofluorescent detection of MRE11 foci following irradiation .	170
Figure 5.11 Analysis of 53BP1 foci in E2 bulk cells following irradiation +/- KU-55933	171
Figure 5.12 Effects of radiation +/-10µM KU-55933 on clonogenic survival of E2, R10 and G7 CSC and bulk cultures	173
Figure 5.13 Effects of radiation +/- KU-55933 on neurosphere formation	175
Figure 6.1 Demonstration of PARP-1 expression by immunohistochemical staining in normal human brain, GBM patient samples (GBM 1 and 2), and orthotopic murine xenografts (G7 CSC and E2 CSC)	182
Figure 6.2 Analysis of PARP-1 and PAR expression in CSC and bulk cells following 5Gy radiation +/- olaparib by Western blotting.....	183
Figure 6.3 Effects of radiation +/- 1µM olaparib on clonogenic survival of CSC and bulk cultures	184
Figure 6.4 Effect of radiation +/- olaparib on neurosphere formation	187

Figures, tables and equations

Figure 6.5 Images of gamma H2AX immunofluorescent staining in E2 CSC and tumour bulk cells exposed to 1 μ M olaparib and 1Gy radiation	189
Figure 6.6 Quantification of gamma H2AX foci following 1Gy +/- 1 μ M olaparib in CENPF positive (G2 cell cycle phase) CSC and bulk cell populations	190
Figure 6.7 Quantification of gamma H2AX foci following 1Gy +/- 1 μ M olaparib in CENPF negative (G1 cell cycle phase) CSC and bulk cell populations	192
Figure 7.1 Analysis of DDR protein expression following 5Gy +/- VE-821 in CSC and bulk cultures	198
Figure 7.2 Effect of VE-821 on cell viability.....	199
Figure 7.3 Effect of 5Gy radiation +/- VE821 on G2/M checkpoint function in E2 and G7 CSC and bulk cultures	201
Figure 7.4 Flow cytometry gating for analysis of pHisH3 positive cells	202
Figure 7.5 Effects of ATR inhibition and VE-821 on clonogenic survival of GBM CSC and bulk cells	203
Figure 7.6 Effects of combination of VE-821 and olaparib on radiosensitivity of E2, G7 and R10 cell lines.	206
Figure 7.7 Neurosphere formation assay in E2 and G7 CSC cultures following combinations of DDR inhibitors and 2Gy	209
Table 1.1 Studies of CSC marker expression and clinical outcome in GBM	37
Table 1.2 Summary of <i>in vitro</i> studies of radiosensitising effects of PARP inhibitors.....	76

Figures, tables and equations	
Table 1.3 Summary of <i>in vivo</i> studies of radiosensitising effects of PARP inhibitors.....	79
Table 2.1 Details of antibodies used, applications and dilutions.....	116
Table 2.2 Secondary antibody details, applications and dilutions	117
Table 3.1 Results of Sanger sequencing of P53 exons 3-10.....	132
Table 4.1 Dose modifying factors for CSC vs tumour bulk cells at 0.37 survival	139
Table 4.2 Surviving fraction at 4Gy values for E2, G7 and R10 CSC and tumour bulk cultures	139
Table 4.3 Surviving fraction at 2Gy values for E2, G7 and R10 CSC and tumour bulk cultures	139
Table 5.1 Sensitiser enhancement ratios at 0.37 survival ($SER_{0.37}$) and surviving fraction at 4Gy (SF4Gy) +/- 10 μ M KU-55933 are tabulated for CSC and bulk cultures of the E2, G7 and R10 cell lines	174
Table 6.1 $SER_{0.37}$ and surviving fraction at 4Gy values (SF4Gy) following PARP inhibition and radiation	185
Table 7.1 $SER_{0.37}$ following ATR inhibition in GBM CSC and bulk cultures	204
Table 7.2 $SER_{0.37}$ for dual ATR and PARP inhibition in GBM CSC and bulk cultures	207
Equation 2.1 The linear quadratic equation.....	100
Equation 2.2 $SER_{0.37}$ ratio.....	100
Equation 2.3 DMF calculation.....	100

List of Publications

Carruthers R, Ahmed S, Strathdee K, Gomez-Roman N, Amoah-Buahin E, Watts C, Chalmers AJ. 2015 **Abrogation of radioresistance in glioblastoma stem-like cells by inhibition of ATM kinase** Mol Oncol Jan 9(1):192-203

Carruthers R, Chalmers AJ 2012. **The potential of PARP inhibitors in neuro-oncology** CNS Oncol. Sep; 1(1):85-97

Ahmed SU, Carruthers R, Gilmour L, Yildirim S, Watts C, Chalmers AJ. Cancer Res. 2015 **Selective inhibition of parallel DNA damage response pathways optimizes radiosensitization of glioblastoma stem-like cells.** pii: canres.3790.2014. [Epub ahead of print]

Carruthers R, Chalmers AJ 2014 **Combination of PARPi with Clinical Radiotherapy** In: Inhibitors for Cancer Therapy (Ed. Sharma R, Curtin N) Springer

List of abbreviations

53BP1	p53 binding protein 1
911	Rad9-Rad1-Hus1 complex
AML	Acute myeloid leukaemia
APE1	Apurinic/apyrimidinic endonuclease
AT	Ataxia telangiectasia
ATM	Ataxia telangiectasia mutated
ATP	Adenosine triphosphate
ATR	Ataxia telangiectasia and Rad 3 related
ATRIP	ATR interacting protein
BCA	Bicinchoninic acid
BER	Base excision repair
bFGF	Basic fibroblast growth factor
BIR	Break induced repair
BLM	Bloom syndrome protein
BRCA1	Breast cancer associated 1, early onset
BRCA2	Breast cancer 2, early onset
BSA	Bovine serum albumin
CDC25a/c	Cell division cycle
CDK	Cyclin dependent kinases
cDNA	Complementary DNA
CENPF	Centromere protein F
Chk1	Checkpoint kinase 1
Chk2	Checkpoint kinase 2
CNS	Central nervous system
CSC	Cancer stem-like cells

List of abbreviations

CXCR4	Chemokine (C-X-C motif) receptor 4
DAB	3'3 diaminobenzidine
DAPI	4',6-Diamidino-2-Phenylindole
DBH	Debromohymenialdisine
DDR	DNA damage response
DMF	Dose modifying factor
DMSO	Dimethyl sulfoxide
DNA	Deoxyribonucleic acid
DNA Lig	DNA ligase
DNA Pol Beta	DNA polymerase beta
DNAPK	DNA dependent protein kinase
DNAPKcs	DNA dependent protein kinase catalytic subunit
dNTP	Deoxynucleoside triphosphates
DSB	Double strand break
DSBR	Double strand break repair
dsDNA	Double stranded DNA
ECL	Enhanced chemiluminescence
ECM	Extra cellular matrix
EGF	Epithelial growth factor
EGFR	Epithelial growth factor receptor
EXO1	Exonuclease 1
FACS	Fluorescence activated cell sorting
FCS	Foetal calf serum
FFPE	Formalin fixed paraffin embedded
FS	Forward scatter
Gamma H2AX	Gamma H2A histone family, member X

List of abbreviations

GBM	Glioblastoma
gDNA	Genomic DNA
GFAP	Glial fibrillary acidic protein
HJ	Holliday junction
HR	Homologous recombination
HRP	Horse radish peroxidase
HSV TK	Herpes simplex virus tyrosine kinase
IRIF	Ionising radiation induced foci
KAP-1	KRAB associated protein 1
L1CAM	L1 cell adhesion molecule
LET	Linear energy transfer
MDC1	Mediator of damage checkpoint 1
MDM2	Mouse double minute 2 homolog
MMEJ	Microhomology mediated end joining
MRE11	Meiotic recombination 11 homolog
MRN	MRE11-Rad50-NBS1 complex
mTOR	Mechanistic target of rapamycin
NAD ⁺	Nicotinamide adenine dinucleotide
NBS1	Nijmegen breakage syndrome 1
NF1	Neurofibromatosis 1
NHEJ	Non homologous end joining
NPC	Neural progenitor cell
p53	Tumour suppressor p53
PALB2	Partner and localiser of BRCA2
PAR	Poly (ADP-ribose)
PARP	Poly (ADP-ribose) polymerase

List of abbreviations

PBS	Phosphate buffered saline
PBST	PBS tween
PCR	Polymerase chain reaction
PDGFR-1	Platelet derived growth factor receptor A
PE	Plating efficiency
pHisH3	Phosphorylated histone H3
PI	Propidium Iodide
PIKK	Phosphatidylinositol3-kinase-related kinases
PNK	Mammalian polynucleotide kinase
Rb1	Retinoblastoma 1
RDS	Radio-resistant DNA synthesis
RNA	Ribonucleic acid
RNF8	Ring finger protein 8
ROS	Reactive oxygen species
RPA	Replication protein A
SDS	Sodium dodecyl sulphate
SDSA	Synthesis dependent strand annealing
SER	Sensitiser enhancement ratio
SiRT1	Silent mating type information regulation 2 homolog 1
SF	Surviving fraction
SMC1	Structural maintenance of chromosomes
SPARC	Secreted protein acidic and rich in cysteine
SS	Side Scatter
SSA	Single strand annealing
SSB	Single strand break
ssDNA	Single stranded DNA

List of abbreviations

TBS	Tris buffered saline
TBSTM	TBST plus 5% marvel
TDP1	Tyrosyl-DNA phosphodiesterase
TGFB	Transforming growth factor beta
TME	Tumour microenvironment
tMVEC	Tumour microvascular endothelial cell
TopBP1	Topoisomerase binding protein 1
VEGF	Vascular endothelial growth factor
XRCC1	X ray repair complementing defective repair in Chinese hamster cells 1
XRCC4	X ray repair cross-complementing protein 4

Chapter 1 Introduction

1.1 Introduction

Glioblastoma (GBM) is the most common primary brain tumour in adults and remains a significant therapeutic challenge. Median survival is 12-15 months despite triple modality therapy consisting of surgical resection, radiotherapy and temozolomide chemotherapy (Stupp et al., 2005), and the disease is characterised by inevitable local recurrence and progression. Recent clinical trials of novel therapeutic agents have been disappointing (Khasraw et al., 2014, Eisele et al., 2014). There is therefore an urgent need to readdress our approach to GBM in order to develop effective therapies which can improve local tumour control, alleviate disabling neurological symptoms of the disease and improve survival for patients.

Given the failure of novel agents with promising *in vitro* activity to improve survival from GBM in recent decades, the validity of current experimental models of cancer has been questioned. In particular, the relevance of serially passaged human cancer cell lines to recapitulate an adequate *in vitro* model of malignant disease has received attention. Intratumoural heterogeneity appears important in determining outcomes from oncological therapy (Marusyk and Polyak, 2010, Gerlinger et al., 2012, Bindra and Glazer, 2005, Patel et al., 2014) and the CSC theory has gained prominence in many solid tumour sites. This hypothesis embraces the concept of functional heterogeneity within tumour tissues and is rapidly gaining clinical relevance. A discussion regarding the CSC hypothesis relevant to GBM follows.

1.2 CSC theory

CSC theory suggests that the organisation of tumour tissue is hierarchical in nature and retains some features of the organisation of normal tissue. In this model of malignant tumours, cancer cells exhibit considerable functional heterogeneity. At the apex of the tumour hierarchy are CSCs, which are a

Introduction

distinct population of tumour cells responsible for maintaining and driving tumour growth which exhibit self-renewal and unlimited proliferative potential. Lower in the tumour hierarchy are tumour cells which are relatively more differentiated and unable to drive tumour growth in the absence of the stem-like population, since these cells lack self renewal and extended proliferative capacity. Cancer cells that lack stem-like properties will be referred to as ‘tumour bulk’ cells for the remainder of this thesis. Despite the central role of CSCs in tumour initiation and propagation it is important to stress that tumour bulk cells still influence the clinical outcome of treatment of a tumour. In reality tumour bulk cells determine the vast majority of volume of disease in a patient, and this tumour compartment is therefore responsible for the symptomatic effects of malignant disease. This is even more so in the case of glioblastoma where the intracranial site of disease means that relatively small increase in tumour volume can cause marked symptomatic deterioration due to the anatomical constraints of the skull. Nevertheless, failure to specifically target CSC populations in glioblastoma and other solid tumour sites will inevitably be associated with treatment failure and recurrence of disease.

1.2.1 Defining CSCs

Self renewal is the cardinal feature of CSCs, and is described as the ability of CSCs to undergo a cell division producing one or two daughter cells which retain the function of self renewal. This ensures the maintenance or expansion of the CSC component of the tumour upon cell division by a CSC. Other features of CSCs are maintained proliferation and capacity for multilineage differentiation. CSCs have an unlimited proliferative capacity in comparison to tumour bulk cells and are able to produce progeny which exhibit features of multilineage differentiation. CSC theory suggests that the CSC subpopulation is vital to the continued growth and existence of a tumour. It is only the CSC subpopulation with the properties of self renewal and unlimited proliferation which can maintain the continued growth of the malignant tissue implying key roles for GBM CSCs in initiating and facilitating tumour recurrence following therapy. The terminology employed when describing CSC theory can be confusing and problematic. ‘Tumour initiating cells,’ ‘tumour propagating cells,’ ‘cancer stem

Introduction

cells' and 'cancer stem-like cells' are examples of terms used in the literature to describe a subpopulation of cancer cells which have increased tumourigenicity and self renewal capability. Although self renewal links both cancerous and normal stem cells, it is important to stress the differences between normal stem cells and CSCs. In CSCs the process of self renewal is deregulated, in comparison to the normal stem cell population where cell division and self renewal are highly organised and tightly regulated processes. It is also important to appreciate that the use of the term 'CSC' does not imply that a normal stem cell is the cell of origin of a particular tumour (however recent studies have confirmed that normal stem cells can be transformed into malignant stem cells (Barker et al., 2009, Lapouge et al., 2011, White et al., 2011)). A recent study by Liu et al suggests that although neural stem cells are the targets of DNA mutations, only oligodendrocyte progenitor cells derived from these mutation bearing neural stem cells exhibit aberrant growth and proliferation. Neural stem cells are therefore the 'cell of mutation' however the 'cell of origin' for glioblastoma is the progeny of the mutated neural stem cell (Liu et al., 2011). Due to these obvious differences between normal and CSCs some authors would judge the term 'cancer stem-like cell' inaccurate or inappropriate. Nevertheless the term 'cancer stem-like cell' does convey the shared properties of these distinct entities and offers a pragmatic solution to the difficulties in terminology experienced when describing this subpopulation of cancer cells.

1.2.2 Tumour heterogeneity and CSC theory

The work of The Cancer Genome Atlas (TCGA) (Verhaak et al., 2010) has described a robust gene expression classification of GBM tumours into 4 main subtypes of proneural, classical, mesenchymal and neural which have clinical utility. The classical subtype is characterised by frequent mutations or amplifications in the gene encoding for EGFR. Mesenchymal subtypes demonstrate frequent mutations in the neurofibromatosis type 1 (NF1) gene and the proneural subtype is characterised by mutations in the p53 gene and platelet-derived growth factor receptor A (PDGFR-A) gene. These classifications appear to have additional clinical significance, with therapy giving greatest benefit in classical type tumours. An analysis of single cell RNA sequencing of

Introduction

430 individual cells from 5 different primary glioblastomas by Patel et al (Patel et al., 2014) however described significant intratumoural heterogeneity in GBM, with the clinical subtype GBM classifiers being expressed variably across tumour cells within different tumours. Furthermore within individual tumours there was evidence of previously unappreciated heterogeneity in expression of diverse transcriptional programmes related to oncogenic signalling, proliferation and immune response. Patel et al also examined CSC populations in the GBM tumours sampled in their study. A ‘stemness signature’ was derived by comparison of *in vitro* CSC cultures and tumour bulk cultures derived from the patient samples examined. Application of the stemness signature to single cell transcriptome profiles revealed the existence of ‘stemness gradients’ within each of the five tumours examined. The authors concluded that *in vitro* models represented phenotypic extremes however *in vivo* there are various degrees of phenotypic stemness exhibited by individual tumour cells. Expression of the stemness signature was most closely correlated with the proneural and classical subtypes, however was underrepresented in cells of the mesenchymal subtype. Survival in patients with proneural tumours was found to correlate inversely with heterogeneity of expression of other tumour subtypes. These studies illustrate the degree of heterogeneity between and within GBM tumours, and highlight the limitations of current *in vitro* models.

1.2.3 Evidence for CSCs

Although the debate surrounding CSC theory has emerged recently, the idea of a hierarchy of structure existing in tumours is not new. In the mid nineteenth century it was proposed that cancer originated from the remnants of embryonic tissues, and heterogeneity in tumour cell populations was noted by the early pathologists in their explorations with light microscopy. In the 1960s a series of experiments in which tumour cells were harvested from patients and then transplanted subcutaneously in autologous manner demonstrated heterogeneity in the ability of tumour cells to recapitulate the patient’s original tumour. Only injections of more than 1×10^6 cells resulted in tumour formation, implying a subset of cells was responsible for tumourigenicity (Brunschwig et al., 1965).

Introduction

The evidence for the existence of a CSC population was initially explored in haematopoietic malignancies, with the demonstration of a rare, slow cycling leukaemic cell population which was responsible for the generation of a proliferative fraction (BD Clarkson, 1974). The development of fluorescence activated cell sorting (FACS) allowed the isolation of specific populations of leukaemic cells facilitating further development of the CSC hypothesis. Studies in acute myeloid leukaemia (AML) in the 1990s demonstrated a population of CD24+CD38- cells from human leukaemia patients (Lapidot et al., 1994), which had the ability to engraft immunocompromised mice in comparison to the majority of AML cells which could not. This led to the proposition of a hierarchical organisation of AML, with a leukaemia initiating CSC population at the apex of this hierarchy. Since then putative CSC populations have been reported in a variety of solid tumours including breast, prostate, pancreas (Hermann et al., 2007), head and neck (Prince et al., 2007), colon (O'Brien et al., 2007) and sarcoma (Wu et al., 2007). However, GBM was the first solid tumour site in which a CSC population was recognised. The existence of CSCs in GBM was first proposed by Ignatova et al who isolated clonogenic neurosphere forming precursors from post-surgical GBM specimens (Ignatova et al., 2002). Singh et al provided further evidence for the existence of GBM CSCs by demonstrating that intracranial tumours could be induced at very high frequency *in vivo* in immunocompromised mice by injection of as few as 100 cells which had been sorted on the basis of the putative stem cell marker CD133 (Singh et al., 2004). These tumours phenotypically resembled the patient specimen and could be serially transplanted. In comparison injection of up to 10^5 CD133 negative cells were unable to induce tumour formation in immunocompromised mice. Hemmati et al undertook a study of paediatric brain tumours and demonstrated the presence of neurosphere forming cells which were multipotent and able to form tumour xenografts. These cells also showed expression of neural stem cell markers (Hemmati et al., 2003).

Three recent investigations have provided important support for the concept of CSCs in different tumour sites. Chen et al utilised a nestin promoter driven transgene coding for GFP and the herpes simplex virus tyrosine kinase (HSV TK) which was expressed specifically in quiescent subventricular zone adult neural

Introduction

stem cells in a genetically engineered mouse model of glioma (Chen et al., 2012). This transgene construct was also found to be expressed in a subset of endogenous glioma tumour cells. On arrest of tumour proliferation in response to treatment with temozolomide, recurrent tumour growth was found to be driven by the GFP labelled CSCs. Furthermore treatment with ganciclovir (which due to HSV TK is toxic to cells expressing the transgene construct) and temozolomide resulted in inhibition of tumour development. This important study demonstrated the reliance of tumour recurrence and regrowth on the CSC population. Driessens et al utilised clonal analysis of squamous skin tumours using genetic lineage tracing to examine the mode of *in vivo* tumour growth (Driessens et al., 2012). This study utilised a transgenic animal model which allows fluorescent YFP labelling of basal papilloma cells via a tamoxifen regulated mutant of *cre* recombinase and the human keratin K14 promoter element which is specifically active in basal layer skin cells. Dosing of mice with tamoxifen was found to label around 1 in 100 basal cells with YFP mediated fluorescence, allowing the fates of individual cells to be followed at various timepoints following tamoxifen induction exposure. Tracking of fluorescently labelled cells demonstrated clonal expansion in the days following induction, however many of these clonal populations disappeared at later timepoints, implying that a high proportion of the originally labelled cellular population did not possess unlimited proliferative capacity. However a fraction of tumour cells had extensive proliferative capacity with CSC characteristics and these clonally derived populations could contribute massively to the tumour cellular population. Schepers et al used lineage retracing in intestinal adenomas to demonstrate that a subset of stem-like cells were responsible for driving growth of adenomas (Schepers et al., 2012). These three papers provide clear support for the hypothesis of hierarchical organisation of cancers and the existence of CSCs.

1.2.4 Experimental models of CSCs

CSCs can be characterised experimentally by examining the key stem properties of self renewal and maintained proliferative potential. This can be achieved via *in vivo* limiting dilution transplantation assay (LDA), which is an experimental

Introduction

technique for quantifying the proportion of biologically active particles in a larger population. Low numbers of CSCs can be shown to recapitulate the tumour of origin when transplanted into immunocompromised mouse models, whilst tumour bulk cells are unable to form tumours even if much higher numbers of tumour bulk cells are transplanted. This represents the gold standard CSC assay. In order to validate CSC enriched populations of cells, LDA must be performed with both putative CSC and tumour bulk populations. Cell viability must be carefully assessed and non-malignant stromal cells excluded from transplantation. A wide range of cell dilutions should be used within the LDA study and a moderate to large number of replicates per dose should be performed in order to achieve a robust statistical analysis. The LDA should also contain concentrations of cells which give both positive and negative results. The CSC theory suggests that a single cell is responsible for tumour initiation (the ‘single hit hypothesis’) and if this holds true then there should be no evidence of co-operating effects between tumour cells. If the single hit hypothesis is not true, then tumour generation will increase greater than expected as cell concentration increases. The statistical methods used in LDA are summarised by Hu et al (Hu and Smyth, 2009). LDA studies are typically time and resource consuming, and consequently robust LDA data is only available in relatively few solid tumour types.

There are various other laboratory assays which seek to define CSC populations, however these are surrogate assays and must be interpreted with care. The neurosphere assay was developed by Reynolds and Weiss who cultured mouse striatal cells in serum free medium in the presence of epidermal growth factor (EGF), which resulted in the death of the majority of cultured cells (Reynolds and Weiss, 1992). However a small proportion of cells survived and continued to undergo cell division, forming spherical structures termed ‘neurospheres’. Early neurospheres were found to be positive for the intermediate neurofilament protein nestin, which is highly expressed in neuroepithelial stem cells. These neurospheres could then be disaggregated and plated out again in serum free medium to form secondary neurospheres. Neurospheres upon removal of mitogens (EGF and fibroblast growth factor, (FGF)) could then be shown to differentiate into the 3 major lineages present in the mammalian central

Introduction

nervous system (CNS), namely astrocytes, neurons and oligodendrocytes. It is important to point out that only a fraction of the cells within a neurosphere represent CSCs, with the majority of the neurosphere being made up of CSC progeny (Ignatova et al., 2002).

Neural stem cell markers have been widely used to identify CSCs. Many putative GBM stem-like cell markers are important antigens associated with neurogenic processes during development and adulthood. Whilst cell sorting of CSC populations based on cell surface markers has greatly facilitated study of CSCs, the limitations of CSC markers must be appreciated. A significant problem in the use of CSC markers to identify GBM CSCs is that a single universal marker for GBM CSCs has not yet been identified. The most commonly used CSC marker in GBM is CD133 (or PROM1). The exact function of CD133 is unknown. CD133+ cells have been shown to initiate tumour formation in immunocompromised mice more efficiently than CD133- cells and CD133 knockdown via shRNA impairs self renewal in GBM CSC populations (Singh et al., 2004). Nevertheless other authors have shown the ability of CD133- cells to initiate tumour formation, whilst some tumours have been found not to have a CD133+ population at all (Beier et al., 2007, Wan et al., 2010). The detection of CD133 relies upon the use of antibodies which recognise 2 different glycosylated epitopes of CD133; AC133 and AC141. These epitopes can be expressed discordantly, and furthermore both can be absent, even in the presence of CD133 protein (Bidlingmaier et al., 2008). The complex issues surrounding detection of CD133 epitopes may underlie some of the diverse outcomes documented in the literature associated with using CD133 as a CSC marker. Whilst CD133 is clearly associated with GBM CSCs in many tumours, it cannot be regarded as a universal CSC marker in GBM. Another cell surface marker commonly used to identify GBM CSCs is nestin. Nestin is an intermediate filament protein which is necessary for self renewal and survival of neural stem cells (Park et al., 2010). Nestin is expressed in subventricular zone cells and a subpopulation of GBM cells and may correlate with dedifferentiated status, enhanced motility, invasive potential and tumour initiating ability (Sanai et al., 2005, Berger et al., 2004). Many other GBM CSC markers have been described including L1CAM (Bao et al., 2008), Sox2 (de la Rocha et al., 2014), CD15 (Mao et al., 2009) and Oct4 (Ikushima et al., 2011).

Introduction

Laterra et al have recently shown that the Oct4 and Sox2 transcription factors induce human glioma cells to transition to a stem-like tumour propagating state (Laterra J, 2014). Furthermore a paper by Suva et al recently established the epigenetic basis of a developmental hierarchy in GBM having identified the existence of a core set of neurodevelopmental transcription factors (POU3F2, Sox2, Sall2, Olig2) essential for GBM propagation (Suva et al., 2014).

It is difficult to estimate the number of GBM CSC lines which are in existence worldwide. There are 7 commercially available glioblastoma cell lines listed by the American Type Culture Collection (ATCC), however the relevance of serially passaged commercial cell lines to contemporary models of glioblastoma has been questioned in view of the importance of tumour heterogeneity. Most studies of the CSC model of glioblastoma rely upon the establishment of primary cell cultures from patient samples, and therefore it is impossible to quantify the number of GBM CSC cultures in existence currently. The establishment of primary cell cultures from patient samples relies upon the selection of tumour cells which can adapt to *in vitro* growth conditions, which again raises questions of whether *in vitro* CSC models are truly representative of tumour *in vivo*. Nevertheless *in vitro* CSC models have been shown to recapitulate patients' tumour more accurately on transplantation into *in vivo* murine orthotopic GBM models (Mannino et al., 2014, Singh et al., 2004), and study of cell lines of limited passage avoids the selection processes which are sometimes observed in extensively passaged cell lines. Most studies of the GBM CSC model utilise around 3 to 6 different primary cell lines in order to ensure a representative study of GBM CSC behaviour.

GBM CSC cultures are generally propagated in non-hypoxic conditions. McCord et al clearly state that their cultures were generated and maintained under conditions of normoxia (McCord et al., 2009), whilst other authors fail to describe precise culture conditions (Bao et al., 2006a, Singh et al., 2004). Gritti et al, who detail a protocol for the establishment of neural stem cell cultures from mouse brain (which has been subsequently used in the establishment of GBM CSC cultures by other authors in this field) suggest 95% oxygen is used at some stages in the propagation of stem cell cultures (Gritti et al., 1996).

Introduction

1.2.5 Clinical relevance of CSCs

The CSC hypothesis proposes that only a subset of tumour cells (CSCs) is responsible for maintaining tumour growth and that CSCs are vital for the viability of tumours. This raises an important issue regarding the effectiveness of current oncological therapy against CSCs: if CSC theory is correct, tumour cure can only be possible if all CSCs are eradicated. Occasionally in clinical practice complete responses to therapy (based on imaging studies) are seen, only for the patient to relapse months later with recurrent disease. This observation could be explained by CSC theory. Oncological therapy may be successful in destroying the majority of bulk tumour cells, but ineffective in treating the relatively small population of CSCs, which results in clearance of macroscopic tumour but later tumour recurrence due to CSC proliferation. This concept is illustrated in figure 1.1. This pattern of recurrence is familiar in GBM, with most tumours being locally recurrent within the initial high dose radiotherapy treatment volume of brain (Hochberg and Pruitt, 1980), and evidence is accumulating for the treatment resistant nature of GBM CSCs. It must be remembered however that often macroscopic disease is present following surgical resection and radiotherapy in GBM, nevertheless the contribution of remaining CSC populations is still likely to be significant as a driver of tumour repopulation and clinical recurrence. Chen et al demonstrated a CSC population to be responsible for driving tumour recurrence following temozolomide therapy (Chen et al., 2012). Bao et al demonstrated radioresistance in CD133+ populations, via upregulation of cell cycle checkpoint and DNA repair pathways, a mechanism which may attenuate responses to other DNA damaging cytotoxic agents (Bao et al., 2006a). The CSC state in other solid tumour types is associated with the expression of high levels of drug efflux transporter pumps conferring the ability to expel cytotoxic agents and enhance cell survival (Beier et al., 2011). Studies report a lack of consensus regarding the effects of temozolomide on GBM CSCs, with some CSC populations being temozolomide sensitive and others resistant.

Introduction

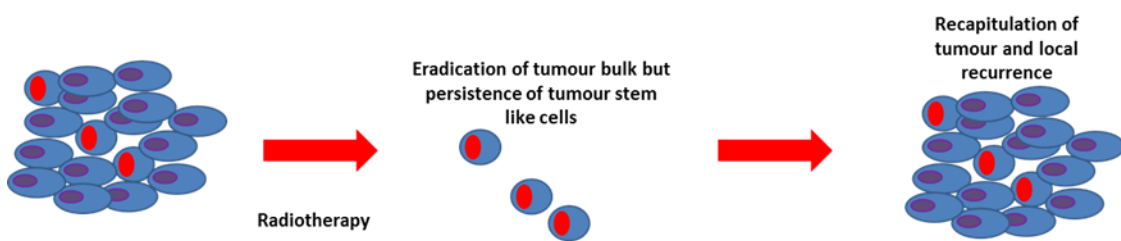


Figure 1.1 Proposed clinical significance of CSC theory

Radiotherapy preferentially eliminates tumour bulk cells, however radioresistant CSCs survive. CSCs repopulate the original tumour leading to clinical recurrence of the tumour many weeks or months following treatment

The clinical relevance of GBM CSCs has also been investigated by reports of the prognostic significance of GBM CSC markers in patient samples. Most of these studies are of a retrospective nature and take the form of correlations between clinical data and quantitative or semi quantitative measurement of CSC marker expression (CD133 and Nestin) by immunohistochemistry, (IHC). The majority of these studies support a correlation between poor prognosis and CSC marker expression. Nevertheless studies differ in regards to how CD133 expression was analysed, with some authors regarding pattern of staining being important as well as quantification of CD133 expression. These studies are summarised in table 1.1.

Introduction

Study	Study population	CSC markers	Outcome
Dahlrot, RH; 2014	239 gliomas	CD133, Nestin	No correlation with CD133 and grade/OS Correlation with nestin and grade Increased nestin in grade II glioma correlated with reduced PFS
Shin, JH; 2013	67 GBMs	CD133	Diffuse CD133 staining associated with poor OS
Shibahara, I; 2013	112 GBMs	CD133	High CD133 expression correlated with reduced time to recurrence
Melquizo, C; 2012	78 GBMs	CD133	CD133 expression not correlated to prognosis
He, J; 2011	59 gliomas	CD133	CD133 expression associated with reduced PFS
Ardebili, S; 2011	26 gliomas	CD133	High CD133 expression associated with reduced OS
Metellus, P; 2011	48 GBMs	CD133	High CD133 expression associated with reduced PFS and OS
Kim, KJ; 2011	88 GBMs	CD133/CD15	CSC marker expression not associated with OS
Paldini, R; 2008	44 GBMs	CD133	High CD133 expression associated with reduced PFS and OS
Chinnaiyan, P; 2008	156 GBMs	Nestin	No prognostic value of nestin expression
Zeppernick, F; 2008	95 gliomas	CD133	Proportion and organisation of CD133+ cells in clusters predicted reduced PFS and OS

Table 1.1 Studies of CSC marker expression and clinical outcome in GBM

Evidence to support the role of GBM CSCs in determining treatment resistance is also provided by studies of patient tumour samples. Tamura et al analysed CD133 expression by IHC in recurrent GBM following treatment with radiotherapy and chemotherapy and compared them to index specimens obtained at first resection. The percentage of CD133 positive cells was found to be significantly higher in recurrent tumours, but only in de novo GBM (Tamura et al., 2013), consistent with the hypothesis that GBM CSCs are capable of surviving radiotherapy. In a separate study of 32 patients undergoing surgery, gamma knife and external beam radiotherapy, Tamura et al demonstrated accumulation of CD133+cells in specimens of recurrent disease, compared to infrequent

Introduction

CD133+ cells in the original resection specimens obtained prior to adjuvant radiotherapy treatment (Tamura et al., 2010). These results support the hypothesis that GBM CSCs are radioresistant, can survive high doses of radiation in vivo and may play a role in initiating tumour recurrence, however may also be consistent with plasticity in the tumour bulk population.

1.2.6 Quiescence of CSCs

It is often suggested that the CSC population is quiescent. However, the evidence for solid tumour CSCs being relatively quiescent in comparison to other tumour cell populations is not entirely clear. Often CSCs are assumed to be slow cycling or quiescent, reflecting their normal tissue stem cell counterparts. However this is likely to be an oversimplification and recent evidence has demonstrated the existence of both actively cycling and quiescent stem cell populations in the normal tissues of mammals (Li and Clevers, 2010), which has implications for assumed CSC quiescence. AML CSCs have been shown to be quiescent, (Ishikawa et al., 2007, Clarkson, 1974) however it is not clear whether this also applies to solid tumour CSCs. Chen et al utilised a Nestin promoter driven GFP transgene in order to study GBM tumour initiating GBM cells (Chen et al., 2012) (described in section 1.2.2). They demonstrated that the subset of GFP expressing tumour cells rarely co-stained for the proliferative marker Ki67, whilst GFP negative tumour cells often co-stained with Ki67. This study may suggest that GBM CSCs are quiescent. Alternatively, the study by Driessens et al (Driessens et al., 2012) (also described in section 1.2.2) demonstrated via mathematical modelling and nucleotide labelling pulse chase experiments that stem tumour cell populations divide and proliferate rapidly. The situation is clearly complex and further investigation of CSC quiescence is warranted.

1.2.7 Maintaining stemness; the influence of tumour microenvironment

Tumours are complex ecosystems comprising tumour cells and a variety of associated non-tumour elements, which together can be termed the ‘tumour

Introduction

microenvironment (TME). In depth review of microenvironmental influences on CSC function is beyond the scope of this chapter, however a short discussion follows, and comprehensive review articles are available (Mannino and Chalmers, 2011).

Evidence suggests that CSCs reside in a specialised microenvironment, in close proximity to endothelial cells in a perivascular niche (Calabrese et al., 2007). The perivascular niche may have a vital role in supporting CSCs and enhancing and maintaining the stem-like phenotype of CSCs and also in promoting radioresistance. The perivascular niche contains many cell types such as pericytes, astrocytes, macrophages, ependymal cells and extracellular matrix (ECM). GBM CSCs are likely to have complex interactions with all of these elements of their surrounding microenvironment. Residence within a perivascular niche appears to sustain the undifferentiated state of nestin and CD133 + cells and supports their proliferation (Calabrese et al., 2007). Studies of proximity of nestin and CD133 expressing tumour cells show them to be residing consistently closer to endothelial cells than nestin or CD133 negative tumour cells, (Calabrese et al., 2007, Christensen et al., 2008, Zeppernick et al., 2008). Two recent studies demonstrated the ability of CD133+ cells to differentiate along the endothelial lineage, allowing a subset of tumour endothelium to be derived directly from tumour cells (Wang et al., 2010, Ricci-Vitiani et al., 2010). The interactions between CSCs and endothelial cells are clearly reciprocal. GBM CSCs have been shown to exert a pro-angiogenic effect via VEGF production (Bao et al., 2006b, Folkins et al., 2009, Salmaggi et al., 2006). Endothelial cells also appear to provide vital support for CSC maintenance. Hovinga et al demonstrated that removal of endothelial cells from a three dimensional GBM CSC culture system resulted in a >50% reduction in neurosphere production from CSC cells (Hovinga et al., 2010). Experiments using co-culture systems have also noted a survival advantage for endothelial cells cultured in the presence of glioma cells following exposure to radiation (Brown et al., 2004, Hovinga et al., 2010). Paracrine signalling by CD133+ cells also appears to increase the apoptotic threshold of endothelial cells, aiding the preservation of the perivascular niche. Infanger et al recently used a 3D *in vitro* scaffold culture system to demonstrate the role of paracrine interleukin 8 signalling in enhancing

Introduction

CSC maintenance and growth *in vitro* and tumour formation *in vivo* (Infanger et al., 2013). The tumour microvasculature also appears to be radioresistant in GBM. Borovski et al demonstrated that tumour microvascular endothelial cells (tMVECs) are highly radioresistant, and become senescent following radiation (Borovski et al., 2013). Senescent tMVECs were detectable in human tumour samples following irradiation. Senescent tMVECS remained viable and were capable of supporting CSC growth with the same efficacy as non senescent tMVECs.

Components of the ECM also appear to have an important influence on CSC function. The perivascular niche contains many components which are unique to its anatomical situation. The vascular basement membrane contains collagen, fibronectin, laminin, heparan sulphate, entactin and vitronectin, whilst tumour ECM surrounding blood vessels contains tenascin C, secreted protein acidic and rich in cysteine (SPARC) and thrombospondin. Most of these components are not found elsewhere in the tumour ECM. Heparan sulphate has the ability to bind basic fibroblast growth factor (bFGF) (Folkman et al., 1988). bFGF has the ability to promote growth of CSCs and inhibit radiation induced apoptosis in GBM CSCs *in vitro* (Bao et al., 2006b). Tenascin C may also have a radioprotective role in the GBM CSC perivascular niche (Mannino and Chalmers, 2011, Midwood and Orend, 2009, Riekki et al., 2001).

1.2.8 Underlying mechanistics of CSC phenotype

Whilst the CSC phenotype has in general been well characterised, the mechanisms underlying expression of the CSC phenotype are only beginning to be elucidated. The importance of epigenetic regulation in cancer initiation and progression is now established and it is hypothesised that epigenetic programs may be partly responsible for intratumoural heterogeneity and may distinguish CSCs from tumour bulk cells. This has been explored in a recent paper by Rheinbay et al (Rheinbay et al., 2013) which presented a comparative analysis of GBM CSC chromatin state which revealed widespread activation of genes in CSCs, the transcription of which would normally be repressed through modulation of chromatin structure by polycomb repressor proteins in comparison to normal

Introduction

human astrocytes and differentiated GBM tumour cells. A large set of developmental transcription factors was found to be activated in GBM CSCs by this process. The most important of these transcription factors was ASCL1, which activates Wnt signalling. Wnt signalling has been shown to be important in maintaining an undifferentiated state in malignant cells, (Zheng et al., 2010). It was speculated that diminished epigenetic silencing and promiscuous transcription factor activation may provide CSCs with a selective advantage in being able to adapt to the requirements of the malignant state.

1.2.9 Controversies surrounding the CSC hypothesis

The existence of CSCs and the main tenets of the CSC hypothesis have been questioned. Quintana et al found frequencies of tumour initiating cells in melanoma (defined as single tumour cells with the ability to recapitulate tumours in immunocompromised mice) to be as high as 25%, and furthermore the frequency of tumour initiating cells within the tumour appeared to change depending on the degree of immunocompromise of the host mouse (Quintana et al., 2010). This supported arguments that the CSC hypothesis was merely a reflection of experimental artefact, and that rather than being a property of a specific tumour population subset, tumourigenicity was inherent to most malignant cells. However the definition of a CSC does not rely upon CSC frequency within a tumour. There is evidence of variation between cancers in terms of the frequency of CSCs and it is possible that in some tumours CSCs make up the majority of the cancer cell population. These tumours will display a very shallow hierarchy in terms of cell function, and indeed could be viewed as being homogenous. The CSC hypothesis may not apply to every cancer type.

Further debate surrounds the concept of stochastic clonal evolution of cancer proposed by Nowell in 1976 and the apparent static phenotype of CSCs (Nowell, 1976). This model suggests that essentially every cancerous cell within a tumour population has a similar malignant proliferative potential, and that intrinsic (e.g. genetic instability) and extrinsic (e.g. hypoxia, immune surveillance) factors determine evolutionary pressures within a tumour and select for more aggressive and better adapted subclones within the tumour cell population. It has been

Introduction

argued that an infrequently occurring cell population within a tumour would be unable to acquire the necessary genetic variation to drive the clonal evolution of ever more aggressive and treatment resistant populations which become more prominent as a cancer progresses. However, the CSC hypothesis and the stochastic clonal evolution models of cancer are not mutually exclusive and can be reconciled. The targets for clonal selection within tumours must exhibit self renewal, since otherwise clonal exhaustion would occur and these populations would quickly die out. Therefore it seems very likely that genetic diversity within CSC populations is the driver of clonal diversity within tumours. Consistent with this, several authors have shown the existence of genetically diverse subclones of leukaemia initiating cells from a single parental tumour (Clappier et al., 2011, Notta et al., 2011, Anderson et al., 2011). Furthermore functionally distinct subclones were related to each other by branching evolution (Notta et al., 2011). Evidence for heterogeneity within GBM CSC populations is presented in the paper by Patel et al, where single cell RNA sequencing revealed the existence of a ‘stemness gradient’ within the tumour CSC subpopulation (Patel et al., 2014).

It is likely that the organisation of solid tumours lies somewhere between the purist hierarchical stem cell model and the stochastic homogeneity suggested by Nowell. There is likely to be some plasticity in the cancer stem cell state, (i.e. some differentiated tumour cells are likely able to dedifferentiate into more stem like cancer cells) however not to the degree where the cancer stem cell model is trivialised. There is now clear evidence for a hierarchical organisation of solid tumours, although this likely varies between and within different tumour sites, with some tumours displaying a very clear or ‘vertical’ hierarchy, and other cancers having a less defined or ‘shallow’ depth of hierarchy.

1.2.10 GBM CSCs and radiotherapy resistance

The idea of CSCs being the underlying cause of radioresistance in GBM is appealing, however evidence presented for the radioresistance of GBM CSCs has not been conclusive.

Introduction

Bao et al published a seminal paper in which the authors described the radioresistance of a CD133+ population of GBM tumour cells (Bao et al., 2006a). The authors demonstrated enrichment of CD133+ populations 48 hours after irradiation in short term cultures from human glioma xenografts and this could also be described after irradiation of *in vivo* glioma xenografts. Irradiated tumour cultures were enriched for CD133+ cells and displayed reduced latency of tumour formation when transplanted in immunocompromised mice, supporting the theory that CD133+ cells were responsible for tumour recurrence after irradiation. Images of colony formation assays were displayed as evidence of increased survival after 5Gy in CD133+ cells in comparison to CD133- cells; however formal clonogenic survival assays accounting for plating efficiency were not performed in this paper. A lower rate of apoptosis in CD133+ cells was proposed to be the main mechanism of preferential survival as shown by decreased activation of caspase 3 and annexin V staining. The main focus of this study centred upon the investigation of altered DNA damage response (DDR) in GBM CSCs. DDR is a term which describes the multitude of cell cycle checkpoint activation and DNA repair pathways instigated by a cell following DNA damage, and will be discussed in more detail later in this chapter. Examination of DDR to radiation in this study showed CD133+ cells have upregulated DDR at baseline and in response to radiation. This took the form of increased levels of phosphorylated DDR proteins such as phosphorylation of ataxia telangiectasia mutated (ATM) at serine 1981 (pATM s1981), phosphorylation of radiation sensitive17 (RAD17) at serine 645 (pRADs645), phosphorylation of checkpoint kinase 1 (Chk1) at serine 345 (pChk1 s345) and phosphorylation of checkpoint kinase 2 (Chk2) at serine 19 (pChk2 s19). These data were described as evidence of enhanced checkpoint response in GBM CSCs, although a detailed analysis of G1/S and G2/M checkpoint kinetics was not undertaken. The alkaline comet assay was employed as an assay of DNA repair. CD133+ cells were found to repair DNA damage more efficiently at 18 and 30 hours post 3Gy compared to CD133- cells. However the alkaline comet assay is mainly a measure of DNA single strand breaks (SSB), which are generally believed to be of less consequence than DNA DSBs to the fate of the irradiated cell. Gamma H2AX foci resolution as a measure of DNA DSBs was also found to be enhanced at 24 hours following 3Gy in CD133+ populations, however this was not performed in a cell cycle phase specific manner. Addition of a Chk1/2 inhibitor debromohymenialdisine appeared to

Introduction

reverse CD133+ radioresistance, however this agent is known to have many off target interactions. The authors concluded that CD133+ GBM cells contribute to glioma radioresistance and tumour repopulation through preferential checkpoint response and enhanced DNA repair.

Further work by the Bao group examined the influence of the L1 cell adhesion molecule (L1CAM) on the previously documented upregulated DDR of GBM CSCs (Bao et al., 2008). L1CAM was previously identified as a putative GBM CSC marker, and in this study was demonstrated to have an influence on altered DDR. L1CAM knockdown attenuated DNA damage checkpoint activation and enhanced DNA repair. L1CAM regulates expression of Nijmegen breakage syndrome 1 protein (NBS1), an important component of the MRN complex (Meiotic recombination 11 homolog (MRE11), Radiation sensitive 50 (Rad50) and NBS1), which is involved in DSB detection and signalling via ATM. Ectopic expression of NBS1 rescued the decreased checkpoint activation and radiosensitivity caused by L1CAM knockdown.

Comparison of the DDR of GBM CSCs to the DDR of neural progenitor cells (NPCs) was carried out by Lim et al (Lim et al., 2012). This study demonstrated increased survival of GBM CSCs relative to the NPCs by cell viability assay following irradiation which appeared to be related to an upregulation of the homologous recombination DNA DSB repair pathway in the GBM CSC populations. Non homologous recombination (NHEJ), another important DSB repair pathway, was not increased in the GBM CSC populations, as measured by a plasmid assay of NHEJ. Quantification of Rad51 foci confirmed the finding of more efficient HR in GBM CSCs in comparison to NPCs. In addition, GBM CSCs were found to exhibit radioresistant DNA synthesis and a defective G1/S and intra S checkpoint. Levels of phosphorylated ATM were lower in GBM CSCs compared to NPCs and the authors speculated that deficient checkpoints facilitated S phase entry and preferential use of HR in S phase and G2. Nevertheless, deficiencies in G1/S checkpoints are common in many tumours due to loss of p53, and are not a unique feature of GBM CSCs, therefore the proposed mechanism does not explain radioresistance of GBM CSCs in comparison to tumour bulk cells. The finding of lower ATM activity appears at first to be at odds with the findings of other

Introduction

investigators who have documented preferential activation of the DDR in GBM CSCs compared to differentiated tumour cells. However the activity of DDR elements in GBM CSCs may still be lower than NPCs, as no comparisons were made in this study between GBM CSCs and tumour bulk cells.

Short et al investigated the effects of targeting homologous recombination repair in newly established glioblastoma cell lines (Short et al., 2011). This study demonstrated that GBM specimens in comparison to normal human astrocytes exhibited upregulation of Radiation sensitive 51 protein (Rad51) and other DNA repair proteins. Rad51 levels were found to be inversely proportional to radiosensitivity and downregulation of Rad51 induced sensitivity to temozolomide treatment. Newly established cell lines which demonstrated expression of the CD133+ marker were extremely sensitive to Rad51 knockdown, suggesting a vital role of HR repair in GBM.

The role of the brain microenvironment in governing radiation responses of CD133+ cells was investigated by Jamal et al (Jamal et al., 2010). This study utilised CD133+ cells from a primary GBM cell line and analysed DDR following radiation exposure *in vitro* and *in vivo* as orthotopic xenografts. This study initially compared the *in vitro* gamma H2AX and 53BP1 response to irradiation in CD133+ cells in neurobasal media versus CD133+ cells in differentiating media. This showed that CD133+ cells in neurobasal media exhibited higher levels of gamma H2AX foci following radiation at timepoints ranging from 0.5 hours to 24 hours in comparison to CD133+ cells grown in differentiating conditions, which may suggest that GBM CSCs are radiosensitive in comparison to differentiated GBM cells at least *in vitro*. However the cell cycle phase of CD133+ cells in neurobasal conditions was not taken into account in the analysis and the authors stated that a higher proportion of CD133+ cells in differentiating media were in phase G0/1, which may account for observed differences in gamma H2AX foci quantification between the CD133+ neurobasal and CD133+ differentiated culture populations, since the quantity of cellular DNA influences gamma H2AX foci numbers. Analysis of orthotopic tumour sections demonstrated faster resolution of gamma H2AX foci following *in vivo* irradiation in comparison to *in vitro* studies. Whilst demonstrating the importance of tumour microenvironment

Introduction

for DDR to DSBs, it is unclear from this study whether this pertains specifically to GBM CSCs, or whether this is generally the case for both CD133+ cells grown in neurobasal and differentiating media.

McCord et al described the radiosensitivity of CD133+ GBM cells in comparison to established glioma cell lines (McCord et al., 2009). The authors argued that investigating survival mechanisms of CD133+ cells which were more treatment sensitive than established laboratory GBM cultures would not advance understanding of GBM therapy resistance. CD133+ cells were shown to be significantly more radiosensitive than established cell lines by clonogenic survival assay. Direct comparison of radiosensitivity of CD133+ and CD133- GBM cells was examined in 2 primary GBM cultures by clonogenic survival assay. In one cell line CD133+ cells were indeed radioresistant, however in the other primary cell line there was no difference in radiosensitivity between CD133+ and CD133- cells. The authors concluded that CD133+ CSC radioresistance is tumour dependent. No evidence for decreased levels of apoptosis following irradiation (as evidenced by lack of a subG1 population on FACS analysis of cell cycle) was found in the CD133+ populations, in contrast to the findings of Bao's study. DNA repair was characterised by neutral comet and RAD51/gamma H2AX foci analysis. All three of these assays demonstrated defective DNA repair in GBM CD133+ cells compared to established glioma cell lines, with the authors concluding that a defect in homologous recombination repair may be responsible. There did not appear to be preferential activation of the G2/M checkpoint in CD133+ cells following irradiation by quantification of mitotic cells. CD133+ cells were shown to have a defective S phase checkpoint however. The comparison of CD133+ cells with established cell lines ignores differences in intrinsic radiosensitivity between different cell lines. Nevertheless the pragmatic question of whether the concept of CSCs actually has relevance to established *in vitro* models of GBM radiation resistance is valid.

A further study of GBM CSC DDR was described by Ropolo et al (Ropolo et al., 2009). The authors of this study identified GBM cell lines which expressed varying levels of the stem-like cell markers CD133 and nestin. The DDR following radiation in GBM cell lines expressing higher levels of CD133 and nestin was

Introduction

compared to GBM cell lines which showed low or no expression of these markers. This approach ignores important differences in intrinsic radiosensitivity between unrelated cell lines. Radiation sensitivity was not in itself quantified and clonogenic survival assays were not performed in this study. The population doubling time of the CD133/nestin expressing cell lines was significantly elevated compared to the other cell lines examined. One primary GBM cell line in this study was cell sorted according to CD133 positivity and DDR following irradiation was evaluated and compared between CD133+ and CD133- cell populations. Upregulation of the cell cycle checkpoint kinases pChk1 and pChk2 in CD133+ cells was confirmed. However there appeared to be no evidence of increased DNA repair in the CD133+ population when assessed by alkaline comet assay or by gamma H2AX foci in comparison to CD133- populations. The authors concluded that prolonged doubling time and elevated levels of cell checkpoint kinases were responsible for increased radiation resistance in GBM CSCs, however enhanced DNA repair was not a feature of these cells. Again the approach of comparing non-isogenic cell lines presents problems. Furthermore evidence of altered cell cycle time and DDR phosphoprotein expression does not necessarily equate to increased radioresistance.

Chang et al analysed radiation sensitivity by cell viability assay in CD133+ and CD133- populations of primary tumour specimens *in vitro* (Chang et al., 2009). This demonstrated enhanced survival of CD133+ populations following radiation. Furthermore, knockdown of silent mating type information regulation 2 homologue 1 (SiRT1) with shRNA induced radiosensitisation in the CD133+ population. SiRT1 is a NAD dependent histone deacetylase and deacetylates p53. It has roles in transcriptional regulation, inhibition of differentiation, regulation of the cell cycle and inhibition of apoptosis and tumourigenesis. Overexpression of SiRT1 has been associated with tumourigenesis and resistance to radiotherapy. There were a limited number of cell lines examined in this study and clonogenic survival assay was not performed.

Zhou et al investigated the radioresistance of two commercially available glioma cell lines (U87 and U251) following fluorescence activated cell sorting for CD133+ and CD133- populations (Zhou et al., 2013). They demonstrated

Introduction

radioresistance of CD133+ populations in comparison to CD133- populations by clonogenic assay, however no attempt at statistical analysis of survival curves or data points was made, and it is therefore impossible to comment on whether the differences seen are significant. Furthermore a DNA repair defect at 4 hours following 2Gy was demonstrated by neutral comet assay. Neutral comet assay is a relatively insensitive assay and usually requires high doses of radiation to produce measurable levels of DNA damage. Overall the findings of this investigation are difficult to interpret.

In the wider literature, investigations of CSC radioresistance have been made in other tumour sites. Desai et al investigated CSC radioresistance in lung cancer (Desai et al., 2014). They utilised cell sorting of CD133+ and CD133- populations in order to compare radioresistance by clonogenic assay in 2 commercially available lung cancer cell lines; A549 and H1299. CD133+ cells were found to be more radioresistant in the A549 cell line, but not in the H1229 cell line. This study relied on CD133+ status alone as a marker of CSC phenotype, and enhanced tumourigenicity and self renewal of CD133+ cell populations *in vivo* was not demonstrated. A549 CD133+ cells showed more efficient DNA repair of DSBs at 24 hours and upregulation of DDR components, whereas H1229 CD133+ cells did not. Interestingly, if H1229 cells were irradiated 2 weeks prior to sorting, CD133+ cells could then be shown to demonstrate radioresistance compared to H1229 CD133- cells. The author concluded that CD133+ cells were able to acquire radioresistance, whereas CD133- cells were not capable of this in the H1229 cell line. Furthermore the authors demonstrated upregulated expression of genes encoding DDR components in CD133+ cells compared to CD133- cells by realtime PCR. This is in contrast to Western blotting studies of CSC DDR components which in general show upregulation of phosphorylated components of DDR following radiation, rather than upregulation of baseline protein expression levels.

Dittfeld et al investigated CD133+ as a marker of radioresistance in 10 commercially available colorectal carcinoma cell lines (Dittfeld et al., 2010). The authors found that cell lines could be separated into those which had distinct CD133+ and CD133- populations, those which were universally CD133-

Introduction

and those which were universally CD133+. Clonogenic survival assays were performed in HCT 116 CD133+ and CD133- cell populations, with no difference being found in radiosensitivity. The authors concluded that CD133 expression could not be interpreted as a marker of CSC radioresistance in the cell lines examined.

Evidence for radioresistance of CSC from the current literature is therefore not conclusive. The initial report by Bao et al received much attention, and since then radioresistance has become an accepted feature of CSCs and has not been intensely scrutinised. Only a minority of studies have performed clonogenic survival assays with formal curve fitting and statistical rigour, and these studies have reported conflicting results regarding CSC radioresistance. Furthermore these data relate to a relatively small number of cell lines. Evidence of upregulated DDR proteins and phosphoproteins in CSCs is more compelling, however this does not equate to radioresistance, which can only conclusively be shown by the gold standard of clonogenic survival assay. A possible explanation for the discordant findings regarding CSC radioresistance may involve the reliance of studies on CD133 expression as a marker of CSC phenotype. Although CD133 expression appears to be a robust marker of stem-like phenotype in some tumours, it is evident from the studies discussed above that CD133 is not a universal marker for the CSC phenotype or for CSC radioresistance.

The underlying reason for the upregulated DDR and subsequent radioresistance proposed in CSCs is not well understood. There appears to be an almost global upregulation of DDR components in CSCs. In particular phosphorylation of DDR proteins appears to be increased in response to irradiation; however phosphorylation can also be upregulated under basal conditions. Upregulation of DDR is not limited to a particular DDR pathway; increased levels of pATM, phosphorylated ataxia telangiectasia and Rad 3 related protein (ATR), phosphorylated DNA dependent protein kinase catalytic subunit (DNAPKcs), Poly (ADP-ribose) polymerase (PARP), poly (ADP-ribose) (PAR), Rad17, pChk1 and pChk2 have all been documented and these elements play roles in diverse DDR pathways including NHEJ, HR, BER and response to replication stress. Given that a global upregulation of DDR pathways is evident in CSCs, and this appears to be

Introduction

a shared trait amongst CSCs, then it seems likely that the underlying stimulus or mechanism of enhanced CSC DDR is fundamental to the CSC state.

Venere et al proposed one such underlying fundamental CSC state to be an increased level of basal reactive oxygen species (ROS) within GBM CSCs (Venere et al., 2014). ROS are generated by cellular metabolism, or can be induced by exogenous insults, such as ionising radiation. ROS induce a variety of DNA damage, however mainly in the form of DNA base damage and SSBs. The authors of this paper showed upregulated basal ROS in CD133+ cells compared to CD133- cells isolated from freshly dissociated GBM tumour xenografts. CD133+ cells also displayed higher levels of oxidative DNA damage in keeping with the finding of elevated ROS levels. Poly (ADP-ribose) polymerase 1 (PARP-1) is integral to the repair of DNA SSBs and the authors demonstrated upregulation of PARP-1 and its product poly (ADP-ribose) (PAR) in GBM CD133+ cells in comparison to CD133- cells. Inhibition of PARP using the well characterised inhibitor olaparib as a single agent produced considerable toxicity to CD133+ GBM cells, however had little effect on CD133- cells. PARP inhibition was shown to reduce neurosphere and *in vivo* tumour generation following irradiation. The authors concluded that the likely reason for upregulation of PARP in GBM CSCs was an increased level of DNA base damage and SSBs secondary to elevated basal ROS. The mechanism of elevated basal ROS in CD133+ cells is unknown, however the authors suggested it may be related to EGFR hyperactivation. This study has provided interesting insights into the potential underlying mechanisms of upregulated DDR in CSCs, however this area requires further study.

1.3 The DNA Damage Response

Further consideration of the issues surrounding GBM CSC radioresistance requires a fuller understanding of the DDR to ionising radiation in mammalian cells. There are multiple pathways involved in DDR, often with huge complexity and some redundancy in function. However in general the cellular response to DNA damage can be summarised by two processes (1) the activation of cell cycle checkpoints and (2) the initiation of DNA repair pathways. These two processes are complementary; the activation of cell cycle checkpoints provides time for the

Introduction

cell to repair DNA before undergoing mitosis. If repair of DNA damage is successful the cell will survive and retain reproductive integrity. If not, the cell may die via apoptosis, mitotic catastrophe or an alternative cell death mechanism. This is summarised in figure 1.2. A comprehensive discussion of all aspects of DDR is not possible within the confines of this thesis however the elements of DDR relevant to the repair of DNA DSBs induced by X-irradiation will be discussed in some detail.

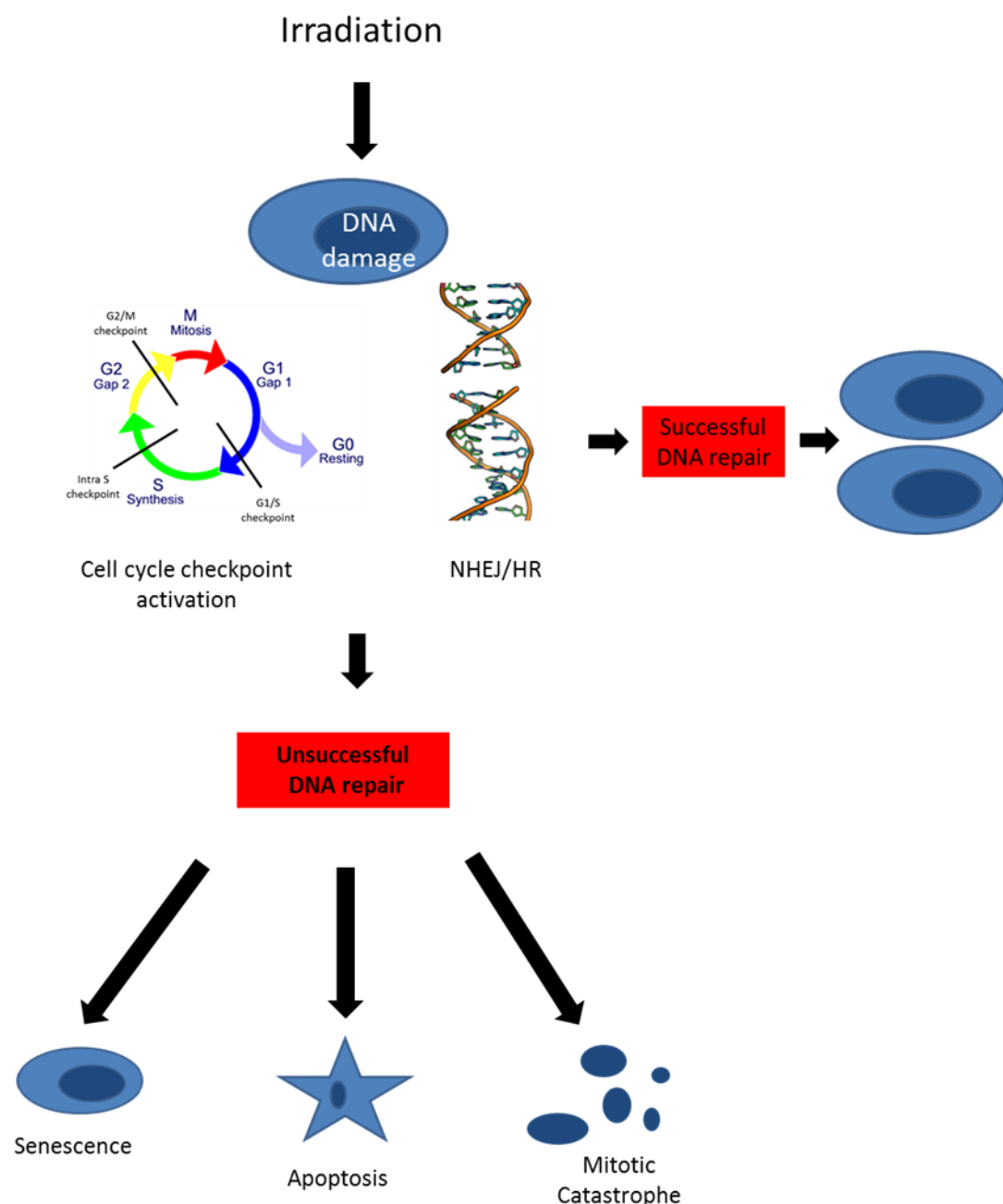


Figure 1.2 Responses of mammalian cells to DNA DSBs induced by gamma irradiation

Introduction

Following induction of DNA DSBs by ionising radiation, a DNA damage response consisting of cell cycle checkpoint activation and DNA repair is generated. If unsuccessful this may result in cell death.

1.3.1 DNA repair processes

A 2Gy dose of radiation will produce on average around 2000 SSBs and 80 DSBs. DNA SSBs are generally readily repaired by the cell and do not normally contribute to the lethal effects of radiation under normal circumstances. SSB repair will not be considered further, other than in the context of the effects of PARP inhibitors later in this chapter. DNA DSBs are much more difficult for cells to repair, and have long been considered the lesion responsible for lethality after exposure to radiation (Ward, 1975, Radford, 1985). Figure 1.3 shows an illustration of DNA DSB repair kinetics in mammalian cells following gamma radiation, adapted from Goodarzi et al (Goodarzi and Jeggo, 2012). There is an initial fast phase of repair lasting 1 to 3 hours which represents DNA DSBs that can be efficiently repaired by the cell. In addition to the fast phase of repair there is a longer ‘tail’ which is termed the slow phase of DNA DSB repair and can extend past 24 hours. It is likely that both slow phase and fast phase repair are occurring simultaneously. If left unrepaired, even a single DNA DSB can result in loss of genetic information and cell death (Frankenberg et al., 1981). Therefore it is unsurprising that mammalian cells have developed complex and highly efficient systems for repair of DNA DSBs. DNA DSBs are repaired by two DDR pathways: homologous recombination (HR) and non-homologous end joining (NHEJ). For a concise review of DNA DSB repair see Shibata and Jeggo (Shibata and Jeggo, 2014).

Introduction

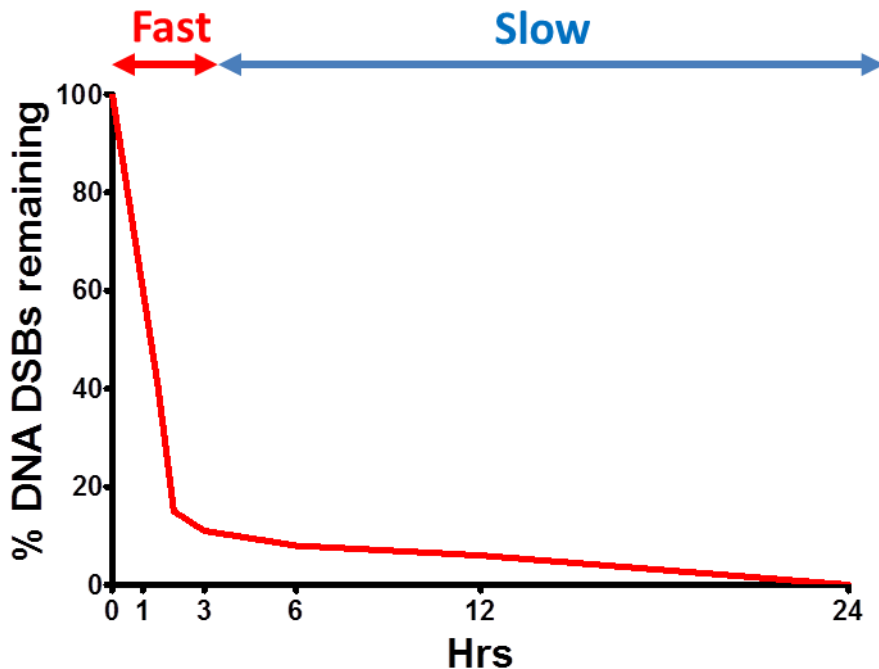


Figure 1.3 Illustrative schematic of kinetics of DNA DSB repair following irradiation in mammalian cells

The majority of DSBs are repaired a short time after irradiation in the ‘fast’ phase of DNA DSB repair via NHEJ. However a subset of DNA DSBs requires much more time for repair, due to complexity and/or chromatin context and is represented by a ‘slow’ phase tail on the above illustration. Slow phase repair is achieved via NHEJ in G1 phase and HR repair in G2 phase. Adapted from (Goodarzi and Jeggo, 2012).

1.3.2 Non Homologous End Joining (NHEJ)

The bulk of DNA DSB repair in mammalian cells is undertaken by NHEJ, and exclusively so in G1 cell cycle phase where cells have a diploid DNA content. NHEJ is involved in both fast phase repair and slow phase repair in G1 cycle cells and in the fast phase of repair in G2 cycle cells (Riballo et al., 2004). NHEJ involves the processing of broken DNA termini to form compatible ends which can then be ligated back together. NHEJ is a simple and efficient method of DNA DSB repair but is error-prone and inherently associated with loss of genetic information. The mechanistics of NHEJ can be simplified into 3 steps; (for a comprehensive review see Weterings et al (Weterings and Chen, 2008)) 1; the capture of both ends of the broken DNA molecule, 2; the bridging of the two

Introduction

broken DNA ends and 3; the religation of the broken DNA molecule. NHEJ generally appears to make the first attempt at rejoining all DNA DSBs, even in G2 phase where HR is possible, due partly to the cellular abundance of Ku70 and Ku80 and their high affinity for DNA termini (Beucher et al., 2009, Shibata et al., 2011). The binding of Ku70/80 to exposed DNA termini occurs within seconds following the creation of a DNA DSB, and initiates the process of NHEJ (Uematsu et al., 2007, Mari et al., 2006). Ku70/80 form a heterodimeric doughnut shaped structure which allows it to load onto the DNA DSB ends (Walker et al., 2001). The Ku-DNA complex then acts as a scaffold for the association of the DNA-PK catalytic subunit (DNAPKcs). From electron microscopy it appears that the association of two Ku70/80 subunits and two DNAPKcs molecules can form a bridge between 2 broken DNA ends, allowing the broken DNA ends to be tethered (DeFazio et al., 2002). Association of DNAPKcs with DNA and a Ku70/80 subunit is necessary for activation of DNAPKcs. Subsequent autophosphorylation of DNAPKcs is required for NHEJ to progress, since the unphosphorylated form of DNAPKcs blocks access for DNA end processing enzymes and ligases. Autophosphorylation of DNAPKcs relieves this block and allows processing of DNA ends in preparation for ligation (Reddy et al., 2004). The block to processing caused by unphosphorylated DNAPKcs is thought to protect DNA ends from inappropriate resection until both ends of the DSB have been brought together in appropriate apposition. DNAPKcs contains multiple phosphorylation sites, which appear to govern the progression of NHEJ events, for example autophosphorylation at T2609 destabilises the interaction of DNAPKcs with DNA allowing access for end processing enzymes such as Artemis whilst further DNAPKcs autophosphorylation at S2056 protects DNA ends from excessive end processing (Weterings et al., 2003). Studies have shown that phosphorylation of DNAPKcs occurs even in the absence of functional DNAPKcs kinase, which suggests that ATM or another PIKK kinase may have a role in the phosphorylation of DNAPKcs (Uematsu et al., 2007, Chen et al., 2007). A recent study by Jiang et al demonstrated that ATM -mediated phosphorylation of DNAPKcs is necessary for Artemis recruitment and end processing of DNA DSBs prior to NHEJ (Jiang et al., 2015).

Introduction

The simplest form of DNA DSB is a clean incision through the phosphodiester backbone of the DNA molecule, leading to two blunt DNA termini that do not require processing and can be simply religated together. However many DNA DSBs resulting from radiation are more complex, with 3' or 5' overhangs that require processing in order to facilitate religation. This could be achieved either by using the overhanging DNA strand to resynthesize nucleotide sequence on the complementary strand or by resection of the overhanging sequence. Many DNA polymerases are capable of synthesising nucleotide sequence during NHEJ, and it appears these come from the common cellular DNA polymerase pool, rather than NHEJ specific polymerases. However, resection of ends during NHEJ appears more specialised and involves the nuclease Artemis (Dahm, 2007, Goodarzi et al., 2006). Artemis appears to be involved in the resection of ‘complex’ ends in NHEJ and is hyperphosphorylated by ATM and DNAPKcs. Artemis in isolation only possesses 5' to 3' exonuclease activity, however by association with DNAPKcs it gains an additional endonuclease function (Niewolik et al., 2006). Other end processing events may be necessary prior to religation by NHEJ. Mammalian polynucleotide kinase (PNK) adds 5' phosphate groups which are necessary for the ligation reaction. 3' phosphoglycolates may require removal prior to ligation, which can be performed by Artemis, APE1, TDP1 and PNK (Weterings and Chen, 2008).

Ligase IV and XRCC4 are responsible for the final stage of NHEJ whereby the tethered and processed DNA ends are brought together and religated. A schematic diagram of NHEJ is shown in figure 1.4.

Introduction

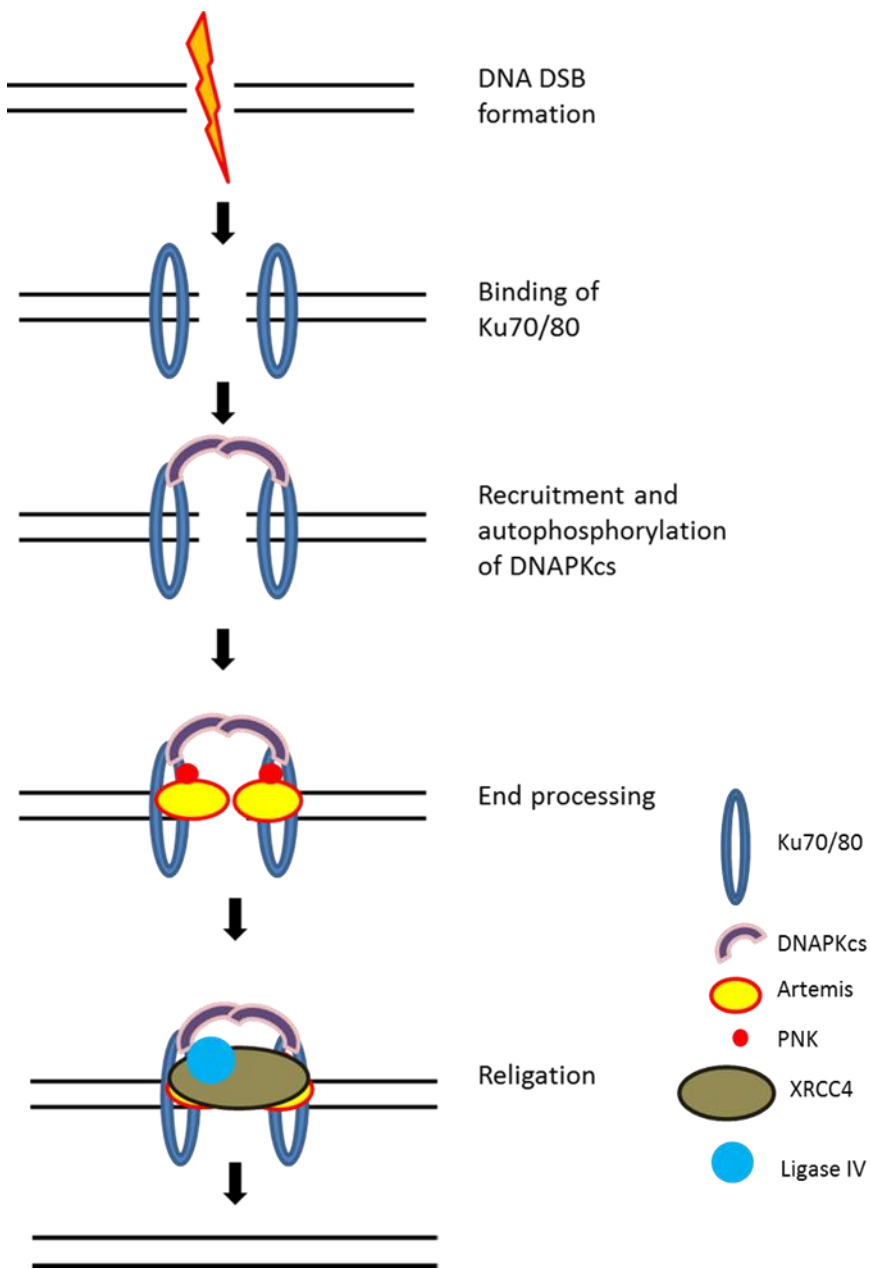


Figure 1.4 Schematic diagram of non homologous end joining (NHEJ) repair

NHEJ is initiated by the binding of Ku70/80, followed by the recruitment of DNAPKcs and its subsequent autophosphorylation. End processing is achieved via artemis and additional factors before the broken DNA ends are ligated.

An alternative mechanism of NHEJ is possible via microhomology mediated end joining (MMEJ) (Roth and Wilson, 1986, Wang et al., 2003). For a detailed review see McVey et al (McVey and Lee, 2008). MMEJ has a requirement for limited MRN dependent end resection and relies upon homologous matching of 5-25 base pairs on both strands in order to correctly align the DNA DSB ends. Any overhanging or mismatched bases are removed and missing bases are inserted.

Introduction

The process is particularly error prone, since it does not identify any sequence lost due to the DSB. MMEJ appears to act as a reserve DSB repair pathway but can also repair DSBs generated at collapse of replication forks. The process is dependent upon ATM, PARP-1, MRE-11, C-Terminal Binding Protein Interacting Protein (CtIP) and DNA ligase IV but operates independently of Ku or DNAPKcs, (McVey and Lee, 2008). It is unknown the extent to which MMEJ contributes to DSB repair in normal cells, however the process can assume importance in cancer cells with defects in other DNA DSB repair pathways (Bentley et al., 2004).

1.3.3 Homologous Recombination (HR)

The homologous recombination (HR) pathway represents a more complex and sophisticated mechanism of DNA DSB repair. Although NHEJ repairs the majority of DNA DSBs, HR contributes to repair of DSBs in specific circumstances, such as the one ended DSB created by collapse of DNA replication forks and a subset of DNA DSBs in G2 repaired via slow kinetics (Jeggo et al., 2011, Helleday et al., 2007, Beucher et al., 2009). HR is conventionally considered limited to the S and G2 phases of the cell cycle, since it relies upon homologous DNA sequence (in the form of a duplicate DNA strand on a sister chromatid) in order to effect repair; it is therefore a highly accurate repair mechanism. There is some evidence however that the normal regulation of HR is dissociated from cell cycle phase in GBM and other tumours, with Rad51 foci being evident outwith S and G2 phases (Short et al., 2007). Nevertheless it is a generally held view that HR can only occur during or after S phase when the cell has duplicated its DNA in preparation for mitosis. A simplified schematic of HR and its subpathways is shown in figure 1.5. For a more detailed review of the process see Filippo et al (San Filippo et al., 2008), Li et al (Li and Heyer, 2008) and Krejci et al (Krejci et al., 2012).

An initiating step in HR is resection of the 5' DNA end of the DSB in order to create 3' SS DNA which can then invade a partner chromosome. Initial end processing is achieved by the MRN complex and CtIP, (Sartori et al., 2007), which facilitate removal of hairpins, bulky adducts and other aberrant DNA end

Introduction

structures and allow repair. End processing creates short 3' tails following resection of 50-100 nucleotides from the 5' break ends. Ku 70/80 has a low affinity for ssDNA making NHEJ less likely once resection has taken place (Dynan and Yoo, 1998). Further resection is undertaken via two pathways. In the first of these BLM and DNA2 physically interact and carry out 5'-3' resection of DNA ends. In the second pathway MRN, RPA and BLM promote the recruitment of EXO1 to DNA ends which can then carry out further processing (Nimonkar et al., 2011, Nimonkar et al., 2008).

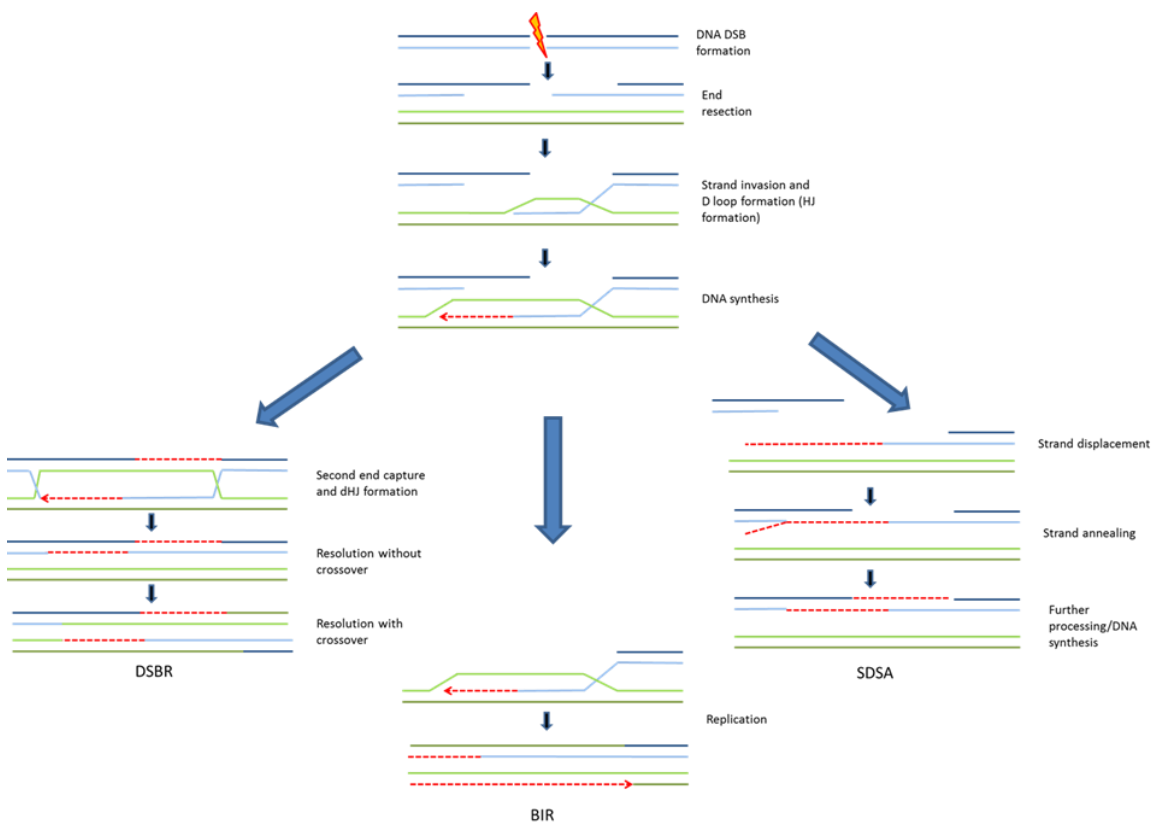


Figure 1.5 Schematic diagrams of homologous recombination (HR) repair and its subpathways

HR repair is initiated by end resection and coating of ssDNA in RPA and subsequently Rad51. The search for homologous sequence on the sister chromatid is initiated by strand invasion and Holliday junction formation. Resolution of the resulting structures can occur via double strand break repair, (DSBR); break induced repair, (BIR); or synthesis dependent strand annealing, (SDSA).

Introduction

Following creation of 3' overhangs, ssDNA is bound by replication protein A (RPA), which protects ssDNA and removes DNA secondary structure in order to facilitate formation of a ‘presynaptic filament,’ which consists of Rad51 coated ssDNA (Wold, 1997, Eggler et al., 2002). Rad51 is a recombinase, i.e. an enzyme which facilitates genetic recombination, and it forms a helical filament on ssDNA which holds DNA in an extended and stretched conformation to aid the search for homology. Loading of Rad51 onto ssDNA can be inhibited by the presence of RPA, due to its high affinity for ssDNA. Rad51 therefore requires additional help from other proteins to facilitate its loading and the efficient formation of the presynaptic filament; these are called ‘recombination mediators’. Breast Cancer 2 (BRCA 2) has an essential role in the loading of Rad51 onto ssDNA and acts as a recombination mediator. BRCA 2 binds DNA, physically interacts with Rad51 and is needed for the formation of Rad51 foci (Tarsounas et al., 2003, San Filippo et al., 2006). BRCA 2 has a role in targeting Rad51 filament formation to the ssDNA-dsDNA junction on RPA coated ssDNA (Yang et al., 2005). Another protein required for this process is PALB2. PALB2 promotes the proper localisation and stability of BRCA2 in chromatin and appears to be crucial for the DNA repair effects of BRCA2 (Xia et al., 2006).

Once assembled, the presynaptic filament captures a duplex DNA molecule and begins its search for homologous sequence. This occurs in a random fashion, with the presynaptic filament making many collisions against the sister duplex DNA molecule until homology is found. Rad51 facilitates the physical connection between the invading DNA strand and DNA duplex structure leading to the formation of heteroduplex DNA ('D loop') with a Holliday Junction (HJ) (see figure 1.5). Following successful invasion of the presynaptic strand, three different routes to repair can occur.

The double strand break repair model (DSBR) requires the capture of the second DNA end which stabilises the D loop and forms a double Holliday junction (dHJ), as shown in Figure 1.5. The dHJ can then be resolved to produce crossover or non crossover products or dissolved to produce non crossover products exclusively. DSBR is used mainly during meiosis. Synthesis dependent strand annealing (SDSA) does not rely upon capture of the second DNA end and instead

Introduction

the invading strand is displaced from the D loop, and then anneals to its own complementary strand or the complementary strand associated with the other end of the DNA break. DNA synthesis completes repair. SDSA is the primary mechanism of DSB prior to mitosis (Nassif et al., 1994).

In the break induced repair pathway (BIR) the D loop turns into a replication fork capable of both lagging and leading strand synthesis (Malkova et al., 1996). An entire chromosome arm can be synthesised in this fashion. BIR is used when there is loss of one strand of DNA in the break or at collapse of replication forks.

All of the above pathways require Rad51; however a Rad51 independent repair pathway exists called single strand annealing (SSA) (Lin et al., 1984). Sequences generated during end processing contain regions of homology in both DNA strands at a DSB site. These homologous sequences can be annealed and ligated, accomplishing DSB repair. The process is similar in mechanism to MMEJ, however remains a distinct pathway of HR.

1.3.3 Choice of DSB repair pathway

In G1 phase of the cell cycle, NHEJ is the preferred method of DSB repair, since HR is not possible. Back up pathways such as MMEJ may also be used, however it is not currently clear under which circumstances alternate pathways are used. However in G2 phase, there are two possible routes which the cell can choose in order to achieve DSB repair, since both NHEJ and HR are possible. In general, most DSBs are repaired by NHEJ even in G2 phase, and NHEJ appears responsible for the fast phase of DSB resolution in G2 (Beucher et al., 2009). It is possible that NHEJ represents the first attempt at repair for all DNA DSBs, with only unsuccessful NHEJ leading to HR (Shibata et al., 2011). However, there appears to be a subset of DNA DSBs in G2 which require HR as a pathway due to complexity or chromatin context, and the factors governing choice of pathway are still a matter of contention. End resection appears to have a major influence on pathway choice, with extensive resection committing to HR repair and excluding further attempts at NHEJ (Shibata et al., 2014). 53BP1 appears to negatively regulate ATM dependent end resection in G1 phase, therefore

Introduction

promoting NHEJ as the primary repair mechanism (Bothmer et al., 2010). In S and G2 phase however, Breast Cancer 1 (BRCA1) appears to promote the removal of p53 Binding Protein 1 (53BP1) in order to facilitate ATM dependent end resection and allow HR to take place (Bunting et al., 2010).

1.3.4 Cell Cycle Checkpoint Control

Mammalian cells have three main cell cycle checkpoints; the G1 checkpoint, intra S checkpoint and G2/M checkpoint. These are shown in figure 1.6. These checkpoints regulate the progression of cells through the cell cycle, preventing a cell from progressing into the next phase of the cell cycle prior to satisfying the requirements of the previous phase. Progression through the cell cycle is controlled by the cyclin dependent kinases (CDKs) and cyclins, the name alluding to their cyclical accumulation and destruction throughout the cell cycle. These proteins form cyclin-CDK complexes whose activity ultimately regulates the machinery responsible for cycle progression. When G0 phase cells enter G1, CDKs 4 and 6 form complexes with D type cyclins to phosphorylate the retinoblastoma protein (Rb1) which inactivates its function as a transcriptional repressor driving the cell forward in the cell cycle. In late G1 CDK2-cyclin E complexes reinforce Rb1 phosphorylation to initiate the gene expression programme required for S phase. Cyclin A-CDK1 is then responsible for driving the cell through G2 phase and into mitosis with cyclin B-CDK1. For a review of cell cycle checkpoint control see Lukas et al (Lukas et al., 2004).

Introduction

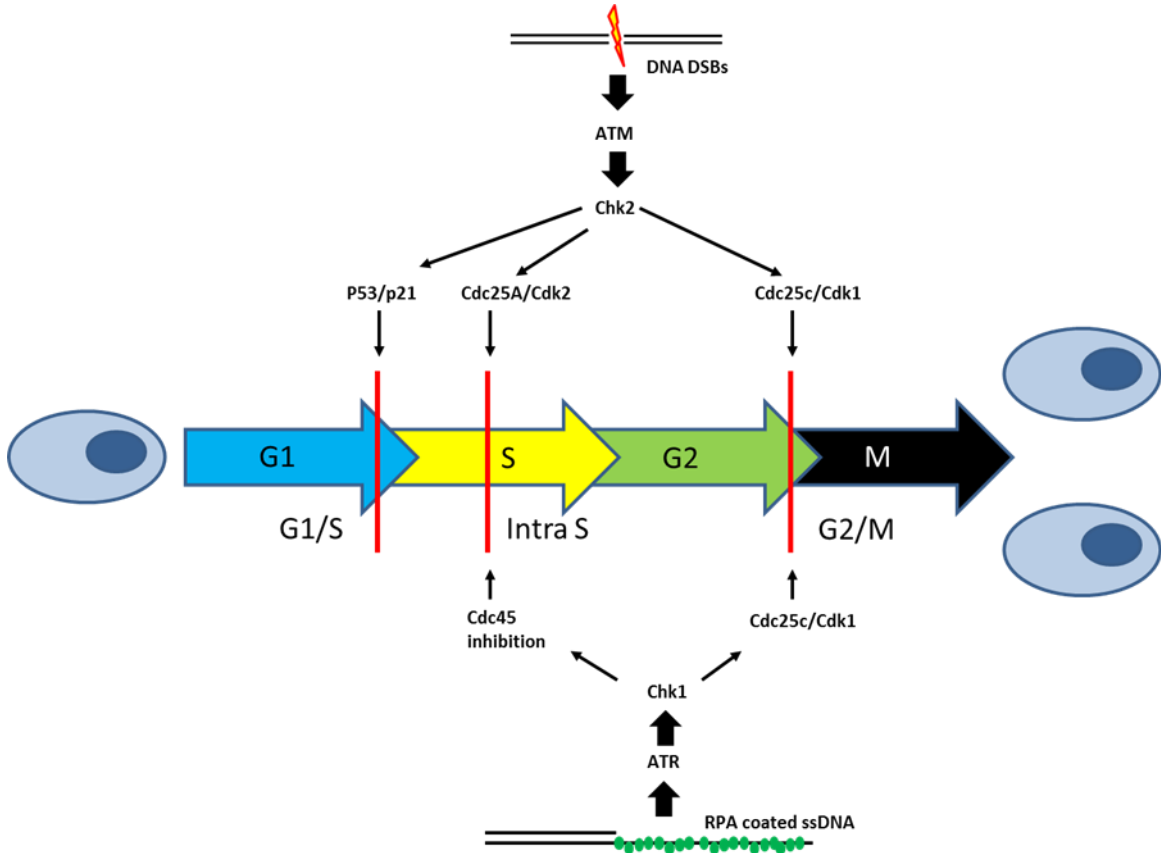


Figure 1.6 The influence of ATR and ATM on cell cycle control in response to DNA damage

Simplified diagram of cell cycle control following activation of the upstream PIKKs ATM and ATR. ATM is activated by DNA DSBs and influences all three major checkpoints, whereas ATR is activated by RPA coated ssDNA and has its major roles in the intra S checkpoint and maintenance of the G2/M checkpoint. Considerable crosstalk exists between the ATM and ATR pathways and DNA end resection initiated by activation of ATM will facilitate ATR activation. See text for details.

The G1 checkpoint is usually very robust in eukaryotic cells, however in malignant cells the G1 checkpoint is frequently absent due to mutations affecting the p53 pathway. GBM tumours frequently lack a G1 checkpoint response to irradiation. Normal G1 checkpoint function requires functioning p53, which is phosphorylated in response to DNA damage by both ATM and Chk2. This leads to a reduction in binding of MDM2 to p53 and p53 activation, resulting in its nuclear accumulation and stabilisation. The increased levels of p53 protein lead to increased transcription of p21, which binds and inhibits CDK2-cyclin E activity, preventing the cell from entering S phase. The G1/S checkpoint is highly sensitive, but limited by the time required for p21 upregulation (Deckbar et al., 2010). An alternative activation of the G1/S checkpoint is mediated via

Introduction

phosphorylation of Cdc25A, again by ATM and Chk2, which then targets Cdc25A for proteosomal degradation. Cdc25A removes inhibitory phosphate groups on CDK2, allowing progression into S phase (Mailand et al., 2000).

The intra S checkpoint is activated in response to replication stress or other difficulties encountered by the cell during S phase and operates to slow DNA replication rather than stop it entirely, and is p53 independent. The S phase checkpoint suppresses origin firing and slows replication fork progression to reduce the rate of further DNA replication. Abnormalities in S phase checkpoints result in the radio-resistant DNA synthesis (RDS) phenotype; i.e. cells are unable to stop or delay the synthesis of DNA following DNA damage. ATR is the primary modulator and amplifier of S phase DDR, with ATM playing a more minor role (Cimprich and Cortez, 2008). ATR is activated by the presence of RPA coated ssDNA, in conjunction with ATR's constitutive interacting partner ATRIP (Zou and Elledge, 2003). ATR can be further activated by direct interactions with DNA topoisomerase 2 binding protein 1 (TopBP1) which can be recruited to junctions of ss and dsDNA by the Rad9-Rad1-Hus1 complex, (911 complex) (Lee and Dunphy, 2010). This may limit the repertoire of the ATR response to lesions occurring at ss-dsDNA junctions. ATR phosphorylates Chk1. Both ATR and Chk1 are recruited to damaged DNA sites. Chk1 dissociates from DNA following activation to phosphorylate its own various substrates, which include the Cdc25 phosphatases (Smits et al., 2006). Activation of the ATR-Chk1 pathway prevents the loading of Cdc45 onto replication origins and prevents subsequent DNA replication. The ATM-Chk2-Cdc25 axis also has an effect on intra S phase checkpoint activation. A distinct pathway involving ATM dependent phosphorylation of SMC1 and SMC3 slows the rate of DNA synthesis or regulates recombinational repair following DNA damage (Willis and Rhind, 2009).

Cancer cells frequently rely upon G2/M checkpoint activation to allow repair of DNA damage prior to entering mitosis, since the G1/S phase checkpoint is often dysfunctional in malignant cells. Progression through the G2/M checkpoint with unrepaired DNA damage can result in cell death and therefore it is essential that control of the G2/M checkpoint is maintained. The protein complex driving mitotic entry through the G2/M barrier is CyclinB1/Cdk1. During G2 phase

Introduction

CyclinB1/Cdk1 is inactive due to phosphorylation of Tyr15 and Thr14 by Wee1 and Myt1 kinases. For entry into mitosis, dephosphorylation of Cdk1 by Cdc25 phosphatases is required. CyclinB1/Cdk1 is usually held in an inactive state by Chk1 dependent inhibition of Cdc25. Once activated, CyclinB1/Cdk1 phosphorylates Wee1 leading to its inactivation and phosphorylates Cdc25 which causes further activation of CyclinB1/Cdk1 complexes in a positive feedback loop ensuring commitment to the mitotic process. Activation of the G2/M checkpoint occurs via ATM and ATR which phosphorylate Chk1 and Chk2 leading to phosphorylation of Cdc25 phosphatases. Xu et al examined the function of ATM in the control of the G2/M checkpoint following irradiation. ATM mutant cells initially demonstrated an inability to activate the G2/M checkpoint but subsequently exhibited exaggerated accumulation of cells in G2 several hours following irradiation (Xu et al., 2002). The early G2/M checkpoint identified in this study was ATM dependent but radiation dose independent. The failure of this checkpoint in AT mutated cells represented the inability of cells irradiated in G2 to arrest appropriately following DNA damage. The second observed phenomenon of an enhanced G2 accumulation of cells many hours after irradiation in ATM mutant cells was related to cells which were in G1 or S phase at the time of irradiation. This is a characteristic of cells with defective S phase checkpoints, rather than being a defining feature of ATM deficiency, since this can be demonstrated in other cell lines which are ATM competent but have defects in the intra S checkpoint. The phenomenon of G2 accumulation is ATM independent and is instead ATR-Chk1 dependent. Shibata et al explored the functioning of the G2/M checkpoint in more detail and describe the initiation of G2/M arrest as ATM dependent. However other mechanisms appear responsible for the maintenance of G2/M arrest. ATM dependent end resection and processing of a subset of DNA DSBs appears to activate ATR and subsequent Chk1 activation appears to have a major role in maintaining G2/M arrest. Likewise continued ATM signalling from unrepaired DSBs also appears to contribute to G2/M arrest maintenance (Shibata et al., 2010). The G2/M checkpoint has a defined threshold of sensitivity and the activation and maintenance of G2/M arrest appears to require around 10-15 DSBs (Deckbar et al., 2007). The G2/M cell cycle checkpoint arrests heavily damaged cells in G2 to provide enhanced time for repair of DSBs and it is proposed that this may be important for slow phase repair in G2 via HR. However the G2/M checkpoint is inherently insensitive

Introduction

and allows cells to enter mitosis with a significant number of DSBs (Deckbar et al., 2011).

1.3.5 Integrating, controlling and amplifying: the DDR phosphatidylinositol 3 kinase-related kinases (PIKKs)

The complex processes governing cell cycle checkpoint arrest and DNA DSB repair require co-ordination and control following detection of DNA damage. Furthermore cellular environment and heterochromatin status must be made conducive to repair. This is achieved by signal transduction kinases which amplify signals from damage detection proteins (such as MRN and Ku) and initiate the phosphorylation of huge numbers of substrates which effect checkpoint activation, chromatin structure and DNA repair. These are the PIKKs; ATM, ATR and DNAPK. Although these proteins have already been mentioned in regard to functions in checkpoint activation and DNA repair a short discussion of their roles as central controllers of the DDR now follows.

1.3.6 ATM and its functions

ATM is a highly prolific kinase which phosphorylates many substrates in response to DNA DSBs. For a detailed review see Shiloh et al (Shiloh and Ziv, 2013). Mutations in ATM are responsible for the radiosensitivity syndrome ‘ataxia-telangiectasia,’ first described in 1975 (Taylor et al., 1975). Cells derived from patients with ataxia telangiectasia show deficient G1/S, S and G2/M checkpoints and a deficiency in DNA DSB repair. ATM is a very large protein with a molecular weight of 350kDa. It exists as inactive dimers or multimers until DNA damage occurs, upon which autophosphorylation at serine 1981 occurs, allowing the dissociation of ATM dimers into active monomers. The exact mechanism of ATM activation is debated in current literature. Some authors have suggested that ATM is activated in response to conformational changes in chromatin following DSB formation, rather than direct contact with DNA (Bakkenist and Kastan, 2003). However, direct contact with DSB ends has also been shown to be important for ATM activation (You et al., 2007). Furthermore the MRN complex is necessary for optimal activation of ATM. MRN is a complex of 3 proteins (MRE-11,

Introduction

Rad50 and NBS-1) and is a detector of DNA DSBs. It is one of the first protein complexes to be recruited to DNA DSB sites. Interaction between NBS1 and ATM appears to be critical to ATM recruitment and retention at DSB sites (Falck et al., 2005, Difilippantonio and Nussenzweig, 2007). Reciprocally, ATM also phosphorylates MRN components (Di Virgilio et al., 2009, Lim et al., 2000), illustrating the complex interactions which take place during the initial detection and transduction of the DDR signal.

ATM phosphorylates a large number of proteins directly however, it also activates several other protein kinases, notably Chk2 and DNAPK which are capable of phosphorylating their own substrate repertoires. Although ATM dominates the DDR of cells in terms of its direct interactions with other DDR proteins, it may have an even greater effect via indirect phosphorylation and activation of other proximal DDR kinases.

The effects of ATM on cellular checkpoint control via its phosphorylation of Chk2 and p53 have been discussed above, however its effects on DNA repair are also significant. ATM mutant cell lines are known to exhibit defective DNA DSB repair. The proportion of DNA DSBs which cannot be repaired in ATM mutant cells is relatively small, and is estimated at around 10-20% of the total DSB burden. ATM has a role in DSB repair in both NHEJ in G1 phase and in NHEJ and HR in G2, and the proportion of ATM dependent DSBs is similar in both phases of the cell cycle. Goodarzi et al investigated the role of ATM in chromatin modification, and demonstrated that ATM has a role in repair of heterochromatic DSBs (Goodarzi et al., 2008). This model proposes that in G1 phase, around 75% of DNA DSBs occur in euchromatin regions, in which NHEJ components can freely access and manipulate the DNA, and therefore ATM is not required for the repair of these lesions. However, in heterochromatic regions, nucleosome flexibility is constrained by factors such as KAP-1, which severely limits the ability of the cell to repair these lesions. In this model, DSBs in heterochromatin are responsible for the slow phase of DSB repair, since the cell has difficulty rejoining DSBs occurring in a hostile chromatin context. ATM is able to phosphorylate KAP-1 and allow sufficient elasticity in DNA tertiary structure to allow repair. It has previously been suggested that ATM's primary role is to deal with complex DNA

Introduction

DSB lesions, since Artemis and ATM defects create epistatic DNA repair defects, and Artemis has a vital role in end resection for facilitation of NHEJ (Riballo et al., 2004). However, the proportion of ATM dependent DNA DSBs appears not to increase following irradiation with high LET radiation types which cause more complex DSBs, which implies that ATM dependent repair is not necessarily associated with complex DNA DSBs.

Nevertheless ATM is also known to have roles in specialised DSB repair mechanisms that are not related to heterochromatin such as VDJ class switching and meiotic recombination. Alvarez-Quilon et al demonstrated that ATM is necessary for the repair of DNA DSBs with blocked ends, and that this requirement was independent of chromatin status (Alvarez-Quilon et al., 2014). The authors speculated that ATM could promote nucleolytic activity to eliminate blockage at DNA ends via the MRN complex, CtIP or Artemis, or it could restrict excessive nucleolytic degradation of DNA ends by inhibiting these same nucleases or by phosphorylation of H2AX. These two models are not necessarily conflicting, since ATM may have roles in both complex DNA lesion repair and modification of chromatin.

1.3.7 ATR and its functions

ATR has a critical role in DDR, however in contrast to ATM, which is concerned with DNA DSB repair, the primary function of ATR is to protect cells from replication stress. Replication stress can be defined as the slowing or stalling of replication forks during duplication of DNA. Cancers in general are known to exhibit high levels of replication stress, which is thought to be induced primarily by oncogene activation, leading to upregulation and increased dependence upon the ATR-Chk1 pathway (Halazonetis et al., 2008). The role of ATR in the DDR is reviewed in Marechal et al, (Marechal and Zou, 2013). ATR has an essential role for survival of proliferating cells and its deletion leads to embryonic lethality in mice and lethality in human cells (Brown and Baltimore, 2000). ATM and ATR share many phosphorylation substrates, however they have distinct roles in DDR and cannot be viewed as redundant in function. ATR is activated by RPA coated ssDNA which recruits and directly binds ATR interacting protein (ATRIP). ATRIP

Introduction

and ATR are constitutively bound, and free ATR protein does not exist in isolation. Any situation leading to the formation of ssDNA will result in the activation of ATR. The important role of ATR and Chk1 in cell cycle checkpoint control has already been discussed. However, both ATR and Chk1 have additional important functions in maintaining the integrity of replication forks. Replication fork collapse is characterised by the dissociation of replisome contents and may result in generation of a DSB. This process is still ambiguous and may be the result of replisome dissociation/migration, nuclease digestion of a reversed fork or by replication run-off (Zeman and Cimprich, 2014). ATR is activated by ssDNA generated at stalled replication forks and acts to stabilise the fork and initiates cell cycle checkpoint activation and inhibition of DNA replication origin firing on a global scale throughout the cell nucleus. ATR activation inhibits origin firing via the phosphorylation of the lysine methyl transferase MLL, which alters chromatin structure around replication origins (Liu et al., 2010). In this manner, the stalled fork can then be restarted when the replication stress stimulus has been resolved.

1.3.8 DNA dependent protein kinase (DNAPK)

DNAPK has a critical role in DDR via its function in NHEJ, as discussed above. It phosphorylates a smaller number of substrates in comparison to ATR and ATM. However DNAPK is able to phosphorylate some substrates of ATM in ATM defective cells, allowing a degree of functional redundancy. In particular DNAPK is able to phosphorylate histone H2AX in the absence of ATM (Stiff et al., 2004).

1.3.9 Ionising radiation induced foci (IRIF)

The co-ordinated and efficient repair of DNA DSBs requires the concentration of repair factors to appropriately modified chromatin structure flanking the DNA DSB. These concentrations of DDR elements can be viewed using immunofluorescent microscopy and have been termed ‘ionising radiation induced foci’ (IRIF). For a comprehensive review on IRIFs see Bekker-Jensen et al (Bekker-Jensen and Mailand, 2010). The elements involved in IRIFs generally do not bind stably and constantly to the DSB; instead they are highly dynamic and

Introduction

shuttle on and off the IRIF. One aspect of IRIFs is the structural modification of chromatin which flanks the DSB, allowing the chromatin to act as a platform for the assembly of DNA repair machinery. Chromatin is modified by phosphorylation and ubiquitylation in order to increase the likelihood of DDR element interaction.

Central to the formation of IRIF is the phosphorylation of histone H2AX on serine 139 to form gamma H2AX which spreads either side of a DSB involving regions 2Mbp to 30Mbp long (Rogakou et al., 1999). ATM is the master phosphorylator of H2AX, however DNAPKcs and ATR can also perform this function (Kinner et al., 2008, Fernandez-Capetillo et al., 2002, Bakkenist and Kastan, 2003, Veuger et al., 2004, Friesner et al., 2005). The specific physiological role of H2AX phosphorylation in DSB is yet to be elucidated in detail, however there is evidence that gamma H2AX interacts with mediator of damage checkpoint 1 (MDC1) and has a high affinity binding site for MDC1 (Stucki et al., 2005). MDC1 facilitates further ATM activation via its interactions with NBS-1 instigating a feedback loop where H2AX phosphorylation can be propagated from the DSB site by ATM mediated phosphorylation. Gamma H2AX formation may have a role in the promotion of DSB repair, however it is not essential for either NHEJ or HR (Chan et al., 2010, Petersen et al., 2001, Bassing et al., 2002). It does, however, affect the efficiency of DNA DSB repair and mice lacking H2AX are radiosensitive (Kao et al., 2006). Some authors have speculated that H2AX phosphorylation may be involved in tethering broken DNA ends (Reina-San-Martin et al., 2003, Ferguson and Alt, 2001). Many other DDR proteins have a role in IRIF formation including 53BP1, BRCA1 and Ring Finger protein 8 (RNF8).

The specific function of IRIFs is debated, and it is likely they fulfil many requirements of efficient DNA DSB repair. IRIFs probably act to protect broken DNA ends from inappropriate translocations; the concentration of repair factors also facilitates increased efficiency in DNA repair and signal amplification. Furthermore by attracting many different repair factors to sites of DSBs the cell has an array of available tools with which to attempt repair; in this scenario not all of the multitude of DDR elements may be used but the availability of several

Introduction

different routes to repair may be beneficial for timely DSB repair (Bekker-Jensen and Mailand, 2010).

1.3.10 The role of PARPs in the DDR

The main processes governing the DDR to DNA DSB formation have been explored, however the repair of single strand DNA breaks may also govern the outcome of irradiation induced DNA damage. X-irradiation causes around 25 times more SSBs than DSBs, however these are usually repaired efficiently by the cell and are of little consequence. However if SSBs are not dealt with efficiently, they can have significant effects on cell survival via the generation of DSBs. The PARP family of proteins is known to facilitate base excision repair (BER) which is one of the main cellular single strand break repair pathways. Since the effects of inhibition of PARPs on GBM CSC radioresistance are studied in this thesis, a brief discussion of PARPs and their role in the DDR now follows.

PARPs form a large protein family with diverse functions in the cell which include DNA repair, mitotic segregation, telomere homeostasis and cell death. PARPs are characterised by the catalytic function of poly (ADP-ribosylation). There are 18 reported family members, however not all have definite poly (ADP-ribose) catalytic function and only PARPs 1-3 have well characterised roles in DNA repair. For an in depth review of PARP function see D'Amours and Burkle (D'Amours et al., 1999, Burkle and Virag, 2013). PARP-1 is the most abundant in cells and its functions are the best understood.

Activated PARP-1 modifies its substrates via the covalent, sequential addition of ADP-ribose molecules which form branching poly (ADP-ribose) (PAR) polymers on the targets of PARP. The substrate from which PAR is formed is nicotinamide adenine dinucleotide (NAD⁺). Poly (ADP-ribosylation) is a commonly occurring post translational modification in the cell. It creates negative charge on target proteins altering their three dimensional structure and subsequent interactions with other proteins and with DNA (Krishnakumar and Kraus, 2010).

Introduction

PARP-1 detects DNA damage, and its rapid binding to damaged DNA results in its activation, see figure 1.7. PARP-1 can bind to a variety of DNA damage structures including SSBs and DSBs (Khodyreva et al., 2010, Chasovskikh et al., 2005, Lonskaya et al., 2005, Potaman et al., 2005) . PARP-1 appears to have a major role in PAR synthesis following DNA damage, as 90% of PAR production is attributable to PARP-1 in this context (Langelier et al., 2010). Basal PAR levels are low however can quickly be increased 10 to 500 fold in the presence of DNA damage (D'Amours et al., 1999). High levels of DNA damage appear to be linked to rapid PARylation, whereas lower levels of DNA damage result in slower PARylation activity (Pion et al., 2005). PAR polymers can exist as short branching structures or long elongated polymers; the latter being degraded more quickly. The relationship between PAR polymer structure and DNA damage remains unclear (Malanga and Althaus, 1994). PARP-2 accounts for 5-10% of PAR production in response to DNA damage and less is known about its function and significance (Menissier de Murcia et al., 2003). PARP-2 appears to bind less effectively to SSBs and instead has a greater role in binding to gap and flap DNA abnormalities (Yelamos et al., 2008, Ame et al., 2009). It can homodimerize or heterodimerize with PARP-1, however the biological outcomes of these interactions is still unclear (Sukhanova et al., 2010).

Introduction

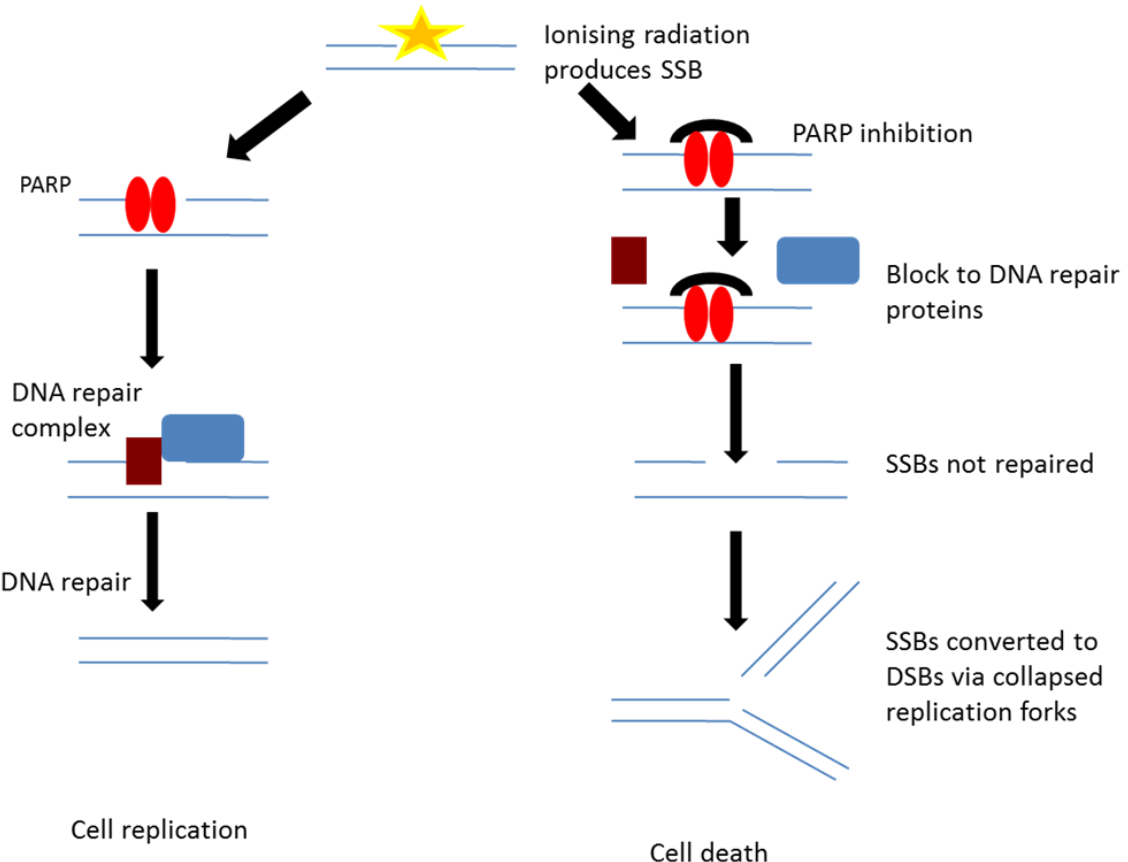


Figure 1.7 Mechanism of radiosensitisation by PARP-1 inhibition

PARP inhibition permits the binding of PARP-1 to DNA SSBs, however prevents the efficient repair of SSBs by inhibiting the recruitment of key BER effectors and by blocking access of repair elements to damage sites. This results in delayed SSB repair and collapse of replication forks as SSBs are converted into DSBs during S phase.

DNA bound PARP can undergo automodification to add long negatively charged PAR polymers (D'Amours et al., 1999). The autoPARylation of PARP-1 allows dissociation of PARP-1 from the DNA molecule, allowing other DNA repair machinery access to the damaged DNA (Zahradka and Ebisuzaki, 1982, Ferro and Olivera, 1982, Lindahl et al., 1995) and facilitating recruitment of various DDR proteins to the damaged sites. The list of substrates for PARP-1 is extensive. PARP-1 can alter DDR protein function by both PARylation and direct interaction.

Although the precise role of PARP-1 in DNA repair is still being elucidated, an important contribution to the repair of SSB lesions is well documented. Rather than being essential for SSB repair, however, PARP-1 increases the efficiency and rate of this process (Fisher et al., 2007, Satoh and Lindahl, 1992, Strom et

Introduction

al., 2011). Activation of PARP-1 promotes the recruitment of the scaffold protein XRCC1 to the site of damage (El-Khamisy et al., 2003). PARP-1 modifies and interacts directly with XRCC1 during this process. Lesions then undergo end processing before being repaired by either short patch or long patch repair. PARP-1 is known to interact with many other SSB repair proteins such as DNA Lig III, DNA Polymerase Beta (DNA Pol Beta) and others. Additionally it appears to have a role in base excision repair (BER) but is not an absolute requirement for the function of this pathway (Strom et al., 2011). The radiosensitising effects of PARP inhibition will be discussed below.

1.4 DDR kinase inhibition as a therapeutic strategy

Given the fundamental role of DDR in determining tumour sensitivity to radiation, inhibition of the DDR in combination with radiotherapy is an appealing therapeutic strategy. DDR inhibition could potentially radiosensitise tumours which are clinically radioresistant, whilst having relatively little effect on normal tissue. The concept of ‘tumour specificity’ is vitally important in cancer therapy, and particularly so when considering increasing the biological effects of ionising radiation. If DDR inhibition were to sensitise normal tissue to the same degree as tumour cells then no therapeutic gain would be made, since any increased tumour effect would be accompanied by an unacceptable increase in toxicity.

There are clearly important differences between the DDR of tumours in comparison to the DDR of normal tissues. DDR presents a barrier to carcinogenesis in the early stages of tumour development (Bartkova et al., 2005). A cell population in the process of carcinogenesis faces pressure to mutate or alter the DDR process in order to tolerate oncogenic proliferative stress. A deficient DDR is in some ways advantageous to tumour cells, giving these cells the capacity to generate genomic instability and heterogeneity, providing adaptability and a survival advantage for the limited resources of the tumour microenvironment. There is evidence to suggest that tumours may be profoundly deficient in some aspects of DDR, rendering them overly dependent on other DDR pathways to carry out efficient DNA repair. Examples of this

Introduction

behaviour are seen in the widespread loss of G1/S checkpoint integrity in solid tumours due to p53 mutation and resulting reliance upon the G2/M checkpoint for cell cycle control. A further example is seen in the context of ‘synthetic lethality’ in HR deficient tumours, which are sensitive to therapies which cause DNA lesions requiring HR for repair such as PARP inhibition. The main reason why radiotherapy is a successful cancer therapy is because tumour cells are less able than the surrounding normal tissue to deal with the DNA damage caused by ionising radiation. The intact DDR of normal tissues ensures a therapeutic ratio exists between tumour and normal tissue, allowing radiation to eradicate tumour cells whilst vital normal tissue structures are able to partially regenerate or tolerate the resulting DNA damage. Therefore pharmacological inhibition of DDR targets a pre-existing weakness inherent to many cancer cells and thus represents a valid and promising therapeutic strategy.

Recently small molecule kinase inhibitors have become commercially available which possess the ability to specifically and potently inhibit individual kinases or proteins within the DDR. Although many of these are not yet advanced enough to be anything more than laboratory tools, others such as the PARP inhibitor class are entering phase I clinical trials in combination with radiotherapy. A discussion on current knowledge and application of DDR kinase inhibition and radiation sensitivity now follows.

1.4.1 PARP inhibition as a radiosensitising strategy

PARP inhibitors are the most developed of DDR kinase inhibition strategies, largely due to early successful trials as monotherapy in a ‘synthetic lethality’ setting (Fong et al., 2009). There are now several PARP inhibitors entering clinical trials including AZD2281 (Olaparib), AG014699 (Rucaparib) and ABT888 (Veliparib). However extensive preclinical investigation into their role as radiosensitising agents has been carried out and is summarised below.

In vitro work has shown PARP inhibition (PARPi) to provide modest radiosensitisation. Sensitiser enhancement ratios (SER), which are a measure of the fold increase in radiation dose necessary to provide the effect seen in the

Introduction

absence of the sensitising drug, have been reported in the range of 1.1 to 1.7, depending on the inhibitor and the cell line tested.

Brock et al (Brock et al., 2004), showed this effect in fibroblast and murine sarcoma cell lines, with SERs (at 10% survival) of 1.4 to 1.6 using the PARP inhibitor INO-1001. Interestingly they also showed an enhanced sensitisation effect when INO-1001 was combined with fractionated radiotherapy, suggesting that PARPi was able to block interfraction repair of sublethal damage. This effect was also reported in a study of glioblastoma cell lines (Dungey et al., 2009).

Other authors have confirmed the radiosensitising effects of PARPi *in vitro* in a variety of different tumour cell lines, summarised in table 1.2. These include head and neck squamous cancer, prostate, glioblastoma, pancreatic, colon, cervix and lung carcinoma cell lines.

Introduction

Author	PARP Inhibitor and radiation dose	Cell line	Assays	Outcome
Brock et al, 2004	INO-1001 10uM, IR 0-8Gy	CHO rodent fibroblast, c37 human fibroblast, SaNH murine sarcoma cell lines	Clonogenic survival and apoptosis	Decreased clonogen survival in PARPi plus IR, effect enhanced by fractionation
Albert et al, 2007	ABT888 (veliparib) 5uM, IR 0-6Gy	H460 lung carcinoma cell lines	Clonogenic survival, apoptosis, endothelial damage assay	No increase in apoptosis Decreased clonogen survival in PARPi plus IR vs IR alone Increased apoptosis Inhibition of endothelial tubule formation
Dungey et al, 2009	AZD2881 (olaparib) 1uM , IR 0-5Gy	T98G and U87MG glioblastoma cell lines	Clonogenic survival, gamma H2AX foci	Decreased clonogenic survival in PARPi plus IR vs IR alone, decreased DNA repair, DNA replication dependent effect of PARPi, Fractionation sensitive effect
Loser et al, 2010	AZD2881 (olaparib) 500nmol/l plus IR 0-8Gy	Human and murine primary cells defective in artemis, ATM, DNA ligase IV	Clonogenic survival, alkaline comet assay, gamma H2AX foci	PARPi radiosensitisation enhanced in ATM, Artemis and DNA ligase IV deficient cells. Clonogenic survival decreased in rapidly dividing and DNA repair deficient cells
Calabrese et al, 2004	AG14361 0.4uM plus IR 8Gy	LoVo and SW620 human colonic carcinoma cell lines	Clonogenic survival	PARPi plus IR decreased survival by inhibiting recovery from potentially lethal damage
Russo et al, 2007	E7016 3-5uM plus IR 0-8Gy	U251 glioblastoma, MiaPaCa pancreatic, DU145 prostatic carcinoma cell lines	Clonogenic survival, gamma H2AX foci, mitotic catastrophe, apoptosis	PARPi plus IR increased clonogenic cell kill and mitotic catastrophe, however no increase in apoptosis
Liu et al, 2008	ABT 888 (veliparib) 2.5uM plus IR 5Gy	H1299 lung cancer cells, DU145 and 22RV1 prostate carcinoma cell lines	Clonogenic survival, repair foci assay	PARPi plus IR reduced clonogenic survival, with effect seen in acute hypoxic cells and oxic cells

Table 1.2 Summary of *in vitro* studies of radiosensitising effects of PARP inhibitors

Introduction

PARP inhibitors have been shown to decrease clonogenic survival and increase apoptosis and mitotic catastrophe in irradiated cells *in vitro*. The pro-apoptotic effects of PARPi vary between studies and may be a cell line dependent effect. Noel et al demonstrated lack of radiosensitivity in asynchronously dividing human cell lines treated with PARPi whilst HeLa cells which were synchronised in S phase were significantly sensitised to radiation by the addition of PARPi, suggesting that sensitisation was dependent upon DNA replication (Noel et al., 2006). This was confirmed by Dungey et al (Dungey et al., 2009) who showed that radiosensitisation was enhanced by synchronisation in S phase and abrogated by aphidicolin (which creates an early S phase block). PARPi delayed repair of DNA damage and was associated with a replication dependent increase in gamma H2AX and Rad51 foci. Again radiosensitisation was increased with a fractionated schedule, indicating impaired repair of sublethal damage in PARPi treated cultures. The authors proposed a mechanism whereby PARPi reduced the rate of SSB repair which, in replicating cells, increased the burden of DSBs due to generation of collapsed replication forks during S phase. They also proposed that the DNA lesions produced by collapsed replication forks in the presence of PARPi might be more complicated and hence more difficult to repair by HR. Persistent binding of chemically inhibited PARP to DNA (via steric hindrance) would prevent efficient recruitment of DNA repair proteins to the lesion, providing an explanation for this theory (Langelier et al., 2012). The observation that PARP inhibition requires DNA replication in order to radiosensitise cells was thought to make an effect via DSB repair unlikely.

The above discussion has important implications for the clinical use of PARPi as radiosensitisers. The radiosensitising effect of PARP inhibition appears to be limited to replicating cells. This would suggest an element of tumour specificity if this approach were used in tumours with significant fractions of replicating cells such as squamous cell carcinomas or glioblastoma, in an organ of the body where critical normal tissues are non replicating (e.g.CNS). The demonstration that the radiosensitising effect is enhanced by clinically relevant doses of fractionated radiation is also of clinical significance.

Introduction

Loser et al investigated the radiosensitising effects of PARPi on cells which were already deficient in DDR pathways, an effect which has been termed “synthetic sickness”. The addition of PARPi to cell lines with a pre-existing DDR pathway abnormality appeared to enhance the radiosensitising effect of PARPi compared with DDR competent cell lines. The underlying mechanism varies according to the specific DDR pathway abnormality, however it appears that the combination of PARPi and radiation induced DNA damage leaves DDR deficient cells more vulnerable to DNA lesions which may otherwise have been repaired by alternative pathways (Loser et al., 2010).

Liu et al (Liu et al., 2008) examined the effects of acute hypoxia on radiosensitisation by PARPi. The PARPi ABT888 was shown to inhibit intracellular PARP activity in prostate and non-small cell lung carcinoma cell lines under conditions of hypoxia. Under conditions of acute hypoxia cells were sensitised to a degree similar to the radiosensitivity of oxic cells. The authors concluded that PARPi with ABT888 remained an effective radiosensitiser under conditions of acute hypoxia; which is an important consideration in translating PARPi into clinical practice, given that most tumours are hypoxic to some degree (Meng et al., 2005, Bindra et al., 2004), and furthermore hypoxia has been characterised as a major determinant of radioresistance (Moulder and Rockwell, 1984). Chronic hypoxia induces downregulation of HR, which may allow targeting of chronically hypoxic cancer cells with a PARPi synthetic lethal strategy. Chan et al have shown that PARPi treated tumour xenografts which showed hypoxic subregions had increased gamma H2AX signalling and reduced survival in an *ex vivo* clonogenic assay. However the specific radiosensitising effects of PARPi in the context of chronic hypoxia were not investigated (Chan et al., 2010). Nevertheless the ability of PARPi to selectively target chronic hypoxic cancer cells is obviously of great clinical interest.

The radiosensitising effects of PARPi have been replicated by several authors in *in vivo* models. The results of these studies are summarised in table 1.3. A recent paper by Tuli et al demonstrated tumour growth inhibition and prolonged survival in an *in vivo* orthotopic model of pancreatic carcinoma (Tuli et al., 2014).

Introduction

Author	PARP inhibitor and radiation dose	Cell line	Assay	Outcome
Khan et al, 2009	GPI-15427 10,30, 100,300mg/kg po, IR 2Gy for 2 days	JHU012 and JHU012 head and neck cancer xenografts	Tumour growth delay, apoptosis	PARPi plus IR inhibited tumour regrowth vs IR Increased apoptosis
Clarke et al, 2009	ABT 888 7.5mg/kg po bd, Temozolomide 33mg/kg/d, IR 20Gy over 11 days	Glioblastoma intracranial xenografts (MGMT hypermethylated)	Animal survival, body weight	PARPi-TMZ-IR prolonged survival vs IR alone, minimal weight loss
Donawho et al, 2007	ABT 888 25mg/kg/d via osmotic pumps, IR 20Gy over 10 days	HCT116 xenograft human colorectal carcinoma	Animal survival	PARPi plus IR increased mean survival time vs IR alone
Albert et al, 2007	ABT 888 25mg/kg ip for 5 days, IR 10Gy over 5 days	H460 xenograft, human lung carcinoma	Tumour growth delay, Ki67 staining, apoptosis, blood vessel density	PARPi plus IR delayed tumour regrowth vs IR alone Decreased tumour vasculature Decreased proliferation Increased apoptosis
Calabrese et al, 2004	AG143615 or 15mg/kg/d ip, IR 10Gy over 5 days	SW620 human colon carcinoma	Tumour growth delay	PARPi plus IR delayed tumour regrowth vs IR alone
Russo et al, 2009	E7016 30mg/kg po, IR 4Gy single fraction	U251 glioblastoma xenograft	Tumour growth delay	PARPi-TMZ-IR delayed tumour regrowth vs IR alone
Tuli et al, 2014	ABT 888 25mg/kg, IR 5Gy single fraction	Pancreatic carcinoma	Tumour growth delay and survival	PARPi plus IR delayed tumour regrowth and prolonged survival

Table 1.3 Summary of *in vivo* studies of radiosensitising effects of PARP inhibitors

Introduction

The radiosensitising effects of PARPi appear to be enhanced in *in vivo* models, with several studies showing radiosensitising effects that exceed those predicted by *in vitro* data. This is unlikely to be explained by radiotherapy fractionation effects alone, since several of the studies also used large single fraction radiotherapy doses similar to those used *in vitro*. PARPi has been shown to have effects on tumour vasculature, which may partly explain the enhanced effects seen in *in vivo*. PARPi have a structural similarity to nicotinamide, which is a potent vasodilator. It has been proposed that PARPi may have a strong vasodilatory effect on tumour vasculature, thus relieving tumour hypoxia, increasing drug delivery and enhancing their radiosensitising effects (Calabrese et al., 2004, Ali et al., 2011a), but the clinical significance of this effect remains to be proven.

Normal tissue toxicity in a PARPi radiosensitisation strategy has not been extensively investigated, partly because most animal models of cancer do not yield clinically meaningful radiation toxicity data. However there are several features of PARPi that predict a degree of tumour specificity. Likely toxicities will of course depend upon the tumour site irradiated. As single agents, PARP inhibitors have been shown to have highly favourable toxicity profiles, consisting of nausea or somnolence syndrome at very high doses, (Fong et al., 2009). Therefore toxicities out with the irradiated field would be unexpected, unless concomitant chemotherapy was also incorporated into treatment. Administration of PARP inhibitors with cytotoxic chemotherapy has resulted in severe myelosuppression in phase I clinical trials however (Samol et al., 2012).

The dependence on DNA replication indicates that rapidly dividing tissues will be sensitised to radiotherapy by PARP inhibition. Hence squamous cell carcinomas, glioblastoma and other highly mitotically active tumours may be most sensitised by PARPi. This also has implications for normal tissue toxicity, since tissues with high cellular turnover such as the oesophagus, mucous membranes, skin, bowel and bone marrow may be sensitised by a PARPi strategy; although only if these sites were also irradiated. Tissues comprised of infrequently dividing cells such as brain, spinal cord, heart and muscle are predicted not to be sensitised by

Introduction

PARPi, although concern must be raised with regard to supporting stromal tissue, e.g. astrocytes in the case of the CNS and vascular endothelial cells.

Given that the vascular endothelium is present in every organ and tumour treated, the endothelium is worthy of specific consideration in terms of the effects of a radiation/PARPi strategy. The cell doubling time of endothelial cells in culture has been estimated from labelling studies to be in the region of 93 to 2300 days, which would classically make it an intermediate to late responding tissue (Hobson and Denekamp, 1984). However there is evidence to suggest a proliferative stimulus is provided by irradiation which would decrease the doubling time of endothelial cells and perhaps increase endothelial sensitivity to PARPi plus radiation (Haveman et al., 2007). A recent paper however has shown that the neurovascular niche was preserved in mouse brain following irradiation, however there was an effect on long term neurogenesis (Bostrom et al., 2013).

It is unknown whether the progenitor stem cells of slowly dividing tissues may be sensitised by PARPi strategies; this would have implications for long term toxicity from this strategy. In particular in the case of the CNS, it is unclear how neural stem cells may respond to PARPi radiosensitisation strategies. Some studies have shown that the subventricular zone of adult mice forebrains contain a population of actively dividing cells, with complete turnover of the resident proliferating cell population occurring every 12-28 days (Craig et al., 1999). These cells could therefore be predicted to experience some radiosensitisation by PARP inhibition, however the effect of PARP inhibition on radiosensitivity of human neural stem cells has not been directly investigated. Nevertheless *in vitro* models of neural stem cells which could be used to assess toxicity of novel DDR inhibitor agents have been described (Meli et al., 2014). Tanori et al demonstrate an *in vivo* characterisation of the effects of ionising radiation on neural stem cells in the murine cerebellum and a similar model could be utilised to explore the toxic effects of PARP inhibition (or other DDR inhibition) plus radiation combinations. Examination of the cells of the subventricular zone of mice for DDR markers such as gamma H2AX 24 hours following treatment with radiation and PARP inhibition would be informative.

Introduction

PARPi has also been observed to accumulate in malignant tissue, an effect which may be related to enhanced levels of DNA damage (which would therefore bind more PARP) in malignant tissue. This may also increase the tumour specificity of PARPi (Calabrese et al., 2004) and limit normal tissue toxicity (Galia et al., 2012a). Potentially PARP inhibition could protect normal tissue from toxicity from radiotherapy. Theoretically, activated PARP will deplete cells of NAD⁺, making it difficult for damaged normal cells to activate energy dependent apoptotic pathways leading to cell death by necrosis and an inflammatory cascade leading to further tissue damage. With PARP inhibition, NAD⁺ would not be exhausted, and cells would be more likely to die from apoptosis. There are some studies looking at the use of PARPi in myocardial reperfusion injury and ovine models of acute lung injury which lend some support to this theory (Roesner et al., 2010, Hamahata et al., 2012). Furthermore it has been found that PARP inhibition is protective in irinotecan induced gastrointestinal toxicity (Tentori et al., 2006).

Laboratory models of the acute and long term toxicities of radiation therapy are being developed and refined(Figley et al., 2013).However, the additional toxicity of PARP inhibition on the acute and late effects of radiation toxicity are yet to be explored in these models.

1.4.2 ATM inhibition as a radiosensitising strategy

In comparison to PARP inhibition, the development of radiosensitisation strategies based on ATM inhibition are at a much earlier stage of development, and no compounds are currently entering clinical trials. Much of the *in vitro* work in this area has explored the use of ATM inhibition as a laboratory tool rather than preclinical investigation as a radiosensitiser.

Golding et al (Golding et al., 2009), explored the use of ATM inhibition as a radiosensitiser in GBM. They demonstrated highly potent radiosensitisation of commercially available GBM cell lines using the ATM inhibitor KU-60019, however radiosensitisation was not quantified by formal estimation of SER_{0.37}. Furthermore the authors demonstrated an effect of ATM inhibition on cell

Introduction

migration and invasion *in vitro*, and speculated that this may be due to effects of ATM inhibition on AKT phosphorylation. They concluded that ATM inhibition was a highly effective radiosensitiser and inhibitor of DDR in glioma. In a further paper, Golding et al explored the combination of ATM inhibition with radiation and temozolomide on commercially available GBM cell lines (Golding et al., 2012). SER_{0.37} was calculated to be 1.8-2.1 depending on the dose of KU-60019 used. The addition of temozolomide did not enhance the radiosensitivity produced by ATM inhibition, (nor did temozolomide actually radiosensitise in the absence of ATM inhibitor). When co-cultured with human astrocytes, the combination of temozolomide and ATM inhibition reduced glioma cell growth by around 70%. Astrocytes did not demonstrate *in vitro* radiosensitisation after exposure to KU-60019. Biddlestone-Thorpe et al explored an *in vivo* GBM model of ATM inhibition and radiation treatment (Biddlestone-Thorpe et al., 2013). *In vivo* administration of KU-60019 required the use of osmotic pumps and convection enhanced delivery, since the drug did not reach therapeutic concentrations in plasma following oral or intraperitoneal administration. KU-60019 significantly prolonged survival and delayed tumour growth in combination with radiation treatment. The investigators explored the influence of p53 status on radiosensitising effects of ATM inhibition. U87 cells, which are known to be wild type for p53, were infected with a mouse retrovirus expressing the p53-281G allele, generating U87 cells with mutant p53. U87-281G cells experience increased radiosensitisation following ATM inhibition *in vitro*, and mice bearing U87-281G xenografts experienced prolonged overall survival with the combination of ATM inhibition and radiation in comparison to mice bearing U87 parental xenografts. Overall survival was not prolonged by ATM inhibition and radiotherapy in the mice with U87 parental xenografts in comparison to radiation alone. The authors concluded that ATM inhibition may be of potential benefit in combination with radiotherapy for GBM with mutated p53.

These three papers represent the most in depth studies of the potential clinical applications of ATM inhibition in glioma. Other studies have demonstrated the potentiating effects of ATM inhibition on cisplatin mediated radiosensitisation of non-small cell lung cancer cells or the radiosensitisation of head and neck squamous carcinoma cell lines by ATM inhibition via interfering RNA (Toulany et

Introduction

al., 2014, Zou et al., 2008). Rainey et al demonstrated that transient ATM inhibition for a period of 4 hours was able to potently radiosensitise HeLa cells *in vitro* (Rainey et al., 2008). Choi et al investigated the consequences of ATM inhibition versus ATM loss. The authors demonstrated distinct effects of ATM inhibition versus ATM loss, manifest by reduced sister chromatid exchange (a marker of homologous recombination) in ATM inhibited irradiated cells which was not apparent in irradiated ATM null cells (Choi et al., 2010).

Current dogma would suggest that inhibition of ATM in combination with radiotherapy will lead to overwhelming normal tissue toxicity, since ATM is one of the central kinases of the DDR. This would limit the use of ATM inhibition as a clinical radiosensitiser. However, there is evidence to suggest that radiosensitivity following ATM inhibition may be tissue specific. A study by Schneider et al demonstrated that astrocytes downregulate ATM expression and lack significant DDR, however retain DNA repair competency via NHEJ (Schneider et al., 2012). In support of this Gosink et al demonstrated that astrocyte radiosensitivity was unaffected by ATM deficiency (Gosink et al., 1999). A further recent study by Moding et al using a murine sarcoma model demonstrated that deletion of the ATM gene had much less of a radiosensitising effect on normal cardiac endothelia than on rapidly proliferating tumour endothelia (Moding et al., 2014). These data suggest that ATM inhibition as a radiosensitising strategy may be clinically achievable, however further study of the potentially toxic effects of ATM inhibition is clearly required.

1.4.3 ATR inhibition as a radiosensitising strategy

Again the effects of ATR inhibition on radiosensitivity are not well characterised and remain at an early stage of development. Wang et al investigated the effects of kinase dead ATR expression on cellular radiosensitivity. They demonstrated that ATR kinase loss radiosensitised cells due to deficient S and G2 cell checkpoints and reduced HR (Wang et al., 2004). Gilad et al demonstrated a requirement for malignant cells to engage the ATR-Chk1 pathway in order to maintain genome stability following oncogenic expression of Ras, implying that

Introduction

suppression of ATR signalling may sensitise cancer cells to DNA damaging agents such as radiation (Gilad et al., 2010).

Until recently a specific and potent inhibitor of ATR has not been available. A study by Reaper et al characterised the effects of a specific and potent inhibitor of ATR, VE-821, in combination with a variety of genotoxic agents in commercially available cell lines. VE-821 was shown to potentiate the effects of cisplatin and ionising radiation. Furthermore the effects of VE-821 were enhanced in cells with a deficiency in the ATM-p53 axis. The authors speculated that ATR inhibition generated DSBs via collapse of replication forks which normally induced an ATM dependent S phase checkpoint response. Cells deficient in ATM or p53 were unable to activate this response and exhibited increased sensitivity to ATR inhibition (Reaper et al., 2011).

Prevo et al investigated radiosensitisation via ATR inhibition in pancreatic carcinoma using VE821. VE821 was found to ablate radiation and gemcitabine induced Chk1 phosphorylation. It also increased the sensitivity of commercially available and primary pancreatic cancer cells to the combination of radiation and gemcitabine in both normoxic and hypoxic conditions, and effectively inhibited radiation induced G2/M arrest. ATR inhibition appeared to increase DNA DSBs following treatment with radiation as assessed by persistent gamma H2AX and 53BP1 foci. Rad51 foci formation was reduced 24 hours after treatment with IR and VE821, suggesting inhibition of HR (Prevo et al., 2012).

Fokas et al used a more potent analogue of VE821, VE822 to study the effects of ATR inhibition on pancreatic cancer cell radiosensitivity *in vivo*. VE822 was found to potently inhibit Chk1 phosphorylation and sensitised pancreatic cancer cells to radiation, both alone and in combination with gemcitabine. In contrast VE822 had no effect on tube formation by human dermal microvascular endothelial cells after radiotherapy and did not affect the clonogenic survival of fibroblasts. Again radiation induced foci (gamma H2AX and 53BP1) were increased by the combination of ATR and radiotherapy whilst Rad51 foci were decreased, implying that ATR inhibition causes an HR defect. The combination of IR and ATR inhibition produced a significant increase in tumour growth delay in

Introduction

subcutaneous pancreatic tumour xenografts. This study also attempted to look at normal toxicity of the IR plus ATR inhibitor combination, by assessing the number of apoptotic jejunal cells and villus tip loss in mice treated with the combination. Neither of these parameters when compared with controls suggested additional toxicity with the addition of ATR inhibition (Fokas et al., 2012).

Pires et al investigated the effects of ATR inhibition on radiotherapy resistant hypoxic tumour cells. Inhibition of ATR with VE821 was shown to sensitise a wide variety of commercially available cell lines to radiation. There was no evidence of more marked effects on p53 mutated cell lines. Severe hypoxia is known to cause replicative stress and DDR activation via ATM and ATR signalling. VE821 was demonstrated to abrogate hypoxia mediated ATR signalling. Importantly, ATR inhibition by VE821 was shown to increase radiation induced cell killing in physiologically relevant hypoxic conditions (Pires et al., 2012).

Sankunny et al demonstrated that inhibition of ATR via siRNA could radiosensitise oral squamous cell carcinoma with distal chromosome arm 11q loss (a marker of relative radioresistance and poor prognosis) (Sankunny et al., 2014). Vavrova et al demonstrated the radiosensitisation of p53 deficient promyelocytic leukaemia cells via ATR inhibition (Vavrova et al., 2013).

1.4.4 Chk1 inhibition as a radiosensitisation strategy

The radiosensitising effects of Chk1 have been investigated by several authors in various tumour sites. Chk1 has important effects on G2/M checkpoint control and in the promotion of Rad51 mediated DNA DSB homologous recombination repair and would therefore be predicted to be a potent radiosensitiser. Many studies have focussed on the radiosensitising effects of Chk1 inhibition on p53 mutant cells since these cells will in theory be dependent on the G2/M checkpoint arrest for DNA repair. Koniaras et al demonstrated that the G2/M checkpoint was independent of p53 and then showed that inhibition of Chk1 (achieved by generation of a dominant negative mutated Chk1 cell line) resulted in radiosensitivity (Koniaras et al., 2001). Sorensen et al further defined the

Introduction

role of Chk1 as an essential kinase for the maintenance of genomic integrity (Sorensen et al., 2005). They demonstrated Chk1 inhibition with two different compounds (UCN01 and CEP3891), and noted an increase in phosphorylation of ATR targets, increased initiation of DNA replication and induction of DNA DSBs. Chen et al further investigated the role of Chk1 inhibition as a potential sensitiser to DNA damaging agents (Chen et al., 2006). The responses of p53 mutated cancer cell lines to radiation were quantified following Chk1 inhibition and compared to the response of p53 wild type cell lines and normal human fibroblasts. Chk1 inhibition was found to potentiate the effects of radiation in p53 mutant cells only.

Investigations of different Chk1 inhibitor compounds in different tumour sites have since been published in breast cancer and pancreatic cancer (Engelke et al., 2013, Ma et al., 2012).

1.4.5 Combination DDR inhibition

The ability to inhibit different targets within the DDR allows the prospect of inhibiting combinations of DDR proteins in order to manipulate radiation sensitivity. There are only a few studies which have undertaken this approach. Vance et al investigated the radiosensitisation of pancreatic cancer cells by inhibition of both Chk1 and PARP in combination (Vance et al., 2011). This study demonstrated radiosensitisation of both p53 wild type and p53 mutants in isogenic cell lines by the combination treatment, however radiosensitisation was greater in the p53 mutated cell lines. Sensitiser enhancement ratios for PARP and Chk1 as mono-inhibition were modest (around 1.5), however the combination of agents produced sensitiser enhancement ratios of above 2. The combination of Chk1 and PARP inhibition caused G2/M dysfunction, inhibition of HR and persistent DDR. The combination treatment did not appear to radiosensitise normal intestinal epithelial cells *in vitro*. The authors speculated that the HR deficiency induced by Chk1 inhibition may sensitise to PARP inhibition via generation of a ‘BRCAness’ phenotype.

Introduction

Hoglund et al demonstrated that the combination of PARP inhibition and Chk2 functional loss elicits a synthetic lethal response in Myc overexpressing lymphoma cells (Hoglund et al., 2011). Booth et al investigated the effects of PARP and Chk1 inhibition in mammary cells and found that PARP inhibition and Chk1 inhibition produced cytotoxic effects (Booth et al., 2013). Furthermore the actions of PARP and Chk1 inhibition were enhanced by ATM knockdown. Peasland et al documented a synthetic lethal effect of the combination of the ATR inhibitor NU-6027 and PARP inhibition (Peasland et al., 2011). However these studies did not include ionising radiation.

Clearly the combination of different DDR inhibitors has the potential to enhance the effects of radiation, and given the redundancy encountered within DDR pathways this may represent a particularly effective way of inducing potent radiosensitisation of resistant cancers. Nevertheless the effects of combination DDR inhibition on normal tissue toxicity will require careful consideration.

1.5 DDR inhibition and GBM CSCs

Investigation of the clinical effects of inhibition of DDR has centred on commercially available cell lines in a broad spectrum of tumour sites, and there are relatively few studies of DDR inhibition and its effects on CSCs. Given that several authors have documented upregulation of DDR in GBM CSCs, DDR inhibition would appear to be an ideal strategy for increasing CSC radiosensitivity.

GBM CSCs were shown to exhibit autophagy as a mode of cell death after knockdown of DNAPKcs in a study by Zhuang et al (Zhuang et al., 2011). CSCs were radiosensitised following knockdown of DNAPKcs however did not exhibit a marked apoptotic response.

Kahn et al investigated the effects of mammalian target of rapamycin complex 1 and 2 (mTORC1m/mTORC2) inhibition on GBM CSC cultures (Kahn et al., 2014). mTORC inhibition by the compound AZD2014 significantly radiosensitised CD133+

Introduction

and CD15+ GBM CSCs isolated from 4 different primary GBM cell lines with SER_{0.1}'s of 1.3-1.5. mTORC inhibition has a small but significant effect on GBM CSC survival in the absence of radiation. This was associated with an increase in unresolved gamma H2AX foci at 24 hours, however no alteration in G2/M checkpoint activation could be detected. *In vivo* studies of orthotopic xenografts showed addition of mTOR inhibition to radiotherapy prolonged survival in mice.

The effects of Chk1 kinase inhibition on GBM CSC radioresistance was studied in the paper by Bao et al (Bao et al., 2006a). Chk1 is consistently upregulated in CSC populations as shown by several investigators, and as such it presents an obvious target for radiosensitisation strategies (Bao et al., 2006a, Ropolo et al., 2009). Bao et al utilised the Chk1/Chk2 inhibitor debromohymenialdine (DBH) and demonstrated that exposure to this agent abrogated CSC radioresistance. However formal clonogenic survival assay was not undertaken, and DBH is known to lack specificity for Chk1 kinase, (see section 1.2.8).

Venere et al investigated the radiosensitising effects of PARP-1 inhibition on GBM CSCs, as discussed earlier in this chapter (Venere et al., 2014). PARP-1 inhibition with olaparib was found to have significant radiosensitising effects on GBM CSCs, however this was not quantified by clonogenic assay.

Raso et al investigated the response of GBM CSCs to radiation plus ATM inhibition (Raso et al., 2012). The authors of this study characterised two glioma cell lines, one of which expressed high levels of CSC markers and the other low or nearly absent expression of a panel of nine CSC markers. Effects of ATM inhibition and radiation were assessed by a cell viability assay. The authors demonstrated radiosensitisation of the CSC marker high expressing cell line. In contrast to this however ATM inhibition appeared to exert a radioprotective effect in the cell line showing poor expression of CSC markers. Culture of the CSC marker expressing cell line in differentiating media removed the radiosensitising effect of ATM. The comparison of two non-isogenic cell lines is problematic in this study, however it is of interest that ATM inhibition only had a radiosensitising effect on CSC populations. Nevertheless it is difficult to reconcile the central position of ATM in the DDR to ionising radiation with a radioprotective effect.

Introduction

Biddlestone-Thorpe et al also conducted an investigation into the radiosensitising effects of ATM inhibition via neurosphere generation assay involving a cell line derived from a genetically engineered mouse model of glioblastoma (Biddlestone-Thorpe et al., 2013). ATM inhibition and radiotherapy was found to significantly reduce the generation of neurospheres. Although these studies have shown ATM inhibition to have effects on DDR and radiosensitivity on GBM CSCs, there is clearly a requirement for further investigation of the effects of ATM inhibition in CSCs.

GBM produce abundant transforming growth factor beta (TGFB) which is known to promote effective DDR. The effects of TGFB on GBM CSCs were investigated by Hardee et al (Hardee et al., 2012). Inhibition of TGFB in combination with radiation produced a marked decrease in neurosphere formation and was shown to decrease DDR as assessed by gamma H2AX and 53BP1 and also reduce induction of self renewal signals Notch1 and CXCR4.

1.6 Conclusion

The emergence of CSC theory in recent decades and the accumulating evidence for its existence in GBM has led to investigators questioning the role of this malignant cellular subpopulation in the clinical behaviour of GBM. The existence of a subpopulation of tumour cells with the properties of self renewal, maintained proliferation and multi lineage differentiation immediately alters the priorities of oncological therapy. If the existence of a CSC population is accepted, then eradication of this tumour cell population becomes the primary aim of curative therapy.

As discussed above, evidence suggests that the cancer stem -like cell population is resistant to many current oncological therapies. Radioresistance of GBM CSCs in particular has received much attention in the scientific literature and this particular property of CSCs is an elegant explanation for the clinical behaviour of

Introduction

this disease. However, the evidence for radioresistance in CSCs is not yet compelling. The original report by Bao et al has not been confirmed by subsequent investigations, and some reports have conflicted with the results of this seminal study. There is a paucity of data quantifying GBM CSC radioresistance in isogenic cell lines using the radiobiological standard of clonogenic survival assay. Furthermore conclusions from existing data are complicated by extensive use of the CD133 marker to define GSCs. Although clearly associated with the CSC state in some tumours, the CD133 marker is not universal for CSCs and this may have contributed to discrepancies in the scientific literature regarding CSCs. Likewise detailed mechanistic studies of CSC checkpoint activation and comprehensive analyses of DNA DSB repair incorporating cell cycle effects have not been demonstrated in the literature. There is therefore a need to undertake these studies in order to clarify and confirm the putative radioresistance of CSCs.

Small molecule DDR inhibitors facilitate the manipulation of DDR in cancer cells to allow sensitisation to radiotherapy, whilst theoretically having little effect on the radiation tolerance of normal tissues. Potentially this could bring significant clinical benefits for patients in terms of local control, palliation and cure, since radioresistance is an important reason for the failure of therapy. However the potential use of DDR inhibitors in GBM CSCs has not been extensively explored. Given data suggesting preferential activation of DDR in CSCs, the manipulation of DDR could provide the means to abrogate putative CSC radioresistance. Furthermore inhibition of specific elements of DDR may allow additional insights into the mechanisms of glioblastoma CSC DNA damage response.

1.7 Aims and objectives

1.7.1 Aims

- 1) To investigate the proposed radioresistance of glioblastoma CSCs
- 2) To characterise the putative upregulated DNA damage response of glioblastoma CSCs and its effects on radioresistance

Introduction

- 3) To investigate the modification of radioresistance in glioblastoma cancer stem-like cells by inhibition of key components of the DNA damage response

1.7.2 Objectives

- 1) To quantify the radioresponse of glioblastoma CSCs using clinically relevant radiobiological assays
- 2) To interrogate altered DNA damage response to radiation in glioblastoma CSCs via *in vitro* quantification of major DDR kinases, assessment of cell cycle responses and assays of DNA double strand break repair
- 3) To quantify the *in vitro* radiosensitising effects of DDR kinase inhibition on GBM CSCs using small molecule DDR inhibitors via clonogenic survival assays
- 4) To investigate the effects of small molecular DDR kinase inhibition on GBM CSC responses to radiation by *in vitro* assays of cell cycle effects and DNA double strand break repair

Chapter 2 Materials and Methods

2.1 Cell culture

All experiments involving primary and commercially available GBM cell lines were performed in a Class II sterile laminar flow hood, using supplied sterile plastic ware and solutions. Aseptic technique was maintained in order to avoid contamination.

2.1.1 Source and derivation of primary GBM cell cultures

The E2, G7 and R10 cell lines were gifted by Dr Colin Watts, University of Cambridge, UK. These cell lines were derived from freshly resected GBM specimens, by the Watts' laboratory in Cambridge. Tissue samples were obtained in accordance with local ethical guidelines. Anonymised tissue was mechanically minced in modified phosphate buffered saline solution (PBS) prior to enzymatic digestion. Single cells were then isolated by filtration through a 40 μ m filter (Falcon, UK) and washed with 10ml red blood cell lysis buffer. Live cells were quantified by trypan blue exclusion, seeded at standard density of 15 000 cells/cm² in CSC media (defined below) and allowed to form primary aggregates. These were collected and plated, without dissociation, onto extracellular matrix (ECM) coated flasks (ECM 1:10 dilution, Sigma, UK) and allowed to form a primary monolayer. As the primary monolayer approached confluence cells were dissociated by incubation with Accutase (Life Technologies) at room temperature and washed with PBS. The cell viability was assessed by light microscopy and cells were reseeded onto ECM-coated flasks at a density of 150 cells/cm² to generate the secondary monolayer. To generate subsequent monolayers cells were seeded at standard density 15 000 cells/cm² at each passage. Cell numbers were expanded in this fashion and aliquots frozen at -80°C in DMSO as a cryopreservant before being transferred to liquid nitrogen.

Materials and Methods

2.1.2 Culture of paired GBM CSC and tumour bulk populations

CSC cultures were maintained in stem cell enriching conditions, in CSC media. This consisted of Adv DMEM F12 medium (Gibco) supplemented with 1% B27 (Invitrogen), 0.5% N2 (Invitrogen), 4 μ g/ml heparin, 20ng/ml fibroblast growth factor 2 (bFGF, Sigma), 20ng/ml epidermal growth factor (EGF Sigma) and 1% L-glutamine. Monolayer CSC cultures were seeded onto MatrigelTM at 1:40 dilution (matrigel : media) coated plastic tissue culture flasks or plasticware. Neurosphere cultures did not require MatrigelTM coated plasticware.

Tumour bulk cultures were derived from CSC cultures by culture in differentiating media for at least 5 passages. This consisted of MEM (Gibco), supplemented with 10% foetal bovine serum (FBS Sigma), 1% L-glutamine and 1% sodium pyruvate. Tumour bulk cultures were grown as adherent monolayers on uncoated plasticware, or for clonogenic assays on MatrigelTM coated plastic ware to minimise experimental variation.

2.1.3 Growth conditions

Tumour bulk cell and CSC cultures were grown as adherent monolayers in flat sided flasks (Corning) of 75cm² and 150cm² containing 10 or 20ml of CSC or differentiating medium respectively in a 37°C humidified incubator, (Galaxy) at 5% CO₂ in air, (21% O₂), gas concentration. Cell cultures were maintained at 37°C, 5% CO₂, 21% O₂ and routinely passaged every 3-4 days. For all experiments, low passage number cells were used (maximum 20, but more commonly 5 to 15).

2.1.4 Serial passaging of cells

Passaging of cells was performed when cells were 70-80% confluent from microscopic appearance. Medium was aspirated off and the cell monolayer washed with phosphate buffered saline solution (PBS Gibco) to remove any remaining medium. Cell monolayers were then treated with 0.5ml Accutase (Gibco) and returned to an incubator for 5 minutes in order for the cells to detach from the growth surface and the flask was agitated. 5ml of media was

Materials and Methods

added to the cell suspension, the suspension was centrifuged at 2000rpm for 2 minutes and media discarded. Cells were then distributed into new flasks with appropriate media, noting the passage number.

2.1.5 Counting cells

Cells were detached from monolayers and centrifuged. 3ml of media was added to the pellet and a single cell suspension created by passing media and cells through a 19 gauge needle 10 times. A further 7ml of media was added and the suspension thoroughly mixed. 10 μ l of suspension was added to each chamber of a haemocytometer and the number of cells in the 3 vertical large squares of the middle column of each chamber was counted. The mean cell count ‘C’ of the two chambers was calculated and the number of cells per ml of suspension was equal to C x 10⁴.

2.1.6 Cell storage and cryopreservation

Cells were detached from monolayers and centrifuged as described. Cells were resuspended in cryopreservative medium, consisting of 1ml DMSO plus 9mls of media. Approximately 1 x10⁶ cells were aliquoted into cryo-vials (Corning) and cells were initially frozen at -80°C before being transferred to liquid nitrogen for long term storage.

2.1.7 Thawing cells from liquid nitrogen

Cryo-vials were removed from liquid nitrogen and thawed rapidly in a 37°C water bath. The thawed cell suspension was then transferred to a 75cm² flask containing 20ml of medium. Cells were allowed to adhere overnight and medium was changed the following day.

Materials and Methods

2.2 Western blot analysis of DDR protein levels

2.2.1 Sample preparation

Cells were harvested from 10cm diameter petri dishes. Medium was aspirated and a PBS wash performed prior to application of 100 μ l of cell lysis buffer (1% sodium dodecyl sulphate (SDS) as an ionic detergent, 50mM Tris pH6.8) plus a protease and phosphatase inhibitor cocktail (Roche). A cell scraper was used to homogenise the lysate and lysate was then passed through a cell shredding spin column (Qiagen). Supernatant was collected and stored at -20°C.

2.2.2 Protein estimation

The PIERCE BCA protein assay kit (PIERCE) was used to estimate the protein concentrations of cell lysates. This assay involves the reduction of Cu²⁺ to Cu⁺ by proteins in the presence of an alkali medium. The Cu⁺ ion is able to chelate two molecules of bicinchoninic acid (BCA) to form a stable purple coloured complex that can be detected at 562nm by spectrophotometer.

Bovine serum albumin (BSA) was used as a standard at various concentrations ranging from 0.2mg/ml to 2mg/ml, and plated in triplicate wells of a 96 well plate. Experimental samples were diluted at a 1:5 ratio in lysis buffer and again plated in triplicate in a 96 well plate. BCA reagents A and B were mixed in the ratio 50:1 and 190 μ l of the mixture was pipetted into each well of the test 96 well plate. Test plates were incubated at room temperature for 30 minutes before being read using a spectrophotometer (Tecan Infinite M200 Pro). The protein concentration of each sample was calculated using linear regression based on the equation obtained from the standard curve of BSA protein standards.

2.2.3 Gel electrophoresis of protein

50mcg of protein was mixed with LDS sample buffer (NuPage) with 5% beta mercaptoethanol (Sigma) and made up to a maximum volume of 25 μ l.

Materials and Methods

Bromophenol blue within the LDS sample buffer allows monitoring of progress of the samples within the gel whilst beta mercaptoethanol denatures samples further by breaking down disulphide bonds. Samples were heated at 100°C for 5 minutes. Samples were then loaded into lanes of either a 4-12% Bis-Tris (NuPage) or 3-8% Tris-Acetate (NuPage) precast gel depending on the molecular weight of the protein to be probed for. 10µl of protein standard (PageRuler Preset or Himark prestained, Invitrogen) was loaded in a parallel lane to allow visualisation of the approximate molecular weight of the detected protein in the test cell lysates to be determined. Electrophoresis of gels was carried out over 1 hour and 30 minutes at 150V using an Invitrogen Mini Cell electrophoresis tank with approximately 700mls of electrophoresis buffer (see appendix 1). Following electrophoresis the gel was removed in preparation for protein transfer.

2.2.4 Protein transfer

Following electrophoresis the gel was transferred into a Biorad mini protean tetra system tank filled with transfer buffer (see appendix 1). Two pieces of fibre pad, filter papers and PVDF membrane (Whatman Pro) were soaked in transfer buffer. The fibre pad, filter paper and gel were then loaded into a cassette, which was placed within a transfer tank in an orientation ensuring migration of proteins toward the nitrocellulose membrane. The electrophoretic transfer was run overnight at 30V.

2.2.5 Immunodetection

Specific antibodies were used to detect the presence of proteins of interest. Following transfer of proteins, membranes were removed from the transfer apparatus and placed in TBS-Tween (see appendix 1) containing 5% non-fat milk (Marvel) (TBSTM) on a rocking platform for 1 hour to block non-specific binding sites on the membrane. Membranes were cut in order to facilitate analysis of multiple proteins of interest. Following blocking, membranes were placed into 5mls of TBSTM or TBST containing 5% bovine serum albumin (Invitrogen) with an appropriate dilution of primary antibody, (see table 2.1). Membranes were incubated on a rocking platform at 4°C overnight and then washed 3 times in

Materials and Methods

TBST before incubation with an appropriate horse-radish peroxidase (HRP) conjugated secondary antibody in TBSTM for 1 hour at room temperature (see table 2.2). Following this, membranes were washed for 10 minutes in TBST and this was repeated 4 times. Protein visualisation was carried out using an enhanced chemiluminescent (ECLtm) kit (Fisher Scientific). The reagents rely upon the HRP-catalysed oxidation of luminol to an excited state in the presence of hydrogen peroxide, which results in the production of visible light as it decays to the ground state. ECL reagents were mixed in the ratio 1:1 and applied to membranes. Membranes were wrapped in plastic film and placed in apposition with high performance photographic film (Carestream Kodak Biomax MR Film) in a dark room for periods of 30 seconds-8 hours in order to achieve optimum band intensities.

2.3 Clonogenic survival analysis

2.3.1 Procedure

6 well plates (Corning) were coated with Matrigeltm at a 1 in 40 dilution. Single cell suspensions of CSCs and tumour bulk cells were prepared and counted as above. 250 cells were aliquoted in a volume of 2mls of medium into each well of the 6 well plates and incubated overnight. Prior to irradiation, medium was aspirated from the plates and replaced with 1ml of medium containing DDR inhibitor in DMSO, an identical concentration of DMSO alone, or medium without DDR inhibitor or DMSO. 6 well plates were then returned to the incubator for 1 hour prior to irradiation. Exposure of individual plates to 0, 1, 2, 3, 4 and 5Gy of radiation was undertaken during each assay; 0Gy control plates were sham irradiated. After irradiation plates were incubated for a period of 24 hours; following this drug or DMSO containing medium was aspirated and replaced with 2mls of fresh medium which did not contain DDR inhibitor agent or DMSO and the plates were incubated for a further 2 weeks in the case of the E2 and R10 cell lines or for 3 weeks in the case of the G7 cell line to allow adequate (>50 cells per colony) colony formation. All control plates were subject to the same number and timing of medium changes throughout the experiment. CSCs were maintained in CSC media throughout the entire assay, and tumour bulk cultures were maintained in differentiating media throughout the entire assay.

Materials and Methods

After this period, colonies were fixed and stained. Medium was aspirated and 1ml of 50% methanol-PBS was aliquoted into each well and left for 15 minutes. This was then replaced by 1ml of methanol (Sigma) and the plates left for a further 15 minutes. Following methanol fixation, colonies were stained with a 1:25 solution of crystal violet/PBS (Sigma) for 3 hours before stain was removed and the plates dried overnight. Colonies of >50cells were counted manually.

2.3.2 Analysis of clonogenic survival assay

Colony counts were obtained from triplicate wells for each condition and each independent experiment was repeated a minimum of 3 times. Only colonies of greater than 50 cells were counted. A mean colony number for each experimental condition from these data was obtained and plating efficiency (PE) calculated by dividing mean number of colonies by the number of cells plated, (250 cells per well). Surviving fractions (SF) were then calculated by dividing the PE of the experimental condition by the PE of the unirradiated control. In the case of DDR inhibitor treatments, SF was calculated with reference to the unirradiated DDR inhibitor exposed control plate, therefore ensuring effects of DDR inhibition in the absence of radiation were taken into account during analyses of clonogenic survival data.

Survival curves are conventionally presented with dose plotted on a linear scale on the x axis and surviving fraction plotted on a logarithmic scale on the y axis. The shape of the survival curve in response to gamma radiation can be described by the linear quadratic model, (Brenner and Hall, 1992). This model describes radiation induced cell killing due to a linear component which is proportional to radiation dose and a quadratic component which is proportional to the square of the dose, (see equation 2.1). A biological interpretation of the linear quadratic model has been attempted, however reconciliation of molecular events and mathematical theory requires much simplification of biological events. In brief it is proposed that lethal lesions induced by single DNA damaging events account for the linear component of the survival curve, whereas the combination of single DNA damaging events to create a lethal lesion accounts for the quadratic

Materials and Methods

component. The linear quadratic model is utilised in clinical practice to compare relative biological effects of different radiotherapy fractionation schedules.

$$SF = \exp(-\alpha d - \beta d^2)$$

Equation 2.1 The linear quadratic equation

Data derived from clonogenic survival experiments were fitted to a linear quadratic model. Regression analysis allowed curve fitting to be performed. Modelling data on the linear quadratic equation also enabled sensitiser enhancement ratios at 0.37 survival (SER_{0.37}) and dose modifying factors for 0.37 survival (DMF_{0.37}) to be estimated. These calculations are detailed in equations 2.2 and 2.3.

$$SER_{0.37} = \frac{d_{0.37}(\text{no drug})}{d_{0.37}(\text{drug})}$$

Equation 2.2 SER_{0.37} ratio

$$DMF_{0.37} = \frac{d_{0.37}(\text{CSC})}{d_{0.37}(\text{tumour bulk})}$$

Equation 2.3 DMF calculation

2.4 Irradiation of cells

Irradiation of all cell cultures was carried out using an XStrahl RS225 radiation unit. This unit generates 195kV X rays. Monolayer cell cultures in T75 flasks with 5ml of media were placed on a Perspex baseboard inside the unit avoiding the penumbra of the radiation field as defined by the distance between the 80% and 20% isodoses as measured by ion chamber. 195kV X rays were delivered using a

Materials and Methods

current of 15mA, which provided a dose rate of 1.5Gy per minute at a distance of 400mm from source.

2.5 Neurosphere assay

Single cell suspensions of CSC cultures were made and cell counts performed. Cells were added to medium in a 50ml test tube (Falcon), in order to achieve a cell dilution of 10 cells per 100 μ l of media. For experiments with DDR inhibitor agents, DDR inhibitor in DMSO, or a corresponding volume of DMSO as a control was added prior to the addition of cells to the medium. The tube was agitated in order to achieve an even dispersal of cells. 100 μ l of the cell suspension was then aliquoted into each well of a 96 well plate in order to achieve a dilution of 10 cells per well. The plates were placed in an incubator at 37°C for one hour prior to irradiation. Each plate was irradiated with 2Gy, or sham irradiated in the case of controls and then returned to the incubator. A further 150 μ l of medium was added to each well 48 hours following irradiation in order to dilute DDR inhibitor drugs. Control plates were treated in a similar manner. 96 well plates were incubated for a period of 3 weeks in the case of the G7 cell line or 4 weeks in the case of R10 and E2 cells lines. Neurospheres were imaged using an Optronix™ Gelcount machine. Neurospheres were assessed and counted manually from images produced by the Optronix™ Gelcount software. Neurosphere diameters were obtained from the same images.

2.6 Gamma H2AX foci analysis

2.6.1 Procedure

19mm diameter circular glass coverslips were placed in the wells of 12 well plates (Corning). These were coated with Matrigel™. Single cell suspensions were created and counted, and 1ml of medium containing 4×10^4 cells was added to each well. Plates were then incubated overnight at 37°C. Both CSC and tumour bulk monolayers were grown on Matrigel™ coated coverslips. Prior to irradiation medium was removed and replaced with medium containing DDR inhibitor agent, or medium containing a similar concentration of DMSO as control. Plates were incubated for 1 hour prior to irradiation as before.

Materials and Methods

intervals following irradiation, medium was removed, cells were washed in PBS and then fixed in 4% paraformaldehyde/PBS for 15 minutes. Paraformaldehyde was then removed and replaced with 1ml PBS and plates were stored at 3-5°C.

2.6.2 Immunostaining

Fixed cells on coverslips were removed from PBS and permeabilised by the addition of 3% Triton-PBS solution for 5 minutes on a rocking platform. 3% Triton-PBS was then aspirated and blocking buffer (0.1% Triton-PBS plus 5% FCS plus 0.5% BSA) subsequently added for a period of 30 minutes on a rocking platform to block non-specific antibody binding sites. A dilution of primary antibody was made in antibody buffer (1% BSA in 0.05% Triton-PBS) and 60µl of this solution was aliquoted onto Parafilmtm, and inverted coverslips were placed on top of the primary antibody/buffer onto Parafilmtm. In the case of gamma H2AX and centromere protein F (CENPF) staining, primary antibodies to these two antigens were incubated simultaneously at 5°C overnight. Following incubation in the primary antibody, coverslips were washed 3 times in 0.05% Triton-PBS on a rocking platform 1 minute per wash. Coverslips were then incubated in antibody buffer with secondary Alexa Fluoro conjugate antibody for 1 hour at 5°C in darkness. Coverslips were washed 3 times in 0.05% Triton PBS and mounted onto glass histology slides with 15µl of 4,’6-Diamidino-2-Phenylindole (DAPI) (Vector laboratories). Coverslips were sealed with nail varnish and allowed to dry.

2.6.3 Confocal microscopy

Z stacks of immunofluorescent staining of cells were obtained on a Zeiss 710 confocal microscope. A minimum of 4 sections were obtained per Z stack at depths of 2.5µm. Microscope settings were kept constant between all experimental conditions.

Materials and Methods

2.6.4 Quantification of gamma H2AX foci

Gamma H2AX foci are commonly quantified manually, leading to significant inter (and intra) observer variation in counts obtained. Often nuclei are scored simply as positive or negative for gamma H2AX foci, or an arbitrary cut off of 10 foci per nucleus is used to define high and low levels of gamma H2AX foci, (Kinner et al., 2008). In order to quantify foci per nucleus in this study, Volocty™ software was utilised in order to provide an image analysis solution for foci quantification. A protocol was developed which allowed automated counting of gamma H2AX foci within DAPI and CENPF stained nuclei. Z stack images were processed by maximum intensity projection (Zen software, Zeiss) to allow quantification. A validation process comparing Volocty™ foci counts in cell nuclei at 1 hour following irradiation was performed (fig 2.1). Median values in this data set of 66 cells from 8 images were not significantly different between automated and manual counting processes.

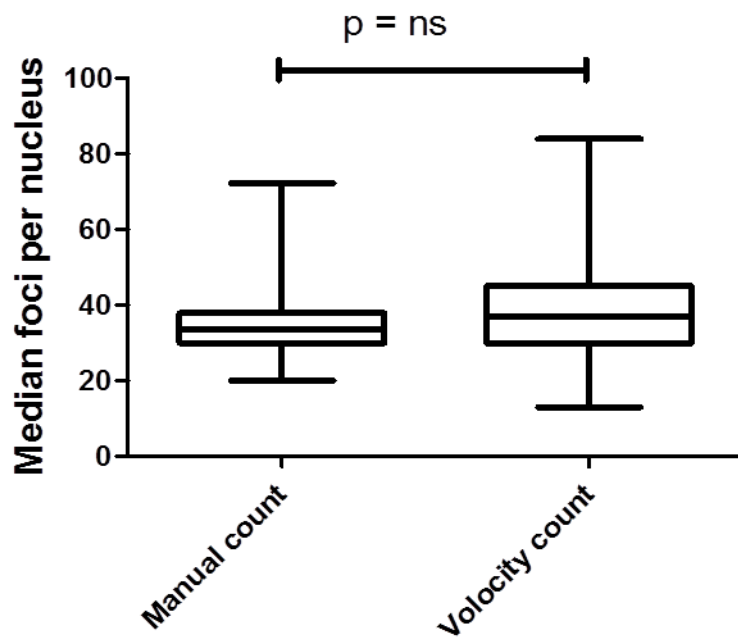


Figure 1.1 Comparison of manual and automated gamma H2AX foci counts by Volocty software.

Gamma H2AX immunofluorescence analysis at 1 hour post 1Gy in the E2 CSC cell cultures in CENPF negative populations. Foci counts were scored manually initially and then quantified using Volocty software; data were summarised by use of the median foci count per nucleus. Medians were compared using the Mann Whitney U test. P value was non-significant.

Materials and Methods

2.7 Neutral Comet Assay

Neutral comet assay is a gel electrophoresis based method which allows detection of DNA DSBs in individual eukaryotic cells, (Olive and Banath, 2006). The main advantage of neutral comet assay is that it provides a direct assay of DNA DSBs which is not dependent on the integrity of DSB signalling, unlike gamma H2AX foci analysis. However there are limitations of the neutral comet assay. It is a relatively insensitive measure of DNA DSBs and can only be used to detect DNA DSBs over a range of around 50 - 10,000 breaks per cell. Some DNA damage (including DSBs), can be repaired rapidly, and unless repair is inhibited, problems in detecting DSBs can be encountered at late timepoints following irradiation. Large doses of radiation are required to initiate DNA damage which is detectable by neutral comet assay. Doses of 20Gy and above are required to provide a quantity of DNA damage reliably detectable by neutral comet. These large doses are not reflective of radiation doses used in clinical practice.

2.7.1 Procedure

Cell cultures in T75 flasks were incubated in media containing ATM inhibitor or a corresponding concentration of DMSO for one hour prior to irradiation. Cell cultures were placed on ice immediately after irradiation in order to inhibit DNA repair. Single cell suspensions in Ca^{2+} free PBS (Trevigen) were made from each experimental condition and cell counts performed. Single cell suspensions were then placed on ice. Suspensions of bleomycin treated control cells supplied by the manufacturer were also prepared in Ca^{2+} free PBS. Low melting point agarose was heated to 100°C in a water bath until molten and then transferred to a 40°C water bath. Cell density of the single cell suspensions was adjusted to 2×10^4 cells/ml. 0.4ml of agarose/cell suspension was mixed with 1.2ml of molten agarose. 50 μ l of agarose/cell suspension was then pipetted onto a comet slide (Trevigen) and left at 4°C to set for 10 minutes. Slides were then submerged in neutral comet lysis buffer (Trevigen) at 4°C for 1 hour. Slides were then submerged in a Tris-Acetate (TA) electrophoresis buffer (see appendix 1) for 30 minutes at room temperature. This procedure was repeated 2 more times. Slides

Materials and Methods

were then submerged in TA buffer in a Trevigen electrophoresis chamber and electrophoresis at 21V was carried out for 45 minutes at 4°C. Slides were then immersed in DNA precipitation buffer (see appendix 1) for 30 minutes and following this were immersed in 70% ethanol-PBS for 30 minutes at room temperature. Slides were then dried at 37°C for 10-15 minutes. 100µl of diluted SYBR-Green (Life-technologies) DNA stain was placed onto each circle of dried agarose and left for 30minutes at room temperature. Excess stain was removed and the slides were allowed to dry completely.

2.7.2 Visualisation and quantification

Comets were visualised by epifluorescent microscopy. Analysis of neutral comets was performed by quantification of the Olive tail moment; a measurement which is defined as the product of tail length and the fraction of total DNA in the tail. Olive tail moment was measured using ImageJ software, using a specific comet assay plugin available at: www.med.unc.edu/microscopy/resources/imagej-plugins-and-macros/comet-assay.

2.8 Immunohistochemistry of formalin fixed, paraffin embedded tumour sections

2.8.1 Procedure

5µm thickness formalin fixed paraffin embedded (FFPE) tissue sections on glass slides were utilised. Sections were deparaffinised in xylene for 5 minutes and then transferred through 99% alcohol for one minute (two changes) and 95% alcohol for one minute (two changes) and then rinsed in tap water. Endogenous peroxidase was blocked by incubating sections in 3% hydrogen peroxide solution for 15 minutes. Antigen retrieval was achieved by boiling sections in citrate buffer solution (see appendix 1), using a pressure cooker and microwave oven. A Vectastain Universal Elite ABC kit was used for immunochemical staining. Blocking of non-specific antibody binding sites was achieved by incubating sections at room temperature for 30 minutes in blocking buffer, (consisting of 1 drop horse serum in 5ml Optimax buffer, Optimaxtm). Primary antibodies were then diluted in Optimax buffer and applied to tissue sections and incubated at

Materials and Methods

4°C overnight. Tissue sections were then washed in PBST (0.2% Tween 20-PBS) for 3 minutes and the wash repeated 3 times. The universal secondary antibody was then applied to the sections and sections were incubated at room temperature for 30 minutes, (2 drops of universal biotinylated secondary antibody, 2 drops horse serum, 5ml Optimax buffer). Sections were washed in PBST on a rocking platform for 6 minutes and the wash repeated 3 times in total. Avidin Biotin HRP complex was prepared by adding 2 drops horse serum, 2 drops of bottle ‘A’, 2 drops of bottle ‘B’ to 5ml of Optimax buffer. 300µl of Avidin Biotin HRP was applied to each section and sections were incubated at room temperature for 30 minutes. Sections were then washed in PBST 3 times over 20 minutes. Vector DAB substrate (3,3’ diaminobenzidine) produces a brown reaction product in the presence of peroxidase (HRP) enzyme. Vector DAB substrate was prepared by adding 84µl of Vector DAB buffer solution, 84µl hydrogen peroxide solution and 200µl DAB stock solution to 5ml of distilled water. Sections were covered in DAB substrate solution and left for 7 minutes until brown staining developed. Excess DAB was disposed of and sections were washed in tap water for 5 minutes. Sections were counterstained with haematoxylin, nuclei were stained with Scotts Tap water and sections were washed once more. Sections were transferred through 95% and 99% alcohol and xylene as before and a coverslip applied to the slides. For each batch of immunohistochemical staining a negative control was present; one tissue section was treated as per the above protocol, however the primary antibody step was omitted.

2.9 Sanger sequencing of p53 in primary GBM cell lines

DNA extraction from E2 CSC, E2 bulk, G7 CSC, G7 bulk and U87 cell lines was performed using a Qiagen DNEasy kit. In brief 5×10^6 cells were centrifuged and resuspended in PBS. 20µl of proteinase K was added. 200µl of buffer ‘AL’ was added and the suspension mixed with an equal volume of ethanol. The mixture was centrifuged in a DNeasy spin column and the flow-through discarded. 500µl of buffer ‘AW1’ was added and the tube centrifuged and flow-through discarded. 500µl of buffer ‘AW2’ was then added and the tube centrifuged and flow-through discarded. DNA was eluted by the addition of buffer ‘AE’ and incubation

Materials and Methods

for 1 minute at room temperature, followed by centrifugation. This step was repeated and extracted DNA stored at -20°C.

Polymerase chain reaction (PCR) was carried out in order to amplify the relevant DNA for Sanger sequencing. Forward and reverse primer sequences covering exons 3 to 10 of the p53 gene were gifted from Dr Patricia Roxburgh (Beatson CRUK Institute, Glasgow). These are detailed in appendix 2. Corresponding oligonucleotide sequences were obtained from Sigma, UK. Lyophilised oligonucleotides were suspended in DNA/RNA free water at a concentration of 200µM, from which a 1:10 diluted working stock was prepared. PCR reagents were obtained from the Qiagen Core Taq PCR kit. 0.2ml thin walled RNA/DNA free reaction tubes (Thermoscientific) were used for PCR reactions. 4µl of genomic DNA (gDNA) was placed in each reaction tube. A master mix containing 1.2µl magnesium chloride (25mM), 4µl PCR buffer, 0.8µl dNTP mixture, 2µl primer stock, 37.6µl water per tube was then added to each reaction, followed finally by 0.4µl Taq polymerase. A negative control containing PCR mastermix and Taq only was run simultaneously to detect spurious DNA contamination of the mastermix preparation.

PCR reactions were run at 94°C for 5 minutes followed by 50 cycles of 96 °C for 10 seconds, 60 °C for 1 minute, and 72 °C for 1 minute. A final annealing temperature of 72 °C for 10 minutes was used with subsequent incubation at 15 °C. A Biorad DNA engine Tetrad 2 was used to carry out PCR reactions.

Amplified DNA was purified by gel electrophoresis. A 2% agarose gel was prepared by dissolving 2g of agarose in 100ml of Tris/Acetate/EDTA (TAE) buffer (see appendix 1). Ethidium bromide (Life Technologies) was added to the gel to a final concentration of 0.2µg/ml. The gel was then cast in the base of an electrophoresis tank and allowed to set at 4°C. 4 µl of DNA loading buffer was added to each PCR product and mixed. 10µl of Generuler 100bp ladder was added to the first lane of the gel and samples loaded in parallel lanes. 300ml of TAE buffer was added to the electrophoresis tank and the gel was run at 80V for 2 hours. DNA bands were visualised by ultraviolet light and a scalpel was used to cut out the visible DNA bands from the gel which were placed into reaction

Materials and Methods

tubes. The Qiaquick extraction kit was used to extract DNA from the gel bands. In brief, the bands were weighed and 3 volumes of buffer ‘QG’ were added followed by incubation at 50 °C in a heatblock. 1 volume of isopropanol was added and the mixture transferred to a spin column. The column was centrifuged and flow-through discarded. This step was repeated. 750µl of buffer ‘PE’ was added and the sample centrifuged. 50µl of DNA elution buffer was added and the flow-through collected and stored at -20 °C. The DNA concentration of each purified PCR product was assayed by Nanodrop estimation.

Sanger sequencing of PCR products was carried out using an Applied Biosystems 3130 genetic analyser and was performed by William Clark and Andrew Keith, (CRUK Beatson Institute, Glasgow). In brief, Sanger sequencing involves the analysis of ssDNA. An oligonucleotide sequence is used to prime the sequence of interest, and initiates a cDNA elongation process via DNA polymerase. A mixture of normal deoxynucleosidetriphosphates (dNTPs; dATP, dGTP, dCTP, dTTP) and corresponding modified fluorescently labelled di-deoxynucleotidetriphosphates (ddNTPs) are supplied for the reaction. Different fluorophores allow detection of different ddNTP analogues. Elongation of cDNA occurs with the addition of dNTPs until a ddNTP is randomly incorporated. Incorporation of a fluorescently labelled ddNTP terminates the elongation reaction and results in the production of a DNA fragment with a fluorescently labelled terminal base. The length of the DNA fragment can be used to inform the position of a dNTP corresponding to the fluorescently labelled ddNTP. Separation of DNA fragments is achieved by gel electrophoresis using a denaturing polyacrylamide urea gel.

Sequence chromatograms generated by the Sanger method were read using ApE software, (<http://biologylabs.utah.edu/jorgensen/wayned/ape/>). Sequence from both forward and reverse primers was utilised and compared to published wild type p53 sequence, (http://p53.iarc.fr/TP53Sequence_NC_000017-9.aspx). Significance of mutations was determined by comparison of the mutated codon sequence to published tables of DNA codons and respective amino acids. The p53 database (http://p53.free.fr/Database/p53_database.html) was consulted for further information on any identified sequence changes in the p53 exons characterised by this study.

Materials and Methods

2.10 Flow cytometric analysis of cell cycle distribution and G2/M checkpoint activation

Flow cytometry was employed to provide analysis of cell cycle distribution and G2/M checkpoint activation.

Briefly, flow cytometry is a method of analysis of cell size, granularity and expression of cell surface markers or of ligands such as propidium iodide (PI) which bind to DNA. A flow cytometer allows the hydrodynamic focussing of a suspension of single cells. Single cells are therefore exposed to a laser one cell at a time. Cells or particles cause scattering of light as they pass through the laser light, which is detected as Forward Scatter (FS) and Side Scatter (SS). FS is light which is scattered at small angles relative to the incident laser light, whereas SS is light scattered at larger angles. FS provides information on cell size, whereas SS provides information on cell granularity. Based on FS and SS values, cells can be separated into different populations, and debris or dead particulate matter excluded. Furthermore, fluorochromes used for detection or staining of target molecules and proteins will emit light when excited by a laser with the corresponding excitation wavelength. Fluorescent stained cells can be detected individually and quantified.

2.10.1 Procedure

Cell cultures grown as monolayers to 30-50% confluence in T75 flasks were utilised. Cells were dissociated using accutase as above, centrifuged and pelleted in 15ml reaction tubes. Pellets were dissociated into single cell suspensions. Cells were then fixed in 70% ethanol and stored at 4°C.

Fixed cells were centrifuged and pelleted and ethanol removed by aspiration. Cell pellets were washed in 5ml 0.05% Triton-PBS and centrifuged. This process was repeated twice. 0.05% Triton-PBS was aspirated and each cell pellet was dissociated into a single cell suspension in 125 μ l of 0.05% Triton-PBS containing a 1:50 dilution of phosphorylated Histone H3 antibody-Alexa 488 conjugate, (see table 2.1) and transferred to a 1.5ml reaction tube. Reaction tubes were

Materials and Methods

incubated at 4°C on a rocking platform for 45 minutes. Reaction tubes were centrifuged and primary antibody mixture removed by gentle aspiration. Cell pellets were dissociated in 400µl of PBS containing 200µg/ml RNase A (to degrade RNA) and 10µg/ml PI and incubated for 10 minutes.

SS and FS characteristics were used to identify cells of interest and a region gate was applied using FloJo software to exclude cellular debris and doublet nuclei (Fig 2.2 and 2.3). The 488nm laser was utilised to excite both PI and alexa fluoro 488 conjugate primary antibodies. PI emission was collected by the FL32 channel (650585/42 emission filter) whilst the FL1 channel detected Alexa 488 emission (53085/3042 emission filter).

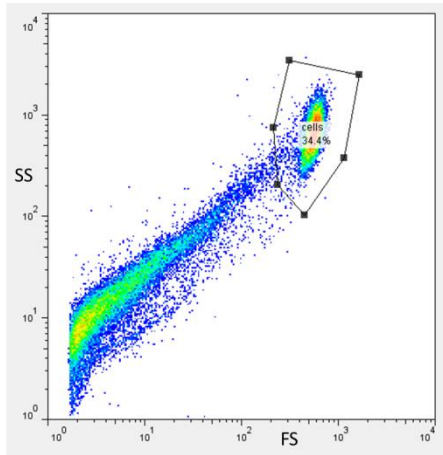


Figure 2.2 Region gating to exclude debris from flow cytometry analyses

Materials and Methods

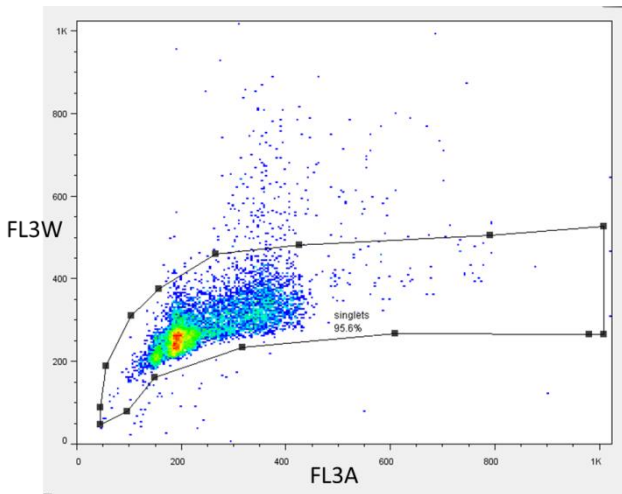


Figure 2.3 Region gating to exclude doublets from flow cytometry analyses

From the PI emission data a cumulative histogram was plotted. PI emission corresponds to DNA content, and allowed the visualisation of two distinct peaks (G1 and G2 phase cells). The amplitude PI signal intensity of the signal from G2 cells was double that of G1 cells. The PI intensity of S phase cells emitted a range of amplitudes is between the G1 and G2 peaks (fig 2.4). The application of a cell cycle profile using FloJo software allowed calculation of the numbers of cells in each phase.

Materials and Methods

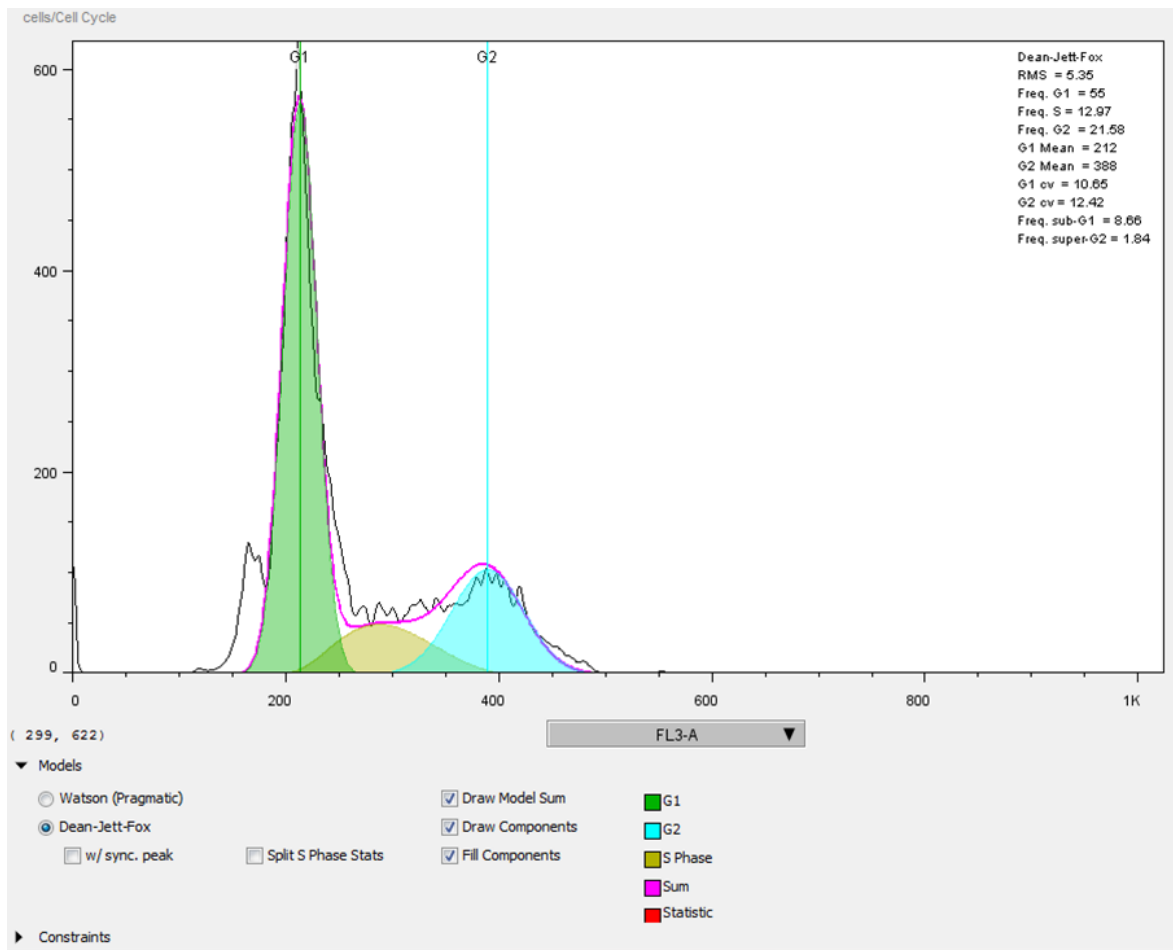


Figure 2.4 Example of cell cycle profile following analysis of PI stained cells using FlowJo software

For analysis of Alexa 488, FL1 signal was plotted against FL3A, and a regional gate was applied in order to facilitate quantification of G2 DNA content cells with bound pHisH3 antibody-alex488 conjugate (fig 2.5).

Materials and Methods

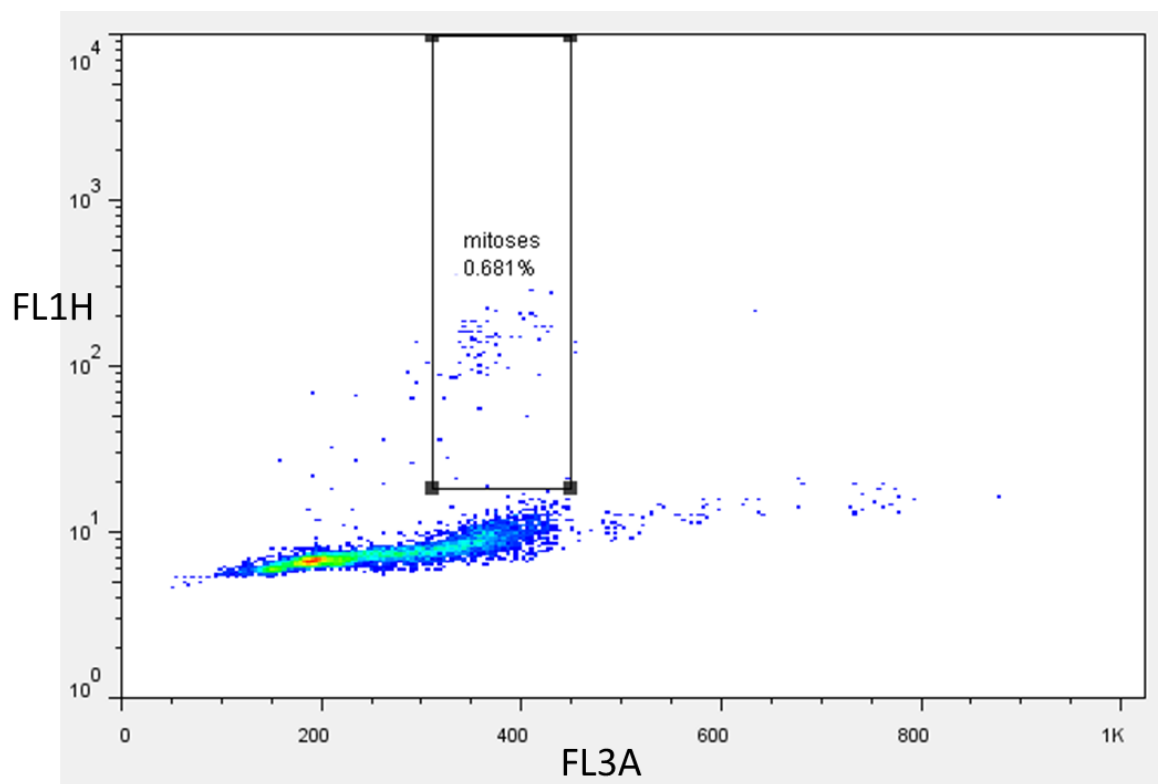


Figure 2.5 Example of regional gating applied to identify mitotic cells labelled with Phosphorylated Histone H3 (pHisH3) Alexa Fluoro 488 conjugate antibody

Materials and Methods

2.11 Cell viability assays

Cell cultures were plated into Matrigel™ coated 96 well plates at a density of 500 cells per well and incubated overnight in 100µl of media. Media was aspirated and replaced with 100µl of media containing DDR inhibitor agent or a corresponding concentration of DMSO. Plates were returned to the incubator for 24 hours, after which DDR inhibitor agent/DMSO media was removed and replaced with fresh media, or alternatively left in DDR inhibitor/DMSO media for a period of 6 days. After a total of 7 days from initial plating, plates were analysed for viable cells using the Cell Titer-Glo assay (Promega). Briefly, this assay relies upon a luciferase reaction, following the lysis of cells and provides a quantification of cell viability based on amount of ATP. Monooxygenation of beetle luciferin is catalysed by luciferase in the presence of Mg²⁺, ATP and oxygen, providing a luminescent signal which is proportional to the amount of ATP present. This can be quantified by means of a luminometer.

96 well plates were treated as per the manufacturer's protocol. 100µl of Cell Titer-glo reagent was added to each test well and the plate placed on an orbital shaker for 2 minutes to induce cell lysis. The plate was then incubated at room temperature for 10 minutes to stabilise luminescent signal and luminescence was recorded using a Promega luminometer with an integration time of 1 second. Readouts from DDR inhibitor agent containing wells were normalised to wells containing DMSO control media.

Materials and Methods

2.12 Statistical Analyses

Mean values were compared using student's t-test and 95% confidence intervals. Minitab and GraphPad Prism were used to calculate statistical significance. Special consideration must be given to the analysis of clonogenic assays and gamma H2AX foci analysis.

2.12.1 Clonogenic assays

Data points of CSC versus bulk, and controls versus drug treatments were analysed for statistical significance using ANOVA. SF2Gy and SF4Gy values were summarised as means and compared using Student's t test. SER0.37 values were expressed as a mean derived from a minimum of 3 independent experiments and a 95% confidence interval for the mean was generated from these data.

2.12.2 Gamma H2AX foci analysis

The distribution of gamma H2AX foci per nucleus was found to exhibit significant right skew, and therefore median foci per nucleus was used as a summary statistic. A mean of medians was generated from a minimum of 3 independent experiments and means were compared using student's t test. For the validation of Volocty counts and manual counting methods for nuclear gamma H2AX foci quantification, a Mann Whitney U test was utilised to compare medians.

Materials and Methods

Antigen	Manufacturers details	Application and dilution
ATM	Abcam 2618	WB 1:1000
pATM ser1981	Novus NB100-307	WB 1:1000
ATR	Santa Cruz N19	WB 1:1000
pATR	Cell signaling 2853	WB 1:1000
Chk2	Cell signaling	WB 1:1000
pChk2 thr68	Cell signaling	WB 1:1000
Chk1	Cell signaling 2345	WB 1:1000
pChk1 ser 345	Cell signaling 2348	WB 1:1000
53BP1	Millipore BP13	IF 1:100
CENPF	Abcam 5	IF 1:100
pH2AX ser 139	Millipore JBW301	IF 1:100
pHis H3 alexa 488 conjugate	Cell signaling 9708	FACS 1:50
PARP-1	Santa Cruz 8007	WB 1:1000 IHC 1:600
PAR	Calbiochem AM80	WB 1:1000
Nestin	Abcam 6320	IF 1:100
Neuron specific beta III tubulin	Abcam 7751	WB 1:1000
Sox2	Abcam 75485	WB 1:1000
CD133	Miltanyi AC133	IF 1:10
Actin	Sigma 090M4758	WB 1:2000

Table 2.1 Details of antibodies used, applications and dilutions

Materials and Methods

Antigen	Manufacturers details	Application and dilution
Alexa® 488 goat anti-mouse IgG (H+L)	Invitrogen A11029	IF 1:250
Alexa® 568 donkey anti-rabbit IgG (H+L)	Invitrogen A10042	IF 1:250
Anti-mouse IgG HRP – Linked antibody	Cell signaling 7076S	WB 1:2000
Anti-Rabbit IgG HRP-Linked antibody	Cell signaling 7074	WB 1:2000
Anti-Goat IgG HRP-Linked antibody	Santa Cruz sc2020	WB 1:2000

Table 2.2 Secondary antibody details, applications and dilutions

Chapter 3 Model characterisation

3.1 Introduction

In order to characterise the radiation response of GBM CSCs, *in vitro* models of the CSC subpopulation and differentiated tumour bulk populations were developed. There have been various approaches to this problem in the past. Cell sorting based on the cell surface marker CD133 has been utilised in several studies to sort populations of marker positive CSCs from non-stem populations, (Bao et al., 2006a, McCord et al., 2009). However a satisfactory universal CSC marker in GBM has not yet been identified and it is likely that CD133 expression does not correlate with CSC phenotype in all GBM tumours. Other investigators have quantified the expression levels of putative CSC markers in a variety of GBM cell lines and classified them as having high or low expression of these markers. Radiosensitivities of high and low CSC marker expressing cell lines were then compared, (Ropolo et al., 2009). However this model ignores important differences in intrinsic radiosensitivity between non isogenic cell lines, limiting the utility of this approach.

A model was developed in which isogenic, paired CSC enriched and CSC depleted cultures were generated from the same primary parental cell line, thus avoiding any problems associated with differing intrinsic radiosensitivities between different cell lines. This was achieved by culturing primary GBM tumour samples in a neurobasal-like CSC media with the addition of epidermal and fibroblast growth factors and in the absence of serum (see chapter 2) to enrich for GBM CSCs. Once these CSC enriched cultures had been established, a model of differentiated or ‘tumour bulk’ cells was generated by culturing them in conventional growth media containing serum without additional growth factors (see chapter 2). CSC enriched and depleted cultures were then characterised by a repertoire of assays including *in vivo* tumourigenicity, neurosphere formation and expression of a panel of CSC and differentiation markers. This culture model has the major advantage of not relying upon a single CSC marker, since there is no universal satisfactory GBM stem cell marker and even CD133 negative cells have been shown to exhibit CSC properties, (Beier et al., 2007).

Model characterisation

Conventional CSC cultures are grown as “neurospheres” since cells grown under these conditions form spheres and fail to adhere to plastic tissue culture flasks. Neurospheres differ from spheroid cultures in that the cells within the neurosphere are thought to represent the progeny of a single cancer stem cell, whereas spheroids represent cellular aggregates of cultured cells. This can be shown by plating single cells into 96 well dishes and demonstrating the generation of neurospheres. Both E2 and G7 CSC cultures produced neurospheres when grown in this manner, (fig 3.1). Bulk cultures on the other hand adhered in the conventional manner to tissue culture flasks producing a monolayer culture. Neurospheres are problematic to work with for the purposes of *in vitro* assays, and the architecture of a particular form of cell culture may provide a further confounding factor when comparing functional differences and radiation sensitivities between CSC and tumour bulk cultures. Therefore GBM CSCs were cultured as monolayers by allowing them to adhere to a MatrigelTM coating which was applied to tissue culture plastics, (fig3.2).

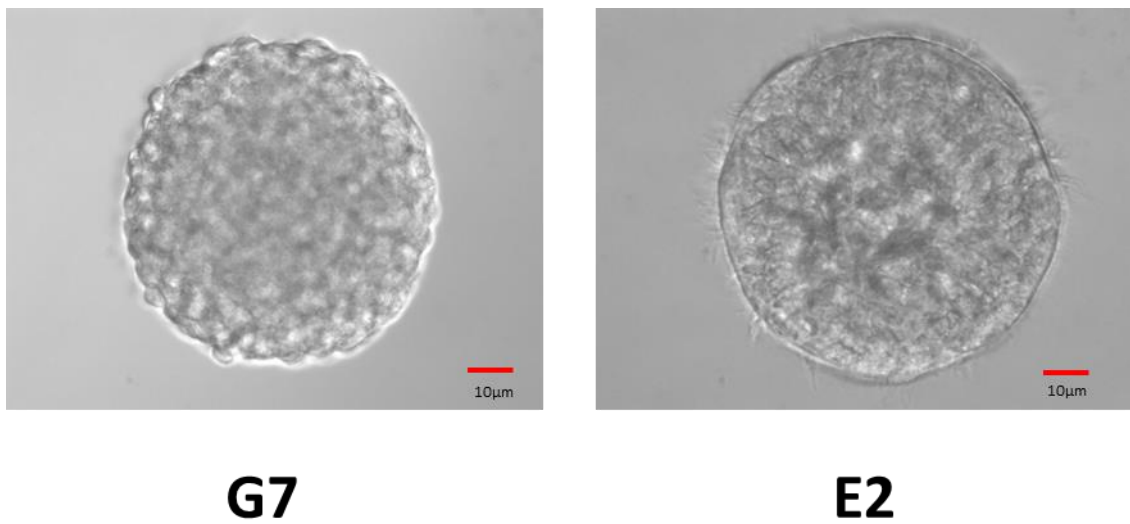


Figure 3.1 Representative images of E2 and G7 neurospheres

E2 and G7 cells were cultured in CSC media in tissue culture flasks and allowed to form neurospheres (10x magnification light microscopy).

Differences between CSC and tumour bulk monolayer MatrigelTM cultures were apparent by inspection under the microscope at low (10x) magnification. Particularly in the E2 cell line the tumour bulk cells appeared spiculated and

Model characterisation

more differentiated in nature, compared to the rounded, seed like undifferentiated appearance of the CSC cultures, (fig 3.2).

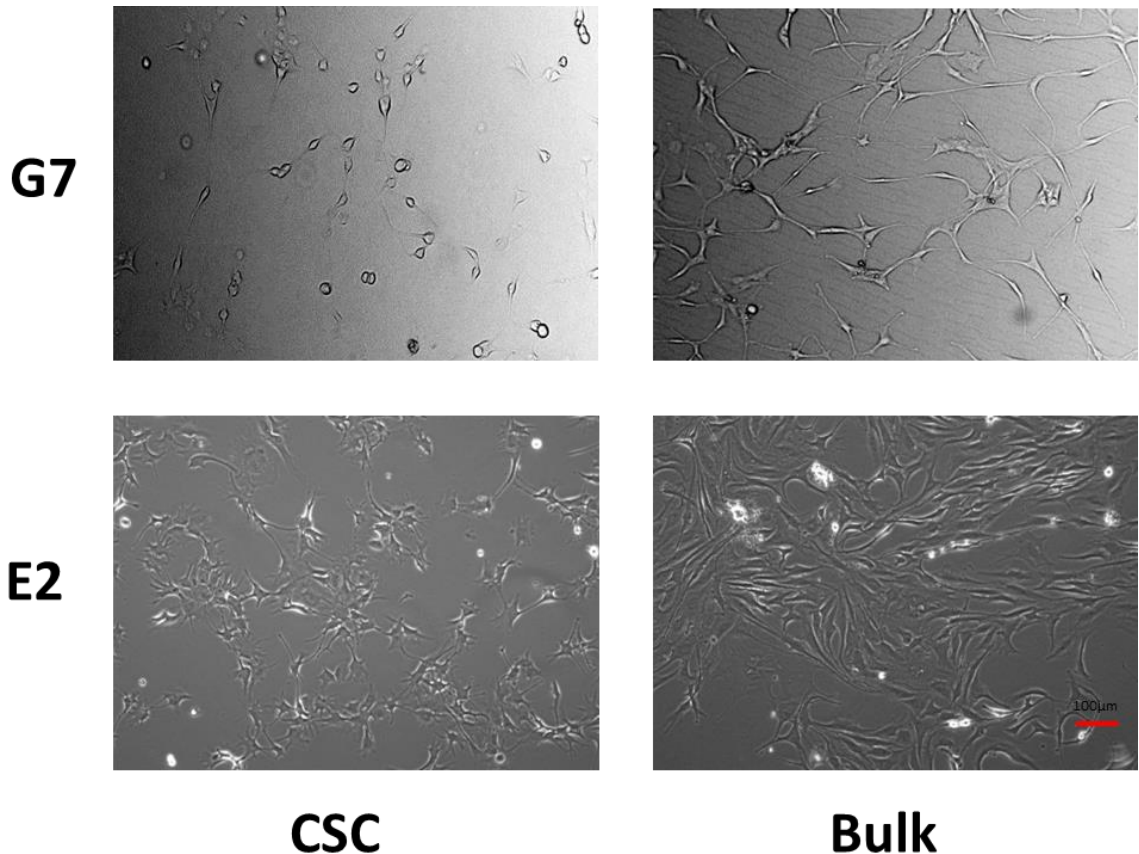


Figure 3.2 Representative images of E2 and G7 monolayer cultures

Representative images of G7 and E2 cell line cultures when cultured as monolayers (10x magnification light microscopy). CSC cultures were grown in CSC media on MatrigelTM coated tissue culture flasks. Bulk cultures were grown in FCS containing media in tissue culture flasks without MatrigelTM.

3.3 Comparison of expression of putative CSC markers in GBM CSC and tumour bulk cultures

As discussed in the introduction to this thesis, a single satisfactory CSC marker does not exist for GBM CSCs, and the functional analysis of CSCs in their ability to recapitulate the parental tumour *in vivo* remains the gold standard method of identifying GBM CSCs. Nevertheless, panels of CSC markers are of value as surrogate indicators of the CSC state. Commonly used CSC markers in GBM are

Model characterisation

CD133, Sox2 and Nestin. Glial fibrillary acidic protein (GFAP) is used as a marker of astrocytic differentiation.

Analysis of the CSC markers Nestin and Sox2 by Western blotting is shown in figure 3.3. The levels of these CSC markers were clearly elevated in CSC cultures of both the E2 and G7 cell lines. The percentage of CD133+ cells and GFAP+ cells in CSC and bulk cultures by FACS analysis are also shown in figure 3.4. The CSC marker CD133 was again clearly and significantly elevated in the CSC cultures of E2 and G7 whilst expression of the astrocytic differentiation marker GFAP was reduced in CSC cultures but significantly elevated in tumour bulk cultures.

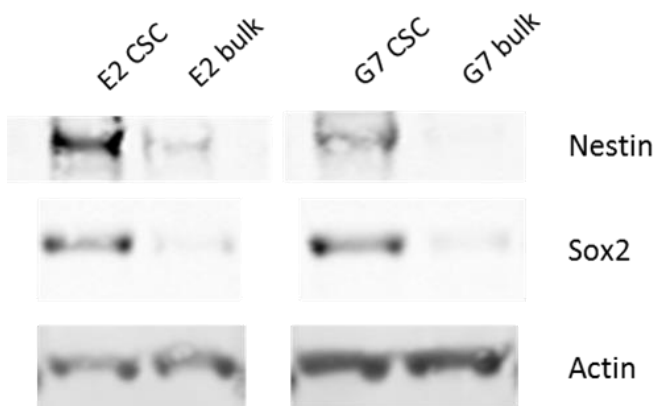


Figure 3.3 Analysis of CSC markers via Western blotting

E2 and G7 CSC and bulk cultures were incubated for 48 hours in their respective media types before lysis for Western blotting. Membranes were probed for the GBM stem markers nestin and sox2

Model characterisation

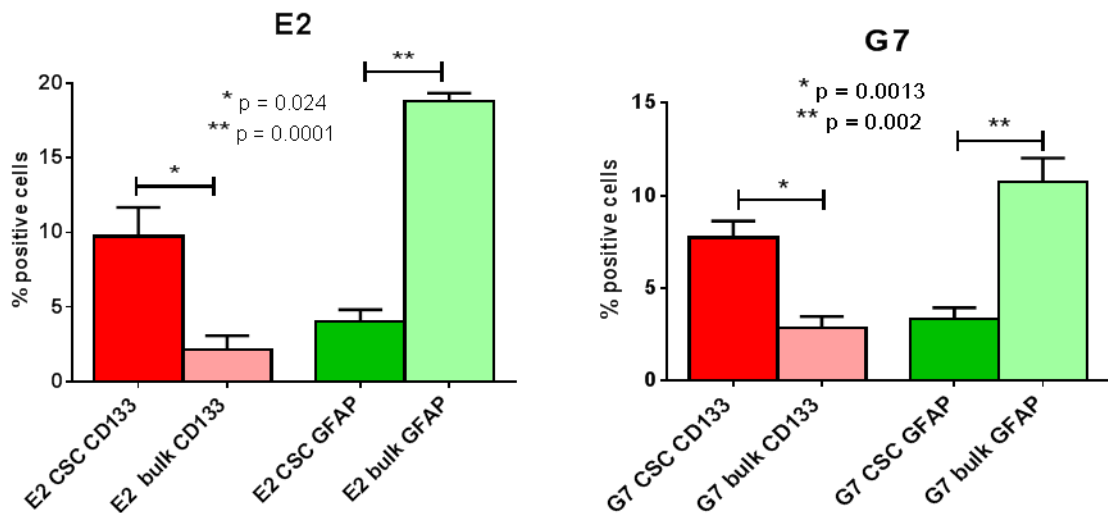


Figure 3.4 Quantification of CD133 expression by flow cytometry

CSC and bulk cultures of both cell lines were dissociated and incubated with CD133 or GFAP antibody respectively and then analysed via flow cytometry using a BD FACSCalibur. Results represent means and SD from 3 independent experiments. P values were generated by student's t test. The data shown in this figure is the work of Dr N Gomez-Roman and Dr S Ahmed, and not the author's own.

These findings were confirmed via immunofluorescent microscopy in the E2 cell line (fig 3.5). Nestin expression was increased in the CSC cultures by immunofluorescence when compared to bulk cultures, however nestin staining was not entirely absent in the tumour bulk culture. This implies either that a CSC population was present in tumour bulk cultures, but depleted compared to CSC culture conditions, or that nestin expression was not specific for CSC and could be observed at lower levels in more differentiated GBM populations. A similar pattern was seen when CD133 staining was performed, (fig 3.5). CD133+ cells were more frequent in CSC cultures compared to the differentiated tumour bulk conditions.

Model characterisation

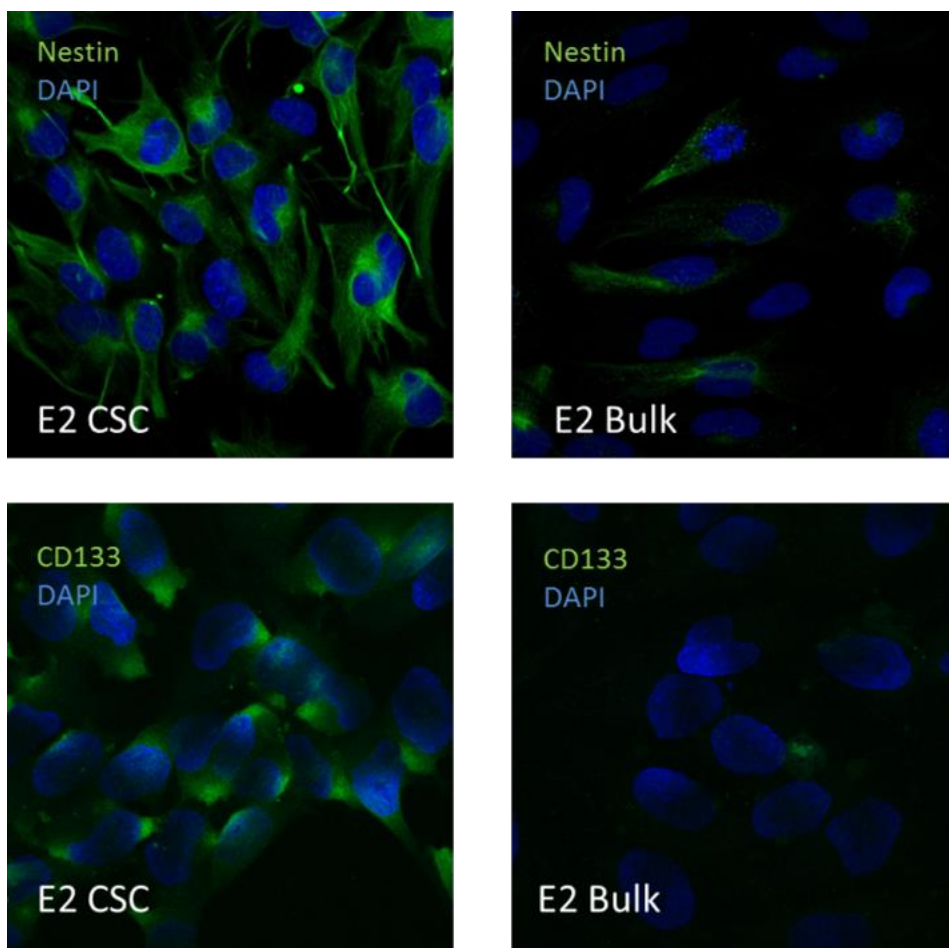


Figure 3.5 Demonstration of immunofluorescent staining for CSC markers in E2 CSC and tumour bulk cells

Cells were grown on MatrigelTM coated circular glass slides until 80% confluent. Cells were then incubated with antibody to nestin (upper panels), or CD133 (lower panels) before being stained with DAPI and visualised using a Zeiss confocal microscope. Cells were incubated with CD133 antibody prior to fixation in order to prevent degradation of the AC133 glycosylated portion of the CD133 antigen. Images represent maximum intensity projections of 6 slice Z stacks.

3.3 Effects of switching media on CSC markers

The model of CSC and bulk tumour cell cultures discussed above was dependent upon the culture conditions which the cell lines were grown in. An investigation of the effects of changing the culture conditions on the CSC or bulk phenotypes of the respective cell lines and culture conditions was undertaken. Established CSC and bulk cultures (i.e. CSC and bulk cell cultures which had been grown in CSC media or bulk media respectively for greater than 5 passages) were used for this experiment. CSC cultures were incubated in bulk media and lysed for Western blotting at timepoints of 0, 2, 12, 24, 48, 72 and 96 hours respectively

Model characterisation

post incubation in bulk media. Established tumour bulk cultures were switched to CSC media and lysed for Western blotting at similar timepoints post incubation in CSC media. The resulting Western blots which were probed for the CSC marker nestin and the differentiation marker GFAP. These are shown for E2 CSC and bulk cultures and G7 CSC and bulk cultures (fig 3.6).

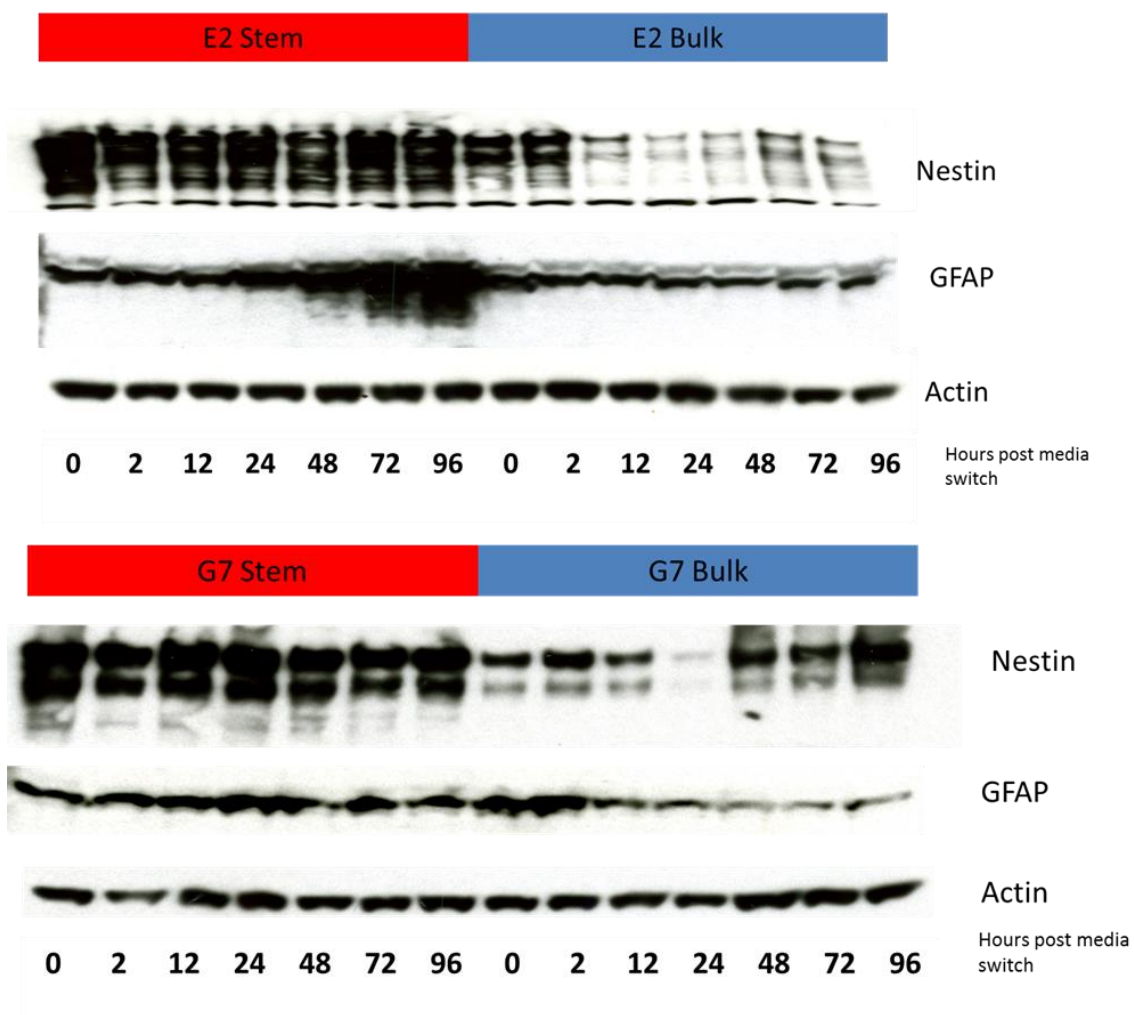


Figure 3.6 Comparison of CSC marker and differentiation marker expression by Western blotting in CSC and bulk cultures following switching of original growth media conditions.

E2 and G7 CSC cultures were incubated in FCS containing bulk media and lysed for Western blotting at the timepoints shown. E2 and G7 bulk cultures were incubated in CSC media and lysed for Western blotting at the timepoints shown. Membranes were probed for the CSC marker nestin and the astrocytic differentiation marker GFAP.

In both G7 and E2 CSC cultures the expression of nestin was maintained, even after 96 hours of incubation in differentiating bulk medium. GFAP levels remained constant in the G7 CSC cell populations, however in the E2 CSCs the

Model characterisation

expression of GFAP increased from 48 hours onwards, demonstrating that a degree of differentiation was occurring in the E2 CSC cultures. The stability of nestin expression over this period of time would suggest that CSC marker expression is a robust and durable feature of CSC cultures and not an artefact of cell culture conditions.

In the E2 and G7 bulk cell cultures, nestin expression decreased on exposure to CSC media. This is an unexpected finding but may have been a non-specific effect of the abrupt withdrawal of foetal calf serum from culture medium. Nestin expression increased from 48 to 96 hours again suggesting a CSC enriching effect occurred, particularly in the G7 cell line.

3.4 *In vivo* validation of the CSC phenotype

CSC markers are unsatisfactory as a sole indicator of the CSC status of tumour cells. CD133 is the most widely used marker of CSCs in GBM, yet CD133- cells have been shown to harbour CSC properties in some tumours, (Beier et al., 2007). Due to the uncertainties associated with putative CSC markers, the culture of GBM CSCs must be validated by *in vivo* transplantation studies. CSCs should display properties of self renewal, multipotency and the ability to initiate tumours at low dilutions on orthotopic transplantation, (Pilkington, 2005, Vescovi et al., 2006).

For these validation studies, 1×10^5 E2 and G7 cells cultured as CSC and bulk cultures were injected as orthotopic transplants into the brains of CD1 nude immunocompromised mice. *In vivo* studies were performed by Dr Lesley Gilmour and Katrina Stevenson. E2 CSCs generated tumours in 100% of mice. Furthermore, CSC culture derived tumours in E2 were highly invasive. HLA1-ABC can be used as a marker for human cells in murine orthotopic tumour transplant models, and is therefore highly specific for the transplanted cells. Ki67 is a mitotic marker which, although not a tumour marker per se, is likely to be positive in mitotically active GBM tumour cells and negative in surrounding mature mouse brain, which can be assumed to be non-dividing. PARP-1 expression is also associated with indices of proliferation and has been reported

Model characterisation

as a GBM tumour cell marker (Galia et al., 2012b). Immunohistochemical staining for HLA1-ABC, PARP-1 or Ki67 detected tumour cells throughout both hemispheres of brain in FFPE sections, (fig 3.7). Quantitative analysis of Ki67 staining in whole brain slices harvested at various timepoints demonstrated increasing tumour burden up to 30 weeks post injection of E2 CSCs, as did quantification of HLA1-ABC, (fig 3.8). In contrast after injection of E2 bulk cells, very few positively staining cells are apparent. These cells are located exclusively around the injection site and fail to infiltrate the brain. E2 bulk cells are therefore non-tumourigenic, (fig 3.8).

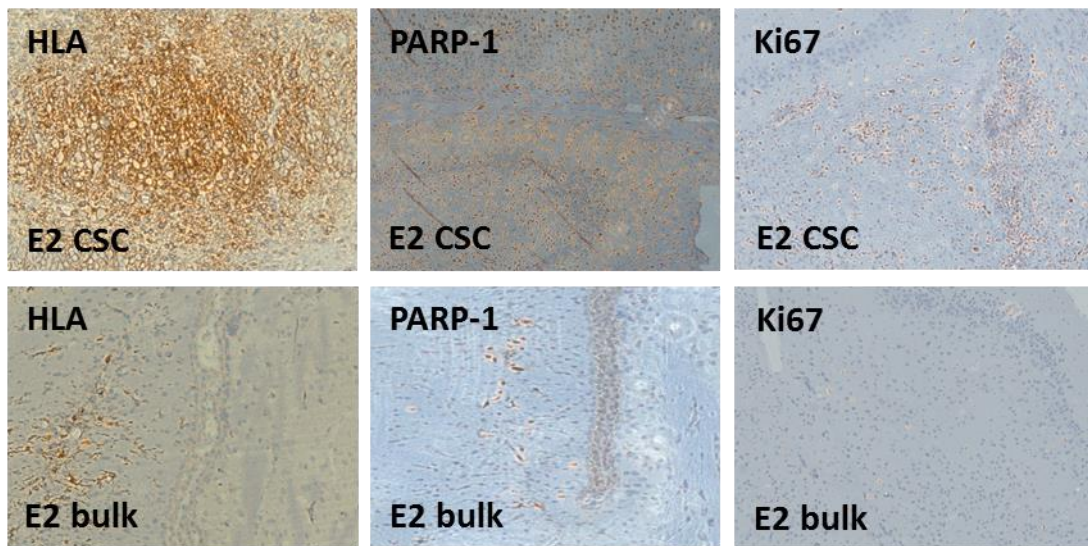


Figure 3.7 Comparison of *in vivo* tumour generation by E2 CSC and bulk cultures

10^5 E2 stem cells or 10^5 E2 bulk cells were orthotopically transplanted into immunocompromised CD1 mice brains. At 16 weeks mice were euthanised and brains were perfusion fixed and sectioned. Representative images of immunohistochemical staining for the human leucocyte antigen HLA1-ABC, the tumour marker PARP-1 and the mitotic cell marker Ki67 are shown in sections of mouse brain. Images were taken at 10x magnification.

Model characterisation

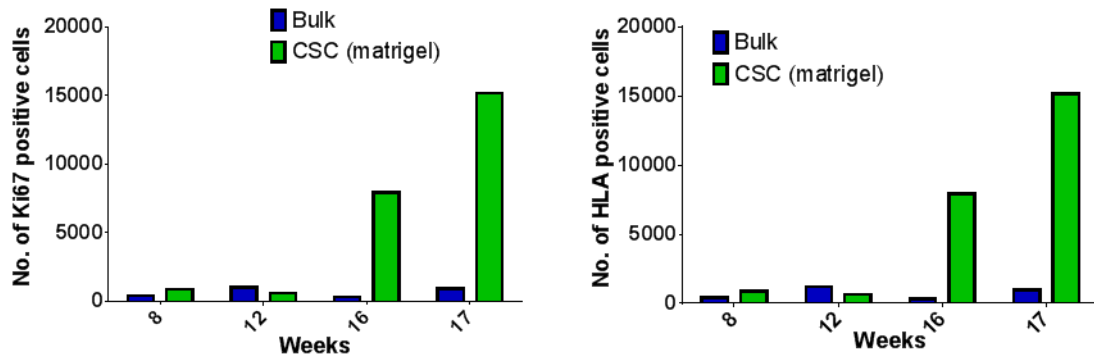


Figure 3.8 Quantification of Ki67 and HLA immunohistochemical staining as a tumour cell marker in sections of murine xenograft tumours derived from E2 CSC and bulk cultures

Quantification of cells staining positive for Ki67 (left panel) and HLA1-ABC (right panel) in sections of xenograft tumours generated in CD1 immunocompromised mice by orthotopic injection of 10^5 E2 CSCs or 10^5 E2 tumour bulk cells. Mice were euthanised at the number of weeks post injection shown and mouse brains were perfusion fixed. Tile scans covering the entire tissue section were taken at 10x magnification using a light microscope and visualised using Carl Zeiss Zen Blue imaging software. Quantification of positively staining cells was carried out using Zen Blue Imaging Software also. This figure represents the work of Dr N Gomez-Roman and S Chahal and is not the authors own.

E2 CSC xenograft sections were stained for CD133, and demonstrated positivity for this CSC marker (fig 3.9). Different patterns of CD133 staining were evident. CD133 staining was observed in perivascular areas (i), generalised regions of tumour (ii) or as isolated infiltrative cells (iii).

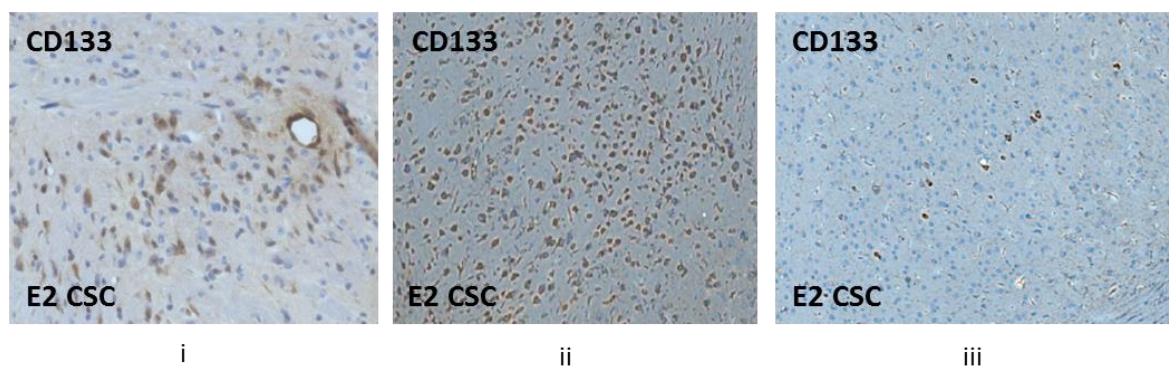


Figure 3.9 Demonstration of patterns of CD133 immunohistochemical staining observed in E2 CSC murine orthotopic intracranial xenograft tumours

Representative images of patterns of immunohistochemical staining for the GBM CSC marker CD133 observed in orthotopic xenograft models generated from E2 CSC cells. Images were taken at 10x magnification.

Model characterisation

Injection of G7 GBM CSCs produced tumours which had invasive margins and recapitulated key features of human GBM. Injection of G7 bulk cells also produced tumours, however these tumours did not recapitulate key features of GBM and failed to infiltrate the brain; representative sections from G7 CSC and bulk xenografts are shown in figure 3.10. Please see Mannino et al for published details of E2 and G7 CSC and bulk cell *in vivo* tumour formation in orthotopic xenograft models, (Mannino et al., 2014), as described in the figures 3.8 and 3.10.

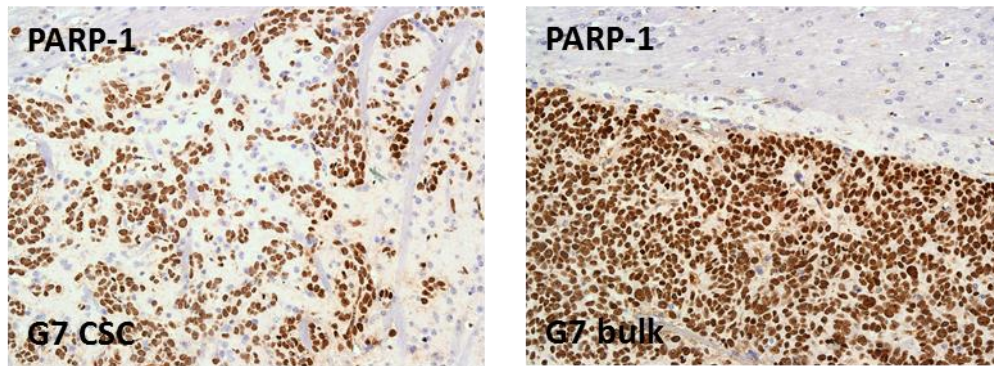


Figure 3.10 Demonstration of PARP-1 expression in G7 CSC and tumour bulk orthotopic xenograft tumours by immunohistochemistry

Representative images of immunohistochemical staining for PARP-1 in orthotopic xenograft tumours generated from injection of 10^5 G7 CSC or bulk cells into a CD1 immunocompromised mouse model. Images obtained at 10x magnification.

3.5 Characterisation of cell proliferation rate in CSC and tumour bulk cultures

Cell proliferation rates of the CSC and bulk cultures of the E2 and G7 cell lines were investigated by cell viability assay using CellTiter-glo[™]. In brief E2 and G7 CSC and tumour bulk cells were seeded into 96 well plates at a density of 200 cells per well and incubated for the time points shown before being analysed using the ATP dependent CellTiter-glo[™] assay. The resulting cell proliferation curves are shown in figure 3.11. These curves show comparable proliferation rates of CSC and tumour bulk cells. Tumour bulk cultures reach confluence arrest earlier than CSC cultures, which is likely a reflection of their increased surface

Model characterisation

area in comparison to the smaller CSC cells, rather than any increase in proliferation rate *per se*.

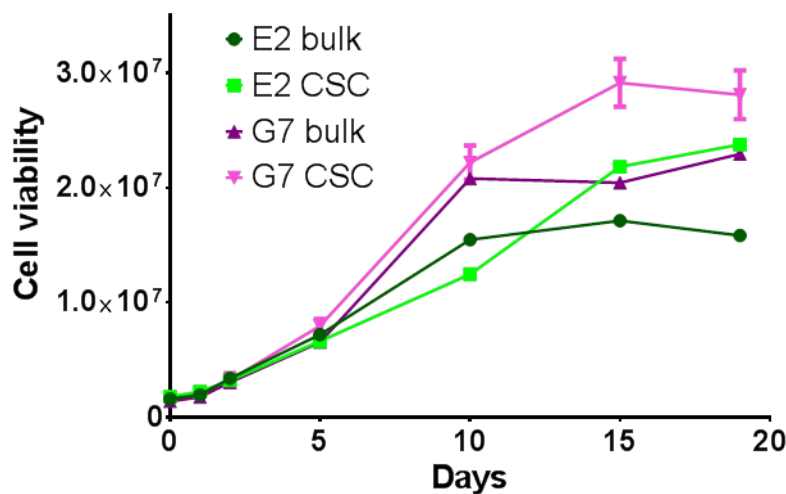


Figure 3.11 Cell proliferation in E2 and G7 CSC and bulk cultures measured by cell viability assay

Graph of cell viability over 20 days following plating of 400 cells per well of a 96 well plate. Data points represent mean with standard deviations. Assay performed in triplicate using CellTiter-glo™. Plates were read on a luminometer at the timepoints shown on the x axis. Points and bars represent mean and SEM of 3 independent experiments

3.6 Cell cycle distribution of stem and bulk cultures

The cell cycle distribution of CSC and bulk cultures of E2 and G7 under basal conditions was characterised. Cells were incubated in PI after ethanol fixation and permeabilisation in order to characterise the cell cycle distribution of CSC and tumour bulk culture populations by FACS analysis. Representative images of cell cycle profiles are shown in figure 3.12.

Model characterisation

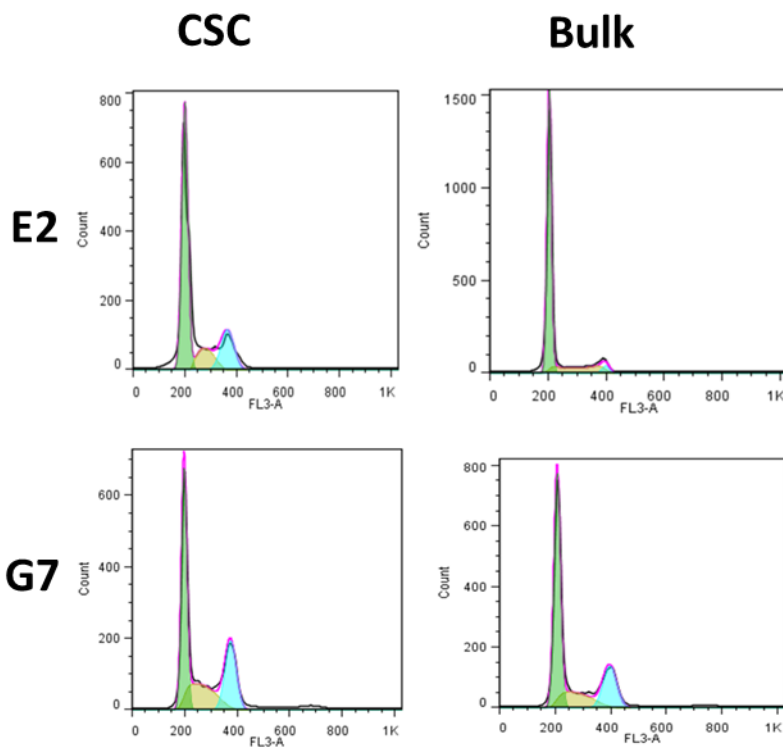


Figure 3.12 Cell cycle profiles of E2 and G7 CSC and tumour bulk cultures under basal conditions

Representative cell cycle profiles for E2 and G7 CSC and bulk cultures. Cell cultures were dissociated and fixed in ethanol before being permeabilised and incubated with 1mg/ml PI and analysed on a BD FACSCalibur.

The percentage of cells in each of G1, S and G2 was quantified for CSC and tumour bulk cultures of both E2 and G7 cell lines. In the E2 cell line there were significant differences in cell cycle distribution between CSC and bulk cells with the proportion of cells in G1 phase being higher in tumour bulk cultures compared to the proportion of cells in G1 phase in E2 CSC cultures. E2 CSC cultures had a greater proportion of cells occupying S and G2 phases in comparison to E2 tumour bulk populations, (fig 3.13). In the G7 cell line similar trends were apparent between CSC and bulk cultures, however only the differences in proportions of G1 and S phase cells reached statistical significance, (fig 3.13).

Model characterisation

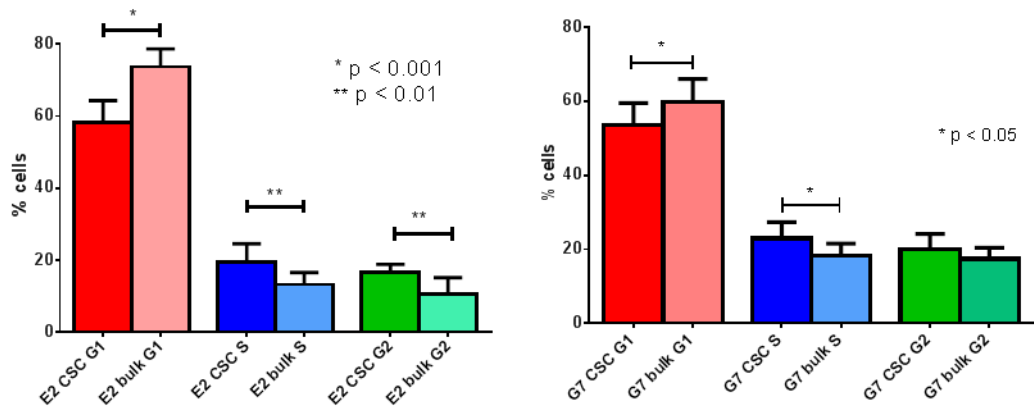


Figure 3.13 Analyses of cell cycle distribution of E2 and G7 CSC and tumour bulk cultures under basal conditions

Quantification of percentage of cells in G1, S and G2 phase of the cell cycle in E2 CSC and tumour bulk (left panel) and G7 CSC and tumour bulk (right panel). Cells were fixed in ethanol and stained with PI prior to analysis. Columns and error bars represent mean and SEM from 9 independent experiments. P values calculated by student's t test.

3.7 Sanger sequencing of p53

The p53 pathway is integral to any cellular response to ionising radiation, and therefore the p53 status of the E2 and G7 cell lines was investigated. Sanger sequencing of the exons 3 to 10 of the p53 gene was performed in both E2 and G7 cell lines in CSC and bulk cultures separately. The U87 cell line, which is known to have wild type p53, was sequenced as a negative control. No mutations were found in E2 in exons 3 to 10 in either CSC or bulk cultures, demonstrating that this cell line has wild type p53. No mutations were found in the G7 cell lines in exons 4 to 10 in either CSC or bulk culture. Exon 3 in G7 was not sequenced due to difficulties obtaining adequate PCR product for sequencing, however only a very small percentage of mutations in p53 in GBM tumours are found outside exons 5-8. The cell line U87 was found to have a p53 R72 polymorphism, however this is of no functional consequence. See table 3.1 for details.

Model characterisation

Exon	G7 CSC	G7 Bulk	E2 CSC	E2 Bulk	U87
3	-	-	WT	WT	WT
4	WT	WT	WT	WT	WT*
5	WT	WT	WT	WT	WT
6	WT	WT	WT	WT	WT
7	WT	WT	WT	WT	WT
8	WT	WT	WT	WT	WT
9	WT	WT	WT	WT	WT
10	WT	WT	WT	WT	WT

Table 3.1 Results of Sanger sequencing of P53 exons 3-10

P53 sequencing results for E2 and G7 CSC and bulk cultures. WT = wild type. DNA was extracted from *in vitro* CSC and tumour bulk cultures of E2 and G7 and PCR product obtained for Sanger sequencing of exons 3 to 10. No mutations were found in exons 3 to 10 for E2. No mutations were found in exons 4 to 10 in G7; however exon 3 was not sequenced in this cell line due to difficulties in obtaining PCR product. U87 is known to have WT p53 and was sequenced as a negative control, however was found to have the p53-R72 polymorphism in exon 4.

3.8 Conclusions

The GBM cell lines E2 and G7, cultured as paired CSC and tumour bulk, were characterised. Upregulation of putative CSC markers Nestin, Sox2 and CD133 by Western blot, immunofluorescent staining and flow cytometry assays could be demonstrated in CSC cultures in comparison to bulk cell cultures. Tumour bulk cultures exhibited reduced levels of CSC marker expression and in contrast had elevated levels of the astrocytic differentiation marker GFAP.

Expression of CSC markers appeared to be retained by CSC cell cultures for up to 96 hours after incubation in differentiating media. Further exploration of the response to CSC and bulk cultures by switch of media conditions could be achieved by extending the timepoints examined in this assay. Furthermore it would have been informative to conduct neurosphere formation assay at the

Model characterisation

various timepoints in order to assess sphere forming capacity of CSC cultures following exposure to differentiating conditions. LDA would be a more robust assessment of CSC tumourigenic potential in this setting. A further avenue of study would be the assessment of gene expression via DNA microarray in CSC and bulk tumour cells at time intervals post exposure to differentiating or stem-like cell enriching media respectively. Unfortunately time and resource constraints during the project prevented these investigations being performed.

Furthermore CSC cultures exhibit enhanced tumourigenicity in an immunocompromised orthotopic xenograft mouse model in the E2 cell line when compared to tumour bulk cultures. The G7 CSC cultures recapitulated features of the parental tumour such as invasion and infiltration whereas the G7 bulk cultures lacked these features, although G7 bulk cells appeared to retain tumourigenicity. Therefore CSC cultures exhibited a robust expression of the CSC phenotype in comparison to tumour bulk cultures thus validating this *in vitro* model.

CSC and bulk cultures exhibit significant differences in cell cycle distribution, with a lower proportion of CSCs being in G1 cell cycle phase under basal conditions in both E2 and G7 cell lines. This has not previously been reported in the wider literature concerning GBM CSCs, and may influence important DDR mechanisms in CSCs. One consequence of this may be increased utilisation of HR DNA DSB repair in GBM CSCs, since preferential occupation of the S and G2 cell cycle phase in GBM CSC populations may facilitate use of this repair pathway in CSCs.

Both E2 and G7 cell lines were found to have wild type p53, with no difference between the CSC and bulk culture populations. Only 38% of primary GBM tumours have mutated p53. The proportion of tumours with mutated p53 in secondary GBM rises to 65% however. Mutations and other abnormalities of the p53 pathway such as MDM3 amplification are however common in GBM, (Nagpal et al., 2006).

Model characterisation

In conclusion it can be shown that *in vitro* CSC and bulk culture models demonstrated increased expression of putative CSC markers and key phenotypic features of GBM CSCs. This is illustrated by increased tumourigenicity in orthotopic mouse models and recapitulation of histological features of the parental tumour.

Chapter 4 Investigation of GBM CSC radioresistance

4.1 Introduction

Previous investigations of GBM CSC radioresistance have not utilised clinically relevant radiobiological measures of radiation sensitivity such as clonogenic survival assay and there is debate in the current scientific literature regarding the radioresistance of GBM CSCs. Bao et al demonstrated that GBM CSCs exhibited radioresistant properties and demonstrated enrichment of the CD133+ population in tumours following irradiation. Furthermore this investigation demonstrated enhanced activation of cell cycle checkpoint proteins in CD133+ GBM cells and more efficient DNA repair after irradiation in the CD133+ population compared to CD133- cells as measured by the alkaline comet assay (Bao et al., 2006a). Images of clonogenic colonies were demonstrated by the authors however formal clonogenic survival assay comparing CD133+ and CD133- populations was not undertaken. Clonogenic survival is a radiobiological standard, and has been shown to correlate with clinical outcome (Bjork-Eriksson et al., 2000, Bjork-Eriksson et al., 1998, West et al., 1997). The investigation by Bao and colleagues also did not include a robust assay of DNA DSB repair (alkaline comet assay is a measure of DNA SSB repair) or a functional measure of cell cycle checkpoint control. Other authors have failed to replicate the findings of Bao et al. McCord et al compared the radiation response of CD133+ GBM cells to that of established GBM cell lines and found that CD133+ GBM cells were radiosensitive in comparison, and exhibited less efficient DNA DSB repair; however this approach ignores probable differences in intrinsic radiosensitivity between different GBM cell lines (McCord et al., 2009). Ropolo et al found that CD133+ GBM cells displayed upregulated phosphorylation of Chk1 and Chk2 kinases under basal conditions and elongated cell cycle durations however found no evidence for enhanced DNA DSB repair (Ropolo et al., 2009).

Given the uncertainty in the literature concerning the proposed radiation resistance of GBM CSCs a key objective of this thesis was to quantify radiation response in GBM CSCs using clinically relevant assays of radiation resistance. Using the model of paired GBM CSC and bulk cultures from a common parental

Investigation of GBM CSC radioresistance

GBM specimen, clonogenic survival assays, examination of cell cycle checkpoint kinetics and phosphoprotein quantification, and interrogation of DNA DSB repair were performed and compared between the CSC and bulk cultures.

4.2 Investigation of radioresistance of GBM CSCs by clonogenic survival assay

Three GBM cell lines (E2, G7 and R10) grown as CSC and bulk cultures were subjected to clonogenic survival assay using a range of radiation doses from 1 to 5Gy. Both CSC and bulk cultures were grown in their respective media throughout the experiment, however bulk cells were seeded onto Matrigel™ coated tissue culture plates in order to minimise differences in experimental conditions. The resulting clonogenic survival curves are shown in figure 4.1. Countable colonies were formed under both conditions and plating efficiencies were similar. All three cell lines could be viewed as radioresistant in both CSC and bulk culture conditions, with surviving fraction at 2Gy (SF_{2Gy}) values above 0.8 in all CSC lines, and SF_{2Gy} above 0.7 in all but the R10 tumour bulk cell line. Radioresistance is a relative term, and is not well defined, nevertheless the SF_{2Gy} of radiosensitive cell line such as a Burkitt's lymphoma can be as low as 0.2. Repair deficient cell lines can also be markedly radiosensitive. Loser et al described the *in vitro* radiation survival of mouse embryonic fibroblast (MEF) cell lines deficient in artemis, ATM and Ligase IV using clonogenic assay (Loser et al., 2010). ATM null MEFs had a SF_{2Gy} of 0.17 and artemis null MEFs had an SF_{2Gy} of 0.16. Ligase IV null MEFS were highly radiosensitive with a SF_{2Gy} of 0.004. These data place the marked radioresistance seen in GBM CSC and tumour bulk cells into context. However the CSC culture populations were significantly more radioresistant than bulk culture populations. This represents the first demonstration of radioresistance in GBM CSCs compared to tumour bulk cultures by clonogenic assay in paired GBM cell lines. Curves were fitted with the linear quadratic equation and dose modifying factors (DMF) calculated at a surviving fraction of 37% (table 4.1). All CSC clonogenic survival curves were significantly different from their corresponding bulk cell clonogenic curves by ANOVA. The dose of radiation required to produce an equivalent decrease in surviving fraction to 37% was 1.3 fold greater for E2 CSCs ($p<0.001$), 1.5 fold greater for

Investigation of GBM CSC radioresistance

G7 CSCs cells ($p = 0.015$) and 1.47 greater for R10 CSCs ($p<0.0001$) than for the corresponding bulk populations. Hence the DMFs for all 3 CSC cultures were similar. The surviving fractions at 4Gy (SF_{4Gy}) are shown in table 4.2 and again these values are significantly greater in the CSC culture populations. SF_{4Gy} values are shown rather than the more conventional SF_{2Gy} because the extreme radioresistance of these cell lines makes the latter parameter less meaningful. SF_{2Gy} remains a more clinically relevant measure of radiation sensitivity however and is shown in table 4.3. The difference in mean SF_{2Gy} values between CSC and tumour bulk populations in the G7 cell line was not statistically significant despite there being significant differences between G7 CSC and tumour bulk in terms of SF_{4Gy} and DMF 0.37 values. Radioresistance of G7 CSCs may only be evident at higher doses of ionising radiation.

Investigation of GBM CSC radioresistance

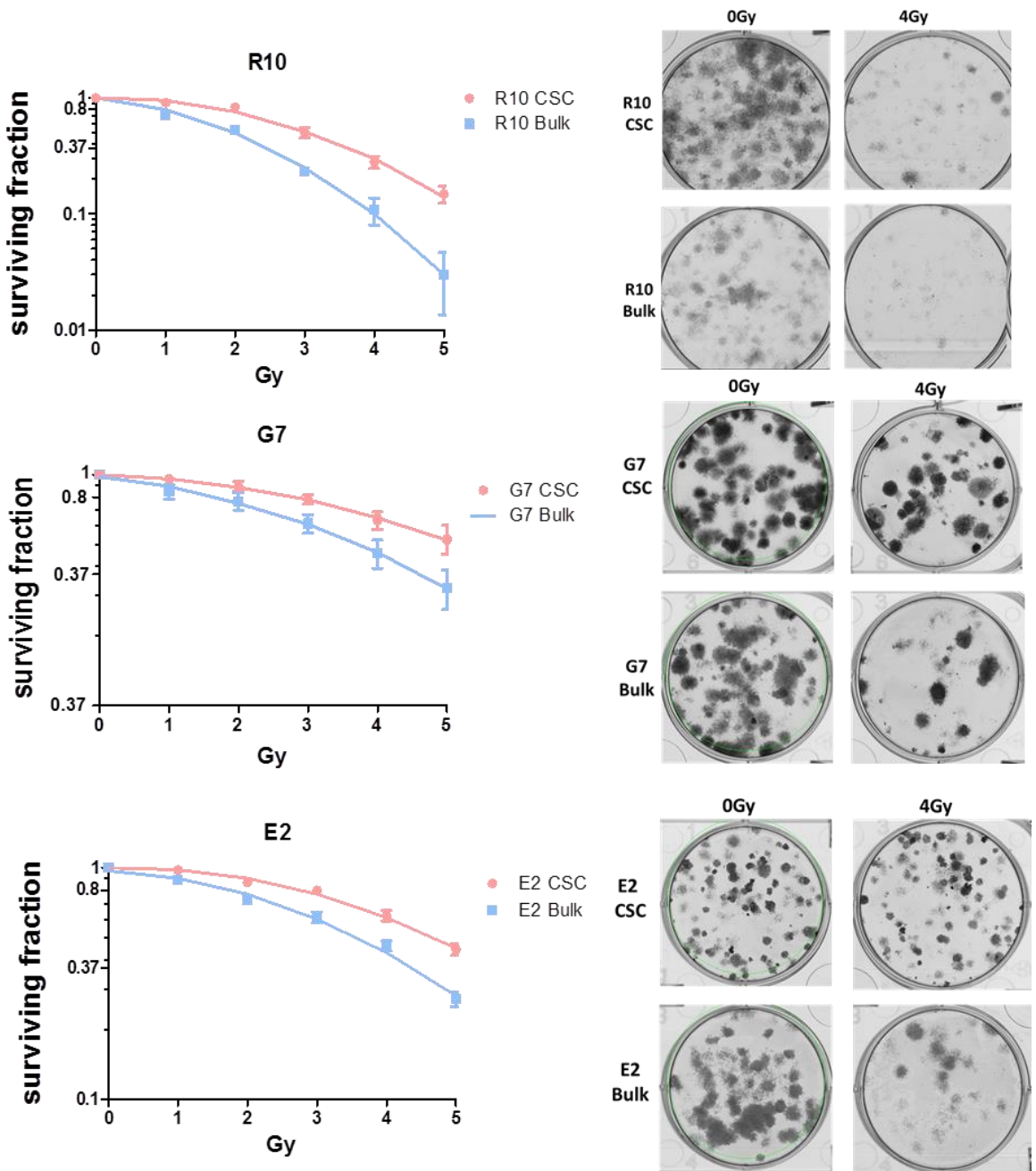


Figure 4.1 Clonogenic survival analysis of CSC versus bulk cultures

Clonogenic survival curves showing response of CSC and tumour bulk cell cultures to ionising radiation in R10, E2 and G7 primary cell cultures. Mean surviving fraction plus SEM of 9 independent experiments is shown for E2 and G7, whilst means plus SEM of 3 independent experiments are shown for R10 fitted to a linear quadratic model. Curves are significantly different by ANOVA (E2 CSC vs bulk cells $p < 0.001$, G7 CSC vs differentiated tumour cells $p < 0.001$, R10 CSC vs differentiated tumour cells $p < 0.0001$). Representative images of colony formation at 0 and 4Gy in each population are shown.

Investigation of GBM CSC radioresistance

DMF 0.37 (95% CI)	
E2 CSC vs bulk	1.30 (1.16, 1.44) (p < 0.001)
G7 CSC vs bulk	1.52 (1.10, 1.93) (p = 0.015)
R10 CSC vs bulk	1.47 (1.41, 1.54) (p < 0.0001)

Table 4.1 Dose modifying factors for CSC vs tumour bulk cells at 0.37 survival

Dose modifying factors at 37% clonogenic survival ($DMF_{0.37}$) with 95% confidence intervals for CSC versus tumour bulk cell cultures of R10, G7 and E2 indicating that CSC cultures are significantly more radioresistant than bulk cell cultures in all cell lines. $DMF_{0.37}$ values were calculated from clonogenic survival data fitted to a linear quadratic model as shown in Figure 4.1. Values shown represent the means of 9 (E2 and G7) or 3 (R10) experiments. P values ($H_0: DMF_{0.37} = 1$) calculated by one sample t test.

	E2 CSC	E2 bulk	G7 CSC	G7 bulk	R10 CSC	R10 bulk
Mean SF4Gy (95% CI)	0.62 (0.56, 0.69)	0.46 (0.41, 0.51)	0.63 (0.52, 0.75)	0.46 (0.33, 0.58)	0.28 (0.21, 0.35)	0.11 (0.053, 0.16)
T test of means	p = 0.001			p = 0.05		p = 0.018

Table 4.2 Surviving fraction at 4Gy values for E2, G7 and R10 CSC and tumour bulk cultures

Mean surviving fractions at 4Gy (SF_{4Gy}) with 95% confidence intervals for CSC and bulk cell cultures of E2, G7 and R10 cell lines. Means of 9 independent experiments each performed in triplicate for E2 and G7, and means of 3 independent experiments in triplicate for the R10 cell line are shown with corresponding 95%CI's. P values for 2 sample t test of mean SF_{4Gy} are also shown.

	E2 CSC	E2 bulk	G7 CSC	G7 bulk	R10 CSC	R10 bulk
Mean SF2Gy (95% CI)	0.86 (0.81, 0.91)	0.72 (0.66, 0.78)	0.893 (0.81, 0.97)	0.744 (0.60, 0.89)	0.83 (0.71, 0.95)	0.53 (0.44, 0.62)
T test of means	p = 0.0020			p = 0.10		p = 0.017

Table 4.3 Surviving fraction at 2Gy values for E2, G7 and R10 CSC and tumour bulk cultures

Mean surviving fractions at 2Gy (SF_{2Gy}) with 95% confidence intervals for CSC and bulk cell cultures of E2, G7 and R10 cell lines. Means of 9 independent experiments each performed in triplicate for E2 and G7, and means of 3 independent experiments in triplicate for the R10 cell line are shown with corresponding 95%CI's. P values were calculated using student's t test.

Investigation of GBM CSC radioresistance

4.3 Investigation of radioresistance of GBM CSCs by neurosphere formation assay

The validity of the clonogenic survival assay data was confirmed by performing neurosphere formation assays. Radioresistance of GBM CSCs was investigated using an assay that was unaffected by the possible confounding factor of different media. Cell sorting using the CD133/AC133 antigen as a CSC marker was performed in E2 CSC cultures, producing a population of E2 CD133+ cells and a population of E2 CD133- cells which could both be maintained in CSC media conditions. These cells were plated into 96 well plates at a density of 10 cells per well and irradiated with 2Gy. After an incubation period of 4 weeks, neurosphere numbers per well were quantified, as shown in figure 4.2.

In figure 4.2 neurosphere forming capacity of the control E2 CD133+ and CD133- cells is detailed in the absence of radiation (top left panel). CD133+ cells have an enhanced ability to produce neurospheres. In addition to forming more neurospheres per plated cell, the neurospheres produced by CD133+ cells had a significantly larger diameter (top right panel). Representative images of the neurospheres produced by CD133+ and CD133- cells are shown.

Furthermore, figure 4.2 shows that CD133+ cells have a significantly enhanced ability to produce neurospheres after exposure to 2Gy when compared to CD133- E2 cells, indicating that CD133+ cells are radioresistant, (lower left panel). This confirms observations from clonogenic survival assays and supports the hypothesis that GBM CSCs are radioresistant. These findings also support the hypothesis that the increased radioresistance observed in CSC populations is an intrinsic property of the GBM CSCs and not a confounding effect of the different culture media used to generate the two different culture types.

Investigation of GBM CSC radioresistance

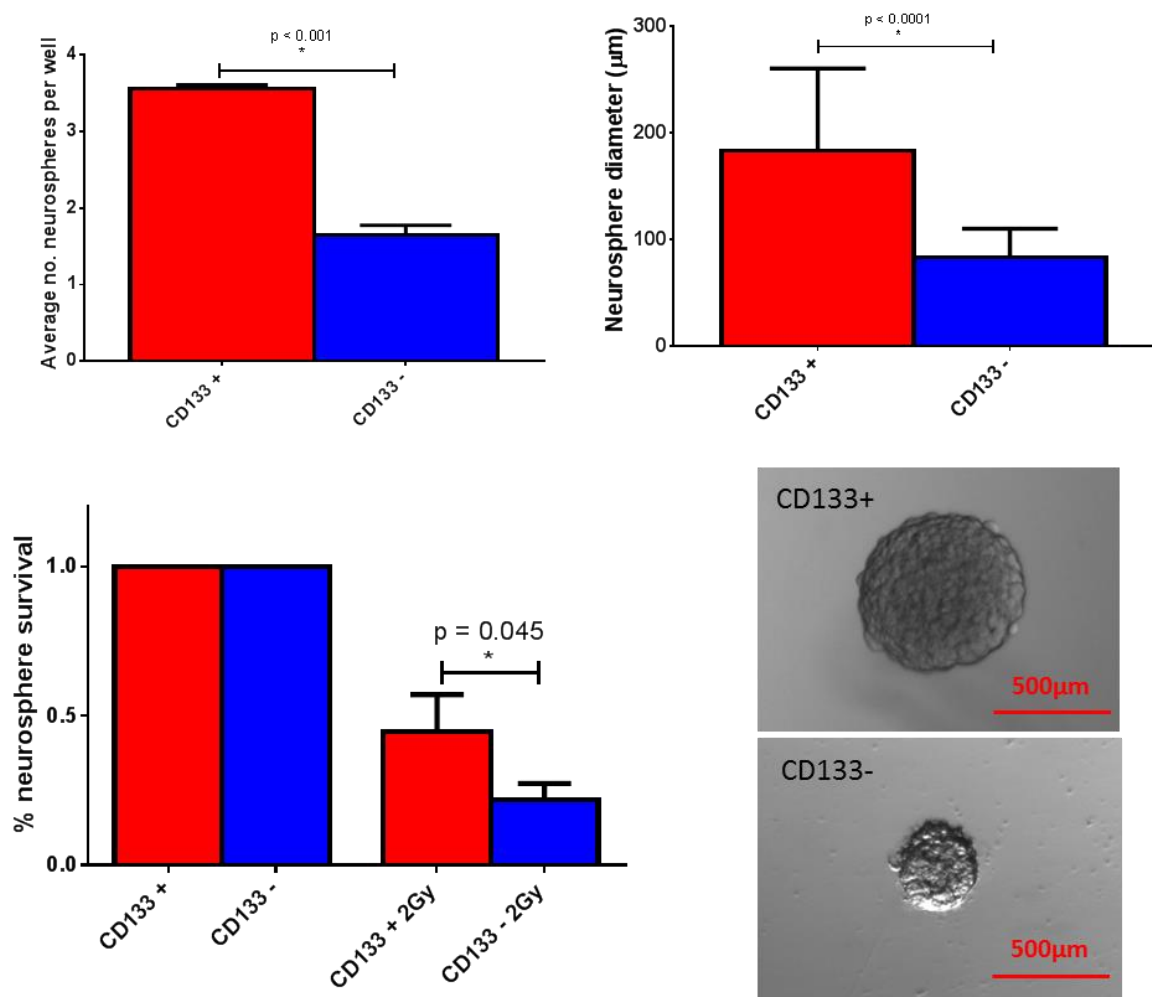


Figure 4.2 Analysis of neurosphere formation in E2 CD133+ and CD133- cells

Top left; neurosphere forming capacity of E2 CD133+ cells and E2 CD133- cells is plotted. Bars represent means plus SEM of 3 independent experiments. P values calculated using student's t test.

Top right; diameters of CD133+ and CD133- neurospheres are plotted, bars represent mean plus SD. Representative images of neurospheres are shown. P values calculated using student's t test.

Bottom left; neurosphere production following 2Gy from CD133+ and CD133- E2 cells; results represent means and SEM from 3 independent experiments. Results are normalised to unirradiated controls. P values calculated using two sample t test.

4.4 Investigation of cell cycle checkpoint phosphoproteins in GBM CSCs

As previously discussed several authors have documented important differences in cell cycle checkpoint activation in CD133+ GBM cells compared to CD133- cells following radiation. However these data are restricted to quantification of phosphorylated checkpoint protein expression and assays of cell doubling times rather than robust analysis of checkpoint function. Cell cycle checkpoint

Investigation of GBM CSC radioresistance

function in CSC and bulk populations following radiation was therefore investigated.

Western blot analysis revealed evidence of an upregulated DDR in GBM CSC cultures compared to bulk cultures in the absence of radiation in the G7 cell line and after radiation in the E2 and R10 cell lines. A radiation dose of 5 Gy induced phosphorylation of ATM at serine 1981 (pATM s1981) to a greater degree in E2 CSC cultures than in E2 bulk cultures. Differences in DDR protein phosphorylation were evident at lower doses of radiation, however 5Gy showed maximal induction of DDR phosphoproteins in both cell lines (personal communication, Dr Shafiq Ahmed). The levels of total ATM were similar between the two populations. Correspondingly the levels of phosphorylated Chk2 at threonine 68 (pChk2 thr68; a major phosphorylation target of ATM) were increased in E2 GBM CSC cultures following 5Gy compared to E2 bulk cultures (fig 4.3). A similar pattern was seen in the R10 cell line, with R10 GBM CSC cultures exhibiting higher levels of pATM s1981 and pChk2 thr68 after 5 Gy radiation compared to R10 bulk cultures (fig 4.3). Levels of phosphorylated ATR serine 428 (pATR s428) and phosphorylated Chk1 serine 345 (pChk1 s345) were also found to be elevated in the E2 CSC population compared to bulk. The phosphorylation of ATR appeared to be upregulated at baseline and was not increased by radiation exposure, whereas the phosphorylation of Chk1 was increased both at baseline and in response to radiation.

Phosphorylation of key DDR proteins was also increased in G7 GBM CSC cultures compared to bulk; however the pattern of upregulation was somewhat different. G7 GBM CSC cultures appeared to have an upregulated baseline level of pATM s1981 and pChk2 thr68 in the absence of radiation, rather than upregulation in response to radiation *per se* (fig 4.3). Total Chk2 levels were increased at baseline in the G7 CSC population compared to bulk. Phosphorylated ATR levels were increased in the G7 CSC cells compared to bulk at baseline, similar to the pattern seen in E2 CSC and bulk.

Investigation of GBM CSC radioresistance

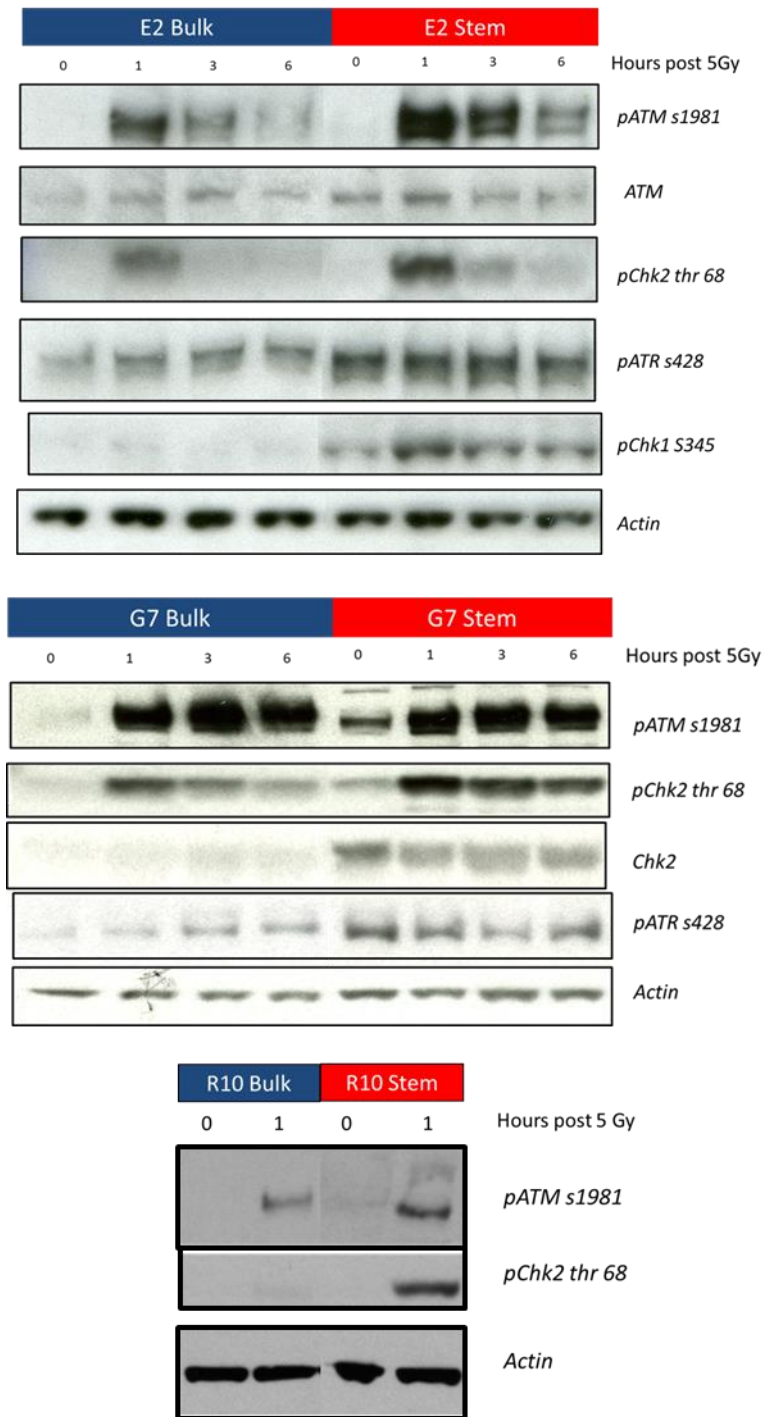


Figure 4.3 DDR protein and phosphoprotein expression by Western blotting in CSC and bulk cells in response to radiation

Western blots comparing levels of pATM s1981 and pChk2 thr68 following 5Gy of ionising radiation in E2, G7 and R10 bulk and CSC populations. Levels of pChk1 s345 and pATR s428 are also shown in the E2 cell line.

4.5 Investigation of cell cycle kinetics in GBM CSC and tumour bulk cultures

It was hypothesised that the differential DDR seen in GBM CSC cells compared to bulk cells would translate into different cell cycle checkpoint kinetics following radiation. In the first instance the G1/S checkpoint was examined by incubation with PI and subsequent flow cytometry. Representative cell cycle profiles are shown in fig 4.4 at 0, 1, 3 and 6 hours following 5Gy of radiation. The proportions of cells in G1, S and G2/M phases were quantified and these results are shown in fig 4.5. The E2 and G7 cell lines showed no G1/S cell cycle checkpoint response to radiation at these timepoints whereas a modest accumulation of cells in G2/M was evident in both cell lines suggesting that the G2/M checkpoint was intact.

G2/M checkpoint activation was investigated in more detail by quantifying the proportion of cells undergoing mitosis in CSC and bulk cultures at various timepoints following radiation. This was achieved by flow cytometric analysis of pHisH3 which is a marker for mitotic cells, (Hans and Dimitrov, 2001). In the E2 cell line CSC cultures exhibited a rapid fall in the percentage of mitotic cells after exposure to 5 Gy. An attenuated reduction in percentage of mitotic cells was observed in E2 bulk cells (fig 4.7). A similar significant effect was observed in G7 CSC compared to bulk cells following 5Gy (fig 4.7). Representative images of the gating used to quantify pHisH3 positive cells is shown (fig 4.6).

These data demonstrate for the first time that the cell cycle phosphoprotein changes described here in GBM CSCs and published previously (Bao et al., 2006a) result in enhanced cell cycle checkpoint activation in GBM CSCs, which is likely to contribute to their radioresistant phenotype.

Investigation of GBM CSC radioresistance

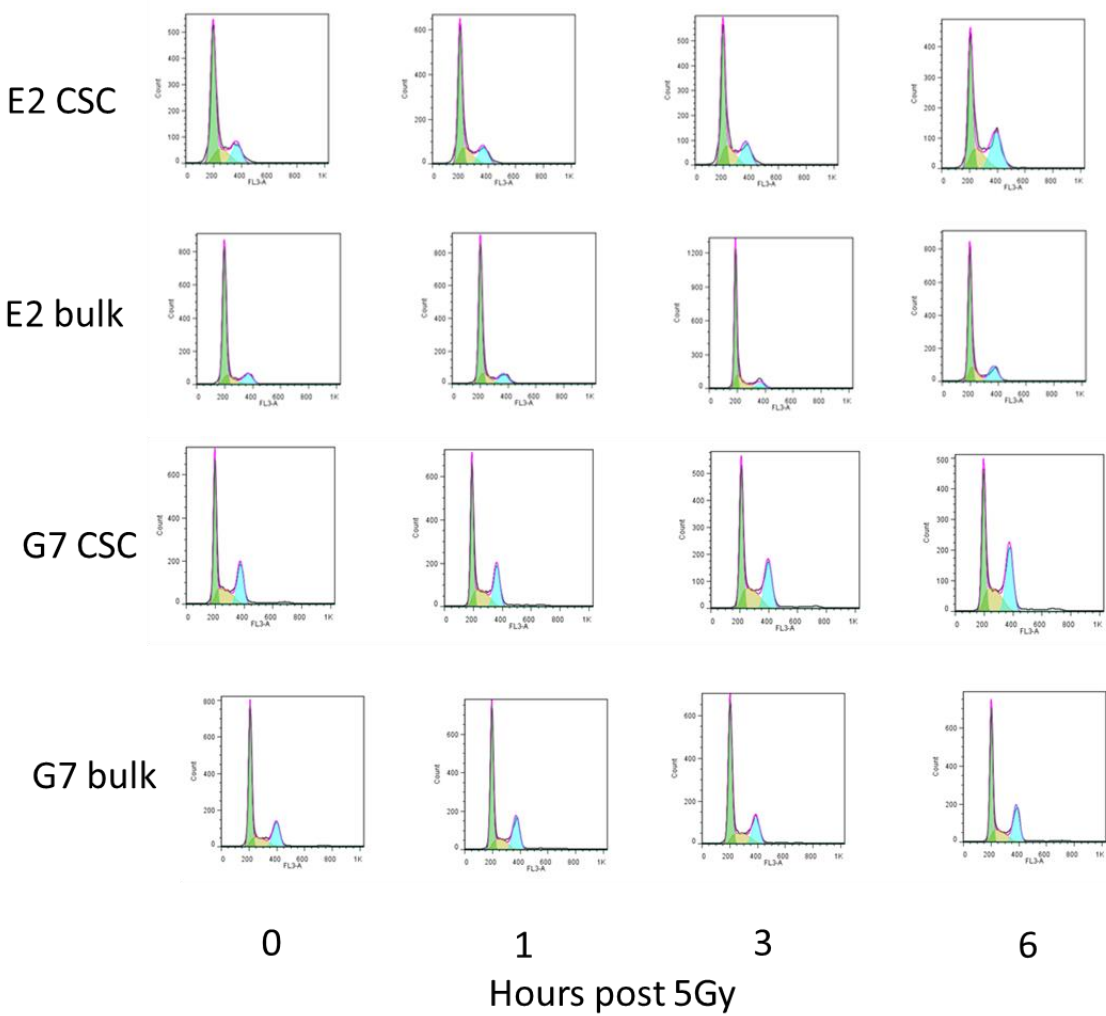


Figure 4.4 Cell cycle profiles of E2 and G7 CSC and tumour bulk cultures following 5Gy radiation exposure

Representative cell cycle profiles of E2 and G7 CSC and bulk cultures treated with 5Gy. Cells fixed with ethanol at timepoints indicated and DNA content analysed by and incubation with PI subsequently facilitating flow cytometric quantification of DNA content.

Investigation of GBM CSC radioresistance

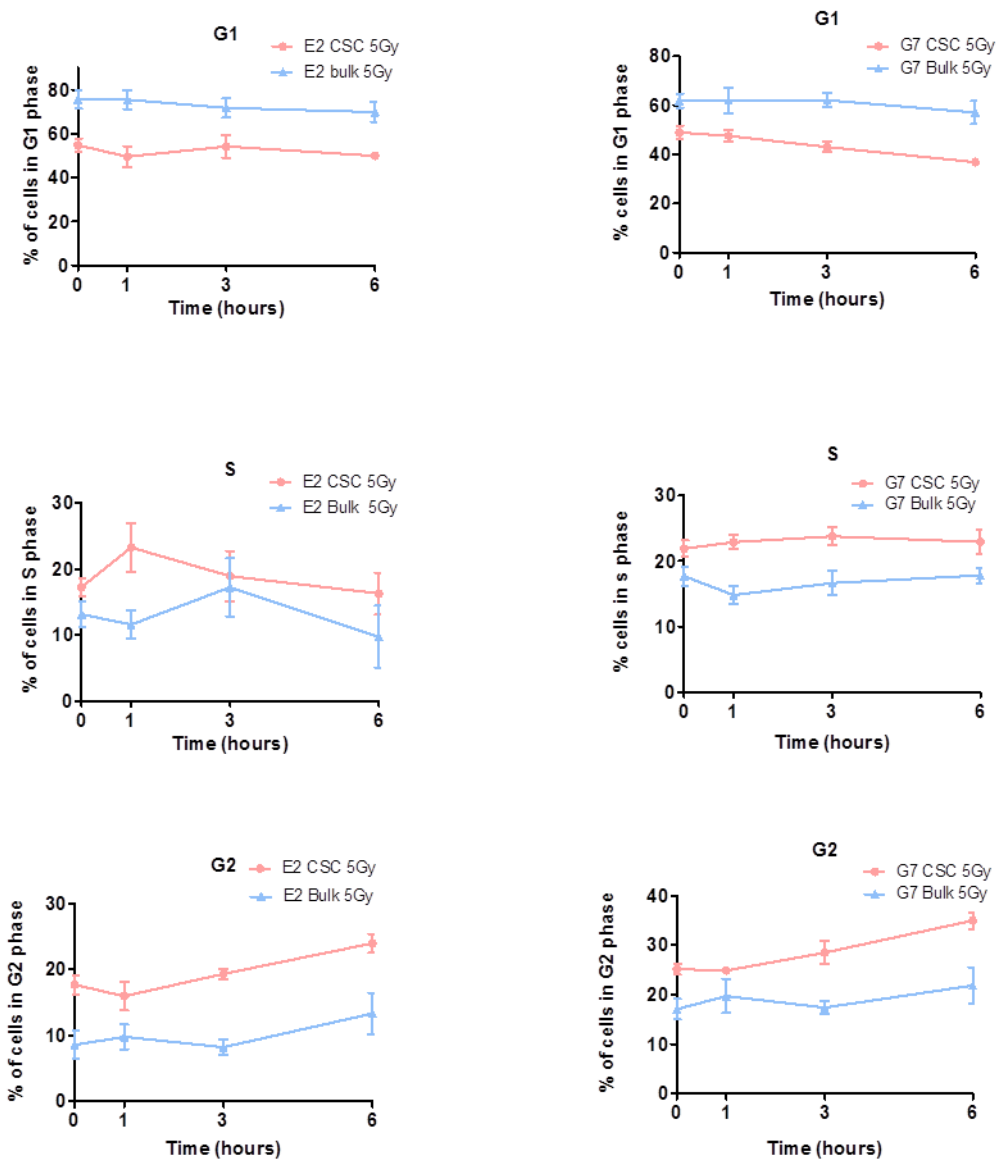


Figure 4.5 Cell cycle phase quantification of cells following ionising radiation exposure in E2 and G7 CSC and tumour bulk cultures

The proportion of cells in G1, S and G2 phases at 0, 1, 3 and 6 hours post 5Gy of radiation was plotted for CSC and tumour bulk cultures of E2 and G7 cell lines. DNA content was measured by flow cytometry following incubation of fixed cells with PI. Data points represent mean and SEM of 3 independent experiments.

Investigation of GBM CSC radioresistance

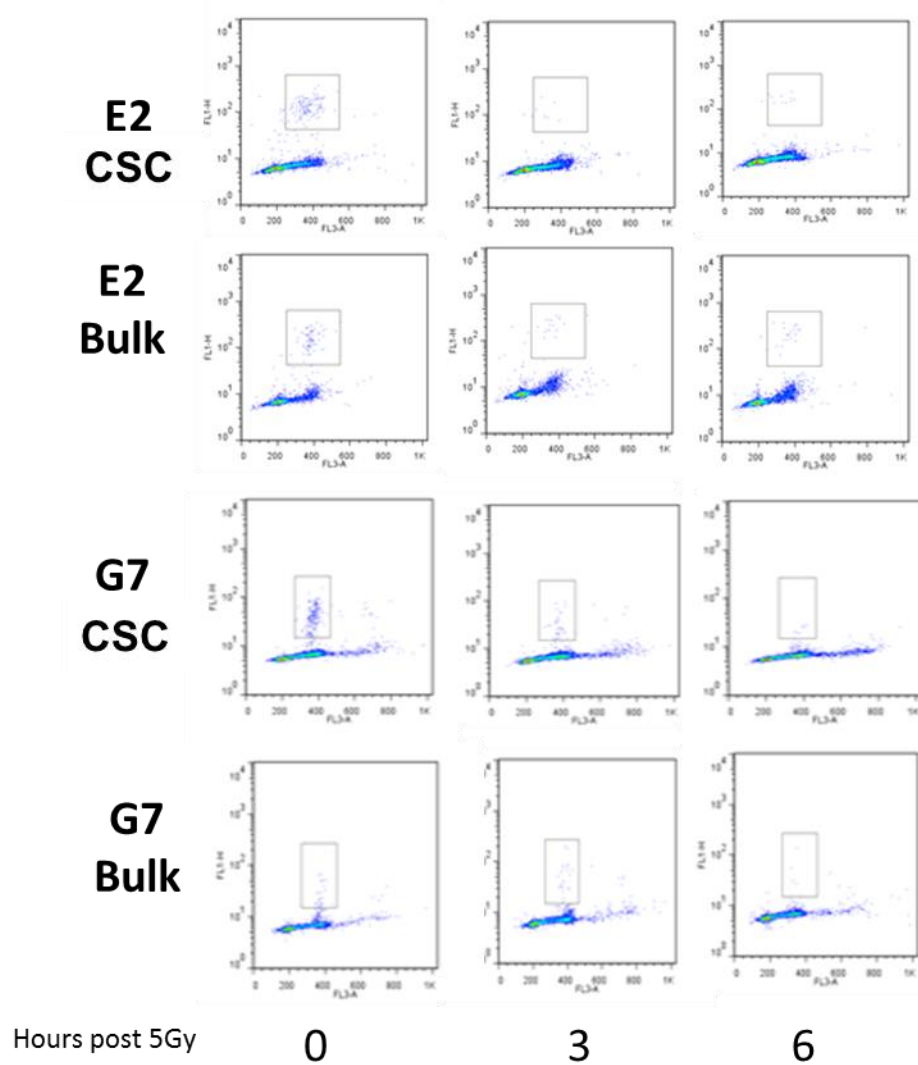


Figure 4.6 Analysis of mitotic cells following ionising radiation by pHisH3

Representative images of gating defining pHisH3 positive cells for flow cytometric quantification of mitotic proportion of CSC and tumour bulk cells of E2 and G7 cell lines post 5Gy.

Investigation of GBM CSC radioresistance

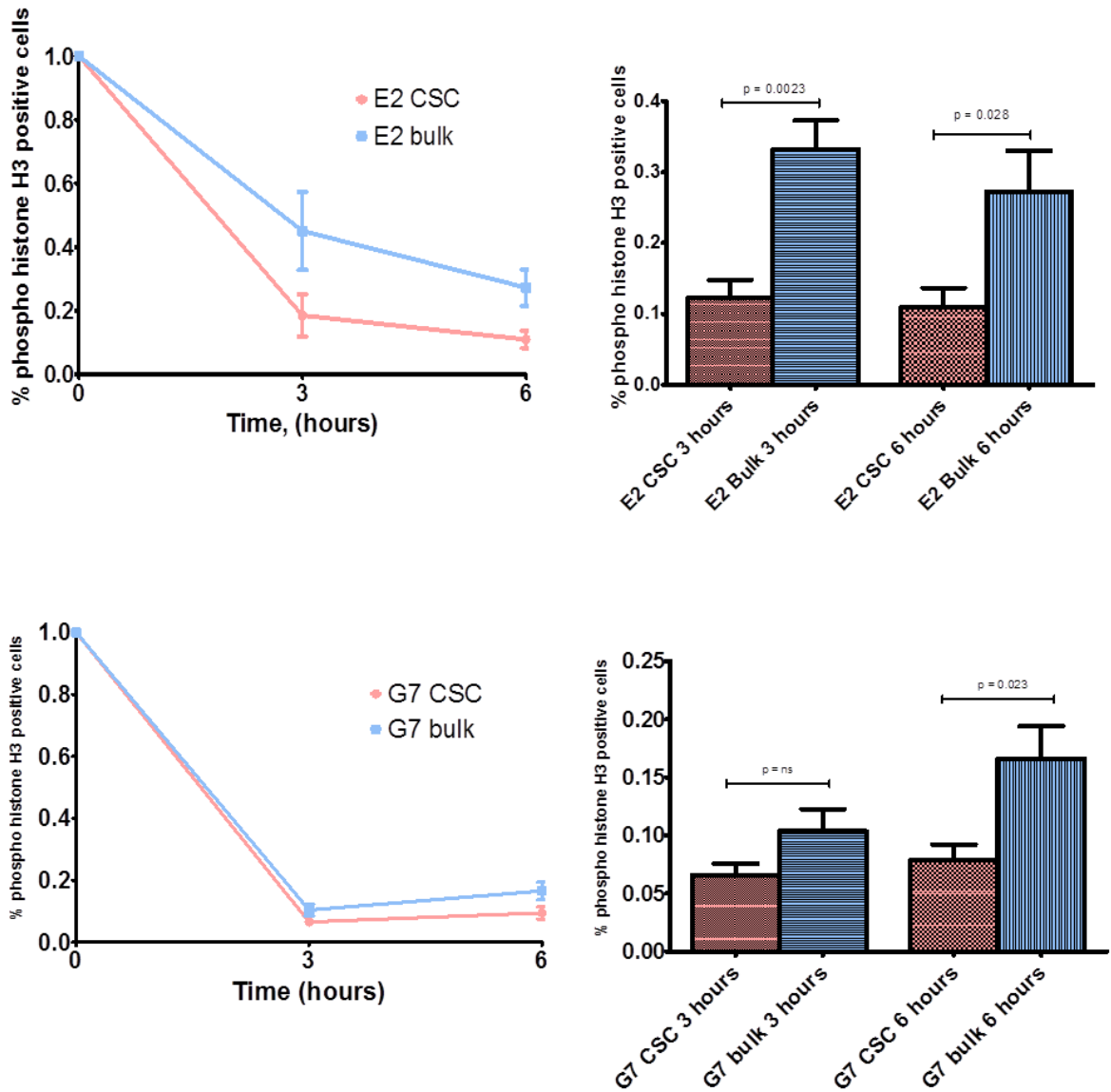


Figure 4.7 Quantification of mitotic cells following ionising radiation by pHisH3

Quantification of proportion of mitotic cells in E2 and G7 CSC and tumour bulk cultures following 5Gy radiation by flow cytometric quantification of pHisH3. Results are plotted as mean +/- SEM of 6 independent experiments normalised to unirradiated controls. Results are plotted as line graphs to illustrate effects on mitotic fraction over time post 5Gy and as column charts to facilitate statistical comparison of timepoints. Columns and error bars represent means and SEM of 6 independent experiments, p values calculated by student's t test.

4.6 Investigation of DNA DSB repair in GBM CSC cultures

Having described changes in cell cycle kinetics contributing to GBM CSC radioresistance an examination of DNA repair in CSC populations was undertaken. Previous authors have addressed this with assays encompassing single strand and double strand DNA damage such as the alkaline comet assay. In this study, a specific examination of DNA DSB repair was performed because DNA DSBs are the key lethal lesions generated by radiotherapy, as well as being

Investigation of GBM CSC radioresistance
the most relevant lesions in terms of clinical radiation resistance in cancers
(Banath et al., 2004).

A quantitative analysis of induction and resolution of DNA DSBs in E2 CSC and bulk cells following radiation exposure was performed by cell cycle phase specific immunofluorescence analysis of gamma H2AX foci using CENPF as a marker of G2 phase cells. Gamma H2AX foci are a marker for DNA DSBs (Sedelnikova et al., 2002). Gamma H2AX represents a phosphorylated histone modification of the histone chromatin component H2AX. H2AX becomes locally phosphorylated in the vicinity of DNA DSBs to form gamma H2AX foci, which are visible and quantifiable using immunofluorescent microscopy. It is generally accepted that each gamma H2AX focus represents the presence of a single DNA DSB, (Kinner et al., 2008). For these experiments a radiation dose of 1Gy was administered in order to be able to quantify DNA DSBs at early timepoints following radiation exposure. Following an initial pilot experiment (fig 4.8), timepoints of 0, 1, 3 and 24 hours were chosen in order to characterise induction, fast phase resolution and slow phase resolution of gamma H2AX foci respectively. As shown in figure 4.8 the number of gamma H2AX foci in CENPF positive populations at 1 hour is increased compared to that seen in the CENPF negative populations consistent with the increased DNA content of G2 phase cells. Per Gy of radiation G2 phase cells will theoretically experience approximately twice the number of DNA DSBs in comparison to G1 phase cells, (Lobrich et al., 2010). Given that this study demonstrated in chapter 3 that GBM CSC cultures have a higher proportion of G2 phase cells compared to bulk cultures, it was necessary to analyse gamma H2AX foci resolution in the G1 and G2 cell cycle phase marker CENPF was incorporated into the gamma H2AX assay used in this study (Liao et al., 1995).

Investigation of GBM CSC radioresistance

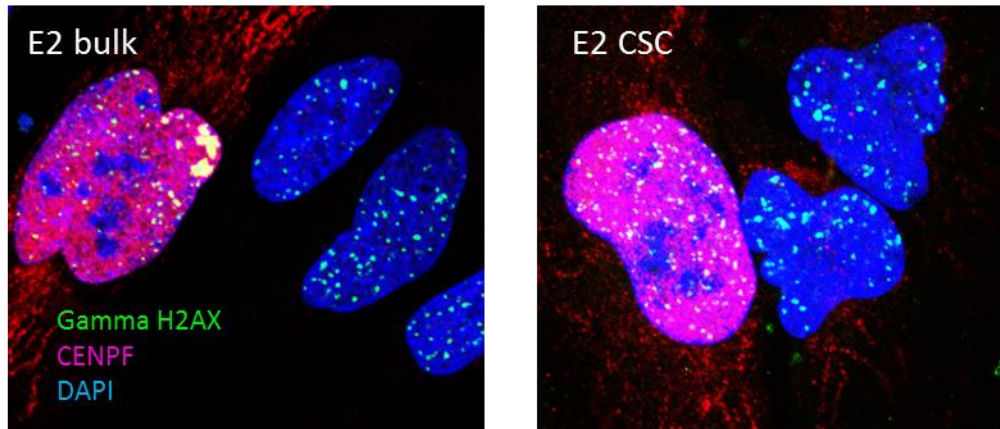
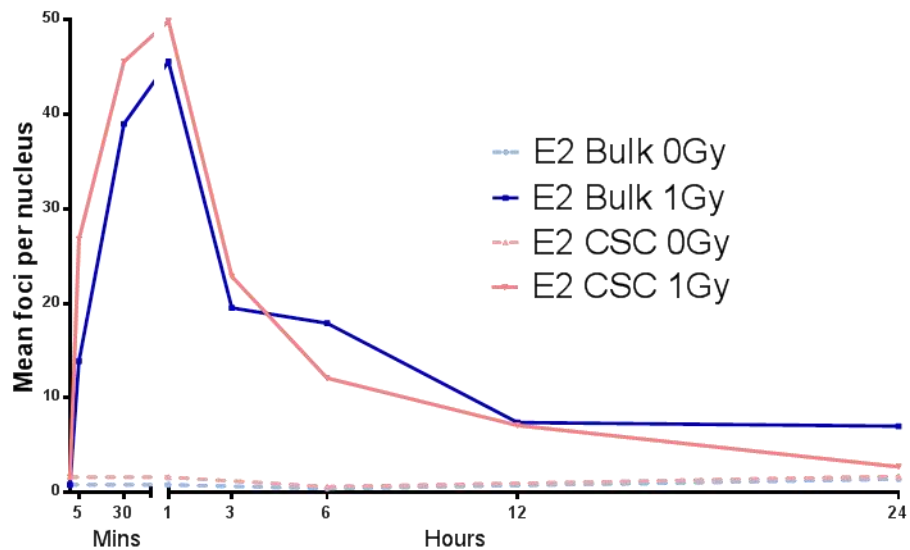


Figure 4.8 Quantification of gamma H2AX foci following 1Gy irradiation (initial pilot experiment)

Gamma H2AX foci quantification following exposure of cells to 1Gy in E2 CSC and bulk cells. Pilot experiment where foci per nucleus were quantified in CENPF negative cells at timepoints of 5mins, 30mins, 1, 3, 6, 12 and 24 hours. Cells were fixed at time points shown and stained with CENPF and gamma H2AX antibodies. Each data point represents mean number of foci per nucleus from 1 experiment. Representative images of gamma H2AX foci and CENPF staining in E2 bulk and CSC are shown at 1 hour post irradiation. Images represent maximum intensity projections of 6 slice Z stacks at 63x magnification using a Zeiss 710 confocal microscope.

Investigation of GBM CSC radioresistance

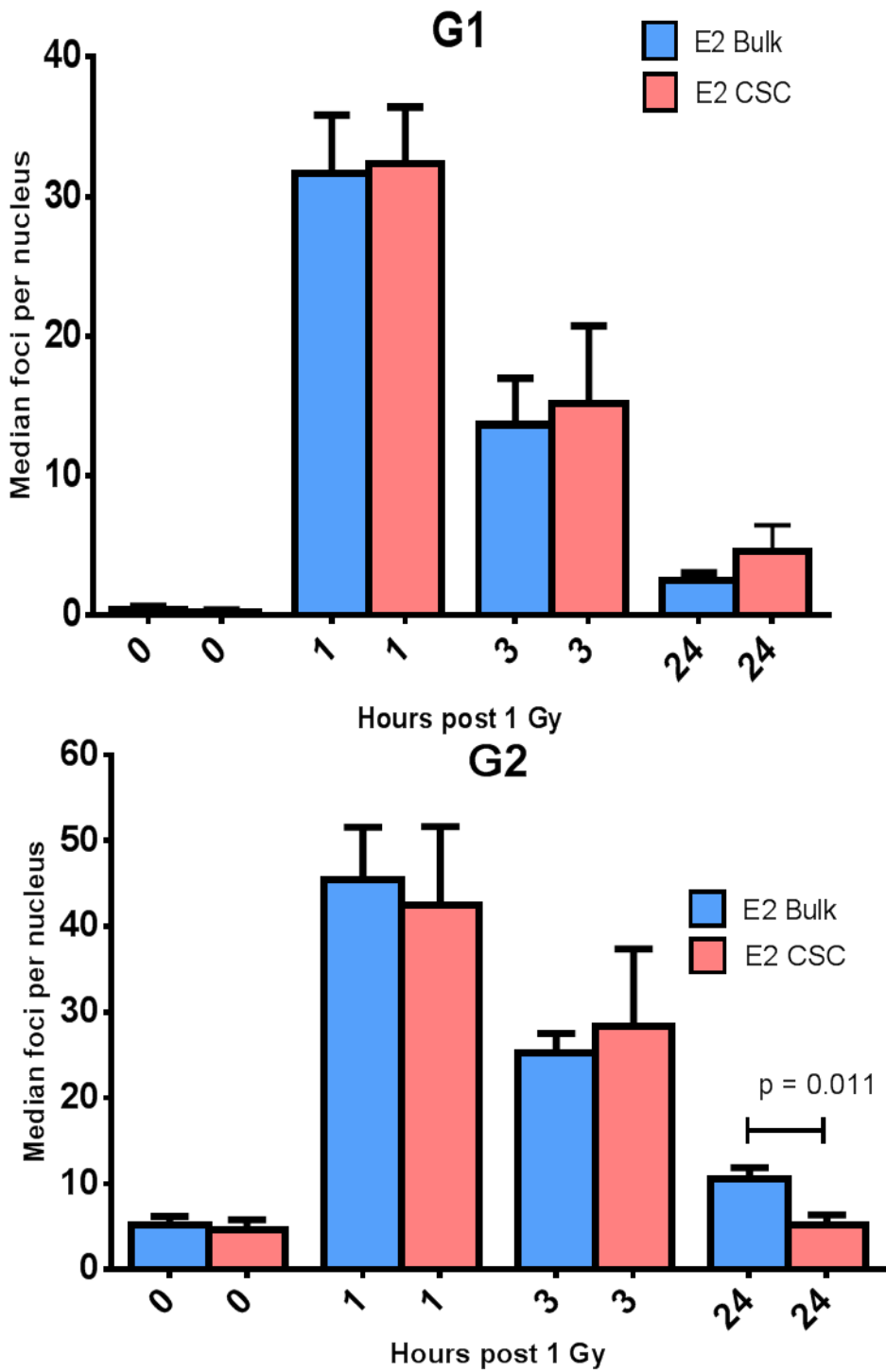


Figure 4.9 Quantification of gamma H2AX foci in CENPF negative and CENPF positive E2 CSC and bulk cell nuclei

Gamma H2AX nuclei were quantified following exposure to 1Gy at timepoints of 0, 1, 3 and 24 hours in CENPF negative (G1) and CENPF positive (G2) cell populations. The median number of foci per nucleus was calculated in 6 independent experiments and the mean of these medians is plotted for each data point with SEM in the graphs above. P values were calculated by student's t test.

Investigation of GBM CSC radioresistance

No difference in induction of gamma H2AX foci between E2 CSC and bulk cell cultures was observed at baseline or at 1 hour following irradiation, and the early or “fast” kinetics of foci resolution did not differ between CSC and bulk populations when measured at the 3 hour time point (fig 4.9). However E2 CSC cultures displayed a significantly enhanced ability to repair DNA DSBs at the 24 hour timepoint compared to E2 bulk culture cells in CENPF positive (i.e. G2) populations. Mean of median foci per nucleus (plus 95% confidence interval) in G2 populations of CSCs was 5.17 (2.78, 7.55) compared to 10.58 (8.09, 13.07) in G2 bulk populations. This would suggest that GBM CSCs are able to resolve DNA DSBs much more efficiently at 24 hours post irradiation than their more differentiated bulk counterparts. The above data demonstrates that GBM CSCs are almost twice as efficient as tumour bulk cells in resolving DNA DSBs at late repair timepoints which would partly explain why GBM CSCs are radioresistant in comparison to tumour bulk cells. There were no statistically significant differences in foci numbers at 24 hours between CSC and bulk cultures in CENPF negative (i.e. G1) populations.

Different patterns of gamma H2AX staining were seen in the nuclei of cells at baseline and in response to radiation. The presence of large radiation induced foci was differentiated from the background non-specific nuclear speckled staining which is produced by antibodies to gamma H2AX. Solid, intense nuclear staining is associated with apoptosis whereas a more diffuse pattern of nuclear staining occurs in S phase cells. ATR is a known phosphorylator of H2AX and will be activated at DNA DSBs produced by the collapse of replication forks in S phase, resulting in gamma H2AX foci which do not represent direct radiation induced DNA DSBs. Furthermore stretches of SS DNA present under conditions of replication stress in S phase cells will activate ATR via ATRIP also resulting in H2AX phosphorylation (Kinner et al., 2008). Gamma H2AX immunofluorescent staining in S phase cells must therefore be interpreted with caution. These patterns of staining were excluded from the analysis as they are not representative of DNA DSBs directly induced by radiation.

4.7 Conclusion

A detailed comparison of radiation resistance in GBM CSC and bulk cultures has been documented. GBM CSCs were significantly more radioresistant than tumour bulk cultures. The dose modifying factor for GBM CSCs relative to tumour bulk cells at 0.37 survival was in the range 1.3-1.5. This magnitude of radioresistance is likely to be clinically significant and supports the hypothesis that CSCs are one of the factors contributing to clinical tumour recurrence after radiotherapy in GBM.

The radioresistance of CSCs was confirmed by neurosphere assay of sorted CD133+ and CD133- cells from an E2 CSC culture population. This assay was not dependent on different cell culture conditions since both CD133+ and CD133- cells could be maintained in neurobasal CSC medium. It is of interest that CD133- cells from this population were still able to form neurospheres, suggesting that although they lack the CD133 CSC marker they still have some proliferative capacity. Nevertheless this proliferative capacity is clearly less than the CD133+ population given that the neurospheres produced were significantly reduced in diameter. The ability of CD133- cells to produce neurospheres was significantly impaired after exposure to 2Gy in comparison to that of CD133+ cells, supporting the hypothesis of GBM CSC radioresistance.

The analysis of cell cycle phosphoproteins in GBM CSCs and bulk cells confirms previously published work documenting upregulation of pChk2 and pATM in response to radiation in GBM CSCs. In addition to the pattern of upregulated phosphorylation of these proteins in response to radiation in the E2 and R10 cell lines, this study also identified upregulated basal levels of cell cycle checkpoint proteins in G7 CSCs. The functional analysis of the G2/M checkpoint using pHisH3 as a mitotic marker in E2 and G7 CSCs demonstrates for the first time that altered levels of cell cycle phosphoproteins are associated with more efficient activation of the G2/M checkpoint. This is a likely contributor to radioresistance. Both G7 and E2 cell lines demonstrated lack of G1/S checkpoint activation following radiation, despite having wild type p53. This likely signifies a defective

Investigation of GBM CSC radioresistance

p53 pathway, which is a common finding in GBM tumours (Cancer Genome Atlas Research, 2008).

A detailed investigation of DNA DSB repair in GBM CSC populations was undertaken. This demonstrated kinetics of gamma H2AX induction and resolution broadly in agreement with previous studies of irradiation induced foci in other cell lines. There is a clear fast phase resolution of foci in the first 3 hours following irradiation followed by a much slower phase of foci resolution stretching from 3 hours to 24 hours. The E2 CSC and bulk G2 cell populations exhibited higher numbers of foci following irradiation compared to G1 cell populations, in keeping with their increased DNA content, however G2 cells did not have double the number of foci compared to G1 phase cells at 1 hour post irradiation. This may reflect a higher degree of aneuploidy in the E2 cell line compared to fibroblast cell lines studied by other authors. This analysis of DNA DSB resolution provides evidence of a significant repair advantage present in GBM CSCs compared to bulk cells. This was evident only at 24 hours post radiation and affected the slow phase of repair of DNA DSBs in G2 phase cells only. The median number of gamma H2AX foci at 24 hours post 1Gy in CSCs was 10.58 vs 5.17 in bulk cell populations. This repair advantage is likely to be clinically significant since it has been shown that the level of unresolved DSBs at 24 hours correlates with radiation sensitivity both *in vitro* and *in vivo* (Banath et al., 2004). This represents an approximate doubling of efficiency of DNA DSB repair at 24 hours post irradiation in the CSC population relative to that seen in the tumour bulk population, and may partly explain the very high radioresistance seen in the CSC population. Other authors have been unable to demonstrate upregulated repair in GBM CSCs. Ropolo et al examined gamma H2AX foci resolution in CD133+ and CD133- cells following radiation and could not show any difference in foci numbers at 24 hours following radiation. However the study by Ropolo et al did not carry out a cell cycle specific examination of foci resolution and furthermore discriminated only between cells with foci and cells without foci, instead of the more comprehensive foci counts per nucleus which were undertaken in this thesis. Studies of CSC DNA DSB repair using the gamma H2AX foci assay in other tumour sites are in agreement with a repair advantage for

Investigation of GBM CSC radioresistance

CSC populations in the slow phase of repair following irradiation (Desai et al., 2014, Frame et al., 2013).

The investigations detailed above show that GBM CSC radioresistance is due to dual mechanisms of efficient activation of the G2/M checkpoint following radiation and increased DNA DSB resolution specifically in the slow phase of DNA DSB repair in G2, which suggests CSCs have increased efficiency in the HR pathway of DNA DSB repair. ATM has been proposed to have a specific contribution to the slow phase of repair of DNA DSBs (Goodarzi et al., 2008, Alvarez-Quilon et al., 2014), and is also a controller of the G2/M cell cycle checkpoint. Given that these investigations have demonstrated upregulated levels of pATM in response to radiation in GBM CSCs, these data suggest that ATM function is key to the radiation resistance seen in GBM CSCs.

Chapter 5 Effects of ATM inhibition on GBM CSC radioresistance

5.1 Introduction

Chapter 4 demonstrated the radioresistance of GBM CSCs was associated with more efficient activation of the G2/M cell cycle checkpoint and increased resolution of DNA DSBs in the slow phase of DNA DSB repair in G2 cells. This was accompanied by increased levels of phosphorylated ATM in response to ionising radiation in GBM CSCs. ATM is an apical kinase in the DDR to ionising radiation, and phosphorylates many effectors of DNA repair. It has key roles both in cell cycle checkpoint activation and DNA DSB repair in response to ionising radiation. Therefore it was hypothesised that GBM CSCs rely upon upregulation of ATM function in order to maintain their radioresistant phenotype and studies of the effects of ATM inhibition in GBM CSC bulk cultures were undertaken.

5.2 Effect of ATM inhibition on upregulated DDR in GBM stem cells

The potent and selective ATM inhibitor KU-55933 was utilised for these studies. A concentration of 10 μ M was chosen from pre-existing literature concerning this compound. Previous studies illustrate that at this concentration KU-55933 specifically inhibits ATM, with no evidence of direct inhibition of DNAPK or ATR (Hickson et al., 2004). In preliminary studies, E2 and G7 CSC and bulk cells were incubated for 1 hour in medium containing 10 μ M KU-55933 prior to 5Gy of radiation and lysed for Western blotting at timepoints of 1, 3 and 6 hours post treatment, (fig. 5.1). ATM inhibition was able to completely inhibit the phosphorylation of Chk2 at threonine 68 (a major phosphorylation target of ATM) in both CSC and bulk cultures of E2 and G7 cell lines. Furthermore autophosphorylation of ATM at serine 1981 was also inhibited by KU-55933. The inhibition of Chk2 phosphorylation would suggest that 10 μ M KU-55933 effectively inhibits function of the ATM kinase in the E2 and G7 cell lines in both CSC and bulk cultures.

Effects of ATM inhibition on GBM CSC radioresistance

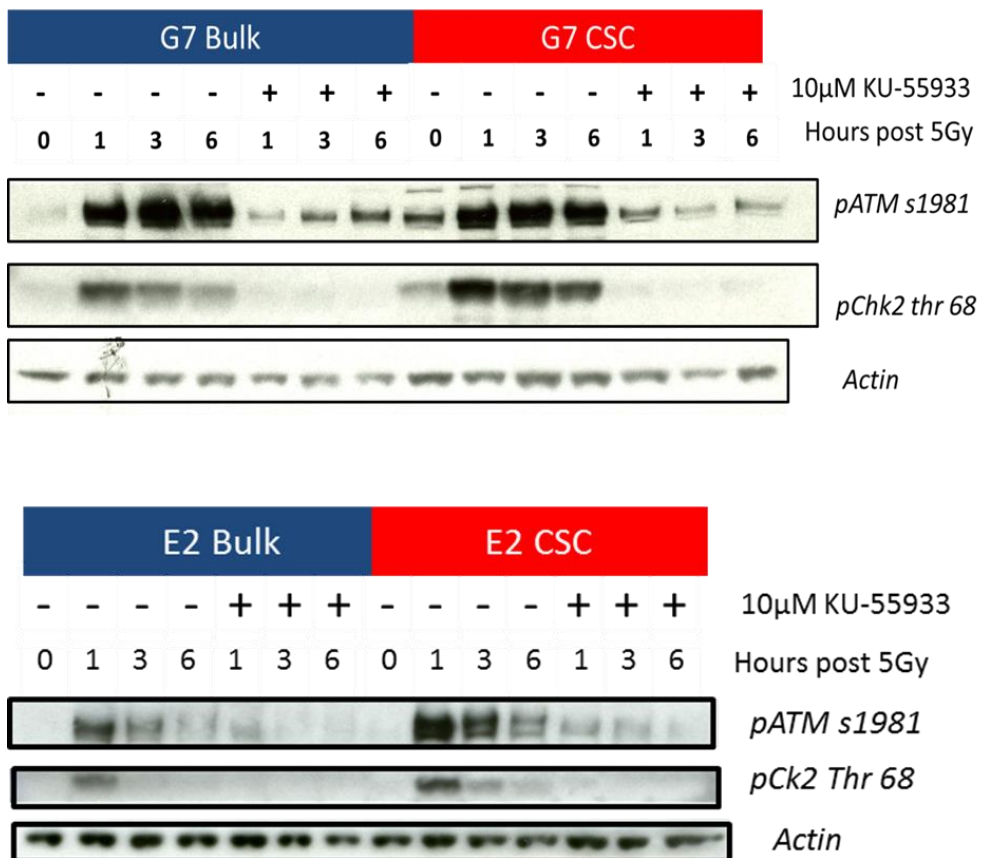


Figure 5.1 Comparison of phosphorylated DDR proteins in CSC and bulk cell cultures following 5Gy radiation +/- KU-55933

E2 and G7 CSC and bulk cultures were incubated with 10µM KU-55933 or a corresponding concentration of DMSO for 1 hour prior to 5Gy radiation. Cells were lysed for Western blotting at timepoints after radiation as shown. Membranes were probed for pATM s1981, pChk2 Thr 68 and actin as a loading control.

5.3 Effect of ATM inhibition in the absence of radiation on cell viability in GBM CSC and bulk cells

Effects of KU-55933 on cell viability in CSC and bulk cultures were assessed using the CellTiter-glotm assay. In brief, CSC and tumour bulk cultures of E2 and G7 were plated onto Matrigeltm plates and incubated with different concentrations of KU-55933 for a period of 24 hours prior to the drug being removed and replaced with fresh CSC or bulk media (fig. 5.2). The experiment was repeated with a longer exposure (6 days) to differing concentrations of KU-55933 in order to assess prolonged exposure to the drug and the effects of cumulative DNA damage (fig. 5.2). Prolonged inhibition with KU-55933 was necessary to assess

Effects of ATM inhibition on GBM CSC radioresistance
effects on the repair of relatively infrequently occurring DNA damage under basal conditions.

24 hour incubation of E2 CSC and bulk cells in media containing 10 μ M KU-55933 produced a 10% decrease in cell viability relative to controls treated with an identical concentration of DMSO. This concentration of drug had a slightly larger effect on the G7 CSC cultures producing a 23% decrease in cell viability. There was no effect on the viability of G7 bulk cultures.

Prolonged 6 day exposure of E2 CSC and bulk cells to 10 μ M KU-55933 had more marked effects on cell viability. Both CSC and bulk viability was reduced relative to controls to 51 and 61% respectively. In G7 CSC and bulk cultures 6 day exposure to 10 μ M KU-55933 had modest effects on CSC and bulk culture viability, reducing CSC culture viability to 76% and bulk culture viability to 84%.

Decreasing cell viability was seen in both cell lines and culture conditions as the concentration of KU-55933 increased. This likely represents non-specific off target effects with very high concentrations of drug.

Effects of ATM inhibition on GBM CSC radioresistance

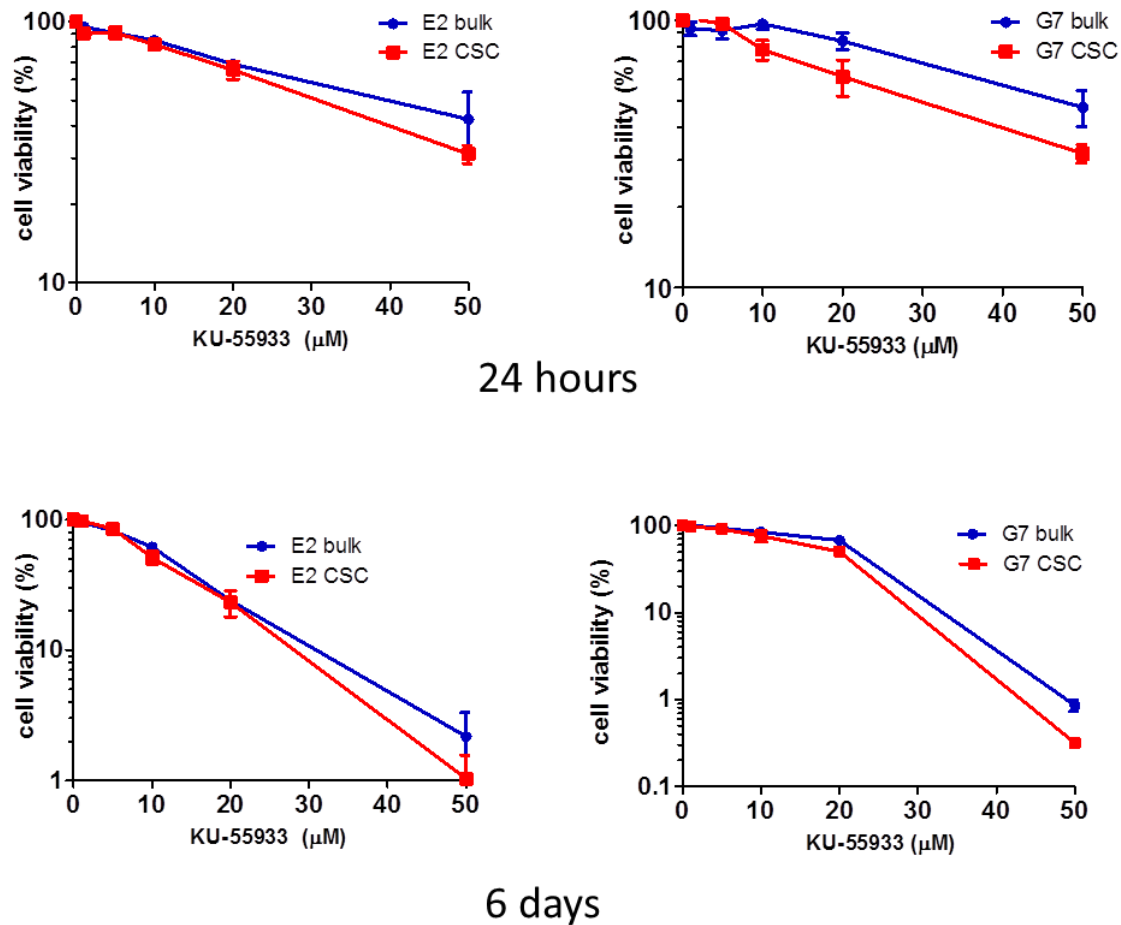


Figure 5.2 Effect of KU-55933 exposure on cell viability in CSC and bulk cultures

E2 and G7 CSC and bulk cultures were plated onto Matrigel™ coated 96 well plates and allowed to adhere. After 24 hours cultures were incubated with incremental concentrations of KU-55933 or corresponding DMSO concentrations for 24 hours prior to media removal and replacement or for 6 days without media removal and replacement. A Cell Titer-glo assay was carried out 7 days post plating of cells and cell viability results of cells exposed to KU-55933 were normalised to those of DMSO controls and plotted as shown. Plotted points represent means +/- SEM from 3 independent experiments.

Effects of ATM inhibition on GBM CSC radioresistance

5.4 Effects of ATM inhibition on G2/M checkpoint activation in GBM CSC and bulk cells

The effects of ATM inhibition on activation of the G2/M checkpoint following radiation were investigated by flow cytometry using pHisH3 as a mitotic marker in CSC and bulk cultures of E2 and G7 cell lines (fig. 5.3). Cell cultures were incubated in 10 μ M KU-55933 for 1 hour prior to 5Gy of radiation before being fixed in ethanol and analysed at the timepoints shown. KU-55933 can be seen to inhibit the G2/M checkpoint in both E2 and G7 CSCs relative to DMSO treated, irradiated controls. CSC cultures still appear to activate the G2/M checkpoint in response to radiation after ATM inhibition, although the degree of activation is much attenuated. The effect in bulk cell cultures however is more marked, particularly in the E2 cell line, where KU-55933 is observed to provide almost complete inhibition of the G2/M checkpoint following irradiation. A similar trend is seen in G7 bulk cells; however the error bars on each data point are wide, making further interpretation difficult.

Representative images of the gating used for the flow cytometric analysis of pHisH3 are shown in figure 5.4.

Effects of ATM inhibition on GBM CSC radioresistance

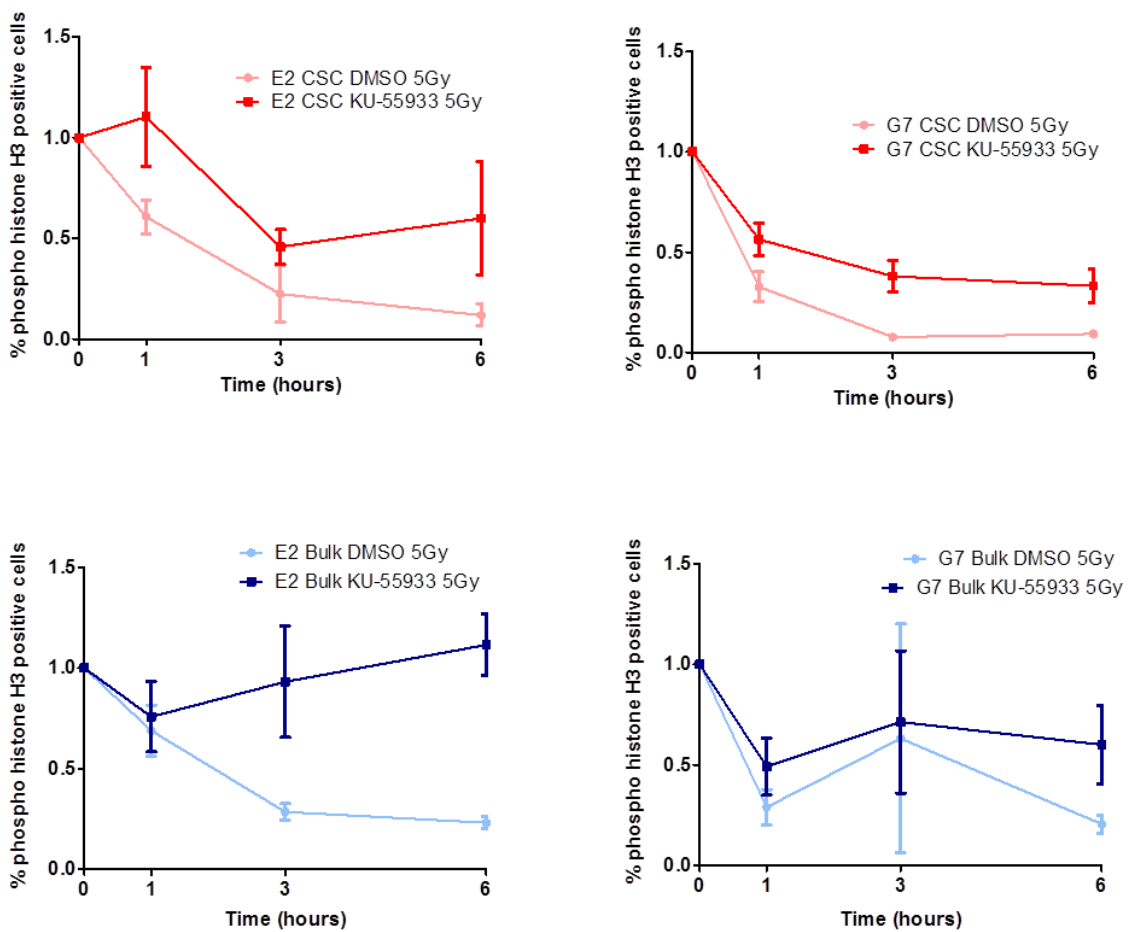


Figure 5.3 Analysis of G2/M checkpoint activation in CSC and bulk cultures following 5Gy radiation +/- KU-55933

E2 and G7 CSC and bulk cultures were plated and allowed to reach 30-40% confluence before being incubated with media containing 10µM KU-55933 or DMSO alone 1 hour prior to 5Gy of radiation. Cells were fixed in ethanol at the timepoints shown before analysis of pHish3 positivity and cell cycle phase was carried out using flow cytometry. Results were normalised to unirradiated controls and plotted as shown. Each data point represents mean +/- SEM from a minimum of 3 independent experiments.

Effects of ATM inhibition on GBM CSC radioresistance

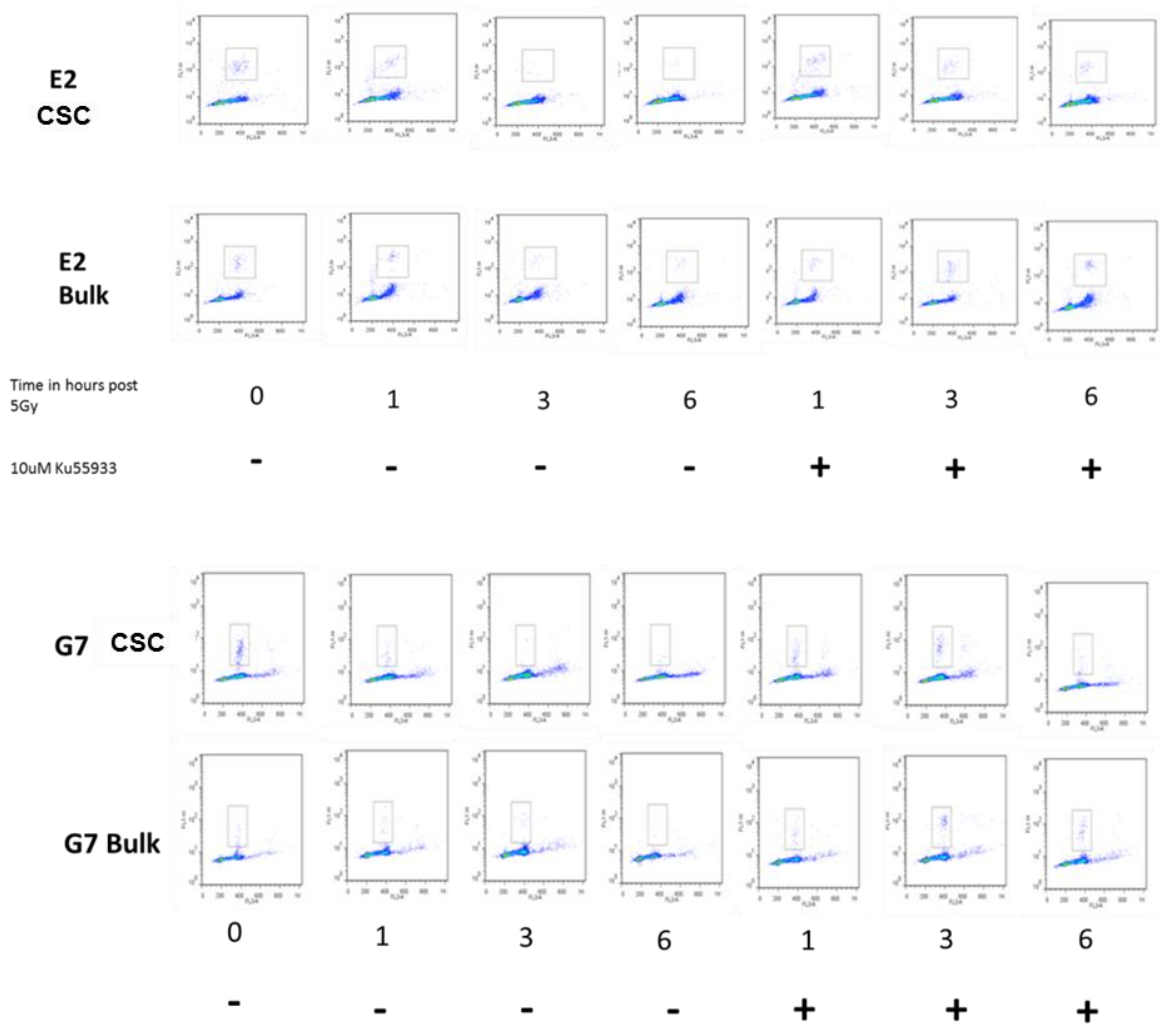


Figure 5.4 Analysis of G2/M checkpoint activation in CSC and bulk cultures following 5Gy radiation +/- KU-55933

Representative images of flow cytometry gating used to identify pHisH3 populations in figure 5.4 in E2 and G7 CSC and tumour bulk cultures

Effects of ATM inhibition on GBM CSC radioresistance

5.5 Effects of ATM inhibition on DNA DSB repair in GBM CSC and bulk cells by Gamma H2AX foci analysis

The effects of ATM inhibition on radiation induced DNA DSB repair in GBM CSC and bulk cultures were investigated by means of quantification of gamma H2AX foci. Representative images of gamma H2AX and CENPF immunofluorescent staining are shown (fig. 5.5). CSC and bulk cultures of E2 cells were incubated in 10 μ M of KU-55933 prior to irradiation with 1Gy and were then fixed at timepoints of 1, 3 and 24 hours and analysed for gamma H2AX foci formation. Populations were again subdivided into G1 and G2 populations using the CENPF cell cycle marker, and foci quantified as median number per cell nucleus (fig. 5.6). A mean of medians was then calculated to provide a summary of foci counts at each timepoint.

Examination of median nuclear gamma H2AX foci number at 24 hours in CENPF positive (G2 cell cycle phase) populations revealed a significant increase in foci numbers in E2 CSCs incubated with KU-55933 compared to DMSO treated controls. Inhibition of ATM completely removed the previously seen efficient repair of DNA DSBs in E2 CSCs at 24 hours in the G2 population. A similar trend was seen in bulk cells in CENPF positive populations at 24 hours post radiation, which did not reach statistical significance ($p = 0.058$). Consistent with ATM being the primary, but not exclusive, phosphorylator of H2AX in response to IR, ATM inhibition produced a marked reduction in Gamma H2AX foci formation at early timepoints (< 3 hours) post irradiation in both CSC and bulk cultures. This finding is discussed in more detail later in this chapter.

No statistically significant effects were seen on late repair (>3 hours) in CENPF negative (G1) CSCs or bulk cells, (fig. 5.7).

Effects of ATM inhibition on GBM CSC radioresistance

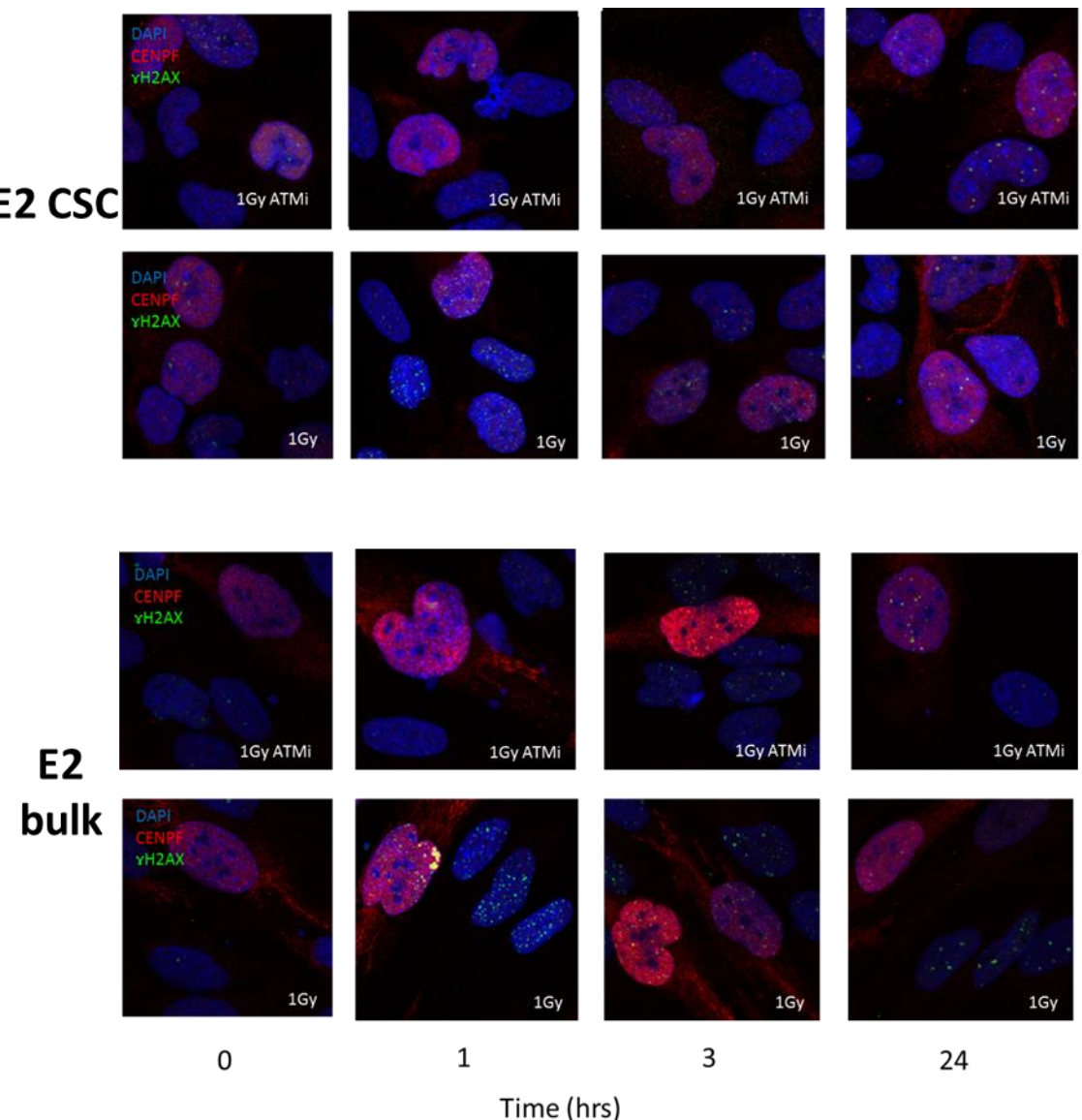


Figure 5.5 Representative images of gamma H2AX foci and CENPF immunofluorescent staining in E2 CSC and bulk cultures

Effects of ATM inhibition on GBM CSC radiosensitivity

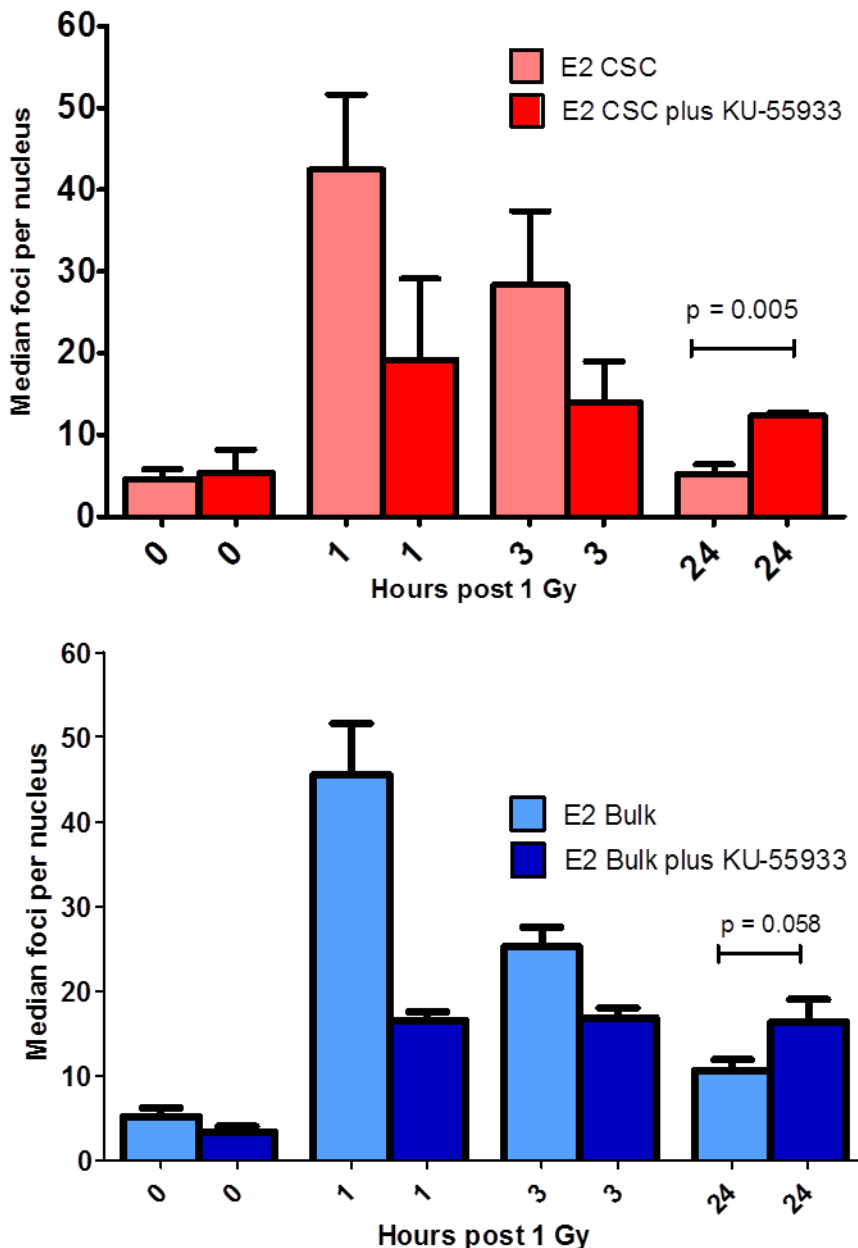


Figure 5.6 Quantification of gamma H2AX foci in CENPF positive (G2 cell cycle phase) E2 CSC and bulk cultures following 1Gy +/- 10µM KU-55933

Analysis of gamma H2AX foci as per figure 5.5, demonstrating median foci count per nucleus in E2 CSC and bulk in CENPF positive (i.e. G2 cell cycle phase) populations at baseline, 1, 3 and 24 hours post 1Gy +/- KU-55933. Each column represents the mean of 3 median foci per nucleus estimations from 3 independent experiments. Error bars represent SEM. P values were calculated by student's t test.

Effects of ATM inhibition on GBM CSC radioresistance

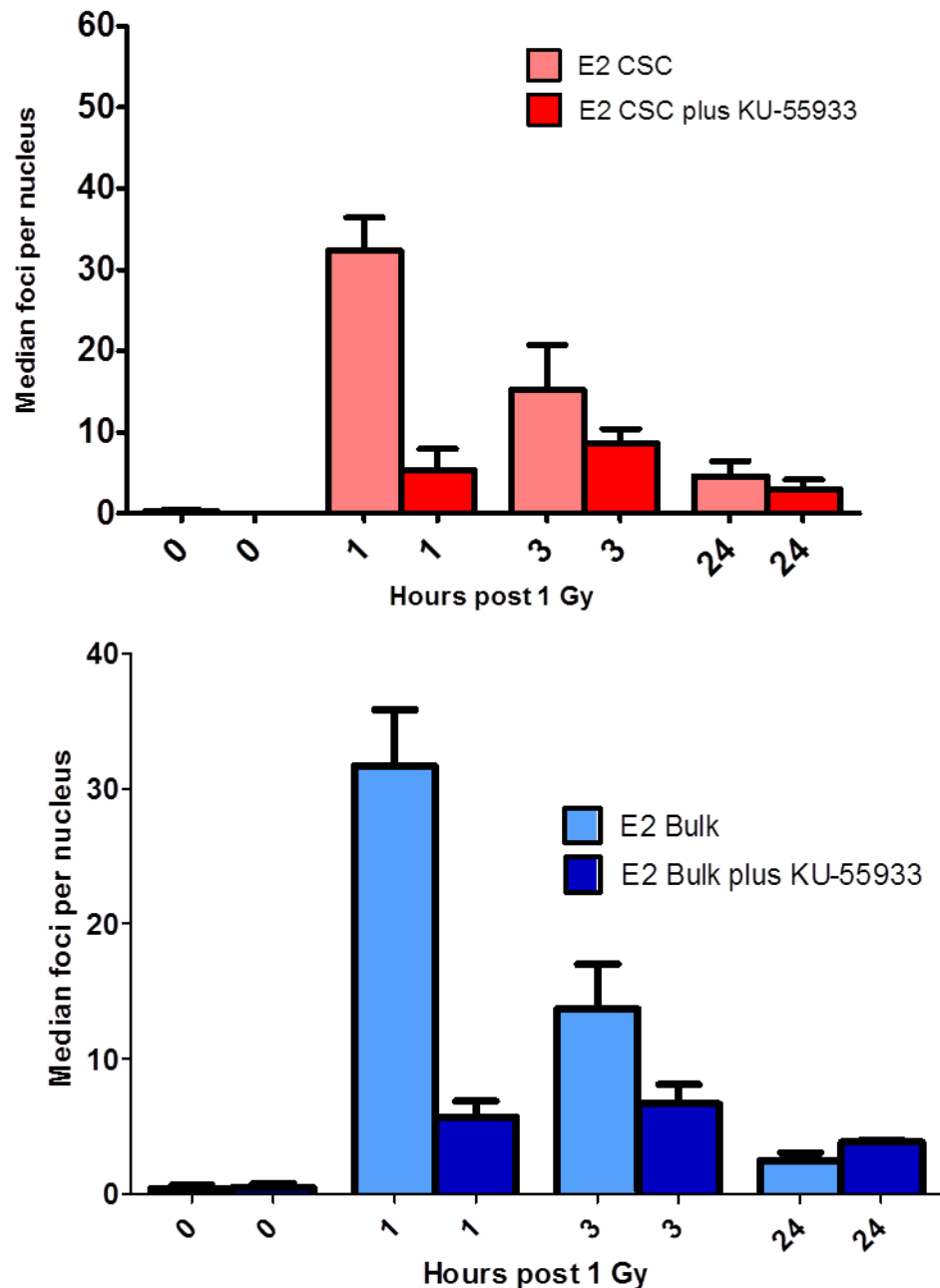


Figure 5.7 Quantification of gamma H2AX foci in CENPF negative (G1 cell cycle phase) E2 CSC and bulk cultures following 1Gy +/- 10µM KU-55933

Analysis of gamma H2AX foci as per figure 5.5, demonstrating median foci count per nucleus in E2 CSC and bulk in CENPF negative (i.e. G1 cell cycle phase) populations at baseline, 1, 3 and 24 hours post 1Gy +/- KU-55933. Each column represents the mean of 3 median foci per nucleus estimations from 3 independent experiments. Error bars represent SEM.

Effects of ATM inhibition on GBM CSC radioresistance

5.6 Effects of ATM inhibition on DNA DSB repair in GBM CSC and bulk tumour cells by neutral comet assay

Further characterisation of the effects of ATM inhibition on DNA DSB repair was undertaken using the neutral comet assay in an attempt to quantify DNA DSBs via an assay which was not reliant upon an ATM mediated signalling cascade, since ATM is the main early phosphorylator of H2AX at early timepoints following radiation exposure. Figure 5.8 shows plots of Olive tail moments in E2 CSC and bulk cultures following exposure to 40Gy plus or minus KU-55933. Preliminary studies suggested the neutral comet assay was not sensitive enough to quantify DNA DSBs following lower, clinically relevant doses of radiation. Cells were analysed 1 hour post irradiation. These data show no significant differences in DNA DSB levels in CSC or bulk cells treated with DMSO or with KU-55933 at 1 hour post irradiation. However these data also fail to show differences between irradiated and unirradiated controls. Given the extreme radioresistance of our GBM cell populations this may represent effective repair of the majority of lesions 1 hour post irradiation, to an extent where the relatively insensitive neutral comet assay was unable to detect a difference between control and irradiated samples. This could also represent failure of the neutral comet assay in this investigation due to operator dependent variables, however commercially available bleomycin treated control cells produced a satisfactory dose response curve, suggesting the execution of the assay was carried out appropriately.

The comet assay was repeated in E2 CSC cultures using a dose of 40Gy, again incubating cells in KU-55933 or a corresponding DMSO concentration for 1 hour prior to irradiation (fig. 5.9). Cell cultures were maintained on ice immediately after radiation in order to inhibit DNA DSB repair. This showed an increase in olive tail moment in cells receiving 40Gy compared to unirradiated controls. There was no decrease in olive tail moment with the addition of KU-55933 relative to cells irradiated in the absence of KU-55933, demonstrating that ATM inhibition although impairing gamma H2AX foci formation at early timepoints in the E2 cell line does not decrease DNA DSB formation. Unirradiated control cells show the formation of a comet tail in figure 5.9. This is explained by relaxation

Effects of ATM inhibition on GBM CSC radiosensitivity
of tertiary chromatin structure during the assay and is expected in control cells
in the neutral comet assay (Olive and Banath, 2006).

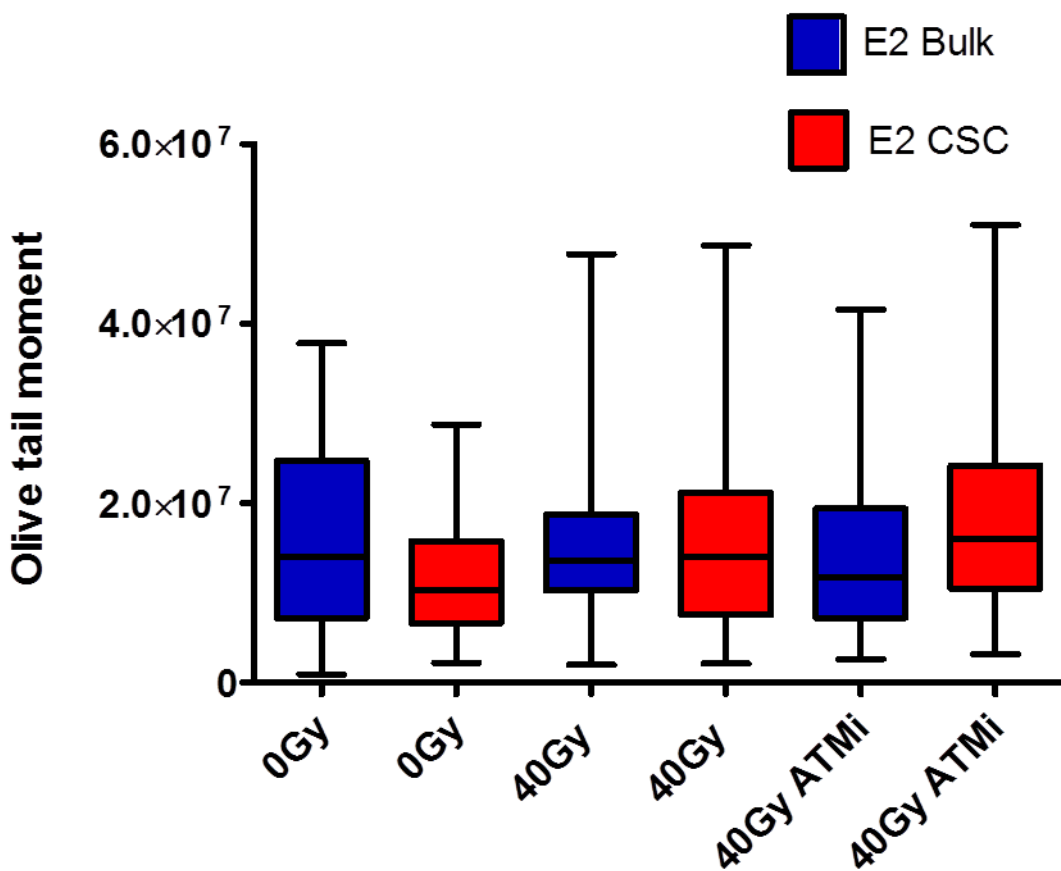


Figure 5.8 Quantification of DNA DSBs in E2 CSC and bulk cultures following radiation +/- 10 μ M KU-55933 by neutral comet assay

Neutral comet assay performed in E2 CSC and bulk cultures after 40Gy, 40Gy plus KU-55933 and in untreated, unirradiated controls. Cultures were incubated in media containing 10 μ M KU-55933 or DMSO 1 hour prior to irradiation with 40Gy and then lysed as per neutral comet protocol 1 hour post irradiation. Neutral comet assay was performed and Olive tail moment was then quantified and medians, interquartile range and range plotted as above. Results are representative of 1 experiment only.

Effects of ATM inhibition on GBM CSC radiosensitivity

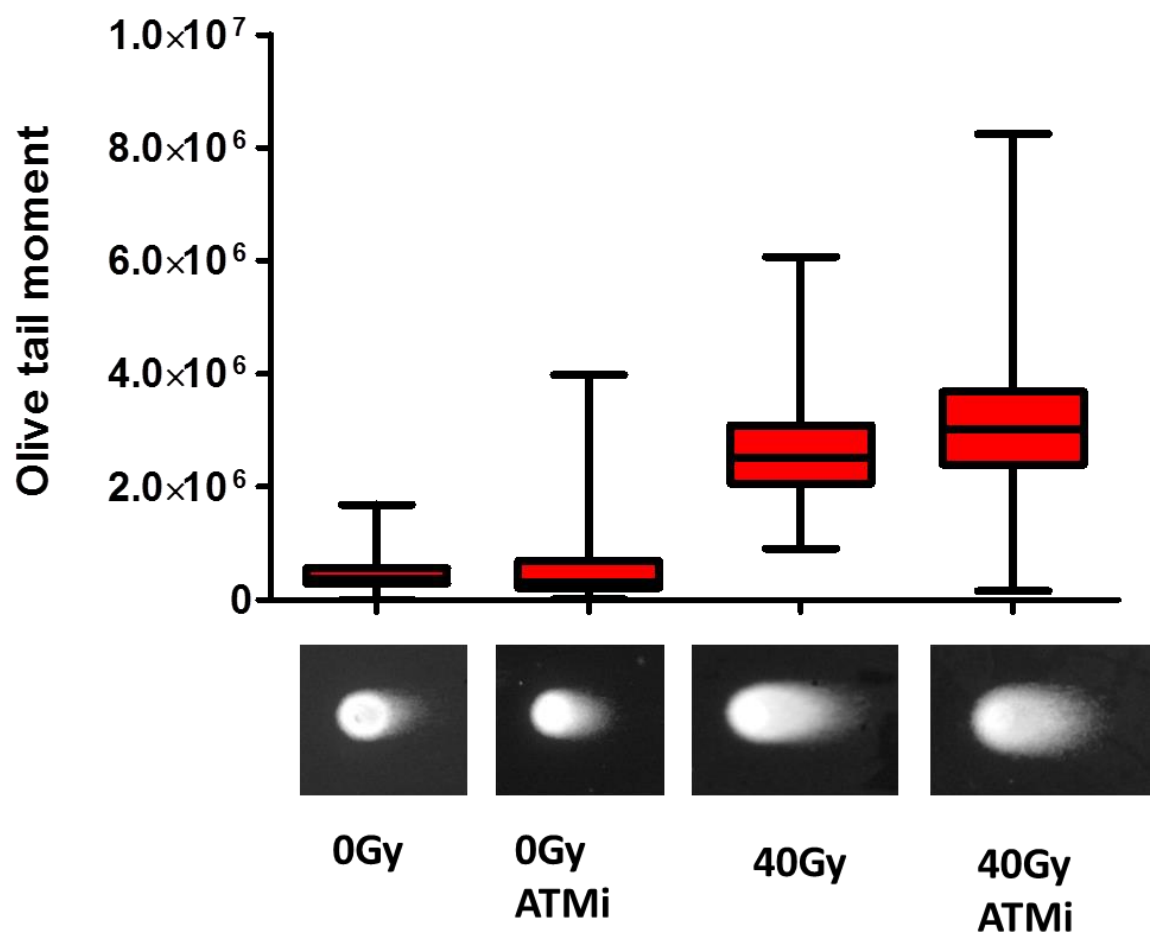


Figure 5.9 Quantification of DNA DSBs in E2 CSC cultures following radiation +/- KU-55933 by neutral comet assay

Neutral comet assay performed in E2 stem cultures quantified and plotted as per fig 5.6a. However cell cultures were placed on ice immediately after irradiation in this experiment to inhibit DNA repair. Cells were lysed and neutral comet assay performed shortly after completion of radiation treatment. Medians of 1 experiment are plotted. Representative images of comets are shown.

Given that the high doses of radiation necessary to detect DNA DSB repair differences with the neutral comet assay are not representative of clinical radiotherapy doses, and the inability to assess DNA repair effects in these cell lines at late or even early timepoints due to the lack of sensitivity of the assay, further use of the neutral comet assay was discontinued.

Effects of ATM inhibition on GBM CSC radioresistance

In view of difficulties experienced with the neutral comet assay attempts were made to quantify a surrogate of DNA DSB formation which did not rely upon ATM function, such as MRE11 foci, NBS1 foci or 53BP1 foci (fig. 5.10). E2 bulk cells were found to produce MRE11 foci following irradiation; however these were unsuitable for quantification. Immunofluorescent staining for NBS1 failed. Formation of 53BP1 foci was found also to be ATM dependent in the E2 cell line at early timepoints post radiation (fig. 5.11).

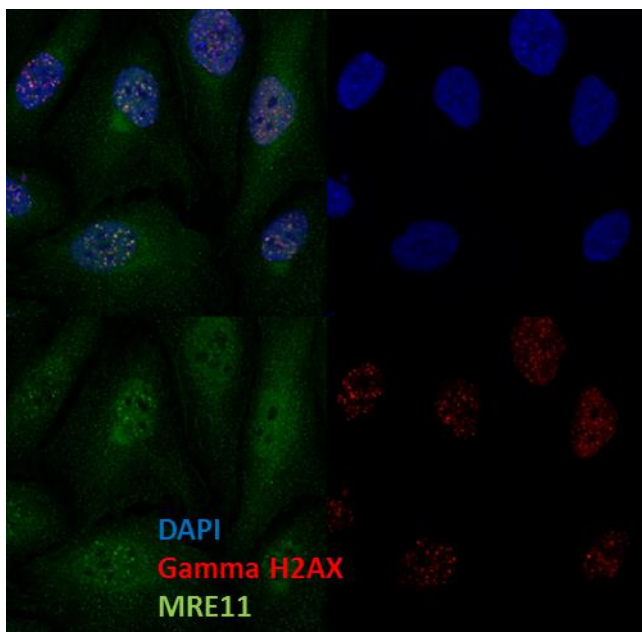


Figure 5.10 Immunofluorescent detection of MRE11 foci following irradiation

E2 bulk cells were fixed at 1 hour post 1Gy of radiation to generate DNA DSBs and stained for Gamma H2AX (red) and MRE11 (green) with DAPI staining of nuclei.

Effects of ATM inhibition on GBM CSC radioresistance

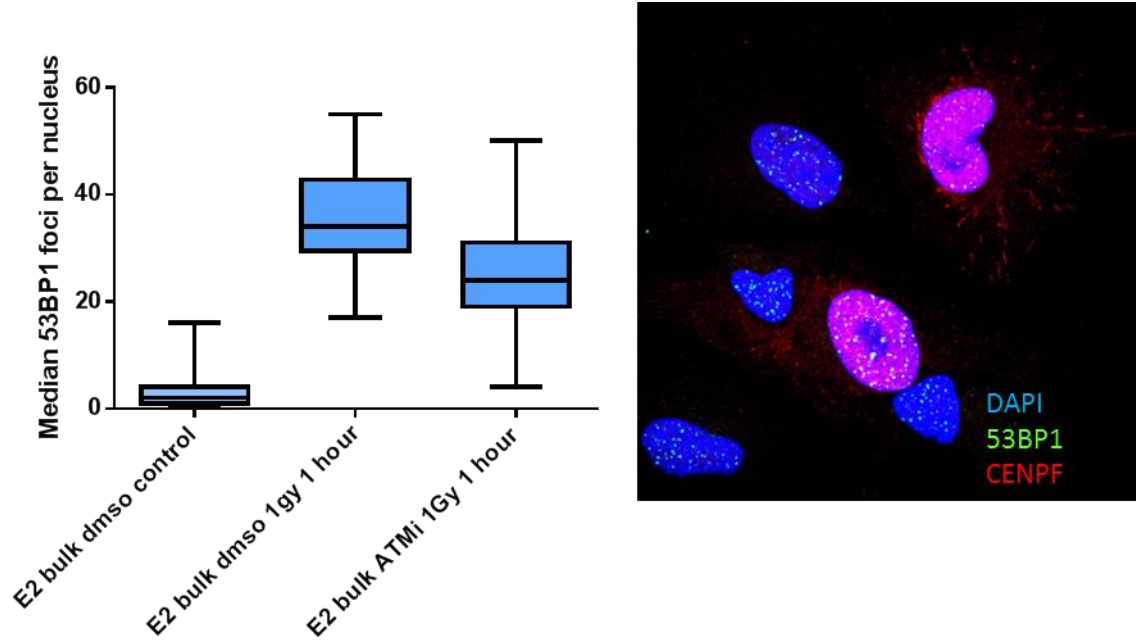


Figure 5.11 Analysis of 53BP1 foci in E2 bulk cells following irradiation +/- KU-55933

E2 bulk cell cultures were irradiated with 1Gy in the presence or absence of KU-55933 fixed at 1 hour post irradiation and stained for CENPF and 53BP1. Median 53BP1 foci per nucleus were quantified in CENPF negative cells. Medians from 1 experiment are plotted. An image of immunofluorescent staining for 53BP1 foci following radiation exposure is shown.

5.7 Effects of ATM inhibition on clonogenic survival of GBM CSC and bulk cultures

The radiosensitising effects of ATM inhibition by KU-55933 on GBM CSC and bulk cultures were investigated by clonogenic survival assay. CSC and bulk cultures were incubated for 1 hour in media containing 10 μ M KU-55933 prior to irradiation and for 24 hours post radiation after which media was replaced. Clonogenic survival curves for CSC and bulk cultures of E2, G7 and R10 are shown in figure 5.12. ATM inhibition demonstrated very potent radiosensitising effects on both CSC and bulk cultures of all three cell lines. ATM inhibition in the absence of radiation had no effect on plating efficiency in any cell line or culture condition.

Application of the linear quadratic equation allowed estimation of a sensitiser enhancement ratio for 0.37 survival ($SER_{0.37}$) in the presence of ATM inhibition. This value represents the fold change in radiation dose necessary to produce a survival of 0.37 in the absence of the sensitising drug. The $SER_{0.37}$ values for ATM inhibition are summarised in table 5.1. ATM inhibition was shown to radiosensitise R10 CSCs to a significantly greater degree than R10 bulk cells for a surviving fraction of 37%. Surviving fraction at 4Gy (SF4Gy) values were also calculated in the presence and absence of KU-55933 and are shown in table 5.1.

Effects of ATM inhibition on GBM CSC radiosensitivity

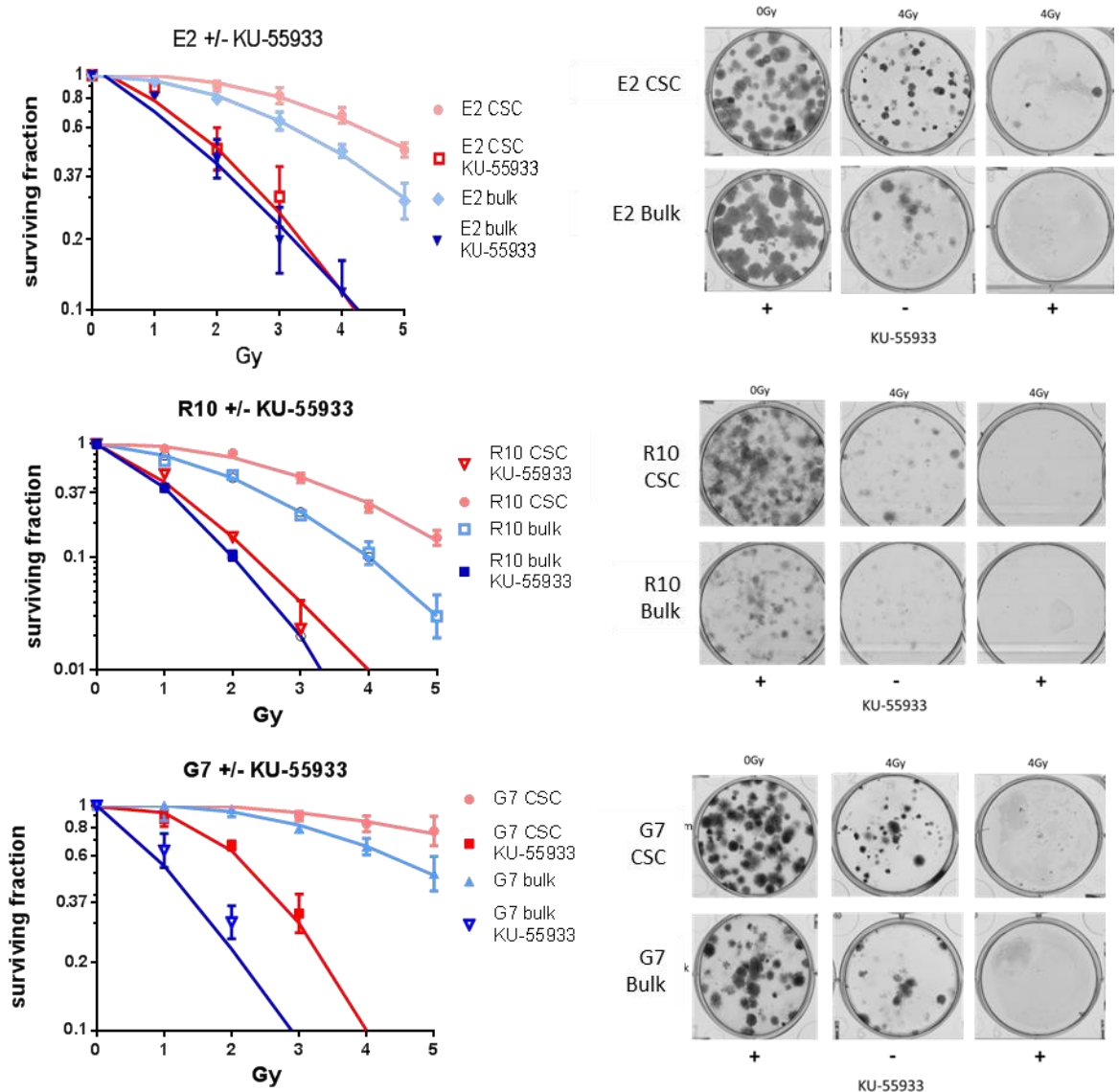


Figure 5.12 Effects of radiation +/- 10 μM KU-55933 on clonogenic survival of E2, R10 and G7 CSC and bulk cultures

Effects of KU-55933 on radiosensitivity of E2, R10 and G7 cell lines. Clonogenic survival curves comparing effects of KU-55933 plus radiation versus radiation alone on CSC and bulk cell cultures in E2, R10 and G7 cell lines. Data points represent mean +/- SEM from 3 independent experiments. Representative images of colony formation at 0 and 4 Gy are also shown.

Effects of ATM inhibition on GBM CSC radioresistance

	SER 0.37 (95% CI)	SF 4Gy (- KU- 55933) (95% CI)	SF 4Gy (+ KU- 55933) (95% CI)
E2 CSC	2.60 (1.72,3.40)	0.67 (0.52, 0.83)	0.088 (0.037, 0.14)
E2 bulk	2.01 (1.27,2.86)	0.48 (0.43, 0.53)	0.11 (0.030, 0.18)
G7 CSC	3.46 (1.75,5.18)	0.83 (0.69, 0.97)	0.096 (0.074, 0.12)
G7 bulk	3.43 (1.99, 4.86)	0.66 (0.54, 0.77)	0.034 (0, 0.1)
R10 CSC	3.17 (2.63, 3.71)	0.28 (0.21, 0.35)	0.12 (0.099, 0.12)
R10 bulk	2.23 (2.16, 2.30)	0.11 (0.053, 0.16)	0

Table 5.1 Sensitiser enhancement ratios at 0.37 survival ($SER_{0.37}$) and surviving fraction at 4Gy (SF4Gy) +/- 10µM KU-55933 are tabulated for CSC and bulk cultures of the E2, G7 and R10 cell lines

To confirm the effects of ATM inhibition and radiation on GBM CSC survival, neurosphere formation assays were conducted in E2 and G7 CSC populations. The extent to which 2Gy inhibited neurosphere formation *in vitro* was significantly increased by treatment with 10µM KU-55933 in both E2 and G7 CSC populations (fig. 5.13). ATM inhibition in the absence of radiation did not affect neurosphere formation.

Effects of ATM inhibition on GBM CSC radiosensitivity

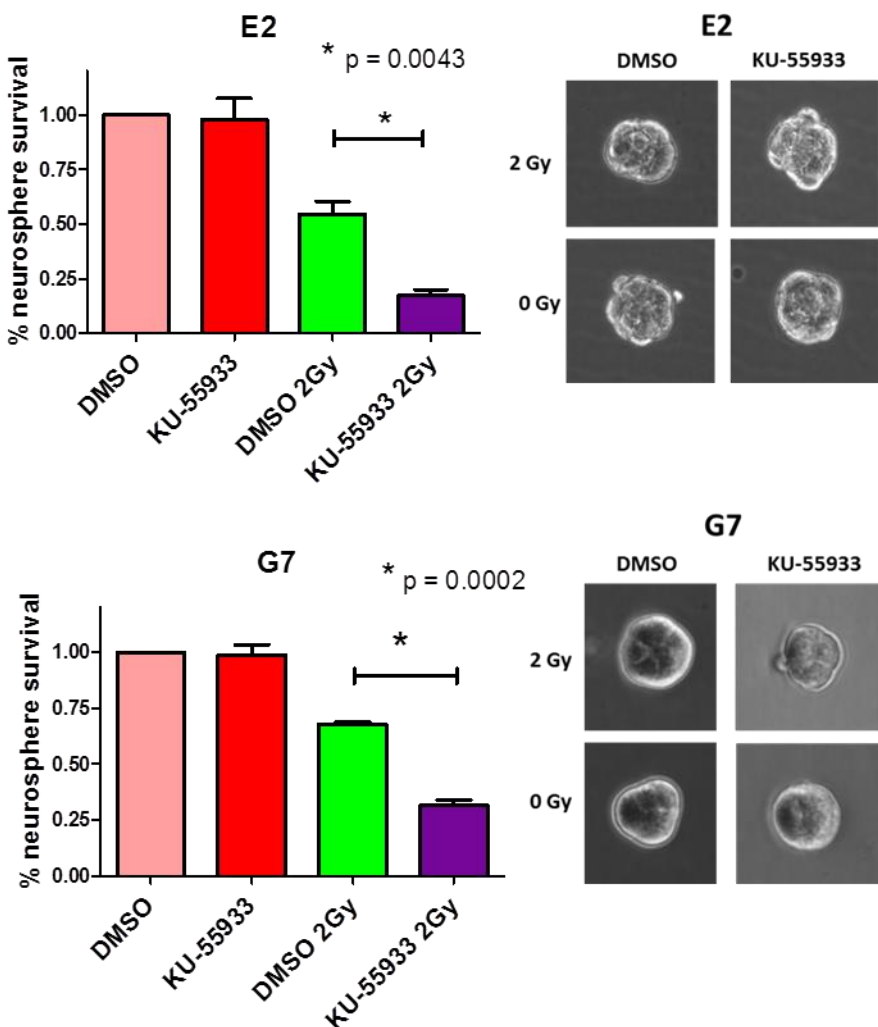


Figure 5.13 Effects of radiation +/- KU-55933 on neurosphere formation

Neurosphere formation assay in E2 and G7 CSC cultures. 10 cells per well were seeded into 96 well plates and treated with KU-55933 or DMSO prior to irradiation with 2 Gy. Neurospheres were quantified manually after incubation for 3 (G7) or 4 weeks (E2) under 5x magnification. Mean plus SEM of 3 independent experiments shown, normalised to control values. Neurosphere forming efficiency of controls (Mean and 95% CI): E2 = 18.56% (15.72, 21.40), G7 = 34.74% (28.50, 40.98). Representative images of neurospheres are shown. P values calculated by student's t test.

5.8 Conclusions

The effects of ATM inhibition on CSC and bulk GBM cultures have been fully characterised. ATM inhibition provided highly potent radiosensitisation of both GBM CSC and bulk cultures, as demonstrated by both clonogenic assay and neurosphere formation assays. The degree of radiosensitisation produced by ATM inhibition when quantified by SER_{0.37} was extremely high and ranged from 2 to 3.5 in the cell lines examined. This is in contrast to radiosensitising agents in

Effects of ATM inhibition on GBM CSC radioresistance

clinical use today, such as cytotoxic chemotherapy drugs, which have SER_{0.37} levels of around 1.3 to 1.8. ATM inhibition clearly has a profound ability to modify the intrinsic radiosensitivity of highly radioresistant tumour cells. This study presents the first evidence of radiosensitisation of GBM CSCs by ATM inhibition using clinically relevant clonogenic survival assays. Vecchio et al (Vecchio et al., 2014) investigated the effects of ATM inhibition on GBM CSC cultures versus differentiated GBM cultures via MTT assay and found ATM inhibition to have a radiosensitising effect in CSCs however, this was in contrast to a radioprotective effect observed in differentiated GBM cells. Clonogenic survival assays are the gold standard for measuring radiobiological effects and the differing results may reflect use of a more robust assay, or be cell line dependent. However it is difficult to relate the profound effects of ATM inhibition on the DDR to a radioprotective effect. In E2 and R10 cells, ATM inhibition completely abrogated the relative radioresistance of CSC's, since the survival curve of the KU-55933 exposed CSCs was superimposed on that of the KU-55933 exposed bulk tumour cells. These data indicate that ATM function is a dominant component of CSC radioresistance in these cell lines.

The complex role of ATM in the cellular DDR to ionising radiation has been characterised by other authors. ATM has both a cell cycle checkpoint role and a DNA repair role. ATM controls both S phase and G2/M checkpoints in response to radiation, and ATM deficient cells are known to exhibit continued S phase progression and abnormal G2/M cell cycle control after irradiation. ATM null cells in particular are noted to exhibit an apparently paradoxical deficient G2/M checkpoint activation following irradiation along with prolonged G2 accumulation. Xu et al (Xu et al., 2002) demonstrated the existence of two molecularly distinct G2/M checkpoints following ionising radiation. The first G2/M checkpoint occurs early following radiation exposure and is ATM dependent, however dose independent. This phenomenon represents failure of cells in G2 at the time of irradiation to progress into mitosis. The second type of radiation induced G2/M checkpoint (described as 'G2 accumulation') is ATM independent and dose dependent, and occurs at later timepoints (around 24 hours in the study by Xu et al) following irradiation and represents G2 accumulation of cells which were in G1 or S phase at the time of irradiation.

Effects of ATM inhibition on GBM CSC radioresistance

G2/M accumulation is a reflection of DNA damaged cells continuing to progress through S phase, and is a feature of cell lines with deficient S phase checkpoints rather than being a specific feature of ATM null cells. G2 accumulation is an ATR dependent process.

Investigations detailed in this thesis demonstrated the ability of ATM inhibition with KU-55933 to inhibit ATM mediated Chk2 phosphorylation in GBM CSC cultures by Western blot. Furthermore the effects of ATM inhibition on the G2/M cell cycle checkpoint were documented, with partial abrogation of radiation mediated G2/M cell cycle checkpoint activation seen in CSC cultures and almost complete abrogation of G2/M cell cycle checkpoint seen in bulk cell cultures. The study presented in this thesis is an analysis of the initial transient ATM dependent G2/M checkpoint occurring early after radiation exposure rather than G2/M accumulation at later timepoints. The analysis of pHish3 presented above demonstrates that CSCs are not completely reliant upon ATM for early G2/M checkpoint activation, in comparison to GBM bulk cells which appear ATM reliant for this function. It may be that an alternative mechanism contributes to activation of the G2/M checkpoint in GBM CSCs. Increased ATR activity in GBM CSCs may be responsible for this effect.

Analysis of gamma H2AX foci resolution in this chapter provided insight into the effects of ATM inhibition on DNA DSB repair following radiation. Other investigators have characterised the role of ATM in DNA DSB repair. ATM has been described as having a specific function in the resolution of DNA DSBs in the slow phase of DNA repair via NHEJ in G1 (Riballo et al., 2004) and HR in G2 (Beucher et al., 2009). This subset of DNA DSBs represents around 10-15% of the overall DSB burden induced by radiotherapy, and ATM appears essential for the repair of these DNA DSBs. ATM may have specific functions required for repair of this subset of radiation induced DSBs (Kuhne et al., 2004). Goodarzi et al presented evidence that ATM facilitated DNA DSB repair in areas of heterochromatin (Goodarzi et al., 2008). In this model ATM facilitates relaxation of densely packed heterochromatin and access to heterochromatic DSB sites by DNA repair machinery via the phosphorylation of KAP1. Inhibition of KAP1 function by siRNA knockdown of KAP1 relieved the DNA DSB repair deficit of ATM

Effects of ATM inhibition on GBM CSC radioresistance

deficient cells in this study. Alvarez-Quilon et al however demonstrated that ATM is required for the repair of DNA DSBs with blocked ends (Alvarez-Quilon et al., 2014). It seems that ATM may have multiple roles in the repair of DSBs which in the absence of ATM activity are otherwise impossible for the cell to repair.

In the studies presented in this chapter, ATM inhibition effectively removed the previously demonstrated repair advantage of GBM CSCs at 24 hours post radiation. This effect was evident only in G2 populations. A similar trend was also seen in bulk cell cultures however again in G2 cell populations exclusively although this failed to reach statistical significance. The excess unresolved gamma H2AX foci in irradiated G2 GBM CSCs treated with ATM inhibitor at 24 hours represents 18% of the DNA DSBs present at 1 hour in the DMSO irradiated G2 GBM CSC controls, which approximates to the 10-15% of overall DNA DSB burden thought to require ATM for repair.

An increase in unresolved gamma H2AX foci was not evident in G1 phase cells following ATM inhibition and radiation in either CSC or bulk cultures in the E2 cell lines. ATM has been shown to contribute to repair of a subset of DNA DSBs repaired by NHEJ in G1 phase (Riballo et al., 2004). Therefore it would have been expected that the G1 populations treated with irradiation and ATM inhibition in this study would also have experienced increased DNA DSBs at 24 hours following irradiation. However, earlier in this study the E2 cell line was demonstrated to have a dysfunctional G1 checkpoint in response to radiation. Therefore cells which are in G1 phase at the time of irradiation will progress into S phase with DNA damage present instead of exhibiting a G1/S cell cycle arrest. It is speculated that the G1 phase cells analysed at 24 hours post irradiation represent cells which have completed DNA repair in S and G2 phase and progressed through mitosis to exist in G1 phase at the time of analysis. As they have completed repair and progressed through mitosis into G1 phase these cells would not exhibit increased levels of gamma H2AX foci following ATM inhibition.

ATM inhibition suppressed phosphorylation of H2AX at early timepoints following irradiation. This was expected, since ATM is known to be the major protein kinase responsible for the phosphorylation of histone H2AX in the early response

Effects of ATM inhibition on GBM CSC radioresistance

to radiation (Burma et al., 2001). DNAPK and ATR are capable of phosphorylating gamma H2AX, (Wang et al., 2005). However, ATM is thought to be more capable of phosphorylation of H2AX due to its ability to become immediately activated by local chromatin modifications associated with DNA breakage. Since chromatin modification occurs over entire chromatin domains, activated ATM will be able to phosphorylate multiple H2AX molecules within each domain (Bakkenist and Kastan, 2003). DNAPK will become activated after direct interaction with Ku, but only after direct binding to a DSB. Therefore the H2AX phosphorylation range of DNAPK will likely be shorter (Stiff et al., 2004). ATR is mainly activated by replication stress associated DNA DSBs after interaction with ATRIP following generation of ssDNA (Zou and Elledge, 2003). Therefore immediate phosphorylation of H2AX by ATR after irradiation appears unlikely (Kinner et al., 2008). The effects on H2AX phosphorylation at early timepoints after irradiation and ATM inhibition are varied in the literature and the effect is likely cell line dependent. Some investigators report no effect of ATM inhibition on early gamma H2AX foci formation after radiation (Beucher et al., 2009), whilst others demonstrate a profound effect of ATM inhibition on H2AX phosphorylation at early timepoints post radiation (Shaheen et al., 2011). Criticism that KU-55933 is non-specifically inhibiting DNAPK in addition to ATM at the concentrations used in these investigations in this chapter is not supported by the available literature. Beucher et al used KU-55933 at a concentration of 20 μ M to achieve ATM inhibition and saw no effect on early phosphorylation of gamma H2AX. The investigations in this thesis used a much lower concentration of 10 μ M KU-55933 which resulted in a profound effect on gamma H2AX formation. It is unlikely that the reduction in gamma H2AX foci formation at these timepoints represents a reduced induction of DNA DSBs. Although the neutral comet assay was unsatisfactory due to its lack of sensitivity at later timepoints following irradiation, there was no reduction in DNA DSBs following radiation and ATM inhibition. The reduction in gamma H2AX foci at early timepoints post radiation plus ATM inhibition therefore likely reflects a reduction in signalling at DSBs.

In conclusion ATM is central to the radioresistance of GBM CSCs. Inhibition of ATM in GBM CSCs is associated with partial abrogation of G2/M checkpoint activation and reduction in efficiency of slow phase DNA DSB repair in G2 phase

Effects of ATM inhibition on GBM CSC radioresistance

GBM CSC populations. ATM inhibition provides highly potent levels of radiosensitisation in both CSC and bulk populations, and completely abrogates CSC radioresistance relative to bulk cells in the E2 and R10 cell lines.

Chapter 6 PARP and GBM CSC radioresistance

6.1 Introduction

The radiosensitising effects of PARP inhibitors on various cell lines have been characterised by several authors (Liu et al., 2008, Dungey et al., 2009, Noel et al., 2006, Albert et al., 2007). PARP inhibition provides modest radiosensitisation in most cell lines, with SER_{0.37} ranging from 1.3 to 1.8. PARP inhibition radiosensitises effectively in hypoxic conditions (Liu et al., 2008). Furthermore, its mechanism of radiosensitisation has been shown to predominantly affect actively replicating cells which may facilitate tumour specific radiosensitisation, since many normal cells within organs of the human body are generally non-dividing or much more slowly proliferating than malignant tissue. *In vivo* studies have shown PARP inhibition to have an even greater radiosensitising effect than those predicted from *in vitro* studies, possibly due to vasodilatory effects on tumour vasculature (Calabrese et al., 2004, Ali et al., 2011b). Furthermore PARP-1 expression is greatly increased in GBM tumour cells and can be used as a tumour marker (Galia et al., 2012b) whilst PARP-1 expression is not present in normal brain. Given these properties, there is great interest in the development of PARP inhibitors as clinical radiosensitisers, particularly in GBM.

Nevertheless, the effect of PARP inhibition on GBM CSC radioresistance is relatively unexplored. A detailed investigation of the role of PARP-1 in GBM CSC radioresistance was undertaken.

6.2 PARP-1 expression in GBM tumour samples

PARP-1 expression in tumour samples was investigated by immunohistochemical staining for PARP-1 as shown in figure 6.1. Two patient GBM samples were stained for PARP-1 in addition to sections from E2 and G7 CSC derived xenografts. Sections of normal human brain were also stained for evaluation of PARP-1 expression. Tumour nuclei appear to stain intensely for PARP-1 in both

PARP and GBM CSC radioresistance

patient GBM samples and in xenografts derived from E2 and G7 CSC cultures. In comparison, normal brain shows no detectable staining of nuclei for PARP-1.

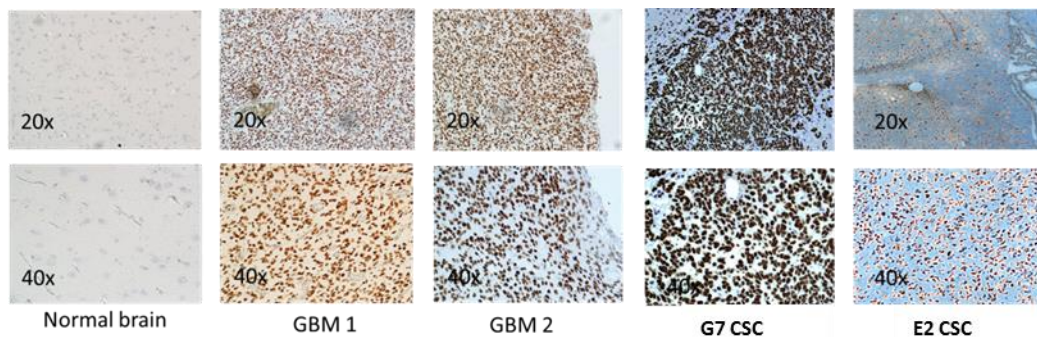


Figure 6.1 Demonstration of PARP-1 expression by immunohistochemical staining in normal human brain, GBM patient samples (GBM 1 and 2), and orthotopic murine xenografts (G7 CSC and E2 CSC)

6.3 Investigation of PARP-1 expression and activity in GBM CSC and bulk cultures

GBM CSC and tumour bulk cultures of E2 and G7 cell lines were incubated with 1 μ M olaparib or a corresponding concentration of DMSO and irradiated with 5Gy. Cells were lysed for Western blotting at timepoints of 0, 1, 3 and 24 hours post radiation. Membranes were then probed for PARP-1, Poly (ADP ribose) (PAR) and actin, as shown in figure 6.2. In both the G7 and E2 cell lines, enhanced expression of PARP-1 was seen in GBM CSC cultures at baseline and after irradiation with 5Gy compared to tumour bulk cultures. Levels of PAR expression were increased in GBM CSC cultures compared to bulk cultures in both cell lines at baseline and after irradiation. The addition of 1 μ M olaparib to cell culture medium 1 hour prior to irradiation with 5Gy abolished PARylation in both GBM CSC and bulk cultures.

PARP and GBM CSC radioresistance

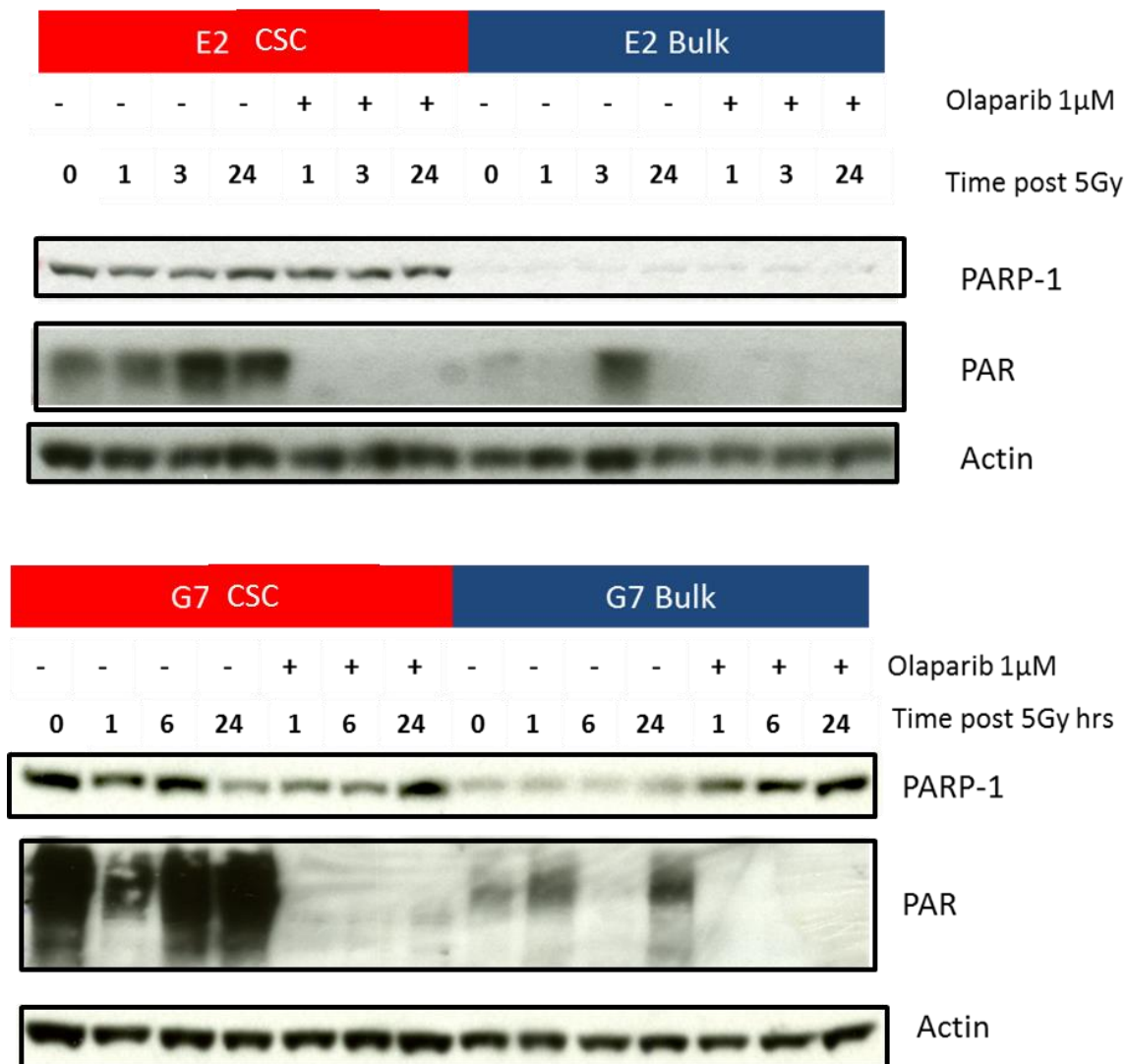


Figure 6.2 Analysis of PARP-1 and PAR expression in CSC and bulk cells following 5Gy radiation +/- olaparib by Western blotting

E2 and G7 CSC and bulk cultures were irradiated with 5Gy after incubation in media containing 1 μ M olaparib or corresponding DMSO concentration. Cultures were then lysed for Western blotting at the time points shown. Membranes were probed for PARP-1, PAR and actin as a loading control.

6.3 Investigation of effects of PARP-1 inhibition on GBM CSC radioresistance

The effects of PARP inhibition on GBM CSC radioresistance were investigated by clonogenic assay. GBM CSC and bulk cultures of the cell lines E2, G7 and R10 were seeded onto Matrigel™ covered plates as described previously. Cell cultures were then incubated with 1 μ M olaparib 1 hour prior to irradiation. Colonies were counted and surviving fractions were plotted in figure 6.3.

PARP and GBM CSC radioresistance

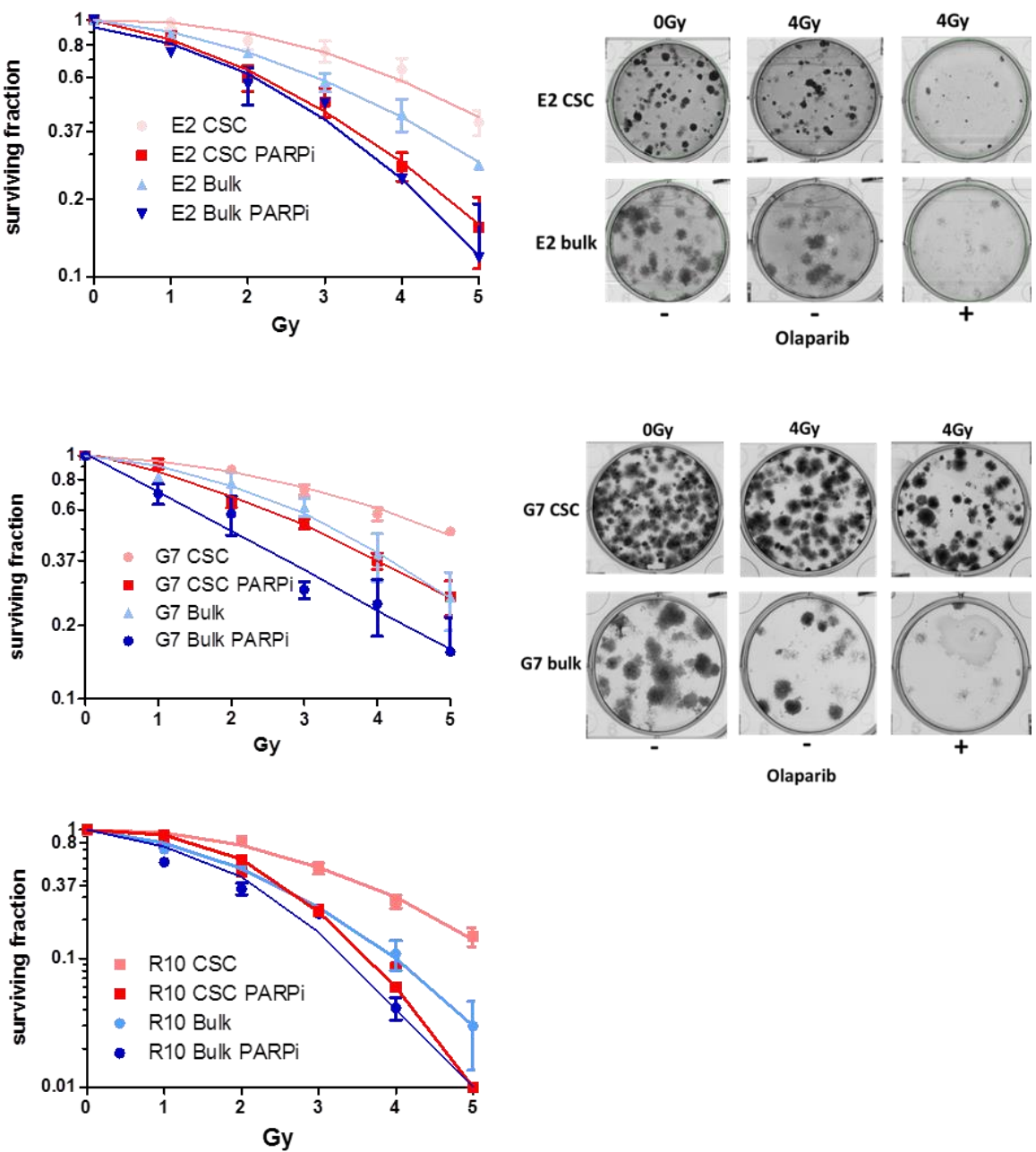


Figure 6.3 Effects of radiation +/- 1 μ M olaparib on clonogenic survival of CSC and bulk cultures

Clonogenic survival curves comparing effects of olaparib plus radiation versus radiation alone on CSC and tumour bulk cultures in E2, G7 and R10 cell lines. Data points represent mean +/- SEM from 3 independent experiments. Representative images of colonies are shown at 0 and 4Gy.

As can be seen in figure 6.3, PARP inhibition radiosensitised E2, G7 and R10 GBM CSC cultures. Treatment with olaparib in combination with radiation reduced colony formation in both GBM CSC and bulk cultures of all 3 cell lines compared to DMSO treated controls. There was no significant effect of PARP inhibition alone on the plating efficiency of any cell line or cell culture condition.

PARP and GBM CSC radioresistance

Calculation of SER_{0.37} for PARP inhibition was performed in all three cell lines for GBM CSC and bulk cultures and is presented in table 6.1. SER_{0.37} values ranged between 1.1 and 1.9 in the cell lines and culture conditions examined. SF4Gy values are also tabulated in table 6.1. Incubation with PARP inhibitor prior to irradiation with 4Gy produced a statistically significant reduction in colony formation in both CSC and bulk cultures of all 3 cell lines.

	SER 0.37 (95% CI)	SF 4Gy (- olaparib) (95% CI)	SF 4Gy (+ olaparib) (95% CI)
E2 CSC	1.93 (1.23, 2.64)	0.64 (0.51, 0.77)	0.27 (0.20, 0.34)
E2 bulk	1.34 (1.19, 1.48)	0.43 (0.31, 0.55)	0.24 (0.22, 0.25)
G7 CSC	1.44 (1.33, 1.54)	0.58 (0.50, 0.65)	0.37 (0.31, 0.42)
G7 bulk	1.52 (1.42, 1.61)	0.39 (0.22, 0.56)	0.25 (0.12, 0.37)
R10 CSC	1.48 (1.20, 1.76)	0.28 (0.21, 0.35)	0.86 (0.066, 0.11)
R10 bulk	1.19 (1.11, 1.26)	0.11 (0.053, 0.16)	0.042 (0.026, 0.057)

Table 6.1 SER_{0.37} and surviving fraction at 4Gy values (SF4Gy) following PARP inhibition and radiation

SER_{0.37} and SF4Gy +/- olaparib are tabulated with corresponding 95% CIs for CSC and bulk cultures of the E2, G7 and R10 cell lines. SER_{0.37} and SF4Gy represent mean values of 3 independent experiments; corresponding 95% confidence intervals are also shown.

The effects of PARP inhibition on radiosensitivity of GBM CSCs were confirmed by neurosphere assay. E2 and G7 GBM CSCs were seeded in 96 well plates at a density of 10 cells per well and treated with 1µM olaparib or a corresponding DMSO concentration before irradiation with 2Gy. 96 well plates were then

PARP and GBM CSC radioresistance

incubated for 3-4 weeks and allowed to form neurospheres. Results plotted normalised to controls are shown in figure 6.4. Treatment with 1 μ M olaparib alone had no effect on generation of neurospheres in either cell line. However combined treatment with olaparib and 2Gy significantly reduced neurosphere production in both cell lines when compared to the effects of 2Gy in the absence of olaparib. Olaparib exposure alone had no effect on the appearance or size of neurospheres.

PARP and GBM CSC radioresistance

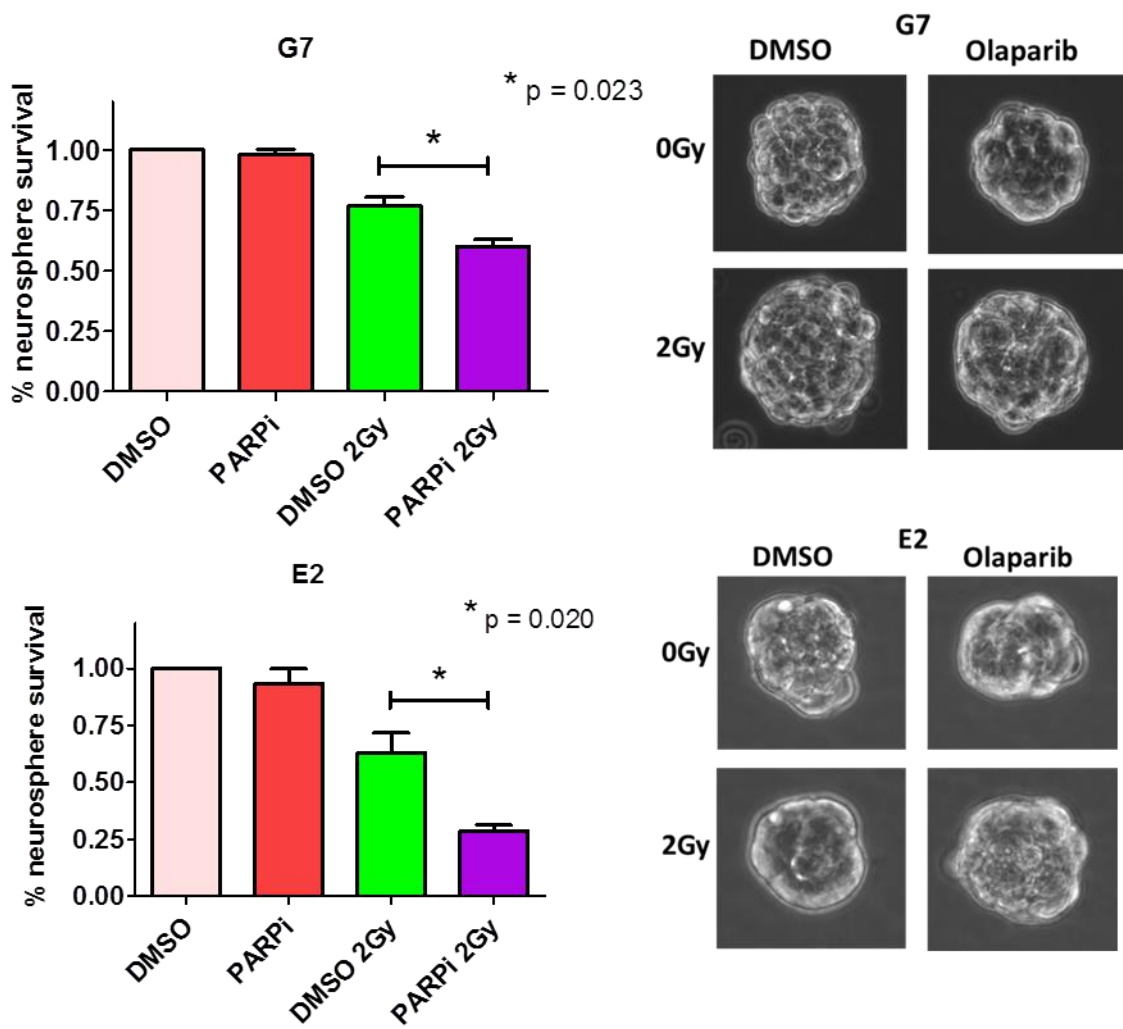


Figure 6.4 Effect of radiation +/- olaparib on neurosphere formation

E2 and G7 CSCs were seeded at a dilution of 10 cells per well into 96 well plates and exposed to olaparib or DMSO prior to irradiation with 2 Gy. Neurospheres were quantified manually after 3 (G7) or 4 weeks (E2) after imaging using an Optronix Gelcount colony counter. Mean plus SEM of 3 independent experiments is shown, normalised to control values. Neurosphere forming efficiency of controls (Mean and 95% CI): E2= 18.56% (15.72, 21.40), G7 =34.74% (28.50, 40.98). Representative images of neurospheres are shown. P values were calculated by student's t test.

6.4 Investigation of effects of PARP inhibition on DNA DSB repair in GBM CSCs

A detailed investigation of DNA DSB repair following radiation and olaparib was undertaken by analysis of gamma H2AX foci, as in chapter 5. E2 GBM CSC and bulk cultures were seeded onto glass coverslips and exposed to 1 μ M olaparib or a corresponding concentration of DMSO in media for a period of 1 hour prior to 1Gy of radiation. Cells were fixed and stained for gamma H2AX and CENPF at timepoints of 0, 1 and 24 hours following radiation. Representative images of staining for CENPF and gamma H2AX are shown in figure 6.5. Cells were assessed to be either CENPF positive (i.e. in S or G2 cell cycle phase) or CENPF negative (i.e. in G1 cell cycle phase) by the investigator.

PARP and GBM CSC radioresistance

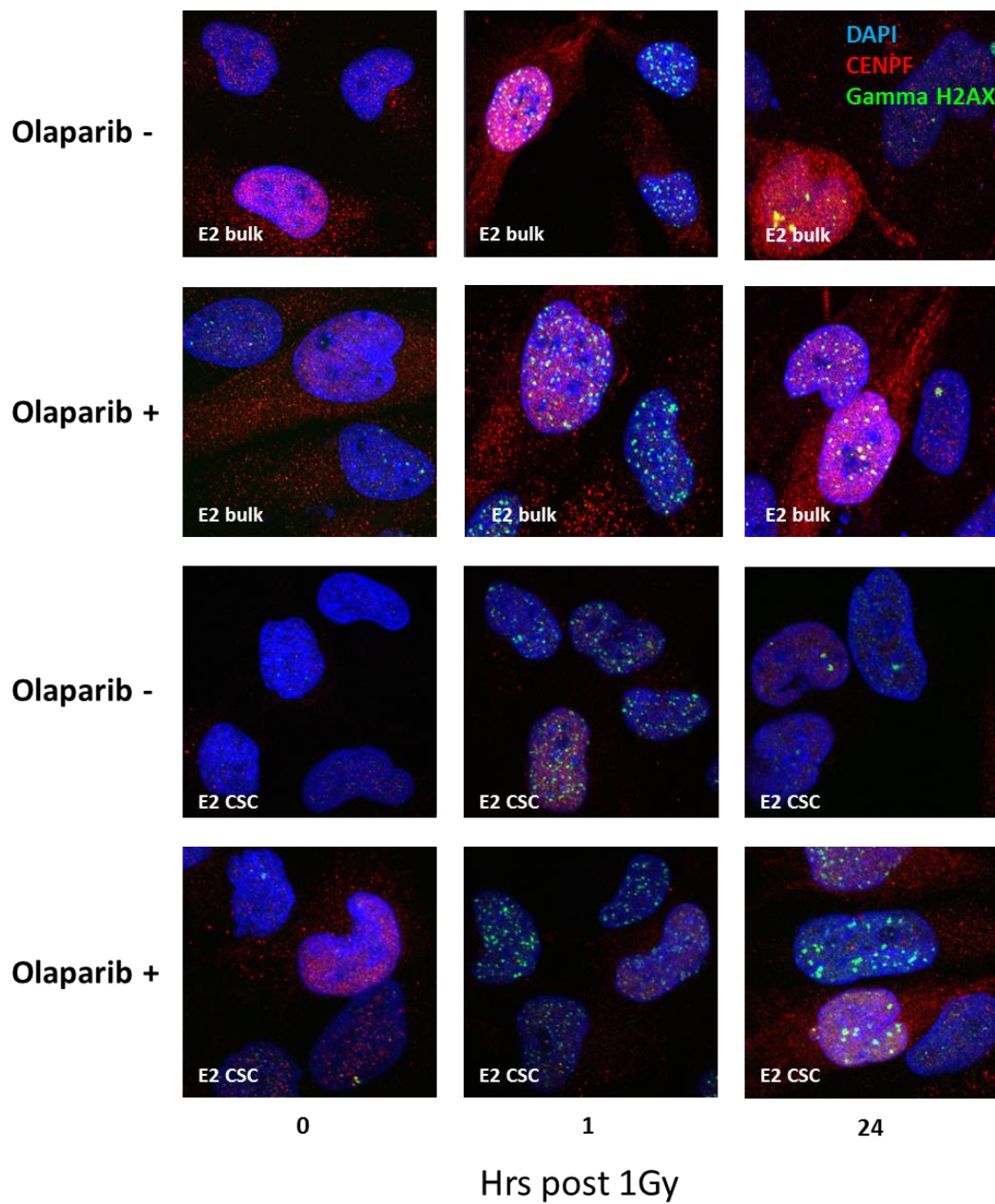


Figure 6.5 Images of gamma H2AX immunofluorescent staining in E2 CSC and tumour bulk cells exposed to 1 μ M olaparib and 1Gy radiation

CENPF and gamma H2AX immunofluorescent staining following incubation with olaparib or DMSO at 0, 1 and 24 hours post irradiation with 1Gy.

Figure 6.6 illustrates the effects of olaparib exposure on the median nuclear gamma H2AX foci in G2 cell cycle phase GBM CSCs and tumour bulk cells of the E2 cell line following 1Gy. There was a significant increase in the mean number of foci per nucleus in both GBM CSC and bulk cultures at 24 hours post

PARP and GBM CSC radioresistance

irradiation and olaparib. There was no significant difference in foci numbers at baseline or 1 hour after irradiation with 1Gy plus olaparib.

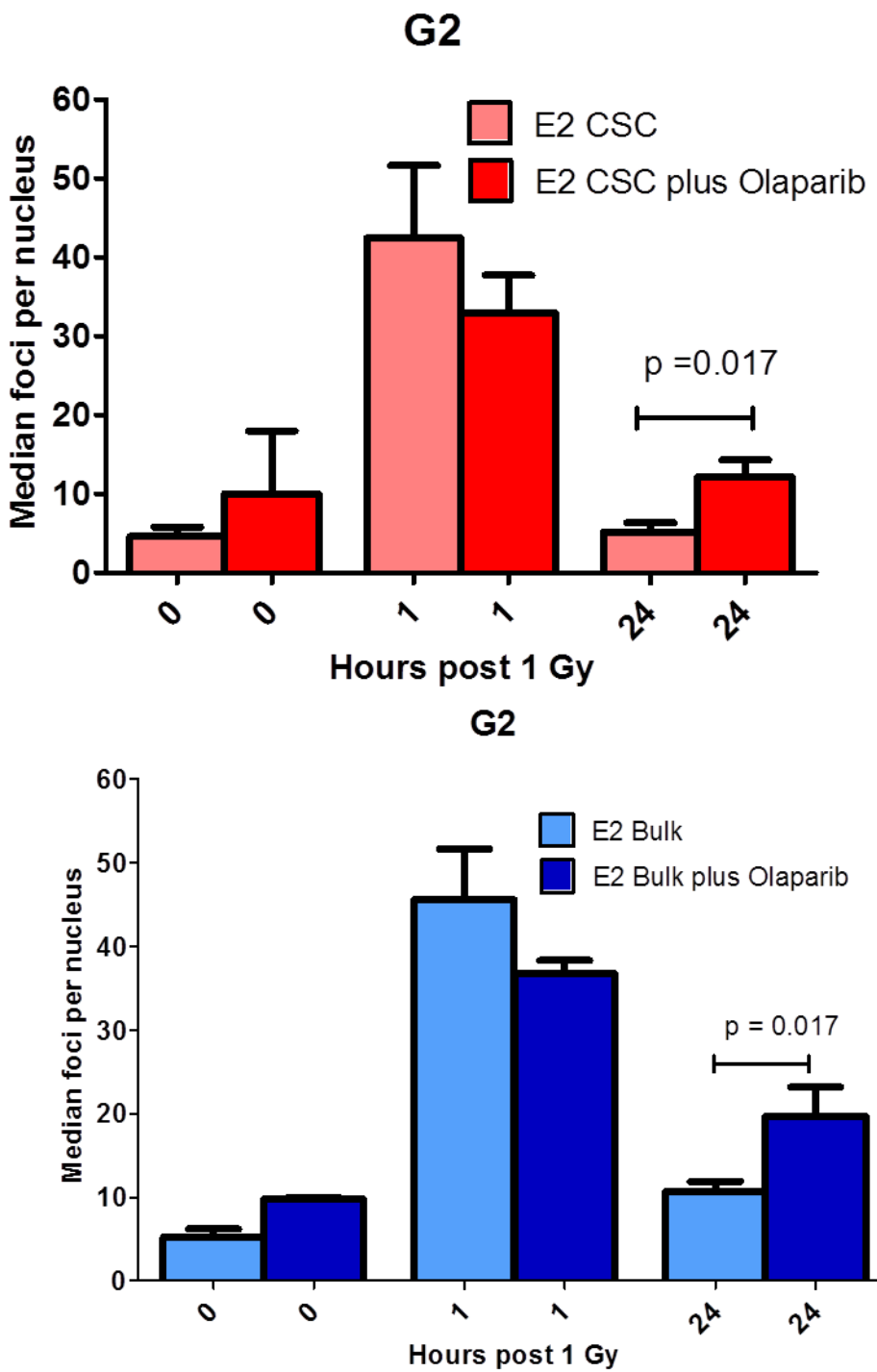


Figure 6.6 Quantification of gamma H2AX foci following 1Gy +/- 1 μ M olaparib in CENPF positive (G2 cell cycle phase) CSC and bulk cell populations

Resolution of gamma H2AX foci in E2 CSC and bulk cultures after treatment with 1Gy in the presence and absence of 1 μ M olaparib in CENPF positive (i.e. S/G2 cell cycle phase) populations. Gamma H2AX foci were quantified at the timepoints shown. Columns represent mean plus SEM of

PARP and GBM CSC radioresistance

3 median nuclear gamma H2AX foci values from independent experiments. P values calculated by student's t test.

Figure 6.7 illustrates the effects of olaparib exposure on radiation induced gamma H2AX foci in G1 cell cycle phase GBM CSCs and tumour bulk cells of the E2 cell line. There were no significant differences in foci number at baseline, 1 or 24 hours in G1 phase cells following 1Gy plus olaparib exposure.

PARP and GBM CSC radioresistance

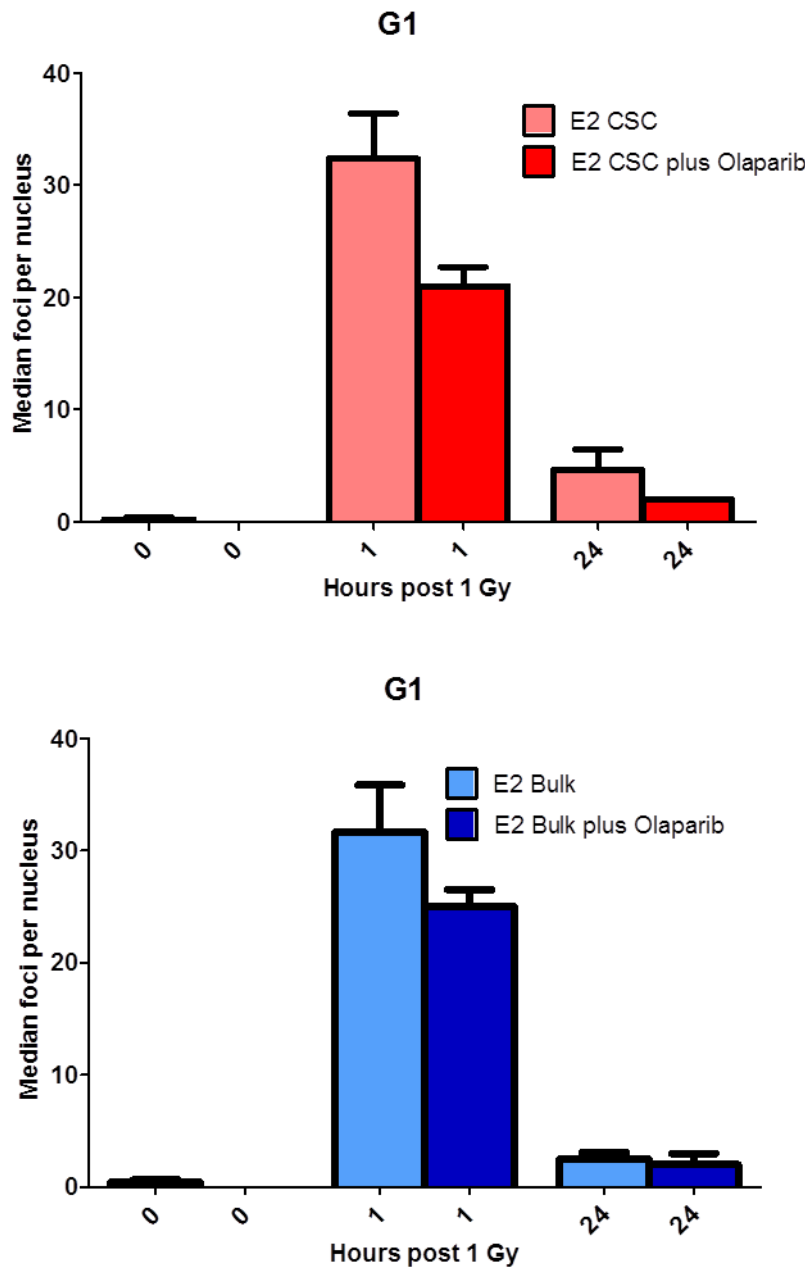


Figure 6.7 Quantification of gamma H2AX foci following 1Gy +/- 1 μ M olaparib in CENPF negative (G1 cell cycle phase) CSC and bulk cell populations

Resolution of gamma H2AX foci in E2 CSC and bulk cultures after treatment with 1Gy in the presence and absence of 1 μ M olaparib in CENPF negative (i.e. G1 cell cycle phase) populations. Gamma H2AX foci were quantified at the timepoints shown. Columns represent mean plus SEM of 3 median nuclear gamma H2AX foci values from independent experiments. Differences between controls and olaparib treated cells are non-significant at all timepoints by student's T test.

6.8 Conclusion

This study presents an investigation of PARP and its importance as a determinant of radiosensitivity in GBM CSCs. Investigations in this chapter have demonstrated the upregulation of PARP-1 in GBM tumour samples in comparison to normal brain, upregulated expression of PARP-1 in GBM CSCs in comparison to tumour bulk cells and inhibition of DNA repair by PARP inhibition in GBM CSCs resulting in radiosensitisation.

Venere et al have investigated the importance of PARP in GBM CSC DDR (Venere et al., 2014). They have shown that PARP-1 and PAR levels are elevated in GBM CSCs, which is in agreement with the results from this thesis. Furthermore it was demonstrated that PARP-1 has an important role in GBM CSC survival. 10 μ M of olaparib was shown to decrease neurosphere formation in CD133+ GBM cells. In contrast, the investigations detailed in this chapter were unable to demonstrate an effect of olaparib on neurosphere formation in the absence of radiation. This likely reflects the use of a much lower (1 μ M) concentration of olaparib, which nevertheless was found to ablate PARylation in GBM CSCs. Venere et al proposed that PARP was upregulated in GBM CSCs in order to efficiently repair damage from an increased level of basal ROS in GBM CSCs. Upregulated basal ROS was demonstrated in CD133+ cells from primary tumour specimens and *in vitro* cultures in keeping with this hypothesis.

GBM CSCs have a marked upregulation of PARP-1 expression in comparison to tumour bulk cells. This is accompanied by increased PARylation of proteins both at baseline and after irradiation. Inhibition of PARP by olaparib radiosensitises GBM CSCs to a modest degree *in vitro* by clonogenic assay. Radiosensitisation with PARP inhibition is also seen in tumour bulk cells. SER_{0.37} values range from 1.2 to 1.9, which is in keeping with the degree of radiosensitisation seen with PARP inhibition in established commercial cell lines (Brock et al., 2004, Dungey et al., 2009). The clonogenic survival curve of the E2 and R10 GBM CSCs treated with olaparib is superimposed on the olaparib treated bulk cell survival curve which suggests complete abrogation of GBM CSC radiation survival advantage. There is therefore a clear trend towards increased radiosensitising effects of

PARP and GBM CSC radioresistance

olaparib in CSCs compared to bulk tumour cells in the E2 and R10 cell lines, which would be in keeping with the overexpression of PARP-1 in CSCs. However the difference between bulk and GBM CSC SER_{0.37} is not statistically significant. These data represent the first demonstration of radiosensitisation by olaparib in GBM CSCs by clonogenic survival assay.

Previous studies have shown an increase in DNA DSB generation following PARP inhibition and radiation when compared to radiation alone (Dungey et al., 2009). In the investigations presented above, the median gamma H2AX foci per nucleus was significantly increased in both CSC and bulk populations in the E2 cell line following 1Gy plus PARP inhibition in G2 cell cycle phase populations. This was not evident in E2 GBM CSC and bulk G1 cell cycle phase cells treated with radiation and olaparib. This result is in keeping with current knowledge on mechanisms of radiosensitivity induced by PARP inhibition.

PARP-1, although having no direct DNA repair enzymatic activity itself, is a key DDR effector and modulates many other proteins involved in DNA repair via PARylation of its substrates (D'Amours et al., 1999). PARP-1 acts as a sensor of DNA damage and will bind to sites of DNA SSBs and will become activated upon DNA binding. Activated PARP is then able to PARylate a wide variety of DDR proteins and have direct interactions with many other DNA repair proteins including XRCC1, DNA Ligase III and DNA Polymerase Beta. AutoPARylation of PARP-1 also occurs, and is important in allowing DNA bound PARP to dissociate from DNA permitting access of other DNA repair machinery to the site of DNA damage. PARP inhibition will prevent the autoPARylation of DNA bound PARP molecules and also the PARylation of its DDR substrates (D'Amours et al., 1999). DNA bound PARP will prevent access to SSB sites by the appropriate DNA repair machinery. Furthermore, PARP will be unable to PARylate and interact with its substrates leading to a defect in SSB repair (Dungey et al., 2009, Zahradka and Ebisuzaki, 1982, Ferro and Olivera, 1982, Lindahl et al., 1995). It is accepted that the main role of PARP-1 is to facilitate SSB repair via Base Excision Repair (BER). PARP is not essential for the function of this pathway; however the presence of functioning PARP greatly improves the rate and efficiency at which BER can be carried out (Fisher et al., 2007, Satoh and Lindahl, 1992, Strom et

PARP and GBM CSC radioresistance

al., 2011, El-Khamisy et al., 2003). The radiosensitising effects of PARP inhibition are related to the role of PARP in SSB repair. Ionising radiation will cause up to 25 times as many SSBs as DSBs, however usually SSBs are repaired quickly and effectively and are of little consequence to the cell. However the presence of PARP inhibition will greatly impede the repair of these SSBs allowing them to be converted into DSBs during S phase DNA replication and subsequent replication fork collapse (Dungey et al., 2009, Brock et al., 2004). The upregulation of PARP-1 demonstrated in GBM CSCs would therefore provide a DNA repair advantage for GBM CSCs contributing to their relative radioresistance.

There are also less well characterised functions of PARP-1 which may confer a benefit for GBM CSC DDR following ionising radiation. PARP-1 is known to contribute to the MMEJ repair pathway of DNA DSB repair. PARP-1 normally directly competes with Ku heterodimers in binding to DNA DSBs; usually the higher affinity of Ku for DSBs prevails, however in the presence of a NHEJ defect, MMEJ achieves prominence (Wang et al., 2006). MMEJ does not normally significantly contribute to DNA DSB repair, however it can be an important pathway in malignant cells (Bentley et al., 2004). MMEJ is known to be sensitive to PARP inhibition.

In conclusion, GBM CSCs exhibit upregulation of PARP-1 expression and elevated levels of PAR both at baseline and in response to radiotherapy. Olaparib effectively reduces levels of PAR following radiation in both CSC and tumour bulk cultures and is associated with preferential radiosensitisation of GBM CSCs compared to tumour bulk cells. Radiosensitisation is associated with an increased median number of DNA DSBs per nucleus at the 24 hour timepoint following irradiation in CSCs in G2 cell cycle phase. These data have clinical significance in relation to the targeting of GBM CSCs in therapeutic strategies. The demonstration that GBM CSCs have increased expression of PARP-1 and increased PARP activity suggests that PARP-1 is a viable therapeutic target. Furthermore the ability of PARP inhibition to preferentially radiosensitise GBM CSCs as demonstrated by clonogenic survival assay in these studies suggests that PARP inhibition may provide enhanced tumour cell kill in combination with

PARP and GBM CSC radioresistance

radiotherapy, which may provide improved local control and survival from GBM.

The combination of PARP inhibition in addition to radiotherapy for GBM is being explored in the PARADIGM study, which is soon to open to recruitment in the UK.

Chapter 7 Radiosensitisation of GBM CSCs by inhibition of ATR and PARP

7.1 Introduction

The reliance of GBM CSCs on both efficient G2/M cell cycle checkpoint activation and enhanced DNA DSB repair was demonstrated in Chapter 4. Whilst potent radiosensitisation was achieved via the inhibition of ATM, ATM inhibition did not completely abrogate the G2/M checkpoint, suggesting alternative mechanisms of G2/M checkpoint activation could be important in cell cycle control in GBM CSCs. GBM CSCs were demonstrated to express high levels of phosphorylated ATR and Chk1 *in vitro* in chapter 4. ATR is known to have a key role in the function of the G2/M cell cycle checkpoint via the activation of Chk1 and subsequent phosphorylation of Cdc25c. It was postulated that ATR might perform an important role in the DDR of GBM CSCs, particularly in relation to G2/M checkpoint response. Therefore an investigation of the effects of ATR inhibition on GBM CSCs was undertaken.

7.2 Effects of VE-821 on ATR function in GBM CSCs

The effects of ATR inhibition were investigated using the specific ATR kinase inhibitor VE-821 (Reaper et al., 2011). G7 CSC and bulk cultures were incubated with incremental doses of VE-821 and subjected to irradiation with 5Gy prior to being lysed and prepared for Western blotting. Blots were probed for phosphorylated ATR ser428 and phosphorylated Chk1 ser345 (fig. 7.1). Phosphorylation at ser428 has been shown to be a marker of activated ATR in response to UV mediated DNA damage, whilst Chk1 is a key substrate of ATR and phosphorylation of Chk1 at s345 provides an indication of ATR function (Vauzour et al., 2007). A concentration of 5 μ M VE-821 was found to produce adequate suppression of the phosphorylation of Chk1 ser345 in G7 GBM CSC cultures following irradiation, (figure 7.1). This is in keeping with published literature regarding VE-821 (Reaper et al., 2011).

Radiosensitisation of GBM CSCs by inhibition of ATR and PARP

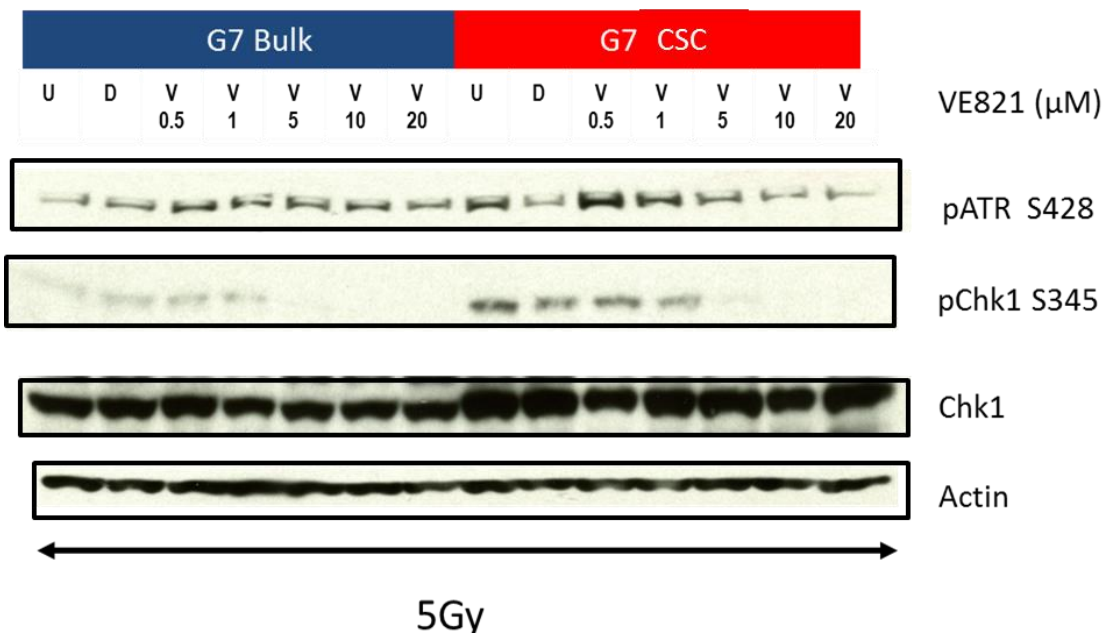


Figure 7.1 Analysis of DDR protein expression following 5Gy +/- VE-821 in CSC and bulk cultures

Investigation of expression of phosphorylated ATR ser428 and phosphorylated Chk1 s345 in G7 CSC and bulk cultures by Western blot 1 hour after exposure to 5Gy and incubation with various concentrations of VE-821 or 0.02% DMSO (D) or media only (U) for 1 hour prior to radiation. Total levels of Chk1 are also shown.

7.3 Effects of VE-821 on cell viability in GBM CSC and bulk cultures

GBM CSC and bulk cultures were incubated for 24 hours in 96 well plates in media containing differing concentrations of VE-821. After 24 hours of exposure to VE-821, the media was replaced with drug-free media. A cell viability (CellTiter-GloTM) assay was then performed 6 days following drug treatment (figure 7.2). 5 μ M VE-821 had a statistically significant effect on the viability of E2 bulk cells and no significant effect on E2 CSC. In the G7 cell line however, exposure to 5 μ M VE-821 for 24 hours decreased cell viability in both CSC and tumour bulk populations. However there was no significant difference in the effect of ATR inhibition on cell viability between CSC and bulk cultures.

Concentrations of VE-821 of 10 μ M and above were associated with marked effects on cell viability in CSC and bulk cultures of both cell lines. Since inhibition of phosphorylation of Chk1 could be demonstrated in the G7 cell line at a concentration of 5 μ M VE-821 and the main focus of the study was

Radiosensitisation of GBM CSCs by inhibition of ATR and PARP

radiosensitisation rather than the effects of VE-821 as a single agent, the concentration of 5 μ M VE-821 was selected for further investigations.

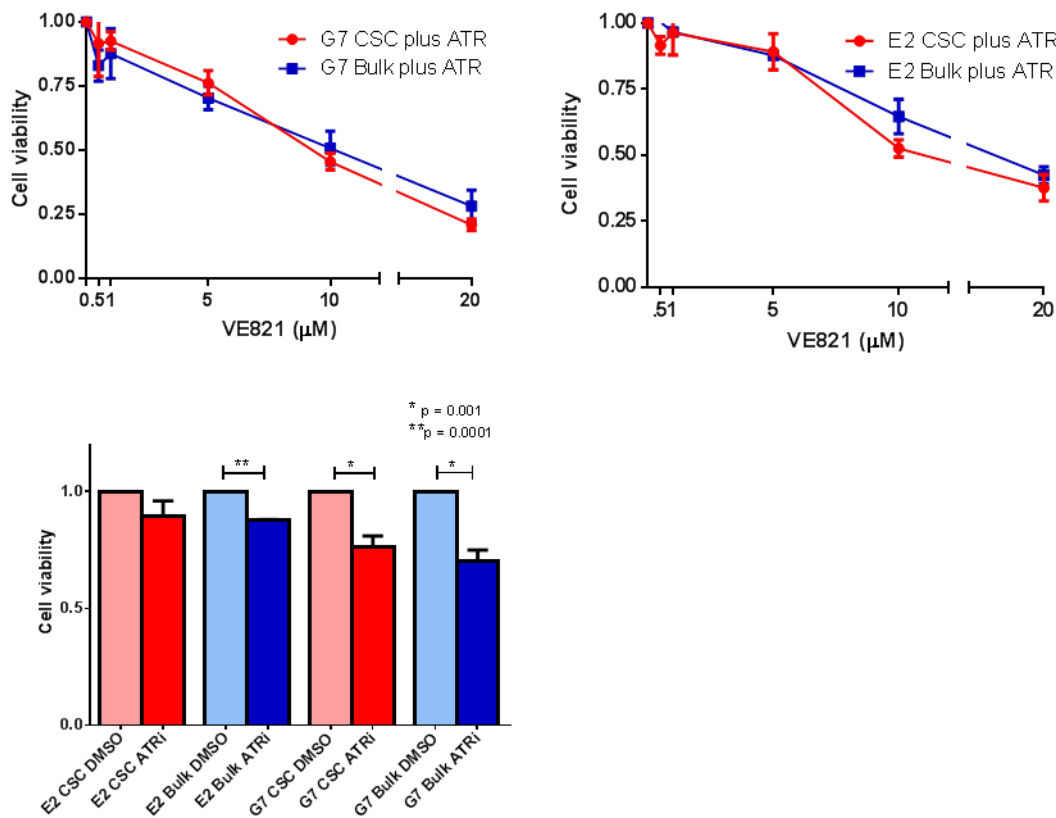


Figure 7.2 Effect of VE-821 on cell viability

Upper panels; investigation of cell viability following 24 hours exposure to incremental concentrations of VE-821 in CSC and bulk cultures of E2 and G7 cell lines. Mean and SEM from 3 results are plotted. Cell viability was assessed by CellTiter-Glo™ analysis performed 6 days after drug treatment. Lower panel; mean cell viability results after exposure to 5 μ M VE-821 are charted as bars and a one sample t test was used to assess whether cell viability was significantly different from controls (normalised data); results from 3 independent experiments. Mean values for cell viability +/- 95% CI's are as follows: E2 CSC 0.9 (0.7, 1.1); E2 bulk 0.88 (0.87, 0.88); G7 CSC 0.76 (0.76, 0.84); G7 bulk 0.70 (0.56, 0.82).

7.4 Effects of VE-821 on the G2/M checkpoint in GBM CSCs

Effects of ATR inhibition on G2/M checkpoint function after radiation were assessed in E2 and G7 GBM CSC and bulk cultures following incubation with 5 μ M VE-821 for 1 hour prior to irradiation with 5Gy. Cells were fixed at timepoints of 0, 3 and 6 hours post irradiation and pHisH3 positive cells were quantified by flow cytometry as in chapter 5.

Radiosensitisation of GBM CSCs by inhibition of ATR and PARP

Results of G2/M checkpoint interrogation are plotted in figure 7.3. ATR inhibition efficiently abolished radiation induced G2/M checkpoint activation and maintenance in the E2 CSC and bulk cultures. VE-821 treated E2 cells failed to show a decrease in mitotic fraction at both 3 and 6 hours following radiation. The mitotic fraction of irradiated cells exposed to ATR inhibition was increased at the 6 hour timepoint relative to DMSO treated, unirradiated control cells.

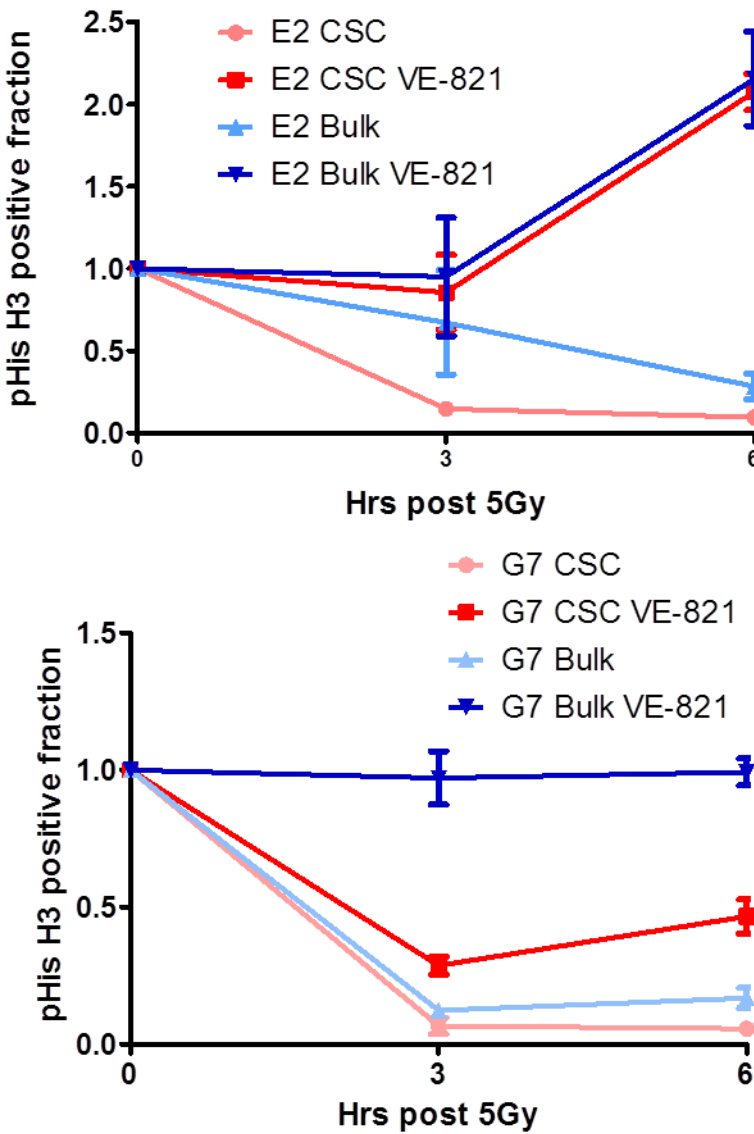


Figure 7.3 Effect of 5Gy radiation +/- VE821 on G2/M checkpoint function in E2 and G7 CSC and bulk cultures

Investigation of G2/M checkpoint function by flow cytometric quantification of pHisH3 positive cells after exposure to 5Gy in the presence of ATR inhibition. E2 and G7 CSC and bulk cultures were incubated with 5 μ M VE-821 or a corresponding concentration of DMSO and then exposed to 5Gy of radiation. Cells were fixed in ethanol at timepoints shown and analysis of pHisH3 and PI incorporation was undertaken via flow cytometry. Each data point represents mean and SEM of a minimum of 3 independent experiments normalised to unirradiated controls.

VE-821 had less effect on G2/M checkpoint function in G7 GBM CSCs following radiation, however. G7 GBM CSCs exhibited an attenuated G2/M checkpoint response to 5Gy radiation in the presence of ATR inhibition. The effect of ATR

Radiosensitisation of GBM CSCs by inhibition of ATR and PARP

inhibition was more marked in G7 bulk cultures, in which the G2/M checkpoint response to 5Gy was completely abolished. However the mitotic population after 5Gy was similar to that of the DMSO treated, unirradiated control cells and no ‘pro-mitotic’ effects above baseline were observed (unlike in E2 cells). Representative images of the flow cytometry gating used in the experiment are shown in figure 7.4

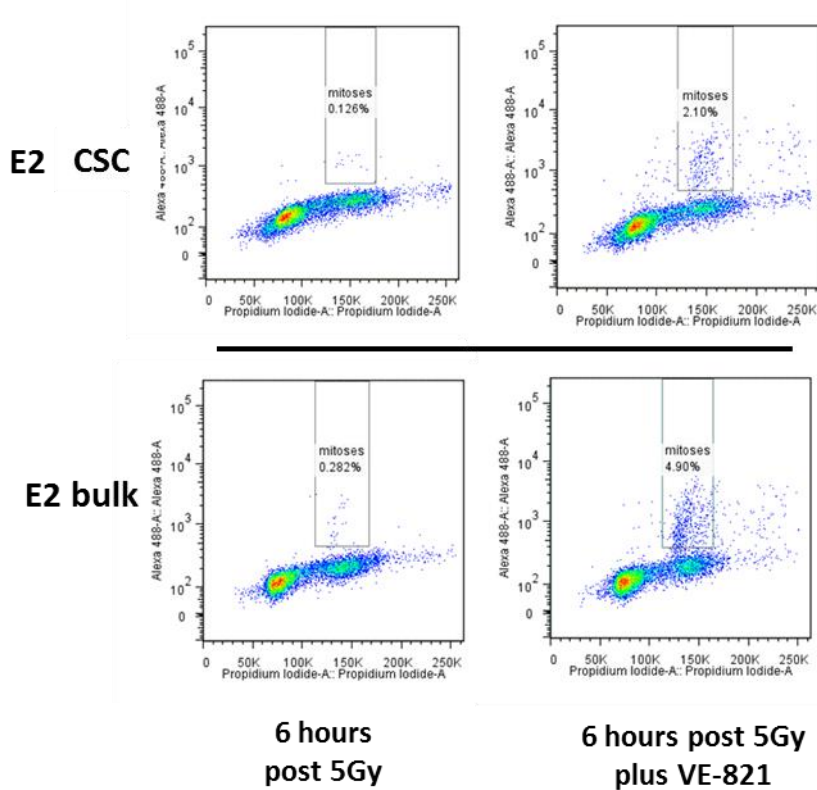


Figure 7.4 Flow cytometry gating for analysis of pHisH3 positive cells

Examples of gating used for the flow cytometric analysis of pHisH3 positive cells in CSC and bulk cultures of the E2 cell line.

7.5 Effects of VE-821 and radiation on clonogenic survival of GBM CSC and bulk cultures

The effect of VE-821 on radioresistance was investigated by clonogenic assay in GBM CSC and bulk cultures of the E2 and G7 cell lines. Cultures were incubated with 5µM VE-821 for one hour prior to irradiation. 24 hours post irradiation drug containing medium was removed and replaced with fresh, drug-free medium.

Radiosensitisation of GBM CSCs by inhibition of ATR and PARP

Clonogenic survival curves are shown in figure 7.5; surviving fractions for combined treatment with radiation and VE-821 were normalised to the surviving fractions of unirradiated VE-821 treated cells during calculation of plating efficiency, therefore eliminating any baseline additive effects of the drug on the analysis of clonogenic survival curves.

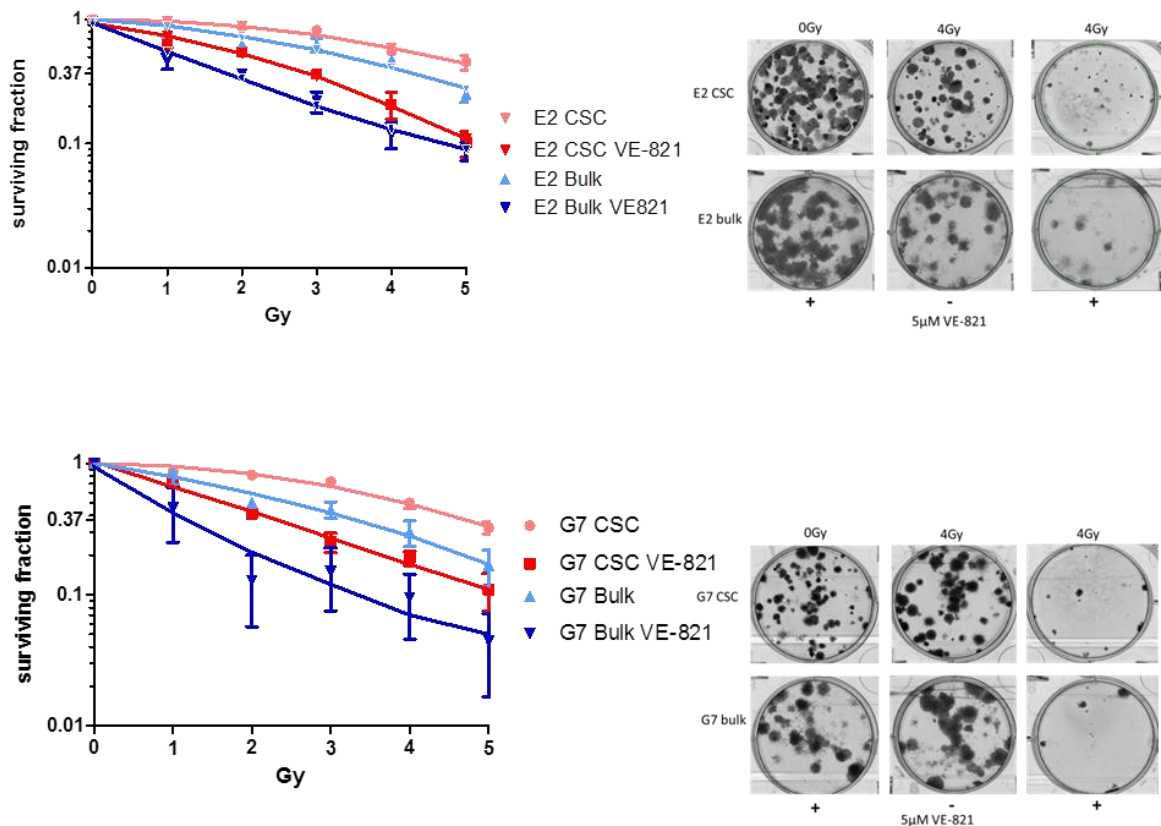


Figure 7.5 Effects of ATR inhibition and VE-821 on clonogenic survival of GBM CSC and bulk cells

Clonogenic survival curves comparing effects of VE-821 plus radiation versus radiation alone on CSC and bulk cell cultures in E2 and G7 cell lines. Data points represent mean +/- SEM from 3 independent experiments. Representative images of colony formation at 0 and 4 Gy are also shown.

ATR inhibition was associated with radiosensitisation of GBM CSCs with SER_{0.37} values of 1.97 in E2 CSC and 2.05 in G7 CSC. In bulk cultures SER_{0.37} values were 2.37 in G7 and 2.56 in E2, (table 7.1). Although SER_{0.37} values were higher in bulk cultures than CSC cultures of both cell lines, these differences were not statistically significant. SF_{4Gy} values were significantly decreased by ATR inhibition in both cell lines and culture types.

	SER 0.37 (95% CI)	SF 4Gy (- VE-821) (95% CI)	SF 4Gy (+ VE-821) (95% CI)
E2 CSC	1.97 (1.85, 2.09)	0.55 (0.47, 0.62)	0.21 (0.11, 0.31)
E2 bulk	2.56 (1.78, 3.33)	0.48 (0.41, 0.54)	0.12 (0.063, 0.17)
G7 CSC	2.05 (1.80, 2.30)	0.50 (0.41, 0.58)	0.19 (0.14, 0.24)
G7 bulk	2.37 (1.95, 2.79)	0.30 (0.17, 0.43)	0.094 (0, 0.19)

Table 7.1 SER_{0.37} following ATR inhibition in GBM CSC and bulk cultures

SER_{0.37} and SF4Gy values represent means of values from 3 independent experiments.

The radiosensitising effects of ATR inhibition were confirmed by neurosphere formation assay in CSC cultures of the E2 and G7 cell lines (figure 7.7). Single cell suspensions were exposed to ATR inhibitor for 1 hour prior to irradiation and then left for 48 hours post irradiation before ATR inhibitor was diluted with the addition of further medium to each well, (see materials and methods). This assay demonstrated that ATR inhibition and radiation in combination significantly reduced the formation of neurospheres relative to CSCs treated with 2Gy radiation only.

7.6 Investigation of combination DDR kinase inhibition on radiosensitivity of GBM CSCs

Inhibition of ATM kinase provided very potent radiosensitisation of GBM CSCs via the dual mechanism of G2/M checkpoint inhibition and inhibition of effective DNA DSB repair, as described in Chapter 5. As discussed in this chapter and chapter 6, ATR and PARP inhibitors as single agents were associated with lower levels of radiosensitisation in CSCs. However ATR inhibition efficiently abrogated

Radiosensitisation of GBM CSCs by inhibition of ATR and PARP

radiation induced G2/M checkpoint function, whilst PARP inhibition was an efficient DNA repair inhibitor. It was hypothesised that the combination of these two agents may provide enhanced radiosensitisation of GBM CSCs, since PARP inhibition would increase the number of unrepaired DNA DSBs following IR, whilst ATR would prevent G2/M checkpoint arrest.

The effect of dual PARP and ATR kinase inhibition on radioresistance of GBM CSCs was therefore investigated. Cell cultures were incubated with 1 μ M olaparib and 5 μ M VE-821 prior to irradiation. Cell media containing olaparib and VE-821 was removed 24 hours after irradiation and replaced with fresh media containing no added inhibitor agents. Figure 7.6 shows cell survival curves in CSC and bulk cultures of E2, G7 and R10 cell lines following dual PARP/ATR inhibition and radiation.

Radiosensitisation of GBM CSCs by inhibition of ATR and PARP

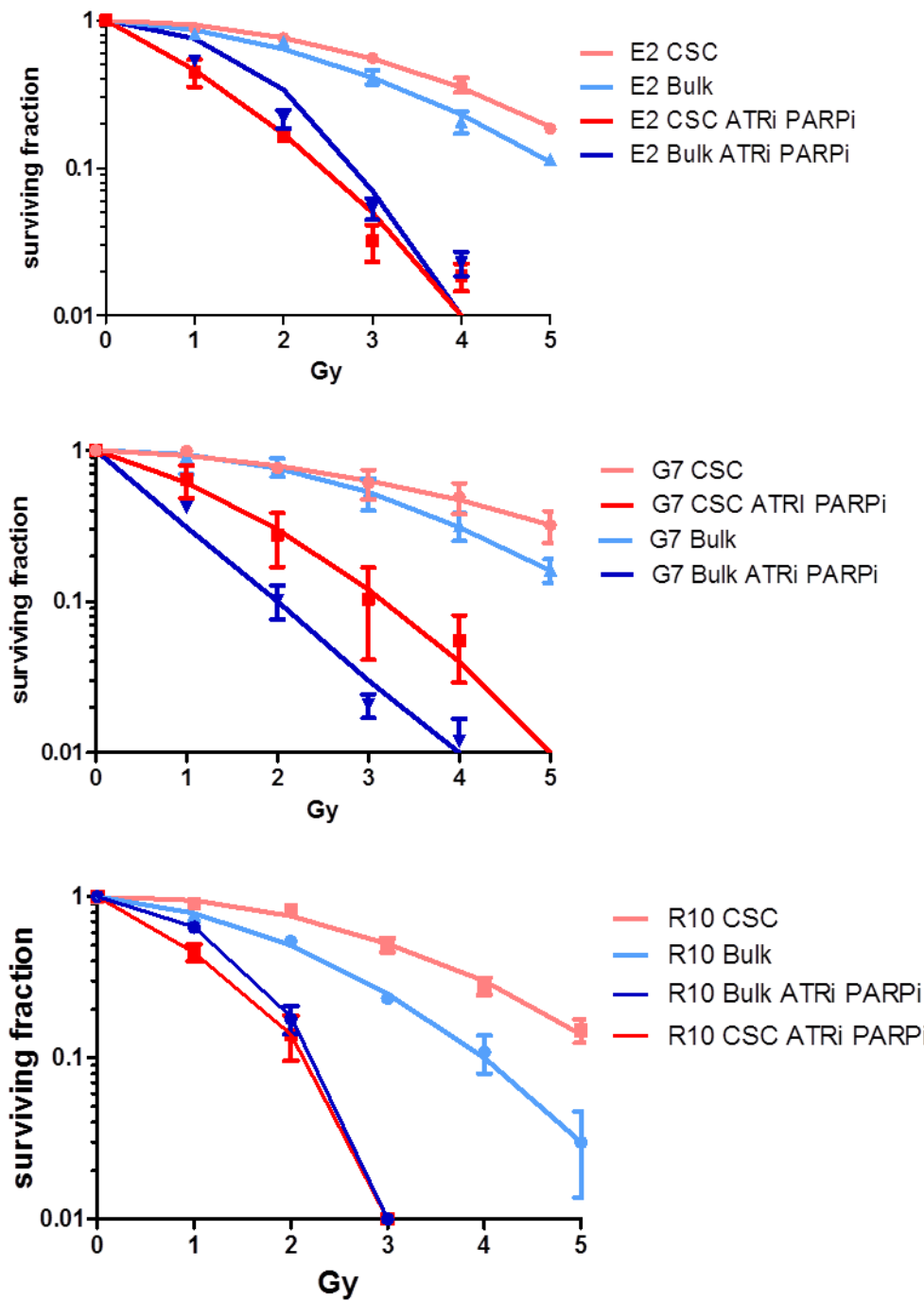


Figure 7.6 Effects of combination of VE-821 and olaparib on radiosensitivity of E2, G7 and R10 cell lines.

Clonogenic survival curves comparing effects of olaparib and VE-821 plus radiation versus radiation alone on CSC and bulk cell cultures in E2, G7 and R10 cell lines. Data points represent mean +/- SEM from 3 independent experiments.

$SER_{0.37}$ values are plotted in table 7.2. These data show that the combination of ATR and PARP inhibition produced highly potent radiosensitisation of GBM CSCs. $SER_{0.37}$ values for the combination of PARP and ATR inhibition ranged from 2 to 3

Radiosensitisation of GBM CSCs by inhibition of ATR and PARP

for CSC cultures of E2, G7 and R10 cells. In R10 and E2 cells, SER_{0.37} values were significantly higher for CSC cultures than for bulk cell cultures, indicating that dual inhibition of ATR and PARP has a particular impact on radiation sensitivity of GBM CSCs, despite the fact that ATR inhibition alone had slightly less effect on the radiosensitivity of CSC than bulk cells. A significant difference was not observed in G7 cells, nevertheless both CSC and bulk cultures of G7 were potently radiosensitised by the combination. Again surviving fractions for ATR and PARP inhibition in combination with radiotherapy were normalised to unirradiated cells treated with ATR and PARP inhibition, therefore eliminating any baseline additive effects of the drugs on the analysis of clonogenic survival curves.

	SER 0.37 (95% CI)	SF 4Gy (- VE-821/olaparib) (95% CI)	SF 4Gy (+ VE- 821/olaparib) (95% CI)
E2 CSC	3.2 (2.53, 3.95)	0.36 (0.28, 0.45)	0.019 (0.012, 0.026)
E2 bulk	1.65 (1.46, 1.88)	0.21 (0.14, 0.27)	0.023 (0.014, 0.031)
G7 CSC	2.06 (1.72, 2.40)	0.59 (0.27, 0.71)	0.055 (0.0042, 0.011)
G7 bulk	2.18 (1.93, 2.44)	0.32 (0.19, 0.45)	0.012 (0.0023, 0.022)
R10 CSC	2.98 (2.30, 3.66)	0.28 (0.21, 0.35)	0
R10 bulk	1.67 (1.44, 1.91)	0.11 (0.053, 0.16)	0

Table 7.2 SER_{0.37} for dual ATR and PARP inhibition in GBM CSC and bulk cultures

SER_{0.37} values and SF4Gy +/- VE-821 plus olaparib are tabulated for CSC and bulk cultures of E2, G7 and R10 cell lines. Mean values from 3 independent experiments with 95% confidence intervals are presented.

Neurosphere formation assays were performed to assess the effects of combined ATR and PARP inhibition in the absence of radiation. This data is presented in figure 7.7 and demonstrates marked inhibition of neurosphere formation by olaparib and VE-821 even in the absence of radiation in both E2 and G7 CSC cell cultures. The combination of PARP and ATR inhibition reduced neurosphere production more efficiently than exposure to 2Gy alone.

Radiosensitisation of GBM CSCs by inhibition of ATR and PARP

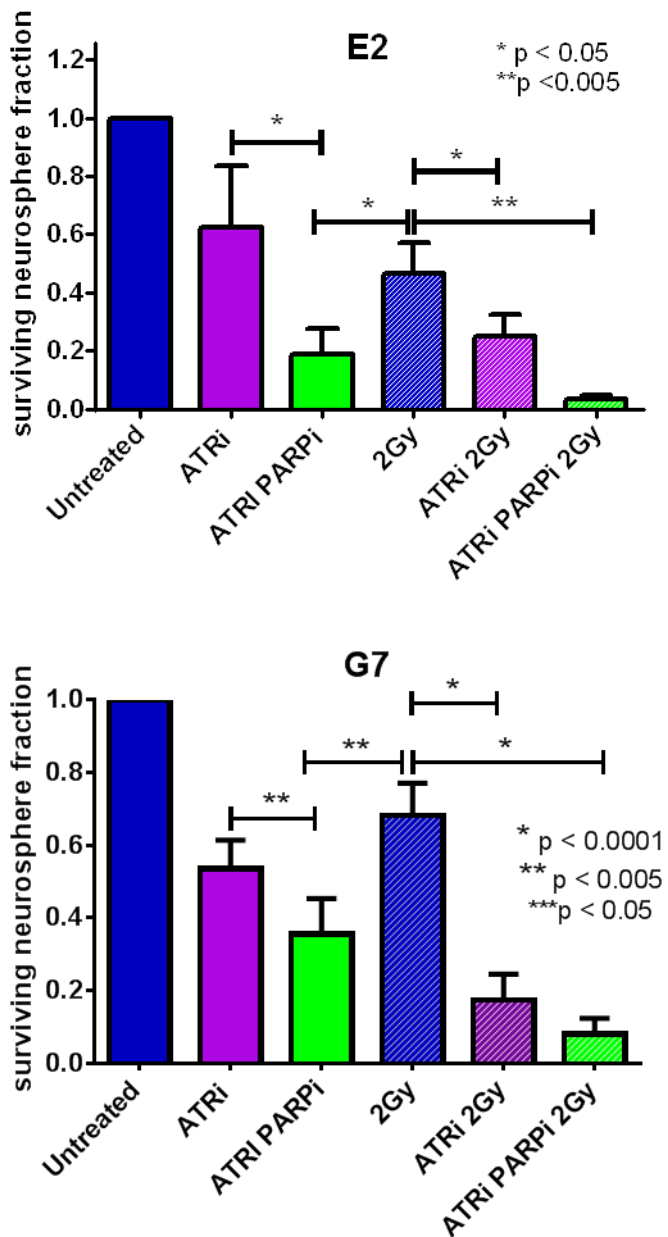


Figure 7.7 Neurosphere formation assay in E2 and G7 CSC cultures following combinations of DDR inhibitors and 2Gy

10 cells per well were seeded into 96 well plates and treated with VE-821, olaparib plus VE-821 or DMSO prior to irradiation with 2 Gy or no irradiation. Neurospheres were quantified manually after 3 (G7) or 4 weeks (E2) after imaging. Mean plus SEM of 3 independent experiments shown, normalised to control values. Student's t test was used to calculate p values.

7.7 Conclusion

In this chapter the effect of ATR inhibition on GBM CSC and bulk cultures was investigated.

A study of ATR inhibition on the G2/M checkpoint in GBM CSCs and bulk cells following irradiation was carried out. ATR inhibition had a very pronounced effect on G2/M checkpoint function in the E2 cell line. Exposure to ATR inhibition following irradiation led to a large increase in mitotic cells in both E2 CSC and bulk populations relative to controls, indicating a vital role for ATR in the control of the G2/M checkpoint in this cell line. ATR inhibition appeared to completely abrogate the efficient IR induced G2/M checkpoint response in E2 CSCs, suggesting that it is the ATR pathway which provides the main mechanism of upregulated G2/M checkpoint function in E2 CSCs compared to bulk cells. Furthermore, the proportion of mitotic cells at 6 hours following irradiation was in excess of the proportion of mitotic cells seen in unirradiated controls. This likely represents an effect of ATR inhibition on the intra-S phase checkpoint in combination with G2/M checkpoint abrogation. Shibata et al examined the importance of ATR in mediating the G2/M checkpoint (Shibata et al., 2010). They demonstrated that ATM is required for initial activation of the G2/M checkpoint, however ATR signalling is then recruited via ATM dependent resection of DSBs requiring repair by homologous recombination. ATR-Chk1 mediated signalling was critical to the maintained activation of the G2/M checkpoint in early timepoints following irradiation. Continued ATM signalling from unrepaired DSBs also contributed to this process. It is of interest that the attenuation of the G2/M checkpoint in the G7 CSC cultures following ATR inhibition and radiation was much less than the degree of effect seen in the E2 CSC cultures. A possible reason for this may be that ATM can compensate for the loss of ATR signalling in the G7 CSC cultures.

Although ATR is an important controller of the G2/M checkpoint, its inhibition is also known to have effects on DNA integrity and repair (Zeman and Cimprich, 2014). As discussed in the introduction, ATR has a vital role in the response to replication stress. ATR stabilises stalled replication forks, slows DNA replication

Radiosensitisation of GBM CSCs by inhibition of ATR and PARP

and activates cellular checkpoints in response to replication stress. Ionising radiation causes a multitude of DNA lesions including pyrimidine lesions, purine lesions, SSBs and DSBs which can be a source of significant replication stress. Upon encountering these lesions DNA polymerases become stalled, whilst DNA helicases continue to unwind the DNA double helix in advance of the replication machinery generating long stretches of ssDNA. This generates an ATR-Chk1 response allowing stabilisation of replication forks, suppression of S phase origin firing and G2/M arrest, providing the cell the means to avoid DSBs caused by collapse of replication forks. ATR can therefore be predicted to play a significant role in the DNA damage response to ionising radiation, particularly in replicating cells, which may account for some of the radiosensitising effects of ATR inhibition. Analysis of gamma H2AX foci was not carried out following the combination of IR and ATR inhibition, however other authors have demonstrated an increase in gamma H2AX foci following ATR inhibition and radiation, in pancreatic carcinoma cell lines (Prevo et al., 2012).

It was observed that the effect of ATR inhibition on the G2/M checkpoint was greater than that seen following ATM inhibition, particularly in the E2 cell line. It was hypothesised that if ATR inhibition was subsequently combined with a DNA repair inhibitor, such as a PARP inhibitor, then highly potent levels of radiosensitisation would be produced in GBM CSCs, given that studies of radioresistance detailed in chapter 4 suggested CSCs rely upon two aspects of DDR; namely efficient cell cycle checkpoint activation combined with more efficient DNA repair. In agreement with this hypothesis, dual ATR and PARP inhibition via the combination of VE-821 and olaparib with radiotherapy produced very potent radiosensitisation of GBM CSCs which could be demonstrated by clonogenic assay and neurosphere assay. Furthermore GBM CSC cultures appeared to experience greater radiosensitisation than bulk cultures in the E2 and R10 cell lines with this combination, with SER_{0.37} being significantly higher in GBM CSC cultures compared to bulk. This combination of DDR inhibitors completely abrogated the increased radioresistance of GBM CSCs in the E2 and R10 cell lines which confirms the importance of DNA repair and cell cycle control in the GBM CSC population. In the G7 cell line, however, CSC cultures still retained their relative radioresistance despite the combination of ATR and PARP

Radiosensitisation of GBM CSCs by inhibition of ATR and PARP

inhibition. This may reflect the reduced attenuation of the G2/M checkpoint seen after radiation and ATR inhibition in this cell line compared to the complete attenuation of the G2/M checkpoint seen after ATR inhibition in the E2 cell line

An interesting observation during the course of these studies was the induction of significant cytotoxicity by the combination of ATR inhibition and PARP inhibition without additional radiation by neurosphere production assay. Reduction in neurosphere production by the combination of ATR and PARP inhibition (without radiation) was significantly greater than that achieved by 2Gy of radiation alone. In contrast, ATM and PARP inhibitors as single agents had no measurable effects on CSC neurosphere production at lowest effective concentration in the absence of radiation, whilst ATR inhibition had a smaller effect on CSC survival.

The mechanism of cytotoxicity of the ATR and PARP inhibitor combination in the absence of radiation requires further investigation. Several possible mechanisms could underlie the effects of dual ATR and PARP inhibition. The observed cytotoxicity may be a form of induced synthetic lethality. Cells lacking BRCA1 or 2 are known to be sensitive to PARP inhibition. In this setting PARP inhibition delays the repair of SSBs arising endogenously from normal cellular metabolism. These lesions result in replication fork collapse and DSB generation, which would normally be dealt with by HR, however the HR deficiency seen in homozygous BRCA 1 or 2 loss results in unrepaired DSBs and cell death. The ATR-Chk1 pathway is known to facilitate HR (Brown et al., 2014) therefore ATR inhibition could induce a ‘BRCAness’ phenotype, producing cytotoxicity on exposure to PARP inhibition. Another possible mechanism involves the role of PARP-1 at collapsed replication forks following an inadequate replication stress response. ATR is required for the stabilisation of stalled replication forks and subsequent activation of Chk1. In the absence of ATR activity, stalled replication forks undergo collapse and DSBs are generated. Bryant et al have shown that PARPs 1 and 2 bind to DSBs formed at collapsed replication forks, and that PARP also binds to short SSB sections of a subset of stalled forks, allowing their detection and the subsequent attraction of MRE11 facilitating resection and replication

Radiosensitisation of GBM CSCs by inhibition of ATR and PARP

restart (Bryant et al., 2009). The upregulation of PARP1 in CSCs may allow for the recovery and repair of stalled/collapsed forks created via ATR inhibition. The inhibition of both elements of this vital repair pathway may result in catastrophic failure of the replication stress response, and synergistic cytotoxic effects.

Peasland et al explored the applications of the ATR inhibitor NU6027 in breast and ovarian carcinoma cell lines and demonstrated a synthetic lethal interaction with PARP inhibition (Peasland et al., 2011). A decrease in RAD51 foci was seen following the combination of ATR and PARP inhibition in comparison to cells treated with PARP inhibition only. The authors hypothesised that ATR inhibition prevented efficient HR and repair of DSBs created via collapse of replication forks following PARP inhibition, leading to cytotoxicity. Nevertheless, the investigations in this chapter represent the first demonstration of radiosensitisation by this drug combination and the first demonstration of cytotoxicity of combined ATR and PARP inhibition in GBM CSCs.

In summary, ATR inhibition appears to provide potent attenuation of the G2/M checkpoint in response to radiation, and radiosensitises GBM CSCs, although to a lesser degree than inhibition of ATM. The combination of checkpoint ablation and repair inhibition via ATR and PARP inhibition provides highly potent radiosensitisation of GBM CSCs and is associated with complete abrogation of the radioresistance seen in some GBM CSC cultures. The combination of ATR and PARP inhibition is also highly effective in reducing neurosphere formation by CSCs in the absence of radiation. These data suggest that the combination of ATR and PARP inhibition should be explored in *in vivo* models of GBM. Dual ATR and PARP inhibition may have promising clinical activity even in the absence of radiation treatment.

Chapter 8 Discussion

8.1 Introduction

This project aimed to investigate the putative radioresistance of GBM CSCs, interrogate the DDR of GBM CSCs to irradiation and characterise the effects of DDR inhibition on the radioresponse of GBM CSCs.

Evidence for radioresistance in GBM CSCs was presented by Bao et al., who demonstrated preferential activation of DDR in response to radiation and increased DNA repair in a CD133+ subpopulation of GBM cells (Bao et al., 2006a). However, subsequent reports have been conflicting regarding the radioresistance of GBM CSCs (Ropolo et al., 2009, McCord et al., 2009). Furthermore the literature in general lacks robust measurement of GBM CSC radioresistance. Some investigations have been unable to demonstrate GBM CSC radioresistance via the gold standard of clonogenic assay (McCord et al., 2009), which has been shown to correlate with clinical outcome (Bjork-Eriksson et al., 2000, West et al., 1997). Instead many investigations have relied upon surrogates of radioresistance such as cell viability assays and demonstration of upregulation of DDR. In addition previous studies have attempted comparison of CSC and tumour bulk radioresponse by comparing non-isogenic cell lines from different parental tumours or by comparing CSC with commercially available cell lines, which ignores differences in intrinsic radiosensitivity and may prove a confounding factor (McCord et al., 2009, Ropolo et al., 2009). Studies of radioresistance in GBM CSCs to date have been highly reliant on the sorting of GBM cell populations using the CD133 marker into CD133 positive and negative subpopulations. Whilst this allows comparison to be made between isogenic CSCs and bulk cells, CD133 is not a universal marker of GBM CSCs and there is evidence that CD133 negative cells can also exhibit CSC properties, which may in part account for the conflicting results seen in the literature. If all of these factors are taken into account, radioresistance in GBM CSC subpopulations has only been robustly investigated by clonogenic assay in a few *in vitro* cell lines, with at times discordant results. Therefore, although radioresistance of GBM CSCs is a widely stated phenomenon, this property of GBM CSCs remains contentious.

Discussion

In addition to investigating the radioresistance of GBM CSCs this project also explored previously documented upregulated DDR in GBM CSCs and investigated the effects of DDR inhibition on this tumour subpopulation. Upregulated DDR in GBM CSCs has been consistently documented by a number of investigators (Bao et al., 2006a, Ropolo et al., 2009), however a detailed analysis of the effects of upregulated DDR expression on the functional endpoints of cell cycle control and DNA DSB repair has not been undertaken. Previous studies have not examined the activation and maintenance of the G2/M checkpoint in GBM CSCs following radiation. Furthermore, studies of DNA DSB repair using gamma H2AX foci in GBM CSCs have not accounted for cell cycle effects, and have provided conflicting data on CSC DSB repair (McCord et al., 2009, Bao et al., 2006a).

A summary discussion of the main findings of the thesis and how these data contribute to current knowledge now follows.

8.2 Modelling GBM CSCs *in vitro*

This project developed a model of GBM CSCs which was not reliant upon the cell surface marker CD133 (see Chapter 3). Instead paired CSC and tumour bulk cultures were derived from a single parental primary GBM cell line. The GBM CSC state was maintained by culture in a serum free neurobasal type medium with supplementation of growth factors, whilst a differentiated tumour bulk phenotype was achieved by culture in FCS containing medium. This model has important advantages over the cell sorting methods described by other authors. In particular, the lack of reliance upon a single GBM CSC marker allows greater heterogeneity in the CSC populations studied in this project. Since there is no accepted universal GBM CSC marker, the possibility of misidentification of the tumour CSC subpopulation is avoided. Furthermore the effects on cellular phenotype of the sorting process are poorly defined, and some authors have questioned whether binding of primary antibody during cell sorting may influence cellular behaviour, although this has not been shown in the case of anti-CD133 antibodies (Taussig et al., 2008).

Discussion

This culture based model of GBM CSC and tumour bulk cells was validated by *in vitro* and *in vivo* methods. Elevated expression levels of CSC markers were demonstrated in GBM CSC cultures in comparison to tumour bulk cultures. In the E2 cell line, GBM CSC cultures were tumourigenic in orthotopic murine GBM models after injection of 10^5 tumour cells, producing highly invasive tumours. In contrast, intracranial injection of 10^5 E2 tumour bulk cells was essentially non-tumourigenic in these mouse models. The G7 GBM CSCs and tumour bulk cultures were both equally tumourigenic in orthotopic models, however G7 GBM CSCs were found to reproduce invasive tumours which recapitulated features of the original parental tumour, in contrast to the G7 bulk cell tumours which had well defined edges and no invasive features (Mannino et al., 2014).

The model described in this project has limitations, since CSC populations and tumour bulk populations are being maintained in different culture conditions, and this could represent a confounding factor in the experiments carried out in this project. However, evidence is accumulating that the CSC state is dependent on microenvironmental influences. CSC phenotype is influenced by the microenvironmental milieu of the perivascular niche, and the CSC state appears to exhibit significant plasticity (Meacham and Morrison, 2013, Vlashi and Pajonk, 2014). The different culture conditions employed in this study recreate some of the tumour microenvironmental cues which are present in the perivascular niche *in vivo* which determine the CSC phenotype. Furthermore criticism could be made of investigations which rely upon cell sorting of CD133+ cells and comparison with CD133- cells. In these investigations it is not clear what the *in vivo* correlate of a CD133- cell maintained in CSC medium is. Certainly CD133- cells can be defined in a negative sense in that they lack the CD133 cell surface marker. However this does not necessarily make them a valid representation of differentiated tumour cells *in vivo*, since they are existing in culture medium which is designed to inhibit differentiation. Nevertheless, the CSC phenotype of the cell cultures described in this project is not a transient cell culture medium based phenomenon. The increased level of expression of the GBM CSC marker nestin appears to be maintained in CSC cultures upon transfer into differentiating tumour bulk medium (chapter 1), which provides further support for the robustness of the GBM CSC model employed in this project. However this

Discussion

model does have certain limitations. CSC cultures utilised in this project are not a pure CSC population; rather these cultures are enriched for CSCs and will also contain some differentiated tumour cells. Likewise bulk cultures grown in FCS containing medium will probably also harbour a subpopulation of CSCs, however this will be depleted in comparison to CSC cultures.

Cell proliferation rates of CSC cultures and tumour bulk cultures were similar following measurement of cell doubling time via cell viability assay in this project, which is in contrast to the opinion that the GBM CSC population is quiescent and divides relatively infrequently. This may represent an artefact of *in vitro* culture of CSC populations in this project. Nevertheless, on review of the literature, CSC quiescence in solid tumours is based mainly on extrapolation of the behaviour of normal stem cell populations. There is relatively little experimental evidence to confirm the quiescence of CSC populations in solid tumours and no studies of proliferation rates of CSCs *in vivo*. Gao et al demonstrated that CD24+ cells in primary ovarian tumours expressed stem cell associated markers such as nestin and were more slowly proliferating than bulk tumour cells up to one week following cell sorting based on this marker (Gao et al., 2010). Dembinski et al identified a slow cycling tumourigenic population of cells in pancreatic tumours, which possessed CSC properties (Dembinski and Krauss, 2009). Nevertheless, conclusive evidence regarding CSC quiescence *in vivo* in GBM is lacking.

This project demonstrated important differences in cell cycle phase occupancy between CSC and bulk cultures. There was a higher proportion of CSCs occupying S and G2 phase of the cell cycle compared to tumour bulk populations. Gao et al demonstrated increased S phase proportions of CSCs compared to tumour bulk cells in ovarian tumours (Gao et al., 2010). Furthermore normal neural embryonic stem cells are known to have a shortened G1-S transition, leading to an overall reduction in cell cycle time (Calegari and Huttner, 2003). The increased proportion of cells in S and G2 phases in CSC populations has important implications for DDR. Conventionally, homologous recombination repair can only occur in late S and G2 phase, and therefore may be important in CSC function, given that CSCs appear to favour S and G2 cell cycle phases. This

Discussion

has critical implications for comparison of DSB repair between CSC and bulk populations, since cells existing in G2 phase will experience a greater number of DNA DSBs than cells in G1 phase following an equivalent radiation exposure due to their higher DNA content (Lobrich et al., 2010). Previous studies of DNA repair in GBM CSCs by gamma H2AX foci quantification have not taken this important factor into account.

8.2 Radioresistance of GBM CSCs

Studies undertaken in this project provide strong support for the contention that GBM CSCs exhibit radioresistance relative to non-CSC tumour cells. The radiation response of 3 GBM cell lines cultured as paired CSC and tumour bulk cultures were subjected to clonogenic analyses of survival following irradiation, which demonstrated radioresistance of the CSC population. Clonogenic data were fitted to a conventional linear quadratic model of survival in order to generate a dose modifying factor for 0.37 survival ($DMF_{0.37}$). $DMF_{0.37}$ for the E2, G7 and R10 CSC cultures relative to tumour bulk cultures was approximately 1.5, indicating that the radiation dose required to produce a 0.37 surviving fraction in CSC cultures was 1.5 times greater than the radiation dose producing 0.37 survival in tumour bulk cultures. This difference in radiosensitivity was statistically significant, and given its magnitude is also likely to be clinically significant. The studies in this thesis therefore provide evidence to support the hypothesis that GBM CSC radioresistance is an important factor in determining disease recurrence in GBM patients. Given concerns regarding confounding effects of medium, the radioresistance of CSCs was confirmed in the E2 cell line by neurosphere production assay of irradiated CD133+ and CD133- sorted cells from the CSC culture population, which demonstrated relative radioresistance of CD133+ cells in comparison to CD133-ve cells.

The study by McCord et al questioned the relevance of GBM CSC radioresistance to current *in vitro* models of GBM (McCord et al., 2009). This study argued that the concept of radioresistant CSCs was irrelevant to current *in vitro* models of GBM, since the established model was more radioresistant than the GBM CSC model. However, all of the GBM CSC cultures subject to clonogenic assay in this

Discussion

thesis demonstrated extremely high levels of radioresistance. SF2Gy for the CSC populations of E2, G7 and R10 were in the range 0.83-0.89. Direct comparison to the commercially available cell lines used in the study by McCord et al is difficult, since SER_{0.37} or other radiobiological parameters were not presented. However the radioresistance of CSC cultures in the present study appears in excess or at least equal to that described by the clonogenic survival curves in commercial GBM cell lines illustrated by McCord et al, and certainly in excess of the CD133+ GBM CSCs used in the McCord study. This suggests that CSC radiation resistance documented in this thesis is relevant to current laboratory GBM models and relevant to the clinical problem of GBM radioresistance.

Similarly to Bao et al, the investigations in this thesis support the concept of increased activation of DDR in GBM CSCs (Bao et al., 2006a). Upregulation of phosphorylated components of the DDR in CSCs in response to radiation was demonstrated in chapter 4. Following irradiation CSCs displayed high levels of pATM s1981 and pChk2 thr68, along with pATR and pChk1 compared to tumour bulk. This study also presents evidence for upregulation of PARP-1 in CSC populations. Increased expression of DDR components does not appear to be limited to a particular pathway and the overall impression from the data in this study and also from published literature is of an almost global pattern of upregulation of DDR elements in CSCs. The underlying process for this phenomenon is unlikely to represent the convergence of multiple alterations in individual DDR pathways, and more likely represents the effect of a process which is fundamental to the CSC phenotypic state. Whether this is due to effects mediated by expression of the CSC marker L1CAM (Bao et al., 2008) or due to the effects of higher baseline reactive oxygen species in CSCs (Venere et al., 2014) is unclear. It is likely that other mechanisms are also responsible.

This thesis presents novel data regarding activation of the G2/M checkpoint in CSCs in response to radiation. Following exposure to 5Gy, CSCs in the E2 and G7 cell lines appeared to activate the G2/M checkpoint to a greater degree than corresponding tumour bulk cultures at 6 hours post radiation. This would be in keeping with the observed higher levels of pATR, pATM, pChk1 and pChk2 in CSC populations since these proteins are known to control the G2/M checkpoint.

Discussion

More efficient activation of the G2/M checkpoint allows attempts at DSB repair to be completed prior to entering mitosis, theoretically allowing CSCs to potentially avoid DSB induced cell death. These data also provide a rationale for therapeutic targeting of the G2/M cell cycle checkpoint in GBM CSCs.

A detailed examination of DSB repair incorporating cell cycle phase was undertaken in GBM CSC and tumour bulk populations using immunofluorescent gamma H2AX foci for DNA DSB quantification following irradiation. Previous studies have examined DNA DSB repair via the gamma H2AX foci assay, however have not undertaken a simultaneous assessment of cell cycle phase. As discussed above, previous studies have ignored the contribution of cell cycle phase to radiation induced DSB burden, which is a potentially important confounding factor when comparing cellular populations which differ in cell cycle phase occupancy. These investigations demonstrated a repair advantage of GBM CSCs relative to tumour bulk cells in G2 phase at 24 hours post radiation. Induction and initial fast phase of DSB resolution appeared similar between CSCs and tumour bulk cells. Quantification of unrepaired gamma H2AX foci at 24 hours has been shown to correlate with clonogenic survival, and these data are in keeping with the clonogenic survival studies performed on CSC and tumour bulk populations in chapter 3 (Banath et al., 2004). The observation that slow phase repair in G2 is enhanced in GBM CSCs is in keeping with an advantage in homologous recombination repair of complex or heterochromatic lesions (Jeggo et al., 2011). An advantage in slow phase DNA DSB repair also implicates ATM function in GBM CSC DSB repair, since ATM has been shown to have a vital role in lesions repaired via slow kinetics. These observations suggest the upregulation of pATM s1981 levels seen in irradiated GBM CSCs have a vital role in the radioresistant phenotype of this cellular subpopulation. Lim et al have previously suggested that HR is a key repair pathway in GBM CSCs, and described a reduced dependency on NHEJ for DSB repair in CSCs (Lim et al., 2012). In a more recent paper they described ablation of the HR pathway by ATM inhibition as having marked effects on GBM CSC survival following irradiation, whilst ablation of NHEJ via DNAPK inhibition did not. ATM inhibition of irradiated cultured GBM CSCs prior to intracranial orthotopic injection appeared to increase survival *in vivo*. They concluded that GBM CSCs are highly reliant upon HR as a mode of

Discussion

repair following radiation (Lim et al., 2014). Nevertheless it can be argued that ATM inhibition does not only affect HR repair. As discussed previously, ATM is involved in NHEJ repair of lesions (again in the slow phase of DNA DSB repair) and has a role in G2/M checkpoint activation. Furthermore it would be difficult to reconcile a relative deficiency in NHEJ with the efficient repair of DNA DSBs seen in G1 phase in GBM CSCs unless an alternative pathway such as MMEJ was being utilised in GBM CSCs. This study did not compare GBM CSCs to non CSC tumour bulk cells and instead used normal neural progenitor cells as a control.

It is unclear why GBM CSCs have upregulation of HR repair in comparison to tumour bulk cells. Investigators have suggested that increased utilisation of HR may reflect a lack of a functioning G1/S checkpoint in response to ionising radiation (Lim et al., 2014, Jeggo et al., 2011). Irradiated cells with a deficient G1/S checkpoint will progress into S phase with DNA damage. This will result in stalling and collapse of replication forks in S phase and subsequent generation of one ended DNA DSBs. This type of DSB has a requirement for HR repair (Jeggo et al., 2011), since NHEJ cannot perform this type of repair. This is an elegant explanation for upregulation of HR in cells with deficient p53 function or deficient G1/S checkpoint function, however it does not explain why GBM CSCs have an HR advantage in comparison to tumour bulk cells, since data from this thesis shows that both have a defective G1/S checkpoint, (despite the E2 and G7 cell lines being p53 wild type). A possible explanation might be that GBM CSCs are somehow more deficient in G1/S checkpoint than tumour bulk cells thus favouring HR, and interestingly mouse embryonic stem cells exhibit this particular feature (Aladjem et al., 1998). However studies of cell cycle distribution following irradiation of CSC and tumour bulk cells in this thesis would not support this hypothesis. Another explanation may be that upregulation of HR repair in GBM CSCs is simply a reflection of the increased proportion of CSCs in S and G2 phase cell cycles compared to tumour bulk cells, however this would not explain the upregulation in DDR signalling seen in GBM CSCs or the more efficient activation of the G2/M checkpoint. Alternately the upregulation of DDR components seen in GBM CSCs (such as pATM and pATR) may be actively promoting HR in G2 phase and facilitating slow phase DSB repair at heterochromatic regions and at collapse of replication forks. However the

Discussion

underlying reason of upregulation of pATM and pATR is not clear. The situation appears complex and further work is required to elucidate underlying mechanisms of HR upregulation in GBM CSCs.

8.3 The role of ATM in GBM CSC radioresistance

The upregulation of pATM in response to radiation in GBM CSCs, enhanced activation of the G2/M checkpoint and more efficient G2 slow phase repair implicates ATM function as being a fundamental determinant of GBM CSC radioresistance. This was explored in detail using the ATM kinase inhibitor KU-55933. ATM inhibition prior to irradiation effectively abrogated phosphorylation of ATM at serine 1981 and Chk2 at threonine 68. Furthermore ATM inhibition partially abrogated the activation of the G2/M checkpoint in GBM CSCs. In contrast complete abrogation of the G2/M checkpoint in the E2 tumour bulk cultures following radiation was observed. A study of gamma H2AX foci resolution following ATM inhibition in the E2 CSC and bulk cultures demonstrated that KU-55933 removed the slow phase repair advantage of GBM CSCs at 24 hours. KU-55933 also had a marked effect on phosphorylation of H2AX at early timepoints following irradiation, an effect related to a reduction in signalling at DSBs rather than a reduction in DSB generation.

The failure of ATM inhibition to completely abrogate the G2/M checkpoint in GBM CSCs implies that another pathway is involved in G2/M checkpoint activation and maintenance in these cells. The ATR-Chk1 pathway would be an obvious candidate. ATM has been implicated in early G2/M checkpoint initiation, whereas the ATR-Chk1 pathway is thought to be important in later continued maintenance of the checkpoint following radiation (Shibata et al., 2010). ATM is necessary for resection of DSBs requiring HR repair; in the process of resection long ssDNA stretches are created which then activate ATR/Chk1 resulting in a ‘switch’ from ATM mediated signalling to ATR mediated signalling at DSBs. Continued ATM signalling from unrepaired DSBs also contributes however. Therefore the mechanism of partial abrogation in GBM CSCs by ATM inhibition becomes apparent; ATM inhibition prevents DSB resection by ATM which in turn reduces activation of ATR. However, the upregulation of pATR which is present

Discussion

at baseline may partially compensate for this effect, resulting in an attenuated G2/M response to radiation in the E2 GBM CSCs under conditions of ATM inhibition.

In E2 bulk cells ATM inhibition appeared to completely abrogate the G2/M checkpoint. Again it could be hypothesised that the ATM to ATR switching process is inhibited by the lack of end resection due to kinase dead ATM. The comparative deficiency in pATR at baseline in the E2 bulk cells compared to CSCs might then lead to total G2/M checkpoint incompetence, since a compensatory upregulation of pATR does not exist in these cells. The situation is more difficult to explain in the G7 CSC and bulk cells, since the experimental variation is greater in G7 tumour bulk, however similar trends are seen.

Further mechanistic insights were gained by the analysis of gamma H2AX foci resolution following ATM inhibition and radiation in the E2 GBM CSC and tumour bulk cultures. In keeping with current literature, ATM inhibition provided a slow phase repair deficit in the G2 phase E2 CSCs at 24 hours. This deficit abrogated the previously documented repair advantage seen at this timepoint in E2 CSCs. Interestingly, ATM inhibition of the E2 tumour bulk cultures produced a trend towards an increase in unresolved gamma H2AX foci at 24 hours, however the effect was non-significant. This may suggest that the E2 tumour bulk cells have a pre-existing deficit in slow phase G2 repair which is either ATM independent, or only partially sensitive to ATM inhibition.

Both CSC and bulk cultures are potently radiosensitised by ATM inhibition as demonstrated by clonogenic assay. SER_{0.37} was in excess of 2.5 in CSCs. Furthermore ATM inhibition had a relatively greater sensitising effect on the CSC cultures of the E2 and R10 cell lines compared to tumour bulk cultures, since the survival curves of the ATM inhibitor treated CSC cultures appeared superimposed on that of the ATM inhibitor treated tumour bulk cultures in these cell lines. This effect was statistically significant in the R10 cell line, with SER_{0.37} for ATM inhibition being significantly greater in the R10 CSCs than the tumour bulk cells.

Discussion

Based on the observations of G2/M checkpoint response and gamma H2AX foci analysis following ATM inhibition and radiation, the E2 tumour bulk cultures are reliant upon ATM kinase function for G2/M checkpoint activation, however ATM inhibition does not affect DNA DSB repair efficiency significantly in tumour bulk populations. In contrast ATM has important roles in G2/M checkpoint activation and DNA DSB repair in E2 CSCs.

These data represent the first characterisation of ATM inhibition in GBM CSCs by clonogenic assay. This investigation is also the first to compare the effects of ATM inhibition in paired tumour bulk and CSC primary cell lines. Other investigations have detailed the response of commercially available cell lines to ATM inhibition (Golding et al., 2012, Golding et al., 2009, Biddlestone-Thorpe et al., 2013), or have looked at cell viability in response to radiation and ATM inhibition (Vecchio et al., 2014). Whilst the radiosensitising effects of ATM inhibition have been extensively explored in immortalised fibroblasts and commercially available immortalised cell lines, these data lend further novel mechanistic insights into the role of ATM in the GBM CSC subpopulation.

8.4 The role of Poly (ADP ribose) polymerase (PARP) in GBM CSC radioresistance

PARP-1 is upregulated in GBM tumour tissue and PARP-1 immunostaining can be utilised as a GBM tumour marker (Galia et al., 2012b). The investigations in this thesis demonstrated that whilst being generally upregulated in GBM tumour cells in comparison to normal brain tissue, PARP-1 and PAR levels are also upregulated specifically in the GBM CSC subpopulation compared to tumour bulk populations. Given these observations it was hypothesised that PARP-1 had an important role in GBM CSC radioresistance.

Venere et al have examined the role of PARP-1 in GBM CSC DNA damage response (Venere et al., 2014). They found that exposure to olaparib at a concentration of 10 μ M over 24 hours greatly reduced the viability of CD133+ cells, but did not affect the viability of CD133- cells. PARP inhibition reduced neurosphere production in CD133+ cells and had significant effects on colony

Discussion

formation by CD133+ cells but not by CD133- cells. It should be noted however that colony formation by CD133+ cells in this study was performed by neurosphere culture, with subsequent induction of monolayer colony formation by addition of FCS. CD133- cells on the other hand were grown as conventional monolayer colonies in FCS containing media. In combination with 3Gy, olaparib prevented recovery of viability in GBM CSC cultures in the 10 days following irradiation. Furthermore olaparib increased gamma H2AX foci formation in irradiated CSCs relative to DMSO treated controls and was associated with increased apoptosis as measured by activated caspase 3/7 activity. Treatment of subcutaneous xenografts with olaparib and radiation reduced tumour volume and inhibited secondary neurosphere formation. The authors also demonstrated upregulated basal ROS levels in CD133+ cells and suggested that this may be an underlying reason for the increased levels of PARP in CSCs. They concluded that targeting of upregulated PARP in GBM CSCs had therapeutic potential.

In comparison to Venere's investigations the studies documented in this thesis found that a much lower concentration of olaparib inhibited PARylation in GBM CSCs. 1 μ M olaparib completely inhibited PARylation in GBM CSCs and this concentration was subsequently used in radiosensitisation studies. No effect of olaparib on neurosphere formation was observed in the absence of radiation. Likewise this concentration of PARP inhibition had no effect on colony formation by CSCs or tumour bulk cells in clonogenic assays. Nevertheless PARP inhibition with 1 μ M olaparib effectively radiosensitised GBM CSCs and tumour bulk cells, with SER_{0.37} in the range 1.4 to 1.9, which is in keeping with other studies of PARP inhibition induced radiosensitisation in commercially available *in vitro* cell lines. Although SER_{0.37} values were not significantly different between CSC and tumour bulk cells following PARP inhibition, a preferential radiosensitising effect of olaparib on CSCs was suggested by examination of clonogenic survival curves. This radiosensitising effect of olaparib on CSCs was confirmed by neurosphere assay following exposure of CSCs to olaparib and 2Gy radiation. In addition a study of gamma H2AX foci resolution in the presence of olaparib was carried out. This showed that exposure to olaparib prior to irradiation caused a reduction in the resolution of gamma H2AX foci at 24 hours in GBM CSCs in G2 phase of the cell cycle. This is in keeping with published literature concerning the mechanism

Discussion

of radiosensitisation of PARP inhibition, which involves the delay of radiation induced SSBs and generation of DSBs during subsequent DNA replication in S phase.

The observation that PARP inhibition had no effect on GBM CSCs in the absence of radiation contradicts the findings of Venere et al, however is likely due to the lower concentrations of olaparib used in this project. Nevertheless, this study demonstrates that a lower dose of olaparib effectively ablates PARylation of proteins in CSCs as demonstrated by Western blot, suggesting that higher concentrations of olaparib may induce other cytotoxic effects not necessarily related to inhibition of PARylation. Jelinic et al investigated the effects of two different PARP inhibitors; olaparib and veliparib (Jelinic and Levine, 2014). They found that olaparib treated cells demonstrated a dramatic decrease in DNA damage repair whereas veliparib did not, irrespective of inhibitory potency. This was a result of cell cycle effects induced by olaparib. Olaparib treatment appeared to induce a G2 arrest in a p53 dependent manner in the cell lines tested in Jelinic's study. The effects of PARP inhibition in CSCs may therefore be dose and inhibitor molecule dependent.

8.5 ATR inhibition and GBM CSC radioresistance

The G2/M checkpoint in GBM CSCs was only partially abrogated by ATM inhibition leading to the hypothesis that ATR may have a significant role in checkpoint control in GBM CSCs. Western blot data also suggested elevated levels of pATR s428 in CSC cultures relative to tumour bulk. Therefore the effects of ATR inhibition in GBM CSCs were investigated. This represents an entirely novel area of study, with no investigations of the effects of ATR inhibition on radiosensitivity of GBM CSCs being available in the current literature.

ATR inhibition with VE-821 provided very effective abrogation of the G2/M checkpoint following irradiation with 5Gy in both E2 CSCs and bulk cultures. Therefore ATR is an important controller of the G2/M checkpoint in the E2 cell line. Interestingly at the 6 hour time point following radiation, there was a large increase in proportion of mitotic cells relative to unirradiated DMSO controls.

Discussion

This may reflect abrogation of the intra S checkpoint and G2/M checkpoint, resulting in a shift of cells into G2 and subsequently into mitosis. The effect in G7 CSCs is different, with a partial inhibition of G2/M checkpoint activation following radiation. However, total abrogation of G2/M checkpoint in the G7 tumour bulk cells was observed.

Radiosensitisation was achieved in both CSC and tumour bulk cultures with ATR inhibition, however the effects were modest, particularly in CSC cultures. SER_{0.37} was approximately 2 in both E2 and G7 CSC cultures. Tumour bulk cultures appeared to be more effectively radiosensitised by ATR inhibition in comparison to CSCs, with SER_{0.37} being in the region of 2.3-2.5 however differences in SER_{0.37} between bulk and CSC were not statistically significant. The radiosensitising effect of ATR inhibition was confirmed by neurosphere assay, with ATR inhibition in combination with 2Gy being associated with a significant decrease in neurosphere formation in both G7 and E2 cell lines in comparison to irradiated controls.

ATR inhibition also produced a significant reduction in neurosphere survival in the E2 and G7 cell lines in the absence of radiation, suggesting that ATR has an important role in CSC renewal and proliferation.

ATR inhibition has been investigated as a potential radiosensitiser of pancreatic carcinoma. Prevo et al investigated the potential of ATR inhibition using VE-821 to sensitise pancreatic carcinoma to radiation and gemcitabine *in vitro*. VE-821 was found to inhibit activation of the G2/M checkpoint and increase DNA damage, via inhibition of homologous recombination, as evidenced by inhibition of Rad51 foci formation. Whether ATR inhibition has a direct effect on the HR pathway is debateable and it seems more likely in this case that ATR inhibition was contributing to DNA damage via indirect effects on HR repair. The inability of ATR inhibited cells to activate the G2/M checkpoint may lead to less efficient HR repair of DNA lesions. ATR inhibition was associated with reduced cancer cell radiosurvival (Prevo et al., 2012). Fokas et al investigated ATR inhibition as a means to radiosensitise pancreatic tumours *in vivo*. This study utilised the compound VE-822, which is a more potent inhibitor of ATR in comparison to VE-

Discussion

821. VE-822 delayed growth of irradiated murine pancreatic xenografts in comparison to irradiated controls. Furthermore ATR inhibition was found not to increase intestinal toxicity in irradiated mice, suggesting ATR inhibition shows a degree of tumour specificity in its radiosensitisation effect (Fokas et al., 2012).

8.6 Combined checkpoint and DSB repair inhibition for optimal radiosensitisation of GBM CSCs

PARP inhibition and ATR inhibition as single agents were both modest radiosensitisers of CSC and bulk cultures in studies conducted in this thesis. PARP inhibition is known to have its major radiosensitising effects via the inhibition of SSB DNA repair and subsequent generation of DNA DSBs, whilst ATR inhibition, although contributing to repair following collapse of replication forks, can be characterised as a significant controller of the G2/M checkpoint. In contrast ATM inhibition provided highly potent radiosensitisation of GBM CSCs through simultaneous effects on DNA DSB repair and G2/M checkpoint abrogation. It was hypothesised that optimal radiosensitisation of GBM CSCs requires inhibition of both these elements of DDR.

Therefore investigations of dual inhibition of G2/M checkpoint control and DSB repair via combined inhibition of ATR and PARP respectively were carried out. Dual ATR and PARP inhibition provided potent radiosensitisation of both CSC and bulk cultures by clonogenic survival assay in all cell lines. Furthermore, E2 and R10 CSCs were radiosensitised by this combination to a significantly greater degree than E2 and R10 tumour bulk cells, which again suggests that the mechanism of CSC radioresistance is due to both cell cycle activation and DNA repair. CSC radioresistance was completely abrogated by blockage of G2/M checkpoint activation and inhibition of DNA repair using olaparib and VE-821 in combination. In contrast in the G7 cell line the radiosurvival advantage of CSCs compared to tumour bulk cells was not altered by this combination suggesting that alternative undefined mechanisms determine CSC radioresistance in this cell line. It can be concluded that in certain GBM tumours, both checkpoint repair and DSB repair are vital to radiation resistance in CSC subpopulations. It is not clear from the investigations carried out whether the effects of ATR and

Discussion

PARP inhibition in combination with radiotherapy represent synergistic or additive effects. Given the molecular DDR mechanisms known to involve both ATR and PARP it would be likely that the effect is synergistic with radiation, however isobologram analysis would be necessary to prove this conclusively. These data suggest therapeutic strategies aimed at radiosensitising GBM CSCs via DDR inhibition require to target both cellular checkpoint control and DSB repair to achieve optimal radiosensitisation.

The study of dual ATR and PARP inhibition as a radiosensitising strategy is entirely novel. Other authors have examined the combination of Chk1 inhibition and PARP inhibition, and found that this combination of DDR inhibition selectively radiosensitised p53 mutant cells in pancreatic carcinoma (Vance et al., 2011). A more recent study by Teng et al examined the effects of ATR and ATM inhibition on the platinum and radiation sensitivity of cervical, ovarian and endometrial carcinoma cell lines (Teng et al., 2015). They demonstrated a profound effect of ATM inhibition on the radiosensitivity of all cell lines tested, however ATM inhibition did not appear to affect platinum sensitivity. The addition of ATR inhibition to ATM inhibition produced even greater levels of radiosensitisation in the cell lines examined.

8.7 Cytotoxic effects of ATR and PARP inhibition in the absence of radiation

A potent cytotoxic effect of ATR and PARP inhibition in combination was observed in both CSC and tumour bulk cultures, even in the absence of radiation. This was demonstrated by neurosphere production assays in the investigations detailed in chapter 7. The effect on neurosphere production of inhibition of ATR and PARP in combination was very marked and was greater than the effect of irradiation with 2Gy alone. It is likely that this was a synergistic effect, since PARP inhibition in the absence of ATR inhibition had no effect, and the effect of ATR and PARP inhibition on neurosphere production was significantly greater than the effect of ATR inhibition alone.

Discussion

Peasland et al demonstrated a synthetic lethal effect of combined PARP and ATR inhibition in commercially available ovarian carcinoma cell lines (Peasland et al., 2011). The authors showed an increase in nuclear gamma H2AX foci and a reduction in Rad51 foci following exposure to both drugs and hypothesised that ATR inhibition produced inhibition of both HR and G2/M arrest, leading to increased sensitivity to the effects of PARP inhibition. Combined ATR and PARP inhibition has not been explored further in recent years, perhaps due to a lack of effective ATR inhibitor compounds. The data presented in this thesis are novel, and the combination of ATR and PARP inhibition would seem particularly appealing in a clinical setting, given the effects seen on CSC radiosensitivity and also in the absence of radiation.

8.8 Clinical utility of DDR inhibition as a GBM radiosensitiser strategy

This project has quantified GBM CSC radioresistance and demonstrated the importance of DDR as a mechanism of radioresistance in this cellular subpopulation. Potent radiosensitisation of CSCs has been achieved by inhibition of key elements of the DDR to ionising radiation, and the sterilisation of this tumour cell population may bring important benefits in terms of local control, palliation of symptoms and possible improved survival for GBM patients. DDR inhibition has obvious therapeutic application, however utilisation of DDR inhibition as a clinical GBM CSC targeted therapy creates additional complexity and several important issues must be explored.

Tumour specificity is a vital property of any clinical radiosensitisation strategy. Only radiosensitisers which increase the radiation sensitivity of tumour cells to a greater degree than that of surrounding normal cells are clinically useful; otherwise the therapeutic ratio of radiation treatment does not change and any clinical benefit from increased tumour cell kill will be outweighed by increased normal tissue toxicity. Evidence suggests that targeting of the DDR may be potentially tumour specific in GBM and other tumour sites.

Bartkova et al described the DDR as a barrier to carcinogenesis, therefore implicating altered DDR as a universal feature of malignant cells (Bartkova et

Discussion

al., 2005). In this seminal study, activation of an ATM/ATR regulated DDR was observed early in tumourigenesis, prior to the development of genomic instability and malignant conversion. Normal proliferating cells did not show evidence of this enhanced DDR. One potential source of enhanced DDR in premalignant cells identified by the authors was that of S phase promoting oncogenes increasing replication stress. Tumourigenic abnormalities that deregulated DNA replication induced DNA damage and checkpoint activation. The authors proposed that activation of the ATM/ATR pathways serve to limit malignant progression, until the DDR is circumvented by events such as p53 mutation that allow the development of further mutations, genetic instability and the complete malignant phenotype. Gorgoulis et al also proposed that cancer development was associated with replication stress and an enhanced DNA damage response prior to the development of p53 mutation and the onset of genomic instability (Gorgoulis et al., 2005).

Many cancer types are known to be deficient in DNA damage responses in comparison to normal tissues. This concept can cause confusion in relation to studies of DDR in CSCs, since CSCs have been shown to have upregulated DDR in comparison to other tumour cells. It is important to remember however that although CSCs may have upregulated DDR relative to non-CSC tumour cells, they are still very likely to harbour abnormalities in DDR function and could therefore be DDR deficient relative to normal cells. Recent studies have used next generation sequencing technologies to explore the different mutations, deletions and copy number alterations occurring in different tumour sites. These have shown that inactivating mutations typically constitute a cancer-specific signature of affected DDR pathways. For example HR repair deficiency appears to be enriched in breast and ovarian cancer, whilst colorectal cancer exhibits alterations in mismatch repair (MMR) and HR (Cancer Genome Atlas, 2012b, Cancer Genome Atlas, 2012a, Cancer Genome Atlas Research, 2011). The concept of altered DDR being fundamental to the process of carcinogenesis provides an explanation for the efficacy of radiotherapy as an oncological therapy. Tumour cells, due to the alterations in DDR necessary to procure the malignant state, may be less able to repair DNA damage than normal tissue, producing a therapeutic ratio between malignant and normal tissue which can be

Discussion

exploited by radiotherapy and other DNA damaging therapies. The result of alterations in the DDR landscape of cancer cells may produce reliance or addiction of cancer cells to particular pathways in order to complete DNA repair as a result of deficiencies in altered pathways or mutations in key DDR genes. These deficiencies in DDR could be further exploited by DDR kinase inhibition in order to enhance radiosensitivity of DDR deficient tumour cells. In view of the fact that normal surrounding tissue would possess a full complement of DDR functions, allowing them to maintain an effective DDR despite radiation and inhibition of a particular element or pathway of the DDR, it is plausible that tumour radiosensitisation could be achieved with little or no increase in normal tissue toxicity.

Evidence to support this hypothesis comes from several published studies. Loser et al demonstrated the increased susceptibility of cells deficient in one or more aspects of DNA DSB repair to the radiosensitising effects of PARP inhibition (Loser et al., 2010). Radiosensitisation of ligase IV deficient fibroblasts by PARP inhibition was explained by inhibition of MMEJ, whilst defective repair of replication associated DNA damage was seen in ATM and Artemis null fibroblasts. The authors concluded that PARP inhibitors would preferentially radiosensitise tumour cells with defective DNA repair in comparison to normal tissues. Biddlesthorpe et al investigated ATM inhibition in GBM and demonstrated increased radiosensitisation of p53 deficient cells by ATM kinase inhibition in comparison to p53 wild type cells. Vance et al showed preferential radiosensitisation of pancreatic cells with p53 mutations to dual Chk1 and PARP inhibition. In general targeting of the ATR/Chk1 pathway results in a tumour specific radiosensitisation effect due to abrogation of the G2/M checkpoint in G1/S checkpoint deficient tumour cells. Normal cells may be more able to tolerate DNA damage in this scenario due to an intact G1/S checkpoint. High levels of replication stress in tumour cells may also facilitate tumour specific radiosensitisation. Fokas et al in their study of radiosensitisation via ATR inhibition in pancreatic cancer xenografts demonstrated no radiosensitising effect of ATR inhibition on normal cells, and in particular examined the effects of ATR inhibition and radiotherapy on the small intestine of mice. The small intestine is a common dose limiting organ in pancreatic cancer radiotherapy in

Discussion

humans. They hypothesised that the tumour specific effect of ATR inhibition may be due to loss of ATM/p53 signalling and exacerbation of replication stress in tumour cells via ATR depletion (Fokas et al., 2012).

The application of DDR inhibition strategies for radiosensitisation will require biomarkers to be developed in order to develop personalised strategies to ensure optimal tumour radiosensitisation. As described above, next generation sequencing technology has allowed the comprehensive sequencing of tumour genomes, facilitating a detailed analysis of mutations, copy number variants and deletions in cells of a particular tumour. It could be envisaged that this information be used to select inhibition of a particular DDR pathway using a specific kinase inhibitor which could facilitate optimal radiosensitisation. For example, a tumour which was deficient in the HR pathway may benefit from PARP inhibition, or cancers with high levels of replication stress may benefit from ATR inhibition. Tumours lacking p53 mediated G1/S checkpoint may usefully be radiosensitised by Chk1 or ATM inhibition. In this way radiosensitiser strategies could in future be tailored to a patient's tumour allowing manipulation of the therapeutic ratio of radiation treatment to its maximum extent.

Other factors may also contribute to the potential tumour specificity of DDR kinase radiosensitisation approaches. Current dogma would suggest that inhibition of central DDR kinases such as ATM and ATR will result in potent and universal radiosensitisation of all tissues, both cancerous and normal within the human body, implying that these strategies would lack tumour specificity. However recent work suggests that DDR pathway utilisation is organ specific, and anatomical location of tumours may allow further tumour specific effects of DDR kinase radiosensitisation. For example, in the brain, astrocytic cells have been shown to have downregulated ATM transcription, yet retain DNA repair proficiency, due to the retention of expression of genes involved in NHEJ (Gosink et al., 1999, Schneider et al., 2012). The studies by Gosink and Schneider suggest that ATM inhibition may allow relative tumour specific radiosensitisation depending upon the anatomical location of tumour in the body. In view of this,

Discussion

GBM may represent an ideal tumour for ATM inhibitor radiosensitisation strategies.

A recent report by Moding et al has highlighted differential effects of ATM inhibition on the radiosensitivity of tumour and normal endothelial cells (Moding et al., 2014). Microvasculature has long been implicated in the long term toxicities associated with radiotherapy, and the effects of any radiosensitising strategy on endothelial tissue must be carefully considered. Moding et al examined the effects on radiosensitivity of ATM deletion in proliferating tumour endothelium in comparison to quiescent cardiac endothelium in a murine sarcoma model. ATM deletion in tumour endothelium led to a significant growth delay in murine tumours following a 20Gy irradiation treatment, however ATM deletion in quiescent cardiac endothelium did not sensitise mice to myocardial necrosis. The authors hypothesised that the radiosensitising effect of ATM deletion is dependent upon the proliferative status of the cell, and confirmed this by demonstrating a reversal of the radiosensitising effect on tumour endothelium by blocking cell cycle progression. With the knowledge that many tumour cells have defective cell cycle checkpoints and enhanced proliferation compared to normal tissue, this may imply that ATM inhibition could exhibit considerable tumour specificity as a radiosensitisation strategy. Furthermore this differential effect of ATM inhibition on tumour vasculature compared to normal tissue vasculature will contribute to tumour specificity. Proliferative status and cell cycle checkpoint competency is not necessarily a comprehensive explanation of effects of ATM inhibition on radiosensitivity however, since fibroblasts in a state of confluence arrest were radiosensitised by ATM inhibition in one study (Kuhne et al., 2004). In keeping with the idea that ATM inhibition may be clinically deliverable, Batey et al demonstrated chemopotentiation via ATM inhibition in murine tumour xenograft models without significant normal tissue toxicity (Batey et al., 2013). Nevertheless, given the catastrophic effects of radiotherapy in AT patients with lymphoma in the 1960's, clinical development of ATM inhibition as a radiosensitising strategy should be cautious (Gotoff et al., 1967). Furthermore development of DDR inhibitor strategies would benefit from adequate models of acute and long term radiation toxicity, which currently are not in existence. Mouse tumour models are inadequate for

Discussion

the measurement of long term toxicity from radiation and large animal radiation studies may provide more adequate data concerning toxicity of DDR inhibition and radiation.

Considerable evidence also exists for the potential tumour specificity of PARP inhibition as a radiosensitiser. In general, PARP inhibition only produces radiosensitivity in replicating cells, since PARP inhibition delays SSB repair resulting in increased DSB generation only if the cell enters S phase. Therefore PARP inhibition could be expected to radiosensitise only tissues which have a significant replicating fraction of cells. Tumours with a high replicative fraction, which includes diverse tumour sites such as GBM, squamous cancers, small cell cancers and lymphomas could therefore be predicted to experience radiosensitisation following PARP inhibition, whereas less mitotically active normal tissues may experience less or no radiosensitisation. Again GBM may represent a particularly favourable site for radiosensitisation using PARP inhibitors, given that many of the normal cellular populations of brain, such as neurons, are terminally differentiated and therefore could be expected to be essentially non-dividing. This thesis also demonstrated the upregulation of expression of PARP-1 in comparison to normal cells in the brain, again suggesting that PARP-1 in particular may be a relatively tumour specific target in GBM. Furthermore the vasodilatory effects of PARP inhibition on tumour vasculature may further enhance efficacy and specificity of this approach by counteracting radioresistance due to tumour hypoxia.

The recent developments in radiotherapy delivery also offer an opportunity to increase therapeutic gains and minimise additional toxicities of DDR inhibitor radiosensitisation strategies. The adoption of intensity modulated radiotherapy (IMRT) technologies have allowed greater conformity in radiation treatment planning, (i.e. how closely the volume of tissue irradiated to high dose matches the targeted high dose volume) and sparing of organs which can be damaged irreparably by ionising radiation such as spinal cord. In the past, radiation treatments were limited by the ability to shape the irradiated volume to closely match the tumour whilst at the same time achieving a dose high enough within the tumour to be clinically effective. Often large volumes of tissue were

Discussion

included in treatment fields, which increased toxicity of the treatment and excluded the possibility of employing radiosensitisation strategies. A case in point is the irradiation of pancreatic tumours, which once proved difficult due to toxicities associated with irradiation of liver, small bowel and kidney; any further increase in normal tissue toxicity by DDR inhibition would have been unacceptable. However IMRT provides highly conformal planning which allows sparing of liver and small bowel and better tolerability which then facilitates therapeutic manoeuvres which may marginally increase toxicity. IMRT and associated dose delivery technologies will also allow sparing of critical structures such as spinal cord. This is important in radiosensitisation strategies since often these structures are irradiated to the limit of their radiation tolerance in conventional radical (curative) radiotherapy treatments. Risking additional radiosensitisation of these critical structures may be unacceptable. However limiting the dose to organs at risk of radiation damage by using IMRT may allow consideration of the use of radiosensitiser agents. Image guided radiotherapy (IGRT) is another recent development which aims to provide better anatomical localisation of radiotherapy beams via tumour imaging during fractionated radiotherapy. Again this can minimise dose to surrounding normal tissues by reducing the margins added to radiotherapy volumes to account for tumour movement and patient setup issues.

Review of current literature would therefore support the assumption that a CSC targeted radiosensitiser strategy mediated by DDR inhibition is, in theory, clinically achievable, particularly in the setting of GBM. Phase I clinical trials of PARP inhibition and radiotherapy are already ongoing in several tumour sites including brain, head and neck cancer, lung cancer and oesophageal cancer and toxicity data is awaited.

8.9 Final Conclusions

This thesis has successfully met its aims and endpoints. The putative radioresistance of GBM CSCs in comparison to tumour bulk cells has been investigated, confirmed and quantified. The upregulated DDR seen by other authors in GBM CSCs has been confirmed, and novel data representing the

Discussion

effects of upregulated DDR on the enhanced activation of the G2/M checkpoint of CSCs in response to radiation has been presented. Investigations of DNA repair mechanisms in GBM CSCs in this thesis have demonstrated enhanced slow phase repair of DNA DSBs in GBM CSCs in G2 cell cycle phase, implicating HR repair in the radioresistance of GBM CSCs.

Studies of the radiosensitising effects of DDR inhibition in GBM CSCs have validated DDR as a suitable target for future GBM CSC directed therapies. Inhibition of ATM, ATR, PARP and dual ATR and PARP inhibition all successfully radiosensitised GBM CSCs at clinically relevant doses of radiation. Further mechanistic insight into GBM CSC radioresistance was achieved following observation of the radiosensitivity of GBM CSCs and tumour bulk cells after exposure to DDR inhibition. Only inhibition of ATM and the combination of ATR and PARP inhibition provided significantly increased radiosensitivity of GBM CSCs relative to tumour bulk cells. This suggests that both cell cycle control and DNA DSB repair are important in mediating GBM CSC radioresistance, since ATM inhibition and the combination of ATR and PARP inhibition affect both these facets of DDR.

Further work is required to validate the effects of DDR inhibition in *in vivo* models of GBM CSCs, which was not carried out due to time constraints. However these investigations are now underway, and will provide data on efficacy and normal tissue toxicity of DDR inhibition as a radiosensitisation strategy.

These data demonstrate that GBM CSCs are highly radioresistant entities which are likely to contribute to the clinical recurrence of GBM tumours following multimodality treatment and influence patient survival from this disease. This thesis would argue that DDR inhibition is a viable potential clinical strategy for targeting radiotherapy resistant GBM CSCs in order to improve local control, palliate symptoms and improve survival in patients with GBM.

Appendix 1

Western blotting

Novex NuPage 4-12% Bis-Tris gels with NuPage MOPS SDS running buffer (NP0001)

Novex NuPage 3-8% Tris-Acetate gels with NuPage Tris/Ace running buffer (LA0041)

NuPage Transfer buffer NP0006-1 (200ml transfer buffer + 300ml methanol + 1500ml distilled water)

TBS-tween: 50mM TRIS (pH7.5) + 150ml NaCl + 0.05% Tween 20

TAE buffer: 242g Tris Base + 57.1 glacial acetic acid + 100ml 0.5M EDTA (final volume made up to 1000ml with distilled water)

TA buffer for neutral comet: 60.57g Tris Base + 204.12g sodium acetate (final volume made up to 500ml with distilled water and pH altered with glacial acetic acid to pH9.0)

DNA precipitation solution for neutral comet: Stock solution: 5.78g of ammonium acetate was solubilised to a final volume of 10ml, then 6.7ml of stock solution was combined with 43.3ml of ethanol to make final solution

Citrate buffer for immunohistochemistry: 1.92g anhydrous citric acid dissolved in 1000ml distilled water and pH adjusted to pH6 with NaOH 1M.

Appendix 2

	Sequence (5'->3')	Template strand	Length	Tm	GC%
E4 PR1					
Forward primer	cttcagACTCCTGAAACAAAC	Plus	23	57.22	39
Reverse primer	CAGCCTCTGGCATTCTGG	Minus	18	60.51	61
Product length	250				
E4 PR2					
Forward primer	TGGATGATTGATGCTGTCC	Plus	20	59.46	45
Reverse primer	ggcattgaagtctcatgaaag	Minus	21	59.69	48
Product length	300				
E5 PR1					
Forward primer	actttcaactctgtctcccttcc	Plus	20	57.71	43
Reverse primer	agccctgtcgctctccag	Minus	20	60.56	63
Product length	250				
E6					
Forward primer	gagagacgcacaggctgg	Plus	19	60.41	63
Reverse primer	cactgacaaccacccttaacc	Minus	21	59.36	52
Product length	231				
E7					
Forward primer	cctcatctgggcctgtgt	Plus	19	61.09	58
Reverse primer	tgatgagaggtggatggtag	Minus	21	59.93	52
Product length	260				
E8					
Forward primer	ggcacaggttaggacctgatt	Plus	21	59.31	52
Reverse primer	ctccctccaccgcttctgt	Minus	19	60.39	58
Product length	229				
E9					
Forward primer	acaagaagcggtggaggag	Plus	19	60.39	58
Reverse primer	ccccaaattgcaggtaaaaca	Minus	20	60.72	45
Product length	247				
E10					
Forward primer	ttgaaccatctttaactcaggt	Plus	23	57.01	35
Reverse primer	ggaatcctatggcttccaa	Minus	20	58.97	45
Product length	240				

References

- ALADJEM, M. I., SPIKE, B. T., RODEWALD, L. W., HOPE, T. J., KLEMM, M., JAENISCH, R. & WAHL, G. M. 1998. ES cells do not activate p53-dependent stress responses and undergo p53-independent apoptosis in response to DNA damage. *Curr Biol*, 8, 145-55.
- ALBERT, J. M., CAO, C., KIM, K. W., WILLEY, C. D., GENG, L., XIAO, D., WANG, H., SANDLER, A., JOHNSON, D. H., COLEVAS, A. D., LOW, J., ROTHENBERG, M. L. & LU, B. 2007. Inhibition of poly(ADP-ribose) polymerase enhances cell death and improves tumor growth delay in irradiated lung cancer models. *Clin Cancer Res*, 13, 3033-42.
- ALI, M., KAMJOO, M., THOMAS, H. D., KYLE, S., PAVLOVSKA, I., BABUR, M., TELFER, B. A., CURTIN, N. J. & WILLIAMS, K. J. 2011a. The clinically active PARP inhibitor AG014699 ameliorates cardiotoxicity but does not enhance the efficacy of doxorubicin, despite improving tumor perfusion and radiation response in mice. *Molecular cancer therapeutics*, 10, 2320-9.
- ALI, M., KAMJOO, M., THOMAS, H. D., KYLE, S., PAVLOVSKA, I., BABUR, M., TELFER, B. A., CURTIN, N. J. & WILLIAMS, K. J. 2011b. The clinically active PARP inhibitor AG014699 ameliorates cardiotoxicity but does not enhance the efficacy of doxorubicin, despite improving tumor perfusion and radiation response in mice. *Mol Cancer Ther*, 10, 2320-9.
- ALVAREZ-QUILON, A., SERRANO-BENITEZ, A., LIEBERMAN, J. A., QUINTERO, C., SANCHEZ-GUTIERREZ, D., ESCUDERO, L. M. & CORTES-LEDESMA, F. 2014. ATM specifically mediates repair of double-strand breaks with blocked DNA ends. *Nat Commun*, 5, 3347.
- AME, J. C., HAKME, A., QUENET, D., FOUQUEREL, E., DANTZER, F. & SCHREIBER, V. 2009. Detection of the nuclear poly(ADP-ribose)-metabolizing enzymes and activities in response to DNA damage. *Methods in molecular biology*, 464, 267-83.
- ANDERSON, K., LUTZ, C., VAN DELFT, F. W., BATEMAN, C. M., GUO, Y., COLMAN, S. M., KEMPSKI, H., MOORMAN, A. V., TITLEY, I., SWANSBURY, J., KEARNEY, L., ENVER, T. & GREAVES, M. 2011. Genetic variegation of clonal architecture and propagating cells in leukaemia. *Nature*, 469, 356-61.
- BAKKENIST, C. J. & KASTAN, M. B. 2003. DNA damage activates ATM through intermolecular autophosphorylation and dimer dissociation. *Nature*, 421, 499-506.
- BANATH, J. P., MACPHAIL, S. H. & OLIVE, P. L. 2004. Radiation sensitivity, H2AX phosphorylation, and kinetics of repair of DNA strand breaks in irradiated cervical cancer cell lines. *Cancer Res*, 64, 7144-9.
- BAO, S., WU, Q., LI, Z., SATHORN-SUMETEE, S., WANG, H., MCLENDON, R. E., HJELMELAND, A. B. & RICH, J. N. 2008. Targeting cancer stem cells through L1CAM suppresses glioma growth. *Cancer Res*, 68, 6043-8.

References

- BAO, S., WU, Q., MCLENDON, R. E., HAO, Y., SHI, Q., HJELMELAND, A. B., DEWHIRST, M. W., BIGNER, D. D. & RICH, J. N. 2006a. Glioma stem cells promote radioresistance by preferential activation of the DNA damage response. *Nature*, 444, 756-60.
- BAO, S., WU, Q., SATHORNSUMETEE, S., HAO, Y., LI, Z., HJELMELAND, A. B., SHI, Q., MCLENDON, R. E., BIGNER, D. D. & RICH, J. N. 2006b. Stem cell-like glioma cells promote tumor angiogenesis through vascular endothelial growth factor. *Cancer Res*, 66, 7843-8.
- BARKER, N., RIDGWAY, R. A., VAN ES, J. H., VAN DE WETERING, M., BEGTHEL, H., VAN DEN BORN, M., DANENBERG, E., CLARKE, A. R., SANSOM, O. J. & CLEVERS, H. 2009. Crypt stem cells as the cells-of-origin of intestinal cancer. *Nature*, 457, 608-11.
- BARTKOVA, J., HOREJSI, Z., KOED, K., KRAMER, A., TORT, F., ZIEGER, K., GULDBERG, P., SEHESTED, M., NESLAND, J. M., LUKAS, C., ORNTOFT, T., LUKAS, J. & BARTEK, J. 2005. DNA damage response as a candidate anti-cancer barrier in early human tumorigenesis. *Nature*, 434, 864-70.
- BASSING, C. H., CHUA, K. F., SEKIGUCHI, J., SUH, H., WHITLOW, S. R., FLEMING, J. C., MONROE, B. C., CICCONE, D. N., YAN, C., VLASAKOVA, K., LIVINGSTON, D. M., FERGUSON, D. O., SCULLY, R. & ALT, F. W. 2002. Increased ionizing radiation sensitivity and genomic instability in the absence of histone H2AX. *Proc Natl Acad Sci U S A*, 99, 8173-8.
- BATEY, M. A., ZHAO, Y., KYLE, S., RICHARDSON, C., SLADE, A., MARTIN, N. M., LAU, A., NEWELL, D. R. & CURTIN, N. J. 2013. Preclinical evaluation of a novel ATM inhibitor, KU59403, in vitro and in vivo in p53 functional and dysfunctional models of human cancer. *Mol Cancer Ther*, 12, 959-67.
- BD CLARKSON, B. R. 1974. Control of Proliferation in Animal Cells. *Control of Proliferation in Animal Cells*. New York: Cold Harbor Spring Laboratory.
- BEIER, D., HAU, P., PROESCHOLDT, M., LOHMEIER, A., WISCHHUSEN, J., OEFNER, P. J., AIGNER, L., BRAWANSKI, A., BOGDAHN, U. & BEIER, C. P. 2007. CD133(+) and CD133(-) glioblastoma-derived cancer stem cells show differential growth characteristics and molecular profiles. *Cancer Res*, 67, 4010-5.
- BEIER, D., SCHULZ, J. B. & BEIER, C. P. 2011. Chemoresistance of glioblastoma cancer stem cells--much more complex than expected. *Mol Cancer*, 10, 128.
- BEKKER-JENSEN, S. & MAILAND, N. 2010. Assembly and function of DNA double-strand break repair foci in mammalian cells. *DNA Repair (Amst)*, 9, 1219-28.
- BENTLEY, J., DIGGLE, C. P., HARNDEN, P., KNOWLES, M. A. & KILTIE, A. E. 2004. DNA double strand break repair in human bladder cancer is error prone and involves microhomology-associated end-joining. *Nucleic Acids Res*, 32, 5249-59.
- BERGER, F., GAY, E., PELLETIER, L., TROPEL, P. & WION, D. 2004. Development of gliomas: potential role of asymmetrical cell division of neural stem cells. *Lancet Oncol*, 5, 511-4.
- BEUCHER, A., BIRRAUX, J., TCHOUANDONG, L., BARTON, O., SHIBATA, A., CONRAD, S., GOODARZI, A. A., KREMLER, A., JEGGO, P. A. & LOBRICH, M. 2009. ATM and Artemis promote

References

- homologous recombination of radiation-induced DNA double-strand breaks in G2. *EMBO J*, 28, 3413-27.
- BIDDLESTONE-THORPE, L., SAJJAD, M., ROSENBERG, E., BECKTA, J. M., VALERIE, N. C., TOKARZ, M., ADAMS, B. R., WAGNER, A. F., KHALIL, A., GILFOR, D., GOLDING, S. E., DEB, S., TEMESI, D. G., LAU, A., O'CONNOR, M. J., CHOE, K. S., PARADA, L. F., LIM, S. K., MUKHOPADHYAY, N. D. & VALERIE, K. 2013. ATM kinase inhibition preferentially sensitizes p53-mutant glioma to ionizing radiation. *Clin Cancer Res*, 19, 3189-200.
- BIDLINGMAIER, S., ZHU, X. & LIU, B. 2008. The utility and limitations of glycosylated human CD133 epitopes in defining cancer stem cells. *J Mol Med (Berl)*, 86, 1025-32.
- BINDRA, R. S. & GLAZER, P. M. 2005. Genetic instability and the tumor microenvironment: towards the concept of microenvironment-induced mutagenesis. *Mutat Res*, 569, 75-85.
- BINDRA, R. S., SCHAFFER, P. J., MENG, A., WOO, J., MASEIDE, K., ROTH, M. E., LIZARDI, P., HEDLEY, D. W., BRISTOW, R. G. & GLAZER, P. M. 2004. Down-regulation of Rad51 and decreased homologous recombination in hypoxic cancer cells. *Molecular and cellular biology*, 24, 8504-18.
- BJORK-ERIKSSON, T., WEST, C., KARLSSON, E. & MERCKE, C. 2000. Tumor radiosensitivity (SF2) is a prognostic factor for local control in head and neck cancers. *Int J Radiat Oncol Biol Phys*, 46, 13-9.
- BJORK-ERIKSSON, T., WEST, C. M., KARLSSON, E., SLEVIN, N. J., DAVIDSON, S. E., JAMES, R. D. & MERCKE, C. 1998. The in vitro radiosensitivity of human head and neck cancers. *Br J Cancer*, 77, 2371-5.
- BOOTH, L., CRUICKSHANKS, N., RIDDER, T., DAI, Y., GRANT, S. & DENT, P. 2013. PARP and CHK inhibitors interact to cause DNA damage and cell death in mammary carcinoma cells. *Cancer Biol Ther*, 14, 458-65.
- BOROVSKI, T., BEKE, P., VAN TELLINGEN, O., RODERMOND, H. M., VERHOEFF, J. J., LASCANO, V., DAALHUISEN, J. B., MEDEMA, J. P. & SPRICK, M. R. 2013. Therapy-resistant tumor microvascular endothelial cells contribute to treatment failure in glioblastoma multiforme. *Oncogene*, 32, 1539-48.
- BOSTROM, M., KALM, M., KARLSSON, N., HELLSTROM ERKENSTAM, N. & BLOMGREN, K. 2013. Irradiation to the young mouse brain caused long-term, progressive depletion of neurogenesis but did not disrupt the neurovascular niche. *J Cereb Blood Flow Metab*.
- BOTHMER, A., ROBBIANI, D. F., FELDHAHN, N., GAZUMYAN, A., NUSSENZWEIG, A. & NUSSENZWEIG, M. C. 2010. 53BP1 regulates DNA resection and the choice between classical and alternative end joining during class switch recombination. *J Exp Med*, 207, 855-65.
- BRENNER, D. J. & HALL, E. J. 1992. The origins and basis of the linear-quadratic model. *Int J Radiat Oncol Biol Phys*, 23, 252-3.

References

- BROCK, W. A., MILAS, L., BERGH, S., LO, R., SZABO, C. & MASON, K. A. 2004. Radiosensitization of human and rodent cell lines by INO-1001, a novel inhibitor of poly(ADP-ribose) polymerase. *Cancer letters*, 205, 155-60.
- BROWN, A. D., SAGER, B. W., GORTHI, A., TONAPI, S. S., BROWN, E. J. & BISHOP, A. J. 2014. ATR suppresses endogenous DNA damage and allows completion of homologous recombination repair. *PLoS One*, 9, e91222.
- BROWN, C. K., KHODAREV, N. N., YU, J., MOO-YOUNG, T., LABAY, E., DARGA, T. E., POSNER, M. C., WEICHSELBAUM, R. R. & MAUCERI, H. J. 2004. Glioblastoma cells block radiation-induced programmed cell death of endothelial cells. *FEBS Lett*, 565, 167-70.
- BROWN, E. J. & BALTIMORE, D. 2000. ATR disruption leads to chromosomal fragmentation and early embryonic lethality. *Genes Dev*, 14, 397-402.
- BRUNSCHWIG, A., SOUTHAM, C. M. & LEVIN, A. G. 1965. Host resistance to cancer. Clinical experiments by homotransplants, autotransplants and admixture of autologous leucocytes. *Ann Surg*, 162, 416-25.
- BRYANT, H. E., PETERMANN, E., SCHULTZ, N., JEMTH, A. S., LOSEVA, O., ISSAEVA, N., JOHANSSON, F., FERNANDEZ, S., MCGLYNN, P. & HELLEDAY, T. 2009. PARP is activated at stalled forks to mediate Mre11-dependent replication restart and recombination. *EMBO J*, 28, 2601-15.
- BUNTING, S. F., CALLEN, E., WONG, N., CHEN, H. T., POLATO, F., GUNN, A., BOTHMER, A., FELDHAHN, N., FERNANDEZ-CAPETILLO, O., CAO, L., XU, X., DENG, C. X., FINKEL, T., NUSSENZWEIG, M., STARK, J. M. & NUSSENZWEIG, A. 2010. 53BP1 inhibits homologous recombination in Brca1-deficient cells by blocking resection of DNA breaks. *Cell*, 141, 243-54.
- BURKLE, A. & VIRAG, L. 2013. Poly(ADP-ribose): PARadigms and PARadoxes. *Mol Aspects Med*.
- BURMA, S., CHEN, B. P., MURPHY, M., KURIMASA, A. & CHEN, D. J. 2001. ATM phosphorylates histone H2AX in response to DNA double-strand breaks. *J Biol Chem*, 276, 42462-7.
- CALABRESE, C., POPPLETON, H., KOCAK, M., HOGG, T. L., FULLER, C., HAMNER, B., OH, E. Y., GABER, M. W., FINKLESTEIN, D., ALLEN, M., FRANK, A., BAYAZITOV, I. T., ZAKHARENKO, S. S., GAJJAR, A., DAVIDOFF, A. & GILBERTSON, R. J. 2007. A perivascular niche for brain tumor stem cells. *Cancer Cell*, 11, 69-82.
- CALABRESE, C. R., ALMASSY, R., BARTON, S., BATEY, M. A., CALVERT, A. H., CANAN-KOCH, S., DURKACZ, B. W., HOSTOMSKY, Z., KUMPF, R. A., KYLE, S., LI, J., MAEGLEY, K., NEWELL, D. R., NOTARIANNI, E., STRATFORD, I. J., SKALITZKY, D., THOMAS, H. D., WANG, L. Z., WEBBER, S. E., WILLIAMS, K. J. & CURTIN, N. J. 2004. Anticancer chemosensitization and radiosensitization by the novel poly(ADP-ribose) polymerase-1 inhibitor AG14361. *Journal of the National Cancer Institute*, 96, 56-67.
- CALEGARI, F. & HUTTNER, W. B. 2003. An inhibition of cyclin-dependent kinases that lengthens, but does not arrest, neuroepithelial cell cycle induces premature neurogenesis. *J Cell Sci*, 116, 4947-55.

References

- CANCER GENOME ATLAS, N. 2012a. Comprehensive molecular characterization of human colon and rectal cancer. *Nature*, 487, 330-7.
- CANCER GENOME ATLAS, N. 2012b. Comprehensive molecular portraits of human breast tumours. *Nature*, 490, 61-70.
- CANCER GENOME ATLAS RESEARCH, N. 2008. Comprehensive genomic characterization defines human glioblastoma genes and core pathways. *Nature*, 455, 1061-8.
- CANCER GENOME ATLAS RESEARCH, N. 2011. Integrated genomic analyses of ovarian carcinoma. *Nature*, 474, 609-15.
- CHAN, N., PIRES, I. M., BENCOKOVA, Z., COACKLEY, C., LUOTO, K. R., BHOGAL, N., LAKSHMAN, M., GOTTIPATI, P., OLIVER, F. J., HELLEDAY, T., HAMMOND, E. M. & BRISTOW, R. G. 2010. Contextual synthetic lethality of cancer cell kill based on the tumor microenvironment. *Cancer research*, 70, 8045-54.
- CHANG, C. J., HSU, C. C., YUNG, M. C., CHEN, K. Y., TZAO, C., WU, W. F., CHOU, H. Y., LEE, Y. Y., LU, K. H., CHIOU, S. H. & MA, H. I. 2009. Enhanced radiosensitivity and radiation-induced apoptosis in glioma CD133-positive cells by knockdown of SirT1 expression. *Biochem Biophys Res Commun*, 380, 236-42.
- CHASOVSKIKH, S., DIMTCHEV, A., SMULSON, M. & DRITSCHILO, A. 2005. DNA transitions induced by binding of PARP-1 to cruciform structures in supercoiled plasmids. *Cytometry. Part A : the journal of the International Society for Analytical Cytology*, 68, 21-7.
- CHEN, B. P., UEMATSU, N., KOBAYASHI, J., LERENTHAL, Y., KREMLER, A., YAJIMA, H., LOBRICH, M., SHILOH, Y. & CHEN, D. J. 2007. Ataxia telangiectasia mutated (ATM) is essential for DNA-PKcs phosphorylations at the Thr-2609 cluster upon DNA double strand break. *J Biol Chem*, 282, 6582-7.
- CHEN, J., LI, Y., YU, T. S., MCKAY, R. M., BURNS, D. K., KERNIE, S. G. & PARADA, L. F. 2012. A restricted cell population propagates glioblastoma growth after chemotherapy. *Nature*, 488, 522-6.
- CHEN, Z., XIAO, Z., GU, W. Z., XUE, J., BUI, M. H., KOVAR, P., LI, G., WANG, G., TAO, Z. F., TONG, Y., LIN, N. H., SHAM, H. L., WANG, J. Y., SOWIN, T. J., ROSENBERG, S. H. & ZHANG, H. 2006. Selective Chk1 inhibitors differentially sensitize p53-deficient cancer cells to cancer therapeutics. *Int J Cancer*, 119, 2784-94.
- CHOI, S., GAMPER, A. M., WHITE, J. S. & BAKKENIST, C. J. 2010. Inhibition of ATM kinase activity does not phenocopy ATM protein disruption: implications for the clinical utility of ATM kinase inhibitors. *Cell Cycle*, 9, 4052-7.
- CHRISTENSEN, K., SCHRODER, H. D. & KRISTENSEN, B. W. 2008. CD133 identifies perivascular niches in grade II-IV astrocytomas. *J Neurooncol*, 90, 157-70.
- CIMPRICH, K. A. & CORTEZ, D. 2008. ATR: an essential regulator of genome integrity. *Nat Rev Mol Cell Biol*, 9, 616-27.

References

- CLAPPIER, E., GERBY, B., SIGAUX, F., DELORD, M., TOUZRI, F., HERNANDEZ, L., BALLERINI, P., BARUCHEL, A., PFLUMIO, F. & SOULIER, J. 2011. Clonal selection in xenografted human T cell acute lymphoblastic leukemia recapitulates gain of malignancy at relapse. *J Exp Med*, 208, 653-61.
- CLARKSON, B. 1974. The survival value of the dormant state in neoplastic and normal populations. In: CLARKSON, B. A. R., R (ed.) *Control of proliferation in animal cells*. New York: Cold Spring Harbor Laboratory.
- CRAIG, C. G., D'SA, R., MORSHEAD, C. M., ROACH, A. & VAN DER KOOY, D. 1999. Migrational analysis of the constitutively proliferating subependyma population in adult mouse forebrain. *Neuroscience*, 93, 1197-206.
- D'AMOURS, D., DESNOYERS, S., D'SILVA, I. & POIRIER, G. G. 1999. Poly(ADP-ribosyl)ation reactions in the regulation of nuclear functions. *The Biochemical journal*, 342 (Pt 2), 249-68.
- DAHM, K. 2007. Functions and regulation of human artemis in double strand break repair. *J Cell Biochem*, 100, 1346-51.
- DE LA ROCHA, A. M., SAMPRON, N., ALONSO, M. M. & MATHEU, A. 2014. Role of SOX family of transcription factors in central nervous system tumors. *Am J Cancer Res*, 4, 312-24.
- DECKBAR, D., BIRRAUX, J., KREMLER, A., TCHOUANDONG, L., BEUCHER, A., WALKER, S., STIFF, T., JEGGO, P. & LOBRICH, M. 2007. Chromosome breakage after G2 checkpoint release. *J Cell Biol*, 176, 749-55.
- DECKBAR, D., JEGGO, P. A. & LOBRICH, M. 2011. Understanding the limitations of radiation-induced cell cycle checkpoints. *Crit Rev Biochem Mol Biol*, 46, 271-83.
- DECKBAR, D., STIFF, T., KOCH, B., REIS, C., LOBRICH, M. & JEGGO, P. A. 2010. The limitations of the G1-S checkpoint. *Cancer Res*, 70, 4412-21.
- DEFAZIO, L. G., STANSEL, R. M., GRIFFITH, J. D. & CHU, G. 2002. Synapsis of DNA ends by DNA-dependent protein kinase. *EMBO J*, 21, 3192-200.
- DEMBINSKI, J. L. & KRAUSS, S. 2009. Characterization and functional analysis of a slow cycling stem cell-like subpopulation in pancreas adenocarcinoma. *Clin Exp Metastasis*, 26, 611-23.
- DESAI, A., WEBB, B. & GERSON, S. L. 2014. CD133+ cells contribute to radioresistance via altered regulation of DNA repair genes in human lung cancer cells. *Radiother Oncol*, 110, 538-45.
- DI VIRGILIO, M., YING, C. Y. & GAUTIER, J. 2009. PIKK-dependent phosphorylation of Mre11 induces MRN complex inactivation by disassembly from chromatin. *DNA Repair (Amst)*, 8, 1311-20.
- DIFILIPPANTONIO, S. & NUSSENZWEIG, A. 2007. The NBS1-ATM connection revisited. *Cell Cycle*, 6, 2366-70.

References

- DITTFELD, C., DIETRICH, A., PEICKERT, S., HERING, S., BAUMANN, M., GRADE, M., RIED, T. & KUNZ-SCHUGHART, L. A. 2010. CD133 expression is not selective for tumor-initiating or radioresistant cell populations in the CRC cell line HCT-116. *Radiother Oncol*, 94, 375-83.
- DRIESSENS, G., BECK, B., CAAUWE, A., SIMONS, B. D. & BLANPAIN, C. 2012. Defining the mode of tumour growth by clonal analysis. *Nature*, 488, 527-30.
- DUNGEY, F. A., CALDECOTT, K. W. & CHALMERS, A. J. 2009. Enhanced radiosensitization of human glioma cells by combining inhibition of poly(ADP-ribose) polymerase with inhibition of heat shock protein 90. *Molecular cancer therapeutics*, 8, 2243-54.
- DYNAN, W. S. & YOO, S. 1998. Interaction of Ku protein and DNA-dependent protein kinase catalytic subunit with nucleic acids. *Nucleic Acids Res*, 26, 1551-9.
- EGGLER, A. L., INMAN, R. B. & COX, M. M. 2002. The Rad51-dependent pairing of long DNA substrates is stabilized by replication protein A. *J Biol Chem*, 277, 39280-8.
- EISELE, G., WICK, A., EISELE, A. C., CLEMENT, P. M., TONN, J., TABATABAI, G., OCHSENBEIN, A., SCHLEGEL, U., NEYNS, B., KREX, D., SIMON, M., NIKKHAH, G., PICARD, M., STUPP, R., WICK, W. & WELLER, M. 2014. Cilengitide treatment of newly diagnosed glioblastoma patients does not alter patterns of progression. *J Neurooncol*, 117, 141-5.
- EL-KHAMISY, S. F., MASUTANI, M., SUZUKI, H. & CALDECOTT, K. W. 2003. A requirement for PARP-1 for the assembly or stability of XRCC1 nuclear foci at sites of oxidative DNA damage. *Nucleic acids research*, 31, 5526-33.
- ENGELKE, C. G., PARSELS, L. A., QIAN, Y., ZHANG, Q., KARNAK, D., ROBERTSON, J. R., TANSKA, D. M., WEI, D., DAVIS, M. A., PARSELS, J. D., ZHAO, L., GREENSON, J. K., LAWRENCE, T. S., MAYBAUM, J. & MORGAN, M. A. 2013. Sensitization of pancreatic cancer to chemoradiation by the Chk1 inhibitor MK8776. *Clin Cancer Res*, 19, 4412-21.
- FALCK, J., COATES, J. & JACKSON, S. P. 2005. Conserved modes of recruitment of ATM, ATR and DNA-PKcs to sites of DNA damage. *Nature*, 434, 605-11.
- FERGUSON, D. O. & ALT, F. W. 2001. DNA double strand break repair and chromosomal translocation: lessons from animal models. *Oncogene*, 20, 5572-9.
- FERNANDEZ-CAPETILLO, O., CHEN, H. T., CELESTE, A., WARD, I., ROMANIENKO, P. J., MORALES, J. C., NAKA, K., XIA, Z., CAMERINI-OTERO, R. D., MOTOYAMA, N., CARPENTER, P. B., BONNER, W. M., CHEN, J. & NUSSENZWEIG, A. 2002. DNA damage-induced G2-M checkpoint activation by histone H2AX and 53BP1. *Nat Cell Biol*, 4, 993-7.
- FERRO, A. M. & OLIVERA, B. M. 1982. Poly(ADP-ribosylation) in vitro. Reaction parameters and enzyme mechanism. *The Journal of biological chemistry*, 257, 7808-13.
- FIGLEY, S. A., CHEN, Y., MAEDA, A., CONROY, L., McMULLEN, J. D., SILVER, J. I., STAPLETON, S., VITKIN, A., LINDSAY, P., BURRELL, K., ZADEH, G., FEHLINGS, M. G. & DACOSTA, R. S. 2013. A spinal cord window chamber model for in vivo longitudinal multimodal optical and acoustic imaging in a murine model. *PLoS One*, 8, e58081.

References

- FISHER, A. E., HOCHEGGER, H., TAKEDA, S. & CALDECOTT, K. W. 2007. Poly(ADP-ribose) polymerase 1 accelerates single-strand break repair in concert with poly(ADP-ribose) glycohydrolase. *Molecular and cellular biology*, 27, 5597-605.
- FOKAS, E., PREVO, R., POLLARD, J. R., REAPER, P. M., CHARLTON, P. A., CORNELISSEN, B., VALLIS, K. A., HAMMOND, E. M., OLCINA, M. M., GILLIES MCKENNA, W., MUSCHEL, R. J. & BRUNNER, T. B. 2012. Targeting ATR in vivo using the novel inhibitor VE-822 results in selective sensitization of pancreatic tumors to radiation. *Cell Death Dis*, 3, e441.
- FOLKINS, C., SHAKED, Y., MAN, S., TANG, T., LEE, C. R., ZHU, Z., HOFFMAN, R. M. & KERBEL, R. S. 2009. Glioma tumor stem-like cells promote tumor angiogenesis and vasculogenesis via vascular endothelial growth factor and stromal-derived factor 1. *Cancer Res*, 69, 7243-51.
- FOLKMAN, J., KLAGSBRUN, M., SASSE, J., WADZINSKI, M., INGBER, D. & VLODAVSKY, I. 1988. A heparin-binding angiogenic protein--basic fibroblast growth factor--is stored within basement membrane. *Am J Pathol*, 130, 393-400.
- FONG, P. C., BOSS, D. S., YAP, T. A., TUTT, A., WU, P., MERGUI-ROELVINK, M., MORTIMER, P., SWAISLAND, H., LAU, A., O'CONNOR, M. J., ASHWORTH, A., CARMICHAEL, J., KAYE, S. B., SCHELLENS, J. H. & DE BONO, J. S. 2009. Inhibition of poly(ADP-ribose) polymerase in tumors from BRCA mutation carriers. *The New England journal of medicine*, 361, 123-34.
- FRAME, F. M., PELLACANI, D., COLLINS, A. T., SIMMS, M. S., MANN, V. M., JONES, G. D., MEUTH, M., BRISTOW, R. G. & MAITLAND, N. J. 2013. HDAC inhibitor confers radiosensitivity to prostate stem-like cells. *Br J Cancer*, 109, 3023-33.
- FRANKENBERG, D., FRANKENBERG-SCHWAGER, M., BLOCHER, D. & HARBICH, R. 1981. Evidence for DNA double-strand breaks as the critical lesions in yeast cells irradiated with sparsely or densely ionizing radiation under oxic or anoxic conditions. *Radiat Res*, 88, 524-32.
- FRIESNER, J. D., LIU, B., CULLIGAN, K. & BRITT, A. B. 2005. Ionizing radiation-dependent gamma-H2AX focus formation requires ataxia telangiectasia mutated and ataxia telangiectasia mutated and Rad3-related. *Mol Biol Cell*, 16, 2566-76.
- GALIA, A., CALOGERO, A. E., CONDORELLI, R., FRAGGETTA, F., LA CORTE, A., RIDOLFO, F., BOSCO, P., CASTIGLIONE, R. & SALEM, M. 2012a. PARP-1 protein expression in glioblastoma multiforme. *European journal of histochemistry : EJH*, 56, e9.
- GALIA, A., CALOGERO, A. E., CONDORELLI, R., FRAGGETTA, F., LA CORTE, A., RIDOLFO, F., BOSCO, P., CASTIGLIONE, R. & SALEM, M. 2012b. PARP-1 protein expression in glioblastoma multiforme. *Eur J Histochem*, 56, e9.
- GAO, M. Q., CHOI, Y. P., KANG, S., YOUN, J. H. & CHO, N. H. 2010. CD24+ cells from hierarchically organized ovarian cancer are enriched in cancer stem cells. *Oncogene*, 29, 2672-80.
- GERLINGER, M., ROWAN, A. J., HORSWELL, S., LARKIN, J., ENDESFELDER, D., GRONROOS, E., MARTINEZ, P., MATTHEWS, N., STEWART, A., TARPEY, P., VARELA, I., PHILLIMORE, B., BEGUM, S., MCDONALD, N. Q., BUTLER, A., JONES, D., RAINES, K., LATIMER, C., SANTOS, C. R., NOHADANI, M., EKLUND, A. C., SPENCER-DENE, B., CLARK, G., PICKERING, L., STAMP, G., GORE, M., SZALLASI, Z., DOWNWARD, J., FUTREAL, P. A. & SWANTON, C. 2012.

References

- Intratumor heterogeneity and branched evolution revealed by multiregion sequencing. *N Engl J Med*, 366, 883-92.
- GILAD, O., NABET, B. Y., RAGLAND, R. L., SCHOPPY, D. W., SMITH, K. D., DURHAM, A. C. & BROWN, E. J. 2010. Combining ATR suppression with oncogenic Ras synergistically increases genomic instability, causing synthetic lethality or tumorigenesis in a dosage-dependent manner. *Cancer Res*, 70, 9693-702.
- GOLDING, S. E., ROSENBERG, E., ADAMS, B. R., WIGNARAJAH, S., BECKTA, J. M., O'CONNOR, M. J. & VALERIE, K. 2012. Dynamic inhibition of ATM kinase provides a strategy for glioblastoma multiforme radiosensitization and growth control. *Cell Cycle*, 11, 1167-73.
- GOLDING, S. E., ROSENBERG, E., VALERIE, N., HUSSAINI, I., FRIGERIO, M., COCKCROFT, X. F., CHONG, W. Y., HUMMERSONE, M., RIGOREAU, L., MENEAR, K. A., O'CONNOR, M. J., POVIRK, L. F., VAN METER, T. & VALERIE, K. 2009. Improved ATM kinase inhibitor KU-60019 radiosensitizes glioma cells, compromises insulin, AKT and ERK prosurvival signaling, and inhibits migration and invasion. *Mol Cancer Ther*, 8, 2894-902.
- GOODARZI, A. A. & JEGGO, P. A. 2012. Irradiation induced foci (IRIF) as a biomarker for radiosensitivity. *Mutat Res*, 736, 39-47.
- GOODARZI, A. A., NOON, A. T., DECKBAR, D., ZIV, Y., SHILOH, Y., LOBRICH, M. & JEGGO, P. A. 2008. ATM signaling facilitates repair of DNA double-strand breaks associated with heterochromatin. *Mol Cell*, 31, 167-77.
- GOODARZI, A. A., YU, Y., RIBALLO, E., DOUGLAS, P., WALKER, S. A., YE, R., HARER, C., MARCHETTI, C., MORRICE, N., JEGGO, P. A. & LEES-MILLER, S. P. 2006. DNA-PK autophosphorylation facilitates Artemis endonuclease activity. *EMBO J*, 25, 3880-9.
- GORGULIS, V. G., VASSILIOU, L. V., KARAKAIDOS, P., ZACHARATOS, P., KOTSINAS, A., LILOGLOU, T., VENERE, M., DITULLIO, R. A., JR., KASTRINAKIS, N. G., LEVY, B., KLETSAS, D., YONETA, A., HERLYN, M., KITTAS, C. & HALAZONETIS, T. D. 2005. Activation of the DNA damage checkpoint and genomic instability in human precancerous lesions. *Nature*, 434, 907-13.
- GOSINK, E. C., CHONG, M. J. & MCKINNON, P. J. 1999. Ataxia telangiectasia mutated deficiency affects astrocyte growth but not radiosensitivity. *Cancer Res*, 59, 5294-8.
- GOTOFF, S. P., AMIRMOOKRI, E. & LIEBNER, E. J. 1967. Ataxia telangiectasia. Neoplasia, untoward response to x-irradiation, and tuberous sclerosis. *Am J Dis Child*, 114, 617-25.
- GRITTI, A., PARATI, E. A., COVA, L., FROLICHSTHAL, P., GALLI, R., WANKE, E., FARAVELLI, L., MORASSUTTI, D. J., ROISEN, F., NICKEL, D. D. & VESCOVI, A. L. 1996. Multipotential stem cells from the adult mouse brain proliferate and self-renew in response to basic fibroblast growth factor. *J Neurosci*, 16, 1091-100.
- HALAZONETIS, T. D., GORGULIS, V. G. & BARTEK, J. 2008. An oncogene-induced DNA damage model for cancer development. *Science*, 319, 1352-5.
- HAMAHATA, A., ENKHBAATAR, P., LANGE, M., YAMAKI, T., SAKURAI, H., SHIMODA, K., NAKAZAWA, H., TRABER, L. D. & TRABER, D. L. 2012. Administration of poly(ADP-ribose)

References

- polymerase inhibitor into bronchial artery attenuates pulmonary pathophysiology after smoke inhalation and burn in an ovine model. *Burns*, 38, 1210-5.
- HANS, F. & DIMITROV, S. 2001. Histone H3 phosphorylation and cell division. *Oncogene*, 20, 3021-7.
- HARDEE, M. E., MARCISCANO, A. E., MEDINA-RAMIREZ, C. M., ZAGZAG, D., NARAYANA, A., LONNING, S. M. & BARCELLOS-HOFF, M. H. 2012. Resistance of glioblastoma-initiating cells to radiation mediated by the tumor microenvironment can be abolished by inhibiting transforming growth factor-beta. *Cancer Res*, 72, 4119-29.
- HAVEMAN, J., RODERMOND, H., VAN BREE, C., WONDERGEM, J. & FRANKEN, N. A. 2007. Residual late radiation damage in mouse stromal tissue assessed by the tumor bed effect. *J Radiat Res*, 48, 107-12.
- HELLEDAY, T., LO, J., VAN GENT, D. C. & ENGELWARD, B. P. 2007. DNA double-strand break repair: from mechanistic understanding to cancer treatment. *DNA Repair (Amst)*, 6, 923-35.
- HEMMATI, H. D., NAKANO, I., LAZAREFF, J. A., MASTERMAN-SMITH, M., GESCHWIND, D. H., BRONNER-FRASER, M. & KORNBLUM, H. I. 2003. Cancerous stem cells can arise from pediatric brain tumors. *Proc Natl Acad Sci U S A*, 100, 15178-83.
- HERMANN, P. C., HUBER, S. L., HERRLER, T., AICHER, A., ELLWART, J. W., GUBA, M., BRUNS, C. J. & HEESCHEN, C. 2007. Distinct populations of cancer stem cells determine tumor growth and metastatic activity in human pancreatic cancer. *Cell Stem Cell*, 1, 313-23.
- HICKSON, I., ZHAO, Y., RICHARDSON, C. J., GREEN, S. J., MARTIN, N. M., ORR, A. I., REAPER, P. M., JACKSON, S. P., CURTIN, N. J. & SMITH, G. C. 2004. Identification and characterization of a novel and specific inhibitor of the ataxia-telangiectasia mutated kinase ATM. *Cancer Res*, 64, 9152-9.
- HOBSON, B. & DENEKAMP, J. 1984. Endothelial proliferation in tumours and normal tissues: continuous labelling studies. *British journal of cancer*, 49, 405-13.
- HOCHBERG, F. H. & PRUITT, A. 1980. Assumptions in the radiotherapy of glioblastoma. *Neurology*, 30, 907-11.
- HOGLUND, A., STROMVALL, K., LI, Y., FORSHELL, L. P. & NILSSON, J. A. 2011. Chk2 deficiency in Myc overexpressing lymphoma cells elicits a synergistic lethal response in combination with PARP inhibition. *Cell Cycle*, 10, 3598-607.
- HOVINGA, K. E., SHIMIZU, F., WANG, R., PANAGIOTAKOS, G., VAN DER HEIJDEN, M., MOAYEDPARDAZI, H., CORREIA, A. S., SOULET, D., MAJOR, T., MENON, J. & TABAR, V. 2010. Inhibition of notch signaling in glioblastoma targets cancer stem cells via an endothelial cell intermediate. *Stem Cells*, 28, 1019-29.
- HU, Y. & SMYTH, G. K. 2009. ELDA: extreme limiting dilution analysis for comparing depleted and enriched populations in stem cell and other assays. *J Immunol Methods*, 347, 70-8.

References

- IGNATOVA, T. N., KUKEKOV, V. G., LAYWELL, E. D., SUSLOV, O. N., VRIONIS, F. D. & STEINDLER, D. A. 2002. Human cortical glial tumors contain neural stem-like cells expressing astrogial and neuronal markers in vitro. *Glia*, 39, 193-206.
- IKUSHIMA, H., TODO, T., INO, Y., TAKAHASHI, M., SAITO, N., MIYAZAWA, K. & MIYAZONO, K. 2011. Glioma-initiating cells retain their tumorigenicity through integration of the Sox axis and Oct4 protein. *J Biol Chem*, 286, 41434-41.
- INFANGER, D. W., CHO, Y., LOPEZ, B. S., MOHANAN, S., LIU, S. C., GURSEL, D., BOOCKVAR, J. A. & FISCHBACH, C. 2013. Glioblastoma stem cells are regulated by interleukin-8 signaling in a tumoral perivascular niche. *Cancer Res*, 73, 7079-89.
- ISHIKAWA, F., YOSHIDA, S., SAITO, Y., HIJIKATA, A., KITAMURA, H., TANAKA, S., NAKAMURA, R., TANAKA, T., TOMIYAMA, H., SAITO, N., FUKATA, M., MIYAMOTO, T., LYONS, B., OHSHIMA, K., UCHIDA, N., TANIGUCHI, S., OHARA, O., AKASHI, K., HARADA, M. & SHULTZ, L. D. 2007. Chemotherapy-resistant human AML stem cells home to and engraft within the bone-marrow endosteal region. *Nat Biotechnol*, 25, 1315-21.
- JAMAL, M., RATH, B. H., WILLIAMS, E. S., CAMPHAUSEN, K. & TOFILON, P. J. 2010. Microenvironmental regulation of glioblastoma radioresponse. *Clin Cancer Res*, 16, 6049-59.
- JEGGO, P. A., GEUTING, V. & LOBRICH, M. 2011. The role of homologous recombination in radiation-induced double-strand break repair. *Radiother Oncol*, 101, 7-12.
- JELINIC, P. & LEVINE, D. A. 2014. New insights into PARP inhibitors' effect on cell cycle and homology-directed DNA damage repair. *Mol Cancer Ther*, 13, 1645-54.
- JIANG, W., CROWE, J. L., LIU, X., NAKAJIMA, S., WANG, Y., LI, C., LEE, B. J., DUBOIS, R. L., LIU, C., YU, X., LAN, L. & ZHA, S. 2015. Differential phosphorylation of DNA-PKcs regulates the interplay between end-processing and end-ligation during nonhomologous end-joining. *Mol Cell*, 58, 172-85.
- KAHN, J., HAYMAN, T. J., JAMAL, M., RATH, B. H., KRAMP, T., CAMPHAUSEN, K. & TOFILON, P. J. 2014. The mTORC1/mTORC2 inhibitor AZD2014 enhances the radiosensitivity of glioblastoma stem-like cells. *Neuro Oncol*, 16, 29-37.
- KAO, J., MILANO, M. T., JAVAHERI, A., GAROFALO, M. C., CHMURA, S. J., WEICHSELBAUM, R. R. & KRON, S. J. 2006. gamma-H2AX as a therapeutic target for improving the efficacy of radiation therapy. *Curr Cancer Drug Targets*, 6, 197-205.
- KHASRAW, M., AMERATUNGA, M. S., GRANT, R., WHEELER, H. & PAVLAKIS, N. 2014. Antiangiogenic therapy for high-grade glioma. *Cochrane Database Syst Rev*, 9, CD008218.
- KHODYREVA, S. N., PRASAD, R., ILINA, E. S., SUKHANOVA, M. V., KUTUZOVA, M. M., LIU, Y., HOU, E. W., WILSON, S. H. & LAVRIK, O. I. 2010. Apurinic/apyrimidinic (AP) site recognition by the 5'-dRP/AP lyase in poly(ADP-ribose) polymerase-1 (PARP-1). *Proceedings of the National Academy of Sciences of the United States of America*, 107, 22090-5.

References

- KINNER, A., WU, W., STAUDT, C. & ILIAKIS, G. 2008. Gamma-H2AX in recognition and signaling of DNA double-strand breaks in the context of chromatin. *Nucleic Acids Res*, 36, 5678-94.
- KONIARAS, K., CUDDIHY, A. R., CHRISTOPOULOS, H., HOGG, A. & O'CONNELL, M. J. 2001. Inhibition of Chk1-dependent G2 DNA damage checkpoint radiosensitizes p53 mutant human cells. *Oncogene*, 20, 7453-63.
- KREJCI, L., ALTMANNOVA, V., SPIREK, M. & ZHAO, X. 2012. Homologous recombination and its regulation. *Nucleic Acids Res*, 40, 5795-818.
- KRISHNAKUMAR, R. & KRAUS, W. L. 2010. The PARP side of the nucleus: molecular actions, physiological outcomes, and clinical targets. *Molecular cell*, 39, 8-24.
- KUHNE, M., RIBALLO, E., RIEF, N., ROTHKAMM, K., JEGGO, P. A. & LOBRICH, M. 2004. A double-strand break repair defect in ATM-deficient cells contributes to radiosensitivity. *Cancer Res*, 64, 500-8.
- LANGELIER, M. F., PLANCK, J. L., ROY, S. & PASCAL, J. M. 2012. Structural basis for DNA damage-dependent poly(ADP-ribosyl)ation by human PARP-1. *Science*, 336, 728-32.
- LANGELIER, M. F., RUHL, D. D., PLANCK, J. L., KRAUS, W. L. & PASCAL, J. M. 2010. The Zn3 domain of human poly(ADP-ribose) polymerase-1 (PARP-1) functions in both DNA-dependent poly(ADP-ribose) synthesis activity and chromatin compaction. *The Journal of biological chemistry*, 285, 18877-87.
- LAPIDOT, T., SIRARD, C., VORMOOR, J., MURDOCH, B., HOANG, T., CACERES-CORTES, J., MINDEN, M., PATERSON, B., CALIGIURI, M. A. & DICK, J. E. 1994. A cell initiating human acute myeloid leukaemia after transplantation into SCID mice. *Nature*, 367, 645-8.
- LAPOUGE, G., YOUSSEF, K. K., VOKAER, B., ACHOURI, Y., MICHAUX, C., SOTIROPOULOU, P. A. & BLANPAIN, C. 2011. Identifying the cellular origin of squamous skin tumors. *Proc Natl Acad Sci U S A*, 108, 7431-6.
- LATERRA J, L.-B. H., BACHCHU L, LI A, CAPLAN M, GUERRERO-CAZARES H, EBERHART C, QUINONES-HINOJOSA, LI Y 2014. Epigenetic regulation of GBM cell stemness and tumor propagating capacity by Oct4 and Sox2. *Neuro Oncol*, iii15.
- LEE, J. & DUNPHY, W. G. 2010. Rad17 plays a central role in establishment of the interaction between TopBP1 and the Rad9-Hus1-Rad1 complex at stalled replication forks. *Mol Biol Cell*, 21, 926-35.
- LI, L. & CLEVERS, H. 2010. Coexistence of quiescent and active adult stem cells in mammals. *Science*, 327, 542-5.
- LI, X. & HEYER, W. D. 2008. Homologous recombination in DNA repair and DNA damage tolerance. *Cell Res*, 18, 99-113.

References

- LIAO, H., WINKFEIN, R. J., MACK, G., RATTNER, J. B. & YEN, T. J. 1995. CENP-F is a protein of the nuclear matrix that assembles onto kinetochores at late G2 and is rapidly degraded after mitosis. *J Cell Biol*, 130, 507-18.
- LIM, D. S., KIM, S. T., XU, B., MASER, R. S., LIN, J., PETRINI, J. H. & KASTAN, M. B. 2000. ATM phosphorylates p95/nbs1 in an S-phase checkpoint pathway. *Nature*, 404, 613-7.
- LIM, Y. C., ROBERTS, T. L., DAY, B. W., HARDING, A., KOZLOV, S., KIJAS, A. W., ENSBEY, K. S., WALKER, D. G. & LAVIN, M. F. 2012. A role for homologous recombination and abnormal cell-cycle progression in radioresistance of glioma-initiating cells. *Mol Cancer Ther*, 11, 1863-72.
- LIM, Y. C., ROBERTS, T. L., DAY, B. W., STRINGER, B. W., KOZLOV, S., FAZRY, S., BRUCE, Z. C., ENSBEY, K. S., WALKER, D. G., BOYD, A. W. & LAVIN, M. F. 2014. Increased sensitivity to ionizing radiation by targeting the homologous recombination pathway in glioma initiating cells. *Mol Oncol*, 8, 1603-15.
- LIN, F. L., SPERLE, K. & STERNBERG, N. 1984. Model for homologous recombination during transfer of DNA into mouse L cells: role for DNA ends in the recombination process. *Mol Cell Biol*, 4, 1020-34.
- LINDAHL, T., SATOH, M. S., POIRIER, G. G. & KLUNGLAND, A. 1995. Post-translational modification of poly(ADP-ribose) polymerase induced by DNA strand breaks. *Trends in biochemical sciences*, 20, 405-11.
- LIU, C., SAGE, J. C., MILLER, M. R., VERHAAK, R. G., HIPPENMEYER, S., VOGEL, H., FOREMAN, O., BRONSON, R. T., NISHIYAMA, A., LUO, L. & ZONG, H. 2011. Mosaic analysis with double markers reveals tumor cell of origin in glioma. *Cell*, 146, 209-21.
- LIU, H., TAKEDA, S., KUMAR, R., WESTERGARD, T. D., BROWN, E. J., PANDITA, T. K., CHENG, E. H. & HSIEH, J. J. 2010. Phosphorylation of MLL by ATR is required for execution of mammalian S-phase checkpoint. *Nature*, 467, 343-6.
- LIU, S. K., COACKLEY, C., KRAUSE, M., JALALI, F., CHAN, N. & BRISTOW, R. G. 2008. A novel poly(ADP-ribose) polymerase inhibitor, ABT-888, radiosensitizes malignant human cell lines under hypoxia. *Radiotherapy and oncology : journal of the European Society for Therapeutic Radiology and Oncology*, 88, 258-68.
- LOBRICH, M., SHIBATA, A., BEUCHER, A., FISHER, A., ENSMINGER, M., GOODARZI, A. A., BARTON, O. & JEGGO, P. A. 2010. gammaH2AX foci analysis for monitoring DNA double-strand break repair: strengths, limitations and optimization. *Cell Cycle*, 9, 662-9.
- LONSKAYA, I., POTAMAN, V. N., SHLYAKHTENKO, L. S., OUSSATCHEVA, E. A., LYUBCHENKO, Y. L. & SOLDATENKOV, V. A. 2005. Regulation of poly(ADP-ribose) polymerase-1 by DNA structure-specific binding. *The Journal of biological chemistry*, 280, 17076-83.
- LOSER, D. A., SHIBATA, A., SHIBATA, A. K., WOODBINE, L. J., JEGGO, P. A. & CHALMERS, A. J. 2010. Sensitization to radiation and alkylating agents by inhibitors of poly(ADP-ribose) polymerase is enhanced in cells deficient in DNA double-strand break repair. *Mol Cancer Ther*, 9, 1775-87.

References

- LUKAS, J., LUKAS, C. & BARTEK, J. 2004. Mammalian cell cycle checkpoints: signalling pathways and their organization in space and time. *DNA Repair (Amst)*, 3, 997-1007.
- MA, Z., YAO, G., ZHOU, B., FAN, Y., GAO, S. & FENG, X. 2012. The Chk1 inhibitor AZD7762 sensitises p53 mutant breast cancer cells to radiation in vitro and in vivo. *Mol Med Rep*, 6, 897-903.
- MAILAND, N., FALCK, J., LUKAS, C., SYLJUASEN, R. G., WELCKER, M., BARTEK, J. & LUKAS, J. 2000. Rapid destruction of human Cdc25A in response to DNA damage. *Science*, 288, 1425-9.
- MALANGA, M. & ALTHAUS, F. R. 1994. Poly(ADP-ribose) molecules formed during DNA repair in vivo. *The Journal of biological chemistry*, 269, 17691-6.
- MALKOVA, A., IVANOV, E. L. & HABER, J. E. 1996. Double-strand break repair in the absence of RAD51 in yeast: a possible role for break-induced DNA replication. *Proc Natl Acad Sci U S A*, 93, 7131-6.
- MANNINO, M. & CHALMERS, A. J. 2011. Radioresistance of glioma stem cells: intrinsic characteristic or property of the 'microenvironment-stem cell unit'? *Mol Oncol*, 5, 374-86.
- MANNINO, M., GOMEZ-ROMAN, N., HOCHEGGER, H. & CHALMERS, A. J. 2014. Differential sensitivity of Glioma stem cells to Aurora kinase A inhibitors: implications for stem cell mitosis and centrosome dynamics. *Stem Cell Res*, 13, 135-43.
- MAO, X. G., ZHANG, X., XUE, X. Y., GUO, G., WANG, P., ZHANG, W., FEI, Z., ZHEN, H. N., YOU, S. W. & YANG, H. 2009. Brain Tumor Stem-Like Cells Identified by Neural Stem Cell Marker CD15. *Transl Oncol*, 2, 247-57.
- MARECHAL, A. & ZOU, L. 2013. DNA damage sensing by the ATM and ATR kinases. *Cold Spring Harb Perspect Biol*, 5.
- MARI, P. O., FLOREA, B. I., PERSENGIEV, S. P., VERKAIK, N. S., BRUGGENWIRTH, H. T., MODESTI, M., GIGLIA-MARI, G., BEZSTAROSTI, K., DEMMERS, J. A., LUIDER, T. M., HOUTSMULLER, A. B. & VAN GENT, D. C. 2006. Dynamic assembly of end-joining complexes requires interaction between Ku70/80 and XRCC4. *Proc Natl Acad Sci U S A*, 103, 18597-602.
- MARUSYK, A. & POLYAK, K. 2010. Tumor heterogeneity: causes and consequences. *Biochim Biophys Acta*, 1805, 105-17.
- MCCORD, A. M., JAMAL, M., WILLIAMS, E. S., CAMPHAUSEN, K. & TOFILON, P. J. 2009. CD133+ glioblastoma stem-like cells are radiosensitive with a defective DNA damage response compared with established cell lines. *Clin Cancer Res*, 15, 5145-53.
- MCVEY, M. & LEE, S. E. 2008. MMEJ repair of double-strand breaks (director's cut): deleted sequences and alternative endings. *Trends Genet*, 24, 529-38.
- MEACHAM, C. E. & MORRISON, S. J. 2013. Tumour heterogeneity and cancer cell plasticity. *Nature*, 501, 328-37.

References

- MELI, L., BARBOSA, H. S., HICKEY, A. M., GASIMLI, L., NIERODE, G., DIOGO, M. M., LINHARDT, R. J., CABRAL, J. M. & DORDICK, J. S. 2014. Three dimensional cellular microarray platform for human neural stem cell differentiation and toxicology. *Stem Cell Res*, 13, 36-47.
- MENG, A. X., JALALI, F., CUDDIHY, A., CHAN, N., BINDRA, R. S., GLAZER, P. M. & BRISTOW, R. G. 2005. Hypoxia down-regulates DNA double strand break repair gene expression in prostate cancer cells. *Radiotherapy and oncology : journal of the European Society for Therapeutic Radiology and Oncology*, 76, 168-76.
- MENISSIER DE MURCIA, J., RICOUL, M., TARTIER, L., NIEDERGANG, C., HUBER, A., DANTZER, F., SCHREIBER, V., AME, J. C., DIERICH, A., LEMEUR, M., SABATIER, L., CHAMBON, P. & DE MURCIA, G. 2003. Functional interaction between PARP-1 and PARP-2 in chromosome stability and embryonic development in mouse. *The EMBO journal*, 22, 2255-63.
- MIDWOOD, K. S. & ORENDS, G. 2009. The role of tenascin-C in tissue injury and tumorigenesis. *J Cell Commun Signal*, 3, 287-310.
- MODING, E. J., LEE, C. L., CASTLE, K. D., OH, P., MAO, L., ZHA, S., MIN, H. D., MA, Y., DAS, S. & KIRSCH, D. G. 2014. Atm deletion with dual recombinase technology preferentially radiosensitizes tumor endothelium. *J Clin Invest*, 124, 3325-38.
- MOULDER, J. E. & ROCKWELL, S. 1984. Hypoxic fractions of solid tumors: experimental techniques, methods of analysis, and a survey of existing data. *Int J Radiat Oncol Biol Phys*, 10, 695-712.
- NAGPAL, J., JAMOONA, A., GULATI, N. D., MOHAN, A., BRAUN, A., MURALI, R. & JHANWAR-UNIYAL, M. 2006. Revisiting the role of p53 in primary and secondary glioblastomas. *Anticancer Res*, 26, 4633-9.
- NASSIF, N., PENNEY, J., PAL, S., ENGELS, W. R. & GLOOR, G. B. 1994. Efficient copying of nonhomologous sequences from ectopic sites via P-element-induced gap repair. *Mol Cell Biol*, 14, 1613-25.
- NIEWOLIK, D., PANNICKE, U., LU, H., MA, Y., WANG, L. C., KULESZA, P., ZANDI, E., LIEBER, M. R. & SCHWARZ, K. 2006. DNA-PKcs dependence of Artemis endonucleolytic activity, differences between hairpins and 5' or 3' overhangs. *J Biol Chem*, 281, 33900-9.
- NIMONKAR, A. V., GENSCHEL, J., KINOSHITA, E., POLACZEK, P., CAMPBELL, J. L., WYMAN, C., MODRICH, P. & KOWALCZYKOWSKI, S. C. 2011. BLM-DNA2-RPA-MRN and EXO1-BLM-RPA-MRN constitute two DNA end resection machineries for human DNA break repair. *Genes Dev*, 25, 350-62.
- NIMONKAR, A. V., OZSOY, A. Z., GENSCHEL, J., MODRICH, P. & KOWALCZYKOWSKI, S. C. 2008. Human exonuclease 1 and BLM helicase interact to resect DNA and initiate DNA repair. *Proc Natl Acad Sci U S A*, 105, 16906-11.
- NOEL, G., GODON, C., FERNET, M., GIOCANTI, N., MEGNIN-CHANET, F. & FAVAUDON, V. 2006. Radiosensitization by the poly(ADP-ribose) polymerase inhibitor 4-amino-1,8-naphthalimide is specific of the S phase of the cell cycle and involves arrest of DNA synthesis. *Molecular cancer therapeutics*, 5, 564-74.

References

- NOTTA, F., MULLIGHAN, C. G., WANG, J. C., POEPLI, A., DOULATOV, S., PHILLIPS, L. A., MA, J., MINDEN, M. D., DOWNING, J. R. & DICK, J. E. 2011. Evolution of human BCR-ABL1 lymphoblastic leukaemia-initiating cells. *Nature*, 469, 362-7.
- NOWELL, P. C. 1976. The clonal evolution of tumor cell populations. *Science*, 194, 23-8.
- O'BRIEN, C. A., POLLETT, A., GALLINGER, S. & DICK, J. E. 2007. A human colon cancer cell capable of initiating tumour growth in immunodeficient mice. *Nature*, 445, 106-10.
- OLIVE, P. L. & BANATH, J. P. 2006. The comet assay: a method to measure DNA damage in individual cells. *Nat Protoc*, 1, 23-9.
- PARK, D., XIANG, A. P., MAO, F. F., ZHANG, L., DI, C. G., LIU, X. M., SHAO, Y., MA, B. F., LEE, J. H., HA, K. S., WALTON, N. & LAHN, B. T. 2010. Nestin is required for the proper self-renewal of neural stem cells. *Stem Cells*, 28, 2162-71.
- PATEL, A. P., TIROSH, I., TROMBETTA, J. J., SHALEK, A. K., GILLESPIE, S. M., WAKIMOTO, H., CAHILL, D. P., NAHED, B. V., CURRY, W. T., MARTUZA, R. L., LOUIS, D. N., ROZENBLATT-ROSEN, O., SUVA, M. L., REGEV, A. & BERNSTEIN, B. E. 2014. Single-cell RNA-seq highlights intratumoral heterogeneity in primary glioblastoma. *Science*, 344, 1396-401.
- PEASLAND, A., WANG, L. Z., ROWLING, E., KYLE, S., CHEN, T., HOPKINS, A., CLIBY, W. A., SARKARIA, J., BEALE, G., EDMONDSON, R. J. & CURTIN, N. J. 2011. Identification and evaluation of a potent novel ATR inhibitor, NU6027, in breast and ovarian cancer cell lines. *Br J Cancer*, 105, 372-81.
- PETERSEN, S., CASELLAS, R., REINA-SAN-MARTIN, B., CHEN, H. T., DIFILIPPANTONIO, M. J., WILSON, P. C., HANITSCH, L., CELESTE, A., MURAMATSU, M., PILCH, D. R., REDON, C., RIED, T., BONNER, W. M., HONJO, T., NUSSENZWEIG, M. C. & NUSSENZWEIG, A. 2001. AID is required to initiate Nbs1/gamma-H2AX focus formation and mutations at sites of class switching. *Nature*, 414, 660-5.
- PILKINGTON, G. J. 2005. Cancer stem cells in the mammalian central nervous system. *Cell Prolif*, 38, 423-33.
- PION, E., ULLMANN, G. M., AME, J. C., GERARD, D., DE MURCIA, G. & BOMBarda, E. 2005. DNA-induced dimerization of poly(ADP-ribose) polymerase-1 triggers its activation. *Biochemistry*, 44, 14670-81.
- PIRES, I. M., OLCINA, M. M., ANBALAGAN, S., POLLARD, J. R., REAPER, P. M., CHARLTON, P. A., MCKENNA, W. G. & HAMMOND, E. M. 2012. Targeting radiation-resistant hypoxic tumour cells through ATR inhibition. *Br J Cancer*, 107, 291-9.
- POTAMAN, V. N., SHLYAKHTENKO, L. S., OUSSATCHeva, E. A., LYUBCHENKO, Y. L. & SOLDATENKOV, V. A. 2005. Specific binding of poly(ADP-ribose) polymerase-1 to cruciform hairpins. *Journal of molecular biology*, 348, 609-15.
- PREVO, R., FOKAS, E., REAPER, P. M., CHARLTON, P. A., POLLARD, J. R., MCKENNA, W. G., MUSCHEL, R. J. & BRUNNER, T. B. 2012. The novel ATR inhibitor VE-821 increases

References

- sensitivity of pancreatic cancer cells to radiation and chemotherapy. *Cancer Biol Ther*, 13, 1072-81.
- PRINCE, M. E., SIVANANDAN, R., KACZOROWSKI, A., WOLF, G. T., KAPLAN, M. J., DALERBA, P., WEISSMAN, I. L., CLARKE, M. F. & AILLES, L. E. 2007. Identification of a subpopulation of cells with cancer stem cell properties in head and neck squamous cell carcinoma. *Proc Natl Acad Sci U S A*, 104, 973-8.
- QUINTANA, E., SHACKLETON, M., FOSTER, H. R., FULLEN, D. R., SABEL, M. S., JOHNSON, T. M. & MORRISON, S. J. 2010. Phenotypic heterogeneity among tumorigenic melanoma cells from patients that is reversible and not hierarchically organized. *Cancer Cell*, 18, 510-23.
- RADFORD, I. R. 1985. The level of induced DNA double-strand breakage correlates with cell killing after X-irradiation. *Int J Radiat Biol Relat Stud Phys Chem Med*, 48, 45-54.
- RAINEY, M. D., CHARLTON, M. E., STANTON, R. V. & KASTAN, M. B. 2008. Transient inhibition of ATM kinase is sufficient to enhance cellular sensitivity to ionizing radiation. *Cancer Res*, 68, 7466-74.
- RASO, A., VECCHIO, D., CAPPELLI, E., ROPOLO, M., POGGI, A., NOZZA, P., BIASSONI, R., MASCELLI, S., CAPRA, V., KALFAS, F., SEVERI, P. & FROSINA, G. 2012. Characterization of glioma stem cells through multiple stem cell markers and their specific sensitization to double-strand break-inducing agents by pharmacological inhibition of ataxia telangiectasia mutated protein. *Brain Pathol*, 22, 677-88.
- REAPER, P. M., GRIFFITHS, M. R., LONG, J. M., CHARRIER, J. D., MACCORMICK, S., CHARLTON, P. A., GOLEC, J. M. & POLLARD, J. R. 2011. Selective killing of ATM- or p53-deficient cancer cells through inhibition of ATR. *Nat Chem Biol*, 7, 428-30.
- REDDY, Y. V., DING, Q., LEES-MILLER, S. P., MEEK, K. & RAMSDEN, D. A. 2004. Non-homologous end joining requires that the DNA-PK complex undergo an autophosphorylation-dependent rearrangement at DNA ends. *J Biol Chem*, 279, 39408-13.
- REINA-SAN-MARTIN, B., DIFILIPPANTONIO, S., HANITSCH, L., MASILAMANI, R. F., NUSSENZWEIG, A. & NUSSENZWEIG, M. C. 2003. H2AX is required for recombination between immunoglobulin switch regions but not for intra-switch region recombination or somatic hypermutation. *J Exp Med*, 197, 1767-78.
- REYNOLDS, B. A. & WEISS, S. 1992. Generation of neurons and astrocytes from isolated cells of the adult mammalian central nervous system. *Science*, 255, 1707-10.
- RHEINBAY, E., SUVA, M. L., GILLESPIE, S. M., WAKIMOTO, H., PATEL, A. P., SHAHID, M., OKSUZ, O., RABKIN, S. D., MARTUZA, R. L., RIVERA, M. N., LOUIS, D. N., KASIF, S., CHI, A. S. & BERNSTEIN, B. E. 2013. An aberrant transcription factor network essential for Wnt signaling and stem cell maintenance in glioblastoma. *Cell Rep*, 3, 1567-79.
- RIBALLO, E., KUHNE, M., RIEF, N., DOHERTY, A., SMITH, G. C., RECIO, M. J., REIS, C., DAHM, K., FRICKE, A., KREMPLER, A., PARKER, A. R., JACKSON, S. P., GENNERY, A., JEGGO, P. A. & LOBRICH, M. 2004. A pathway of double-strand break rejoining dependent upon ATM, Artemis, and proteins locating to gamma-H2AX foci. *Mol Cell*, 16, 715-24.

References

- RICCI-VITIANI, L., PALLINI, R., BIFFONI, M., TODARO, M., INVERNICI, G., CENCI, T., MAIRA, G., PARATI, E. A., STASSI, G., LAROCCA, L. M. & DE MARIA, R. 2010. Tumour vascularization via endothelial differentiation of glioblastoma stem-like cells. *Nature*, 468, 824-8.
- RIEKKI, R., JUKKOLA, A., OIKARINEN, A. & KALLIOINEN, M. 2001. Radiation therapy induces tenascin expression and angiogenesis in human skin. *Acta Derm Venereol*, 81, 329-33.
- ROESNER, J. P., MERSMANN, J., BERGT, S., BOHNENBERG, K., BARTHUBER, C., SZABO, C., NOLDE-SCHOMBURG, G. E. & ZACHAROWSKI, K. 2010. Therapeutic injection of PARP inhibitor INO-1001 preserves cardiac function in porcine myocardial ischemia and reperfusion without reducing infarct size. *Shock*, 33, 507-12.
- ROGAKOU, E. P., BOON, C., REDON, C. & BONNER, W. M. 1999. Megabase chromatin domains involved in DNA double-strand breaks in vivo. *J Cell Biol*, 146, 905-16.
- ROPOLO, M., DAGA, A., GRIFFERO, F., FORESTA, M., CASARTELLI, G., ZUNINO, A., POGGI, A., CAPPELLI, E., ZONA, G., SPAZIANTE, R., CORTE, G. & FROSINA, G. 2009. Comparative analysis of DNA repair in stem and nonstem glioma cell cultures. *Mol Cancer Res*, 7, 383-92.
- ROTH, D. B. & WILSON, J. H. 1986. Nonhomologous recombination in mammalian cells: role for short sequence homologies in the joining reaction. *Mol Cell Biol*, 6, 4295-304.
- SALMAGGI, A., BOIARDI, A., GELATI, M., RUSSO, A., CALATOZZOLO, C., CIUSANI, E., SCIACCA, F. L., OTTOLINA, A., PARATI, E. A., LA PORTA, C., ALESSANDRI, G., MARRAS, C., CROCI, D. & DE ROSSI, M. 2006. Glioblastoma-derived tumorospheres identify a population of tumor stem-like cells with angiogenic potential and enhanced multidrug resistance phenotype. *Glia*, 54, 850-60.
- SAMOL, J., RANSON, M., SCOTT, E., MACPHERSON, E., CARMICHAEL, J., THOMAS, A. & CASSIDY, J. 2012. Safety and tolerability of the poly(ADP-ribose) polymerase (PARP) inhibitor, olaparib (AZD2281) in combination with topotecan for the treatment of patients with advanced solid tumors: a phase I study. *Invest New Drugs*, 30, 1493-500.
- SAN FILIPPO, J., CHI, P., SEHORN, M. G., ETCHIN, J., KREJCI, L. & SUNG, P. 2006. Recombination mediator and Rad51 targeting activities of a human BRCA2 polypeptide. *J Biol Chem*, 281, 11649-57.
- SAN FILIPPO, J., SUNG, P. & KLEIN, H. 2008. Mechanism of eukaryotic homologous recombination. *Annu Rev Biochem*, 77, 229-57.
- SANAI, N., ALVAREZ-BUYLLA, A. & BERGER, M. S. 2005. Neural stem cells and the origin of gliomas. *N Engl J Med*, 353, 811-22.
- SANKUNNY, M., PARIKH, R. A., LEWIS, D. W., GOODING, W. E., SAUNDERS, W. S. & GOLLIN, S. M. 2014. Targeted inhibition of ATR or CHEK1 reverses radioresistance in oral squamous cell carcinoma cells with distal chromosome arm 11q loss. *Genes Chromosomes Cancer*, 53, 129-43.

References

- SARTORI, A. A., LUKAS, C., COATES, J., MISTRIK, M., FU, S., BARTEK, J., BAER, R., LUKAS, J. & JACKSON, S. P. 2007. Human CtIP promotes DNA end resection. *Nature*, 450, 509-14.
- SATOH, M. S. & LINDAHL, T. 1992. Role of poly(ADP-ribose) formation in DNA repair. *Nature*, 356, 356-8.
- SCHEPERS, A. G., SNIPPERT, H. J., STANGE, D. E., VAN DEN BORN, M., VAN ES, J. H., VAN DE WETERING, M. & CLEVERS, H. 2012. Lineage tracing reveals Lgr5+ stem cell activity in mouse intestinal adenomas. *Science*, 337, 730-5.
- SCHNEIDER, L., FUMAGALLI, M. & D'ADDÀ DI FAGAGNA, F. 2012. Terminally differentiated astrocytes lack DNA damage response signaling and are radioresistant but retain DNA repair proficiency. *Cell Death Differ*, 19, 582-91.
- SEDELNIKOVA, O. A., ROGAKOU, E. P., PANYUTIN, I. G. & BONNER, W. M. 2002. Quantitative detection of (125)IdU-induced DNA double-strand breaks with gamma-H2AX antibody. *Radiat Res*, 158, 486-92.
- SHAHEEN, F. S., ZNOJEK, P., FISHER, A., WEBSTER, M., PLUMMER, R., GAUGHAN, L., SMITH, G. C., LEUNG, H. Y., CURTIN, N. J. & ROBSON, C. N. 2011. Targeting the DNA double strand break repair machinery in prostate cancer. *PLoS One*, 6, e20311.
- SHIBATA, A., BARTON, O., NOON, A. T., DAHM, K., DECKBAR, D., GOODARZI, A. A., LOBRICH, M. & JEGGO, P. A. 2010. Role of ATM and the damage response mediator proteins 53BP1 and MDC1 in the maintenance of G(2)/M checkpoint arrest. *Mol Cell Biol*, 30, 3371-83.
- SHIBATA, A., CONRAD, S., BIRRAUX, J., GEUTING, V., BARTON, O., ISMAIL, A., KAKAROUGKAS, A., MEEK, K., TAUCHER-SCHOLZ, G., LOBRICH, M. & JEGGO, P. A. 2011. Factors determining DNA double-strand break repair pathway choice in G2 phase. *EMBO J*, 30, 1079-92.
- SHIBATA, A. & JEGGO, P. A. 2014. DNA double-strand break repair in a cellular context. *Clin Oncol (R Coll Radiol)*, 26, 243-9.
- SHIBATA, A., MOIANI, D., ARVAI, A. S., PERRY, J., HARDING, S. M., GENOIS, M. M., MAITY, R., VAN ROSSUM-FIKKERT, S., KERTOKALIO, A., ROMOLI, F., ISMAIL, A., ISMALAJ, E., PETRICCI, E., NEALE, M. J., BRISTOW, R. G., MASSON, J. Y., WYMAN, C., JEGGO, P. A. & TAINER, J. A. 2014. DNA double-strand break repair pathway choice is directed by distinct MRE11 nuclease activities. *Mol Cell*, 53, 7-18.
- SHILOH, Y. & ZIV, Y. 2013. The ATM protein kinase: regulating the cellular response to genotoxic stress, and more. *Nat Rev Mol Cell Biol*, 14, 197-210.
- SHORT, S. C., GIAMPIERI, S., WORKU, M., ALCAIDE-GERMAN, M., SIOFTANOS, G., BOURNE, S., LIO, K. I., SHAKED-RABI, M. & MARTINDALE, C. 2011. Rad51 inhibition is an effective means of targeting DNA repair in glioma models and CD133+ tumor-derived cells. *Neuro Oncol*, 13, 487-99.
- SHORT, S. C., MARTINDALE, C., BOURNE, S., BRAND, G., WOODCOCK, M. & JOHNSTON, P. 2007. DNA repair after irradiation in glioma cells and normal human astrocytes. *Neuro Oncol*, 9, 404-11.

References

- SINGH, S. K., HAWKINS, C., CLARKE, I. D., SQUIRE, J. A., BAYANI, J., HIDE, T., HENKELMAN, R. M., CUSIMANO, M. D. & DIRKS, P. B. 2004. Identification of human brain tumour initiating cells. *Nature*, 432, 396-401.
- SMITS, V. A., REAPER, P. M. & JACKSON, S. P. 2006. Rapid PIKK-dependent release of Chk1 from chromatin promotes the DNA-damage checkpoint response. *Curr Biol*, 16, 150-9.
- SORENSEN, C. S., HANSEN, L. T., DZIEGIELEWSKI, J., SYLIUASEN, R. G., LUNDIN, C., BARTEK, J. & HELLEDAY, T. 2005. The cell-cycle checkpoint kinase Chk1 is required for mammalian homologous recombination repair. *Nat Cell Biol*, 7, 195-201.
- STIFF, T., O'DRISCOLL, M., RIEF, N., IWABUCHI, K., LOBRICH, M. & JEGGO, P. A. 2004. ATM and DNA-PK function redundantly to phosphorylate H2AX after exposure to ionizing radiation. *Cancer Res*, 64, 2390-6.
- STROM, C. E., JOHANSSON, F., UHLEN, M., SZIGYARTO, C. A., ERIXON, K. & HELLEDAY, T. 2011. Poly (ADP-ribose) polymerase (PARP) is not involved in base excision repair but PARP inhibition traps a single-strand intermediate. *Nucleic acids research*, 39, 3166-75.
- STUCKI, M., CLAPPERTON, J. A., MOHAMMAD, D., YAFFE, M. B., SMERDON, S. J. & JACKSON, S. P. 2005. MDC1 directly binds phosphorylated histone H2AX to regulate cellular responses to DNA double-strand breaks. *Cell*, 123, 1213-26.
- STUPP, R., MASON, W. P., VAN DEN BENT, M. J., WELLER, M., FISHER, B., TAPHOORN, M. J., BELANGER, K., BRANDES, A. A., MAROSI, C., BOGDAHN, U., CURSCHMANN, J., JANZER, R. C., LUDWIN, S. K., GORLIA, T., ALLGEIER, A., LACOMBE, D., CAIRNCROSS, J. G., EISENHAUER, E., MIRIMANOFF, R. O., EUROPEAN ORGANISATION FOR, R., TREATMENT OF CANCER BRAIN, T., RADIOTHERAPY, G. & NATIONAL CANCER INSTITUTE OF CANADA CLINICAL TRIALS, G. 2005. Radiotherapy plus concomitant and adjuvant temozolomide for glioblastoma. *N Engl J Med*, 352, 987-96.
- SUKHANOVA, M., KHODYREVA, S. & LAVRIK, O. 2010. Poly(ADP-ribose) polymerase 1 regulates activity of DNA polymerase beta in long patch base excision repair. *Mutation research*, 685, 80-9.
- SUVA, M. L., RHEINBAY, E., GILLESPIE, S. M., PATEL, A. P., WAKIMOTO, H., RABKIN, S. D., RIGGI, N., CHI, A. S., CAHILL, D. P., NAHED, B. V., CURRY, W. T., MARTUZA, R. L., RIVERA, M. N., ROSSETTI, N., KASIF, S., BEIK, S., KADRI, S., TIROSH, I., WORTMAN, I., SHALEK, A. K., ROZENBLATT-ROSEN, O., REGEV, A., LOUIS, D. N. & BERNSTEIN, B. E. 2014. Reconstructing and reprogramming the tumor-propagating potential of glioblastoma stem-like cells. *Cell*, 157, 580-94.
- TAMURA, K., AOYAGI, M., ANDO, N., OGISHIMA, T., WAKIMOTO, H., YAMAMOTO, M. & OHNO, K. 2013. Expansion of CD133-positive glioma cells in recurrent de novo glioblastomas after radiotherapy and chemotherapy. *J Neurosurg*, 119, 1145-55.
- TAMURA, K., AOYAGI, M., WAKIMOTO, H., ANDO, N., NARAI, T., YAMAMOTO, M. & OHNO, K. 2010. Accumulation of CD133-positive glioma cells after high-dose irradiation by Gamma Knife surgery plus external beam radiation. *J Neurosurg*, 113, 310-8.

References

- TARSOUNAS, M., DAVIES, D. & WEST, S. C. 2003. BRCA2-dependent and independent formation of RAD51 nuclear foci. *Oncogene*, 22, 1115-23.
- TAUSSIG, D. C., MIRAKI-MOUD, F., ANJOS-AFONSO, F., PEARCE, D. J., ALLEN, K., RIDLER, C., LILLINGTON, D., OAKERVEE, H., CAVENAGH, J., AGRAWAL, S. G., LISTER, T. A., GRIBBEN, J. G. & BONNET, D. 2008. Anti-CD38 antibody-mediated clearance of human repopulating cells masks the heterogeneity of leukemia-initiating cells. *Blood*, 112, 568-75.
- TAYLOR, A. M., HARNDEN, D. G., ARLETT, C. F., HARCOURT, S. A., LEHMANN, A. R., STEVENS, S. & BRIDGES, B. A. 1975. Ataxia telangiectasia: a human mutation with abnormal radiation sensitivity. *Nature*, 258, 427-9.
- TENG, P., BATEMAN, N. W., DARCY, K. M., HAMILTON, C. A., MAXWELL, G. L., BAKKENIST, C. J. & CONRADS, T. P. 2015. Pharmacologic inhibition of ATR and ATM offers clinically important distinctions to enhancing platinum or radiation response in ovarian, endometrial, and cervical cancer cells. *Gynecol Oncol*.
- TENTORI, L., LEONETTI, C., SCARSELLA, M., MUZI, A., MAZZON, E., VERGATI, M., FORINI, O., LAPIDUS, R., XU, W., DORIO, A. S., ZHANG, J., CUZZOCREA, S. & GRAZIANI, G. 2006. Inhibition of poly(ADP-ribose) polymerase prevents irinotecan-induced intestinal damage and enhances irinotecan/temozolomide efficacy against colon carcinoma. *FASEB J*, 20, 1709-11.
- TOULANY, M., MIHATSCH, J., HOLLER, M., CHAACOUAY, H. & RODEMANN, H. P. 2014. Cisplatin-mediated radiosensitization of non-small cell lung cancer cells is stimulated by ATM inhibition. *Radiother Oncol*, 111, 228-36.
- TULI, R., SURMAK, A. J., REYES, J., ARMOUR, M., HACKER-PRIETZ, A., WONG, J., DEWEENE, T. L. & HERMAN, J. M. 2014. Radiosensitization of Pancreatic Cancer Cells In Vitro and In Vivo through Poly (ADP-ribose) Polymerase Inhibition with ABT-888. *Transl Oncol*.
- UEMATSU, N., WETERINGS, E., YANO, K., MOROTOMI-YANO, K., JAKOB, B., TAUCHER-SCHOLZ, G., MARI, P. O., VAN GENT, D. C., CHEN, B. P. & CHEN, D. J. 2007. Autophosphorylation of DNA-PKCS regulates its dynamics at DNA double-strand breaks. *J Cell Biol*, 177, 219-29.
- VANCE, S., LIU, E., ZHAO, L., PARSELS, J. D., PARSELS, L. A., BROWN, J. L., MAYBAUM, J., LAWRENCE, T. S. & MORGAN, M. A. 2011. Selective radiosensitization of p53 mutant pancreatic cancer cells by combined inhibition of Chk1 and PARP1. *Cell Cycle*, 10, 4321-9.
- VAUZOUR, D., VAFEIADOU, K., RICE-EVANS, C., CADENAS, E. & SPENCER, J. P. 2007. Inhibition of cellular proliferation by the genistein metabolite 5,7,3',4'-tetrahydroxyisoflavone is mediated by DNA damage and activation of the ATR signalling pathway. *Arch Biochem Biophys*, 468, 159-66.
- VAVROVA, J., ZARYBNICKA, L., LUKASOVA, E., REZACOVA, M., NOVOTNA, E., SINKOROVA, Z., TICHY, A., PEJCHAL, J. & DURISOVA, K. 2013. Inhibition of ATR kinase with the selective inhibitor VE-821 results in radiosensitization of cells of promyelocytic leukaemia (HL-60). *Radiat Environ Biophys*, 52, 471-9.

References

- VECCHIO, D., DAGA, A., CARRA, E., MARUBBI, D., BAIO, G., NEUMAIER, C. E., VAGGE, S., CORVO, R., PIA BRISIGOTTI, M., LOUIS RAVETTI, J., ZUNINO, A., POGGI, A., MASCELLI, S., RASO, A. & FROSINA, G. 2014. Predictability, efficacy and safety of radiosensitization of glioblastoma-initiating cells by the ATM inhibitor KU-60019. *Int J Cancer*, 135, 479-91.
- VENERE, M., HAMERLIK, P., WU, Q., RASMUSSEN, R. D., SONG, L. A., VASANJI, A., TENLEY, N., FLAVAHAN, W. A., HJELMELAND, A. B., BARTEK, J. & RICH, J. N. 2014. Therapeutic targeting of constitutive PARP activation compromises stem cell phenotype and survival of glioblastoma-initiating cells. *Cell Death Differ*, 21, 258-69.
- VERHAAK, R. G., HOADLEY, K. A., PURDOM, E., WANG, V., QI, Y., WILKERSON, M. D., MILLER, C. R., DING, L., GOLUB, T., MESIROV, J. P., ALEXE, G., LAWRENCE, M., O'KELLY, M., TAMAYO, P., WEIR, B. A., GABRIEL, S., WINCKLER, W., GUPTA, S., JAKKULA, L., FEILER, H. S., HODGSON, J. G., JAMES, C. D., SARKARIA, J. N., BRENNAN, C., KAHN, A., SPELLMAN, P. T., WILSON, R. K., SPEED, T. P., GRAY, J. W., MEYERSON, M., GETZ, G., PEROU, C. M., HAYES, D. N. & CANCER GENOME ATLAS RESEARCH, N. 2010. Integrated genomic analysis identifies clinically relevant subtypes of glioblastoma characterized by abnormalities in PDGFRA, IDH1, EGFR, and NF1. *Cancer Cell*, 17, 98-110.
- VESCOVI, A. L., GALLI, R. & REYNOLDS, B. A. 2006. Brain tumour stem cells. *Nat Rev Cancer*, 6, 425-36.
- VEUGER, S. J., CURTIN, N. J., SMITH, G. C. & DURKACZ, B. W. 2004. Effects of novel inhibitors of poly(ADP-ribose) polymerase-1 and the DNA-dependent protein kinase on enzyme activities and DNA repair. *Oncogene*, 23, 7322-9.
- VLASHI, E. & PAJONK, F. 2014. Cancer stem cells, cancer cell plasticity and radiation therapy. *Semin Cancer Biol*.
- WALKER, J. R., CORPINA, R. A. & GOLDBERG, J. 2001. Structure of the Ku heterodimer bound to DNA and its implications for double-strand break repair. *Nature*, 412, 607-14.
- WAN, F., ZHANG, S., XIE, R., GAO, B., CAMPOS, B., HEROLD-MENDE, C. & LEI, T. 2010. The utility and limitations of neurosphere assay, CD133 immunophenotyping and side population assay in glioma stem cell research. *Brain Pathol*, 20, 877-89.
- WANG, H., PERRAULT, A. R., TAKEDA, Y., QIN, W., WANG, H. & ILIAKIS, G. 2003. Biochemical evidence for Ku-independent backup pathways of NHEJ. *Nucleic Acids Res*, 31, 5377-88.
- WANG, H., WANG, H., POWELL, S. N., ILIAKIS, G. & WANG, Y. 2004. ATR affecting cell radiosensitivity is dependent on homologous recombination repair but independent of nonhomologous end joining. *Cancer Res*, 64, 7139-43.
- WANG, H., WANG, M., WANG, H., BOCKER, W. & ILIAKIS, G. 2005. Complex H2AX phosphorylation patterns by multiple kinases including ATM and DNA-PK in human cells exposed to ionizing radiation and treated with kinase inhibitors. *J Cell Physiol*, 202, 492-502.
- WANG, M., WU, W., WU, W., ROSIDI, B., ZHANG, L., WANG, H. & ILIAKIS, G. 2006. PARP-1 and Ku compete for repair of DNA double strand breaks by distinct NHEJ pathways. *Nucleic Acids Res*, 34, 6170-82.

References

- WANG, R., CHADALAVADA, K., WILSHIRE, J., KOWALIK, U., HOVINGA, K. E., GEBER, A., FLIGELMAN, B., LEVERSCHA, M., BRENNAN, C. & TABAR, V. 2010. Glioblastoma stem-like cells give rise to tumour endothelium. *Nature*, 468, 829-33.
- WARD, J. F. 1975. Radiation-induced strand breakage in DNA. *Basic Life Sci*, 5B, 471-2.
- WEST, C. M., DAVIDSON, S. E., ROBERTS, S. A. & HUNTER, R. D. 1997. The independence of intrinsic radiosensitivity as a prognostic factor for patient response to radiotherapy of carcinoma of the cervix. *Br J Cancer*, 76, 1184-90.
- WETERINGS, E. & CHEN, D. J. 2008. The endless tale of non-homologous end-joining. *Cell Res*, 18, 114-24.
- WETERINGS, E., VERKAIK, N. S., BRUGGENWIRTH, H. T., HOEIJMAKERS, J. H. & VAN GENT, D. C. 2003. The role of DNA dependent protein kinase in synapsis of DNA ends. *Nucleic Acids Res*, 31, 7238-46.
- WHITE, A. C., TRAN, K., KHUU, J., DANG, C., CUI, Y., BINDER, S. W. & LOWRY, W. E. 2011. Defining the origins of Ras/p53-mediated squamous cell carcinoma. *Proc Natl Acad Sci U S A*, 108, 7425-30.
- WILLIS, N. & RHIND, N. 2009. Regulation of DNA replication by the S-phase DNA damage checkpoint. *Cell Div*, 4, 13.
- WOLD, M. S. 1997. Replication protein A: a heterotrimeric, single-stranded DNA-binding protein required for eukaryotic DNA metabolism. *Annu Rev Biochem*, 66, 61-92.
- WU, C., WEI, Q., UTOMO, V., NADESAN, P., WHETSTONE, H., KANDEL, R., WUNDER, J. S. & ALMAN, B. A. 2007. Side population cells isolated from mesenchymal neoplasms have tumor initiating potential. *Cancer Res*, 67, 8216-22.
- XIA, B., SHENG, Q., NAKANISHI, K., OHASHI, A., WU, J., CHRIST, N., LIU, X., JASIN, M., COUCH, F. J. & LIVINGSTON, D. M. 2006. Control of BRCA2 cellular and clinical functions by a nuclear partner, PALB2. *Mol Cell*, 22, 719-29.
- XU, B., KIM, S. T., LIM, D. S. & KASTAN, M. B. 2002. Two molecularly distinct G(2)/M checkpoints are induced by ionizing irradiation. *Mol Cell Biol*, 22, 1049-59.
- YANG, H., LI, Q., FAN, J., HOLLOMAN, W. K. & PAVLETICH, N. P. 2005. The BRCA2 homologue Brh2 nucleates RAD51 filament formation at a dsDNA-ssDNA junction. *Nature*, 433, 653-7.
- YELAMOS, J., SCHREIBER, V. & DANTZER, F. 2008. Toward specific functions of poly(ADP-ribose) polymerase-2. *Trends in molecular medicine*, 14, 169-78.
- YOU, Z., BAILIS, J. M., JOHNSON, S. A., DILWORTH, S. M. & HUNTER, T. 2007. Rapid activation of ATM on DNA flanking double-strand breaks. *Nat Cell Biol*, 9, 1311-8.

References

- ZAHRADKA, P. & EBISUZAKI, K. 1982. A shuttle mechanism for DNA-protein interactions. The regulation of poly(ADP-ribose) polymerase. *European journal of biochemistry / FEBS*, 127, 579-85.
- ZEMAN, M. K. & CIMPRICH, K. A. 2014. Causes and consequences of replication stress. *Nat Cell Biol*, 16, 2-9.
- ZEPPERNICK, F., AHMADI, R., CAMPOS, B., DICTUS, C., HELMKE, B. M., BECKER, N., LICHTER, P., UNTERBERG, A., RADLWIMMER, B. & HEROLD-MENDE, C. C. 2008. Stem cell marker CD133 affects clinical outcome in glioma patients. *Clin Cancer Res*, 14, 123-9.
- ZHENG, H., YING, H., WIEDEMAYER, R., YAN, H., QUAYLE, S. N., IVANOVA, E. V., PAIK, J. H., ZHANG, H., XIAO, Y., PERRY, S. R., HU, J., VINJAMOORI, A., GAN, B., SAHIN, E., CHHEDA, M. G., BRENNAN, C., WANG, Y. A., HAHN, W. C., CHIN, L. & DEPINHO, R. A. 2010. PLAGL2 regulates Wnt signaling to impede differentiation in neural stem cells and gliomas. *Cancer Cell*, 17, 497-509.
- ZHOU, W., SUN, M., LI, G. H., WU, Y. Z., WANG, Y., JIN, F., ZHANG, Y. Y., YANG, L. & WANG, D. L. 2013. Activation of the phosphorylation of ATM contributes to radiosensitivity of glioma stem cells. *Oncol Rep*, 30, 1793-801.
- ZHUANG, W., LI, B., LONG, L., CHEN, L., HUANG, Q. & LIANG, Z. Q. 2011. Knockdown of the DNA-dependent protein kinase catalytic subunit radiosensitizes glioma-initiating cells by inducing autophagy. *Brain Res*, 1371, 7-15.
- ZOU, J., QIAO, X., YE, H., YANG, Y., ZHENG, X., ZHAO, H. & LIU, S. 2008. Antisense inhibition of ATM gene enhances the radiosensitivity of head and neck squamous cell carcinoma in mice. *J Exp Clin Cancer Res*, 27, 56.
- ZOU, L. & ELLEDGE, S. J. 2003. Sensing DNA damage through ATRIP recognition of RPA-ssDNA complexes. *Science*, 300, 1542-8.